

13

A Study of Aminolaevulinic Acid Synthase

Carolyn Joy Nahman
MB.ChB.

Thesis presented for the degree of
DOCTOR OF PHILOSOPHY
In the Department of Medicine
UNIVERSITY OF CAPE TOWN
August 2001

The copyright of this thesis vests in the author. No quotation from it or information derived from it is to be published without full acknowledgement of the source. The thesis is to be used for private study or non-commercial research purposes only.

Published by the University of Cape Town (UCT) in terms of the non-exclusive license granted to UCT by the author.

DECLARATION

I, Carolyn Joy Nahman, hereby declare that the work on which this thesis is based is my original work (except where acknowledgements indicate otherwise) and that neither the whole work, nor any part of it has been, is being, or is to be submitted for another degree in this or any other university.

I empower the University to reproduce for the purpose of research either the whole or any portion of the contents in any manner whatsoever.

Signed by candidate

Signature

Date 10 September 2001

Abstract

Delta-aminolaevulinic acid synthase (ALAS) is the first enzyme in the haem biosynthetic pathway, and in mammals is present in two isoforms – differing in regulation and encoded for on different chromosomes. The hepatic form is up-regulated in states of haem deficiency and thus implicated in the acute attack of porphyria. Given the large numbers of patients who suffer from an acute form of porphyria in South Africa the regulation of the human hepatic form of the enzyme is of considerable interest.

In vitro studies of the enzyme are difficult as it is a highly unstable mitochondrial matrix protein with a short half-life. Much of the current knowledge about this enzyme has been derived from studies using rat livers, or chicken embryo livers, rendered porphyrinogenic by treating the animals with a variety of chemicals, which generally cause super-induction of the enzyme – and thus may not reflect true physiological regulation of the enzyme. Therefore, direct knowledge of the human hepatic isoform of ALAS is limited.

In this study, polyclonal antibodies were raised to a fragment of human ALAS in order to study tissue distribution, immunohistochemically. A positive control to assess ALA synthase antibody specificity was developed, using transient transfections of ALA synthase in COS cells. Following this, immunohistochemical studies were undertaken, looking at staining for ALA synthase in multiple human tissue samples, using surgical biopsy material and post-mortem material, including a patient who died of acute porphyria.

ALA synthase was detected in hepatocytes, proximal convoluted tubule cells in the kidney, zona reticularis in the adrenal gland, myocytes, myocardium, bronchial glands of the lung, oesophageal epithelium, endocrine glands of the colon, anterior pituitary cells and neurones. Very little ALA synthase was detected in stomach and small intestine. The apparent high concentrations of ALA synthase in neurones (including dendrites and axons) has not been documented previously. This result sheds light on the theories about the acute attack of porphyria being related to neuronal haem deficiency or direct neurotoxicity of ALA.

Acknowledgements

I would like to thank my supervisors Professor Ralph Kirsch, for inviting me to do research in his department, and Professor Peter Meissner, for agreeing to let me work in the porphyria division. Many thanks also go to Renate Scholle – who taught me the fundamentals of molecular biology and laboratory techniques, and encouraged me on the many occasions when experiments failed; to Prof. Mario Ehlers – for welcoming me into his molecular biology lab; to Ingrid Baumgarten – for teaching me loads about lymphocyte transformations and culture (even though it wasn't finally used in this thesis); to Anne Corrigan – who taught me much about working with glutathione transferase in particular, and protein purifications in general; to the immuno lab for letting me loose on the precious DAKO machine; to Arieh Katz and his lab for letting me “borrow” reagents for the COS cell transfections.

Much thanks also go to my lab colleagues who helped made working in a lab such fun, and who were a shoulder to cry on when things just weren't working – including Fernanda, Sylva, Nicole, Heinrich, Ed, Anthony, Zenda and Kerry.

Special thanks go to Prof. Dave Bishop, who kindly gave us the cDNA for human hepatic ALA synthase – without this generous gift, this thesis would not have been possible.

Most of all I want to thank my ever-patient husband, Philip – with “just one more year on my PhD”, and my daughter Talya, who often was told, “Mummy just needs to spend a little longer at the computer.” Without them this project would not have been completed.

Table of Contents

| | |
|-----------------------------|---------|
| Abstract | iii |
| Acknowledgements | iv |
| Table of contents | v-viii |
| Index of Tables and Figures | ix-xiii |

Table of Contents

Chapter 1 - The haem pathway and porphyria

| | |
|-----------------------------------------------------------------|---------|
| Haem Biosynthetic pathway | 2 - 29 |
| <i>Historical Background</i> | 2 |
| <i>Structure and chemistry of porphyrins and porphyrinogens</i> | 4 |
| <i>Enzymology of haem biosynthesis</i> | 6 |
| The porphyrias | 30 - 47 |
| <i>Introduction</i> | 30 |
| <i>The hepatic porphyrias</i> | 33 |
| <i>The Erythropoietic porphyrias</i> | 41 |
| Summary | 48 |

Chapter 2 - The role of ALAS in Haem Biosynthesis

| | |
|-------------------------------------------------------------------------------|-------|
| Regulation of haem biosynthesis in higher vertebrates | 52 |
| A comparison of housekeeping and erythroid ALA synthase sequences | 53-54 |
| The regulation of erythroid ALA synthase | 55-60 |
| The regulation of housekeeping ALA synthase | 61-67 |
| The role of ALA synthase in the pathogenesis of the acute attack of porphyria | 68-72 |
| Summary - | 73 |

Chapter 3 - The production of antibodies to ALA synthase

| | |
|---------------------------------------------------------------------------------------------|--------|
| 3.1 Introduction | 74-76 |
| 3.2 Materials and Methods | |
| Materials | 77 |
| Methods | 77-90 |
| 1. Computer predictions on the hydrophobicity and other characteristics of ALA synthase | 77 |
| 2. Design of primers | 78 |
| 3. PCR and cloning | 78 |
| 4. Expression and purification of fusion proteins in <i>E.coli</i> | 81 |
| 5. Standard purification technique for SJ GST fusion proteins | 82 |
| 6. CDNB assays to screen for GST activity | 83 |
| 7. Purification of insoluble GST proteins according to the method of Frangioni and van Neel | 84 |
| 8. Further modification of purification of insoluble GST fusion proteins | 86 |
| 9. Western blotting | 87 |
| 10. Preparation of antigen and production of antibody | 88 |
| 3.3 Results and discussion | 90-104 |
| 1. Computer predicted analyses | 90 |
| 2. ALA synthase fragments chosen for expression in <i>E.Coli</i> | 93 |
| 3. PCR and cloning | 97 |
| 4. Expression and purification of fusion proteins in <i>E.Coli</i> | 99 |
| 5. Western blotting | 102 |
| 6. Production of antibodies to ALA synthase fragment 3 | 102 |
| Summary | 105 |

Chapter 4 - Characterisation of the Antibody Produced to the GST-Fragment 3 Fusion Protein

| | |
|-----------------------------------------------------------------------|---------|
| 4.1 Introduction | 107 |
| 4.2 Materials and Methods | |
| Materials | 108 |
| Methods | 108-120 |
| 1. Cytosolic preparation of human liver | 108 |
| 2. Double immunodiffusion to test for the presence of human μ GST | 109 |
| 3. Human GST purification | 110 |
| 4. Western blots | 110 |
| 5. Construction of the His-ALA-synthase-EGFP and cloning strategies | 110 |
| 6. COS cell transfections with DEAE dextran | 118 |
| 7. Visualization of EGFP using fluorescent microscope | 118 |
| 8. Immunocytochemistry of transfected COS cells | 118 |

Index of Tables and Figures

1. Index of Tables

Chapter 1 - The haem pathway and porphyria

| | |
|---------------------------------------------------------------------------------------|----|
| Table 1.1 Historical classifications of the porphyrias. | 31 |
| Table 1.2 Classification of porphyria according to clinical expression of the disease | 32 |

Chapter 3 - The production of antibodies to ALA synthase

| | |
|-------------------------------------------------------------------------|----|
| Table 3.3.1 Instability indices of selected proteins | 92 |
| Table 3.3.2 The primers for amplification of the ALA synthase fragments | 97 |

Chapter 4 - Characterisation of the Antibody Produced to the GST-Fragment 3 Fusion Protein

| | |
|--------------------------------------------------------------------|-----|
| Table 4.2.1 Primers for amplification of the ALA synthase fragment | 113 |
|--------------------------------------------------------------------|-----|

Chapter 5 – Further characterization of the antibody

| | |
|------------------------------------------------------------------------------|-----|
| Table 5.3.1 Immunocytochemistry results of all foetal liver samples analysed | 134 |
|------------------------------------------------------------------------------|-----|

Chapter 6 - Immunohistological examination of ALA synthase in human tissue

| | |
|--------------------------------------------------------------------------------------|------|
| Table 6.3.1. Staining intensity in resected and post-mortem liver specimens | 143. |
| Table 6.3.2. Staining intensity in surgical adrenal specimens. | 145 |
| Table 6.3.3. Staining intensity in surgical and post mortem kidney specimens | 147 |
| Table 6.3.4. Staining intensity in ovary samples | 149 |
| Table 6.3.5. Staining intensity in testis specimens | 151 |
| Table 6.3.6. Staining intensity of brain using antibody to ALA synthase. | 152 |
| Table 6.3.7. Staining intensity of oesophagus using antibody to ALA synthase | 155 |
| Table 6.3.8. Staining intensity of stomach using antibody to ALA synthase. | 158 |
| Table 6.3.9. Staining intensity of lung using antibody to ALA synthase. | 163 |
| Table 6.3.10. Staining intensity of myocardium using antibody to ALA synthase. | 166 |
| Table 6.3.10 Table showing summary of immunostaining in all tissues for ALA synthase | 168 |

2. Index of Figures

Chapter 1 the haem pathway and porphyria

| | |
|--------------------------------------------------------------------------------------|----|
| Fig 1.1 The chemical structure of haem. | 5 |
| Fig 1.2 The haem biosynthetic pathway | 7 |
| Fig 1.3 The chemical structure of glycine, succinyl Coenzyme A and ALA | 8 |
| Fig 1.4 Formation of Porphobilinogen (PBG) from 2 ALA molecules. | 9 |
| Fig 1.5 The polymerization of four ALA molecules to form hydroxymethylbilane. | 13 |
| Fig 1.6 Formation of Uroporphyrinogen III, | 16 |
| Fig 1.7 Decarboxylation of Uroporphyrinogen III | 18 |
| Fig 1.8 The chemical structures of coproporphyrinogen III and protoporphyrinogen IX. | 21 |
| Fig 1.9 The chemical structures of protoporphyrinogen IX and Protoporphyrin IX. | 24 |
| Fig 1.10 The chemical structures of protoporphyrin IX and protohaem IX. | 26 |

Chapter 2- The role of ALAS in Haem Biosynthesis

| | |
|-----------------------------------------------------------------------------------------------------------------------------------|----|
| Fig 2.1 Alignment of the amino acid sequences of erythroid and hepatic ALA synthase | 54 |
| Fig 2.2 Diagram illustrating amplification and maturation sequences of the development of red blood cells from the pronormoblasts | 56 |
| Fig 2.3 Proposed model for regulation of erythroid ALA synthase and globin mRNA in erythroid cells | 60 |

Chapter 3 - The production of antibodies to ALA synthase

| | |
|-----------------------------------------------------------------------------------------------------------------------------------|----|
| Fig 3.2.1 Structure of the pGEX-2T vector | 79 |
| Fig 3.3.1 A hydrophobicity plot of the ALA synthase sequence | 91 |
| Fig 3.3.2 Predicted secondary structure of ALA synthase | 93 |
| Fig 3.3.3 Sequence of ALA synthase showing predicted accessible residues | 94 |
| Fig. 3.3.4 Amino acid sequence of ALA synthase displaying the fragments chosen for expression and purification in <i>E.coli</i> . | 96 |
| Fig 3.3.5 PCR amplification of the 4 fragments of the ALA synthase gene | 98 |
| Fig 3.3.6 The purified plasmid preparations pFP1; pFP2; pFP3; pFP4 | |

| | |
|-------------------------------------------------------------------------------------------------|-----|
| subjected to a <i>Bam HI</i> and <i>Eco RI</i> restriction enzyme analysis | 99 |
| Fig 3.3.7 The purified fusion proteins 1 to 4 | 100 |
| Fig 3.3.8 Western blots performed using anti <i>Schistosoma japonicum</i> GST antibodies | 102 |
| Fig 3.3.9 Elisa performed to test antisera from a rabbit immunized with FP 3 | 104 |
| Fig 3.3.10 Western blotting of purified FP 3 | 105 |

Chapter 4 - Characterisation of the Antibody Produced to the GST-Fragment 3 Fusion Protein

| | |
|--------------------------------------------------------------------------------------------------------------------------------------------------------------------------------------------------|-----|
| Fig 4.2.1 The structure of pEGFP | 112 |
| Fig 4.2.2. The cloning strategy for sub-cloning the processed ALA synthase into the Eukaryotic expression vector, pEGFP | 117 |
| Fig 4.2.3 Schematic representation of the HRP-Streptavidin-Biotin Anti-rabbit Immune complex method | 120 |
| Fig 4.3.1 Immunodiffusion, showing in the rosettes labelled "a" and "b", the cross-reactivity of rabbit anti-human μ GST (central well) and cytosol from liver "B"(peripheral wells). | 121 |
| Fig 4.3.2 SDS polyacrylamide gel(10%) of lig 3 and human GST and Western blots of human GST and FP 3, using antibody to <i>Schistosoma japonicum</i> (B) and to μ GST(C). | 122 |
| Fig 4.3.3 PCR amplification, followed by <i>Eco RI</i> and <i>Bsm I</i> digest of the His-ALA S fragment electrophoresed on a 2% agarose gel and stained with ethidium bromide. | 123 |
| Fig 4.3.4 The purified plasmid preparation of pGEM ALA S has been subjected to an <i>Eco RI</i> and <i>Bsm I</i> restriction enzyme digestion | 124 |
| Fig 4.3.5 Purified plasmid preparations of pEGFP and pEGFP-ALAS, and <i>Eco RI</i> and <i>Not I</i> restriction enzyme analysis of these plasmids. | 125 |
| Fig 4.3.6 Fluorescent microscopy of COS cells transfected with pEGFP-ALAS | 126 |
| Fig 4.3.7 Immunostaining of COS cells with non-immunized rabbit serum visualized at 100 times magnification | 127 |
| Fig 4.3.8 Immunostaining of COS cells using anti-sera to FP3 visualized at 400 times magnification | 128 |

Chapter 5 – Further characterization of the antibody

- Fig 5.1.1** The fragment of ALA synthase (F3) to which antibodies were generated is aligned with the corresponding area of erythroid ALA synthase. 130
- Fig 5.1.2** The fragment of ALA synthase (F3) to which antibodies were generated is aligned with the corresponding area of rat ALA synthase. 131
- Fig 5.3.1** Immunostaining for ALA synthase in foetal liver 134
- Fig 5.3.2.** Immunocytochemistry of rat liver, using antisera to human ALA synthase. 135

Chapter 6 - Immunohistological examination of ALA synthase in human tissue

- Fig 6.2.1** Schematic representation of the HRP-Streptavidin-Biotin anti-rabbit immune complex method 139
- Fig 6.3.1.a** Typical immunohistological examination of a surgical liver specimen using antisera to ALA synthase, viewed at 100 times magnification. 143
- Fig. 6.3.1.b** Typical immunohistological examination of a surgical liver specimen using antisera to ALA synthase, viewed at 200 times magnification. 144
- Fig 6.3.2.a** Adrenal gland at 40X magnification. 145
- Fig 6.3.2.b** The zona reticularis of the adrenal cortex at 200 times magnification. 146
- Fig 6.3.2.c** Adrenal medulla at 200X magnification. 146
- Fig 6.3.3.a** Staining of kidney for ALA synthase at 40 times magnification. 148
- Fig 6.3.3.b** Histological staining of kidney for ALA synthase at 100 times magnification. 148
- Fig 6.3.4** Typical immunohistological staining for ALA synthase in pre-menopausal resected ovary. 150
- Fig 6.3.5.a** Photograph of immunohistological examination of testis using antibody to hepatic ALA synthase at 100 times magnification. 151
- Fig 6.3.5.b** Photograph of immunohistological examination of testis using antibody to hepatic ALA synthase at 200 times magnification. 152
- Fig 6.3.6.a** Photograph of immunohistological examination of brain using antibody to hepatic ALA synthase at 200 times magnification. 153
- Fig 6.3.6.b** A typical immunohistological examination of post mortem brain tissue using antibodies to ALA synthase. 154
- Fig 6.3.7** Immunohistological examination of post-mortem anterior pituitary specimen at 200 times magnification. 155

| | |
|--------------------------------------------------------------------------------------------------------------------------------------|-----|
| Fig 6.3.8.a Immunohistological examination of a specimen of resected oesophagus at 40 times magnification. | 156 |
| Fig 6.3.8.b Immunohistological examination of a specimen of resected oesophagus at 100 times magnification. | 157 |
| Fig 6.3.9 Immunohistological examination of resected stomach using antibody to ALA synthase. | 159 |
| Fig 6.3.10 Immunohistological examination of duodenum using antibody to ALA synthase | 160 |
| Fig 6.3.11 Immunohistological examination of pancreas using antibody to ALA synthase. | 161 |
| Fig 6.3.12.a Immunohistological examination of colon using antibody to ALA synthase at 100 times magnification. | 162 |
| Fig 6.3.12.b Immunohistological examination of colon using antibody to ALA synthase at 200 times magnification. | 162 |
| Fig 6.3.13 Immunohistological examination of skeletal muscle using antibody to ALA synthase at 100 times magnification. | 163 |
| Fig 6.3.14.a Immunohistological examination of lung using antibody to ALA synthase at 40 times magnification. | 165 |
| Fig 6.3.14.b Immunohistological examination of lung using antibody to ALA synthase at 100 times magnification. | 166 |
| Fig 6.3.15.a Immunohistological examination of cardiac muscle using antibody to ALA synthase at a magnification of 100 times. | 167 |
| Fig 6.3.15.b Immunohistological examination of cardiac muscle using antibody to ALA synthase at a magnification of 400 times. | 167 |

Chapter 7- Immunohistochemical examination of ALA synthase in a patient who died during an acute attack of AIP.

| | |
|-----------------------------------------------------------------------------------------------------------|-----|
| Fig 7.3.1 A Haematoxylin and Eosin stained section of HK's liver viewed at 400 times magnification | 175 |
| Fig 7.3.2 A Perl's stain of HK's liver viewed at 400 times magnification | 175 |
| Fig 7.3.3.a Liver at 100 times magnification from patient HK | 177 |
| Fig 7.3.3.b Liver at 400 times magnification from patient HK | 177 |
| Fig 7.3.4.a Adrenal cortex at 100 times magnification. | 178 |
| Fig 7.3.4.b Adrenal medulla at 100 times magnification | 178 |
| Fig 7.3.5.a Kidney at 100 times magnification | 179 |
| Fig 7.3.5.b Kidney at 200 times magnification | 179 |
| Fig 7.3.6 Myocardium at 100 times magnification | 180 |
| Fig 7.3.7 Skeletal muscle from HK viewed at 100 times magnification | 181 |
| Fig 7.3.8 Anterior pituitary viewed at 100 times magnification | 182 |

Chapter One

Literature Review 1 – The Haem Pathway and Porphyria

Haem is an iron-containing protoporphyrin complex which, when conjugated to a variety of proteins, plays an important role in cellular metabolism and is involved in reduction of molecular oxygen, hydroxylation and electron transfer in energy generation and cellular respiration as well as oxygen transport (Beri and Chandra, 1993). It is therefore considered that haem biosynthesis is a key biological process in both prokaryotic and eukaryotic cells.

In all living organisms haem is synthesized via a specific pathway involving a series of chemical reactions and modifications of various porphyrin intermediates (see Fig 1.2). Organisms that have lost the ability to synthesize haem are therefore dependent on host cells for their existence. In earlier terrestrial life forms it would appear that primitive chemical systems existed in which abiotic synthesis of porphyrin-like compounds existed.

While this work is primarily concerned with detailed study of one specific protein, the first and rate-determining enzyme of haem biosynthesis, δ -aminolevulinic acid (ALA) synthase, this chapter serves to describe the context within which ALA synthase can be viewed. It will cover general aspects of haem biosynthesis, the enzymes of haem biosynthesis and the porphyrias (disorders of haem biosynthesis). The regulation of ALA synthase is reviewed in necessary detail in Chapter 2.

Haem Biosynthetic Pathway

Historical Background

Scherer first alluded to the existence of porphyrins in 1841 when he showed that iron was not responsible for the red colour of blood. The colour of blood had been attributed to the presence of iron until that time. Iron was washed out of dried concentrated blood, using sulfuric acid, and the remaining residue became a blood-red colour after this was heated with alcohol. Shortly thereafter, in 1844, Mulder described a purple-red fluid, not containing iron, which he called, "iron-free haematin." In 1871, Hoppe-Seyler was the first person to use the term porphyrin ("haematoporphyrin"), to describe the "iron-free haematin". Interestingly, Hoppe-Seyler (1879) rediscovered the red fluorescence while studying the porphyrin in chlorophyll, which he called phylloporphyrin. The word porphyrin is derived from the Greek word *porphuros*, meaning "purple".

Schultz (1874) described a 33-year-old patient who suffered with severe skin photosensitivity from the age of three, and passed wine red urine. On investigation the urine was found to contain a pigment with a spectrum similar to that of haematoporphyrin (Baumstark, 1874). In the interpretation of these findings Baumstark (1874) suggested that these urinary porphyrin pigments were originating from an "error of synthesis", a fact that was confirmed only fifty years later.

Over the latter half of the 19th century, further cases of "porphyria", started being described. This was partially due to the use of the hypnotics, sulphonyl, tetronal, and trional. Many chemists at that time were describing a variety of these "porphyrins" – found in the urine of patients suffering from both natural forms of porphyria, and patients who had ingested lead or sulphonyl. Around the turn of the 20th century, structures of a variety of porphyrin intermediates were described. Notably, protoporphyrin was identified (Laidlaw, 1904) and subsequently, the correct tetrapyrrole structure of haem proposed by Kuster (1912). However, at that time other scientists had reservations about the stability of such a large ring structure and his work was unfortunately rejected.

The remarkable work by Fischer (1915) and other workers resulted in the differentiation of the natural haem from haematoporphyrin, which was correctly named, protoporphyrin. Fischer's work on haem continued until his death in 1945. He was awarded the Nobel Prize for Chemistry, in 1930, for his work on the chemical synthesis of haematin.

The terminology used for the tetrapyrrole biosynthetic pathway intermediates, the porphyrins, was applied to the description of diseases of the haem pathway in 1937, when the diseases were called "the porphyrias" (Waldenstrom, 1937).

The isolation of crystalline porphobilinogen (PBG) from the urine of acute intermittent porphyria patients was another important milestone in the understanding of this pathway (Westall, 1952). Cookson and Rimington (1954) elucidated the monopyrrole structure of PBG. This compound (PBG) was shown to be enzymatically converted into uroporphyrinogen when incubated with chicken red cell haemolysate (Falk et al, 1953).

Subsequent attempts to study the tetrapyrrole biosynthetic pathway using uroporphyrin-III, which had been prepared from turacin (a copper complex of uroporphyrin-III found in the feathers of a bird species, the Cape Loerie) by the removal of the bound copper ions, were not successful (Rimington, 1939). The reasons for this only became clear when it was realised that the actual intermediate substrates of the tetrapyrrole pathway reactions were porphyrinogens, the reduced forms of porphyrins (Bogorad, 1955).

Studies carried out in suitable animal models provided important information on the systematic biochemical description of the haem (tetrapyrrole) biosynthetic pathway. Various investigators studied the incorporation of radiolabelled precursors at different steps of the pathway during the formation of the haem molecule. Initial studies described how [¹⁵N]glycine and [¹⁴C]glycine were incorporated into haem in humans and other animals (Shemin and Wittenberg, 1946; Muir and Neuberger, 1950; Shemin et al, 1955. *In vitro* labelling studies with [¹⁴C]acetate (Shemin and Wittenberg, 1951), using avian erythrocyte preparations, established that succinyl-CoA was the 4-carbon compound, from

the tricarboxylic acid cycle, which provided some of the carbon atoms in the haem macrocycle (Gibson et al, 1958).

Subsequently, it was demonstrated that 5-aminolaevulinic acid (ALA) was the committed precursor leading to the synthesis of all the porphyrin intermediates (Shemin and Russell, 1953; Neuberger and Scott, 1953). During this same period it was shown that PBG is the monopyrrole precursor for all the tetrapyrrole synthesis in this pathway (Falk et al, 1953). Thus, the porphyrin biosynthetic pathway was well established by the mid-50's.

Structure and Chemistry of Porphyrins and Porphyrinogens

Haem consists of a porphyrin molecule, protoporphyrin-IX, containing an iron atom in the center. Protoporphyrin-IX (PP-IX) is a rigid planar molecule consisting of four pyrrole rings linked by 4 methene bridges. Two propionic acid, two vinyl and 4 methyl side chains are attached to the pyrrole rings (Beri and Chandra, 1993) as shown in Fig 1.1.

The porphyrin nomenclature used is generally that which was designated by Hans Fischer (Fischer and Orth, 1968), in which the four pyrrole rings are called A, B, C and D and the four methene bridges α , β , γ and δ . The eight side chains are attached at the positions designated 1 – 8 by Fischer. The designation IX was assigned to the isomer found in nature, after Fischer and his co-workers discovered that the protoporphyrin purified from haem corresponded to the ninth, out of 15 possible isomers that they had proposed.

The IUPAC-IUB (Joint Commission on Biochemical Nomenclature, 1980) designated the four pyrrole rings as A B C D and the side chains have been numbered 1-8 with side chains 1 and 2 occurring on the pyrrole A, 3 and 4 on B etc. Thus, PP-IX can be described as 1,3,5,8-methyl, 2,4, -vinyl, 6,7- propionate porphyrin.

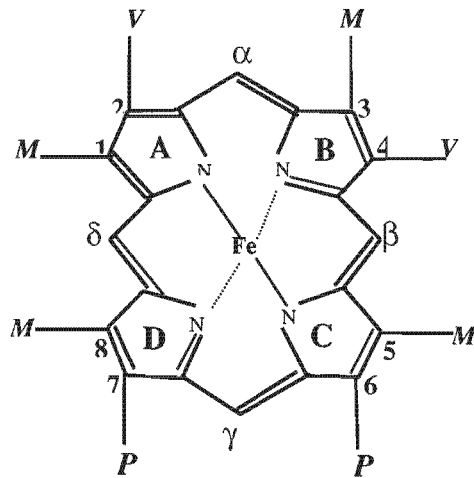


Fig 1.1 The chemical structure of haem. The Fischer nomenclature is indicated, as described in the text above. *M* = methyl ($-\text{CH}_3$), *V* = vinyl ($-\text{CH}=\text{CH}_2$), and *P* = propionate ($-\text{CH}_2\text{CH}_2\text{COOH}$) groups.

PP-IX has the capacity to bind metals, most commonly iron (to form haem), magnesium (to form chlorophyll's) and cobalt to form vitamin B12 (Scott et al 1972; Battersby and McDonald, 1975; Jones, 1976; Bissell and Schmidt, 1987). The iron atom in the ferrous (2+) oxidative state can form 5 or 6 ligand bonds, depending on whether an oxygen molecule is present. Four of the bonds are to the pyrrole nitrogen's of the porphyrins and lie in the plane of the porphyrin ring. The fifth bond tends to be to an amino acid of an apoprotein molecule, often to a nitrogen atom of the imidazole group of histidine.

All porphyrins are brightly colored and when not bound to metals, fluoresce red, in light at the wavelength of about 400nm. They also display a strong light absorption band at around 400nm – the region of the spectrum known as the Soret band, as well as four absorption bands in the visible spectrum.

The side chain substituents attached to the rings are important in determining the physical characteristics of the porphyrins. As biological intermediates, the porphyrins exist as the unconjugated less stable reduced forms, the porphyrinogens. Porphyrinogens are relatively non-aromatic compounds, with less rigid structural properties (Smith, 1975), are unable to bind metals, are colourless and do not fluoresce under ultraviolet light.

Enzymology of Haem Biosynthesis

Haem biosynthesis can be viewed in the most general terms as consisting of a series of “pyrrolic” chemical reactions and modifications, catalysed and linked by the so-called haem biosynthetic enzymes, forming an irreversible, unbranched metabolic pathway. The enzymes of the pathway are located sequentially in the mitochondria, cytoplasm, and finally mitochondria (Dailey, 1990) (see Fig 1.2, below).

In a wide variety of organisms, the sequence of reactions in this pathway is highly conserved after the initial reaction involving ALA synthesis. Both photosynthetic and non-photosynthetic organisms share a common pathway and generally have almost identical enzymes catalysing the reactions from condensation of 2 ALA molecules, to the formation of protoporphyrin-IX.

In mammals ALA, the first committed precursor, is synthesized in a single reaction from glycine and succinyl-CoA, by the mitochondrial matrix enzyme ALA synthase, the enzyme of interest to this dissertation. In plants, algae and some bacteria ALA is synthesized from the intact carbon skeleton of glutamate in three sequential enzymatic steps via what is referred to as the C₅ pathway (Beale and Weinstein, 1990).

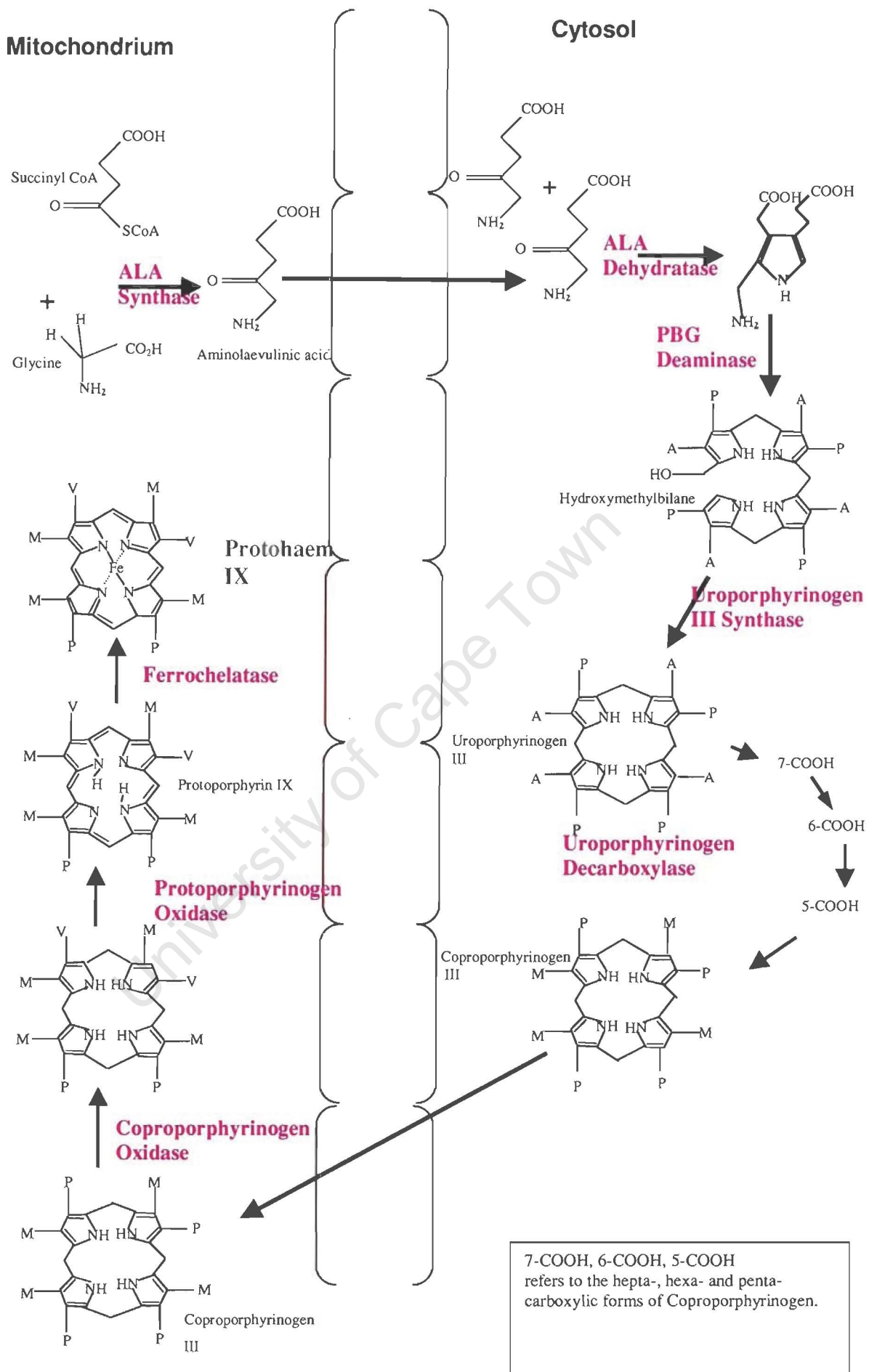


Fig 1.2 The haem biosynthetic pathway

It is convenient to describe the synthesis of haem in four stages – firstly the formation of the pyrrole, secondly the assembly of the tetra-pyrrole macrocycle, thirdly the modifications of the porphyrin side-chains and lastly the final oxidative step and the insertion of the iron atom.

Formation of the pyrrole

1. Synthesis of δ -aminolevulinic acid (ALA) by ALA synthase [EC 2.3.1.37]

As mentioned above, in plants, algae and some bacterial systems (e.g. *E.Coli*), the synthesis of ALA occurs from glutamate by a C₅ pathway. The 5-carbon glutamate skeleton is activated when it binds to tRNA_{glu} and is then reduced to glutamate-1-semialdehyde and converted (by transamination) to its isomer, ALA (Beale and Weinstein, 1990). This thesis is predominantly concerned with the C₄ pathway, which occurs in many prokaryotic and all animal cells. In animal cells the pathway proceeds with the condensation of succinyl CoA (from the citric acid cycle) and glycine to form ALA, by the enzyme ALA synthase.

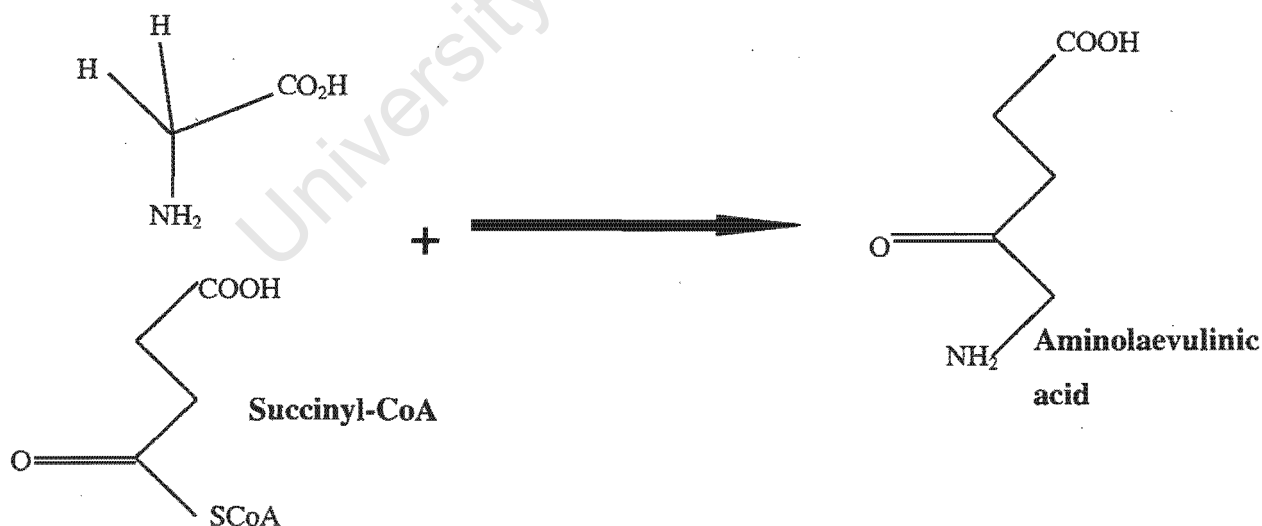


Fig 1.3 The chemical structure of glycine, and succinyl Coenzyme A (CoA) and aminolaevulinic acid. ALA synthase catalyses the condensation of glycine and succinyl CoA to form the first committed precursor in the haem pathway.

Early work by Shemin and co-workers (1945, 1955) was performed using both [^{15}N] and [^{14}C] labelled glycine, and initially established that the α -carbon and nitrogen, but not the carboxyl carbon are incorporated into haem. Shemin et al (1951) subsequently performed labelling experiments with [^{14}C]acetate, and were able to demonstrate that the remaining carbon atoms in haem are derived from succinyl CoA. The glycine and succinyl CoA condense to form the molecule 2-amino, 3-ketoadipic acid that is then decarboxylated to form ALA (Shemin and Russell, 1955). The [^{14}C]-ALA that had been chemically synthesized was incorporated into haem by whole cells (Shemin, 1953).

Further details about ALA synthase – in particular the regulation of ALA synthase will be discussed in detail in Chapter 2.

2. Formation of porphobilinogen (PBG) by ALA Dehydratase [EC 4.2.1.24] (Porphobilinogen Synthase)

The next step in the haem biosynthetic pathway takes place in the cytosol and it involves the condensation of two ALA molecules, in a series of stages involving an aldol condensation and formation of a Schiff-base (Shemin, 1976) with the elimination of two water molecules, to form the monopyrrole, porphobilinogen (2nd reaction, Fig 1.2) (Jordan and Seehra, 1980).

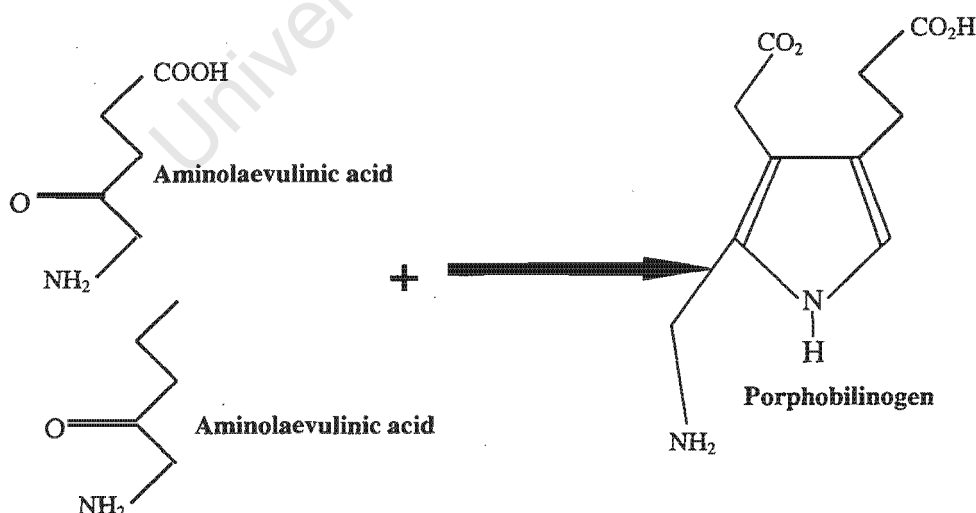


Fig 1.4. Formation of Porphobilinogen (PBG) from 2 ALA molecules.

The multi-subunit, cytoplasmic enzyme, ALA dehydratase, catalyses this reaction. An important role of this enzymatic reaction is to ensure the correct positioning of the two ALA molecules to ensure formation of correct product. Because 2-aminoketones like ALA are intrinsically reactive, other products such as the dehydropyrazine can easily form by non-enzymatic dimerization. Thus two ALA molecules are bound to two different positions on the ALA dehydratase. This helps to achieve specific molecular spacing, which allows the one ALA molecule to contribute to the acetate and amino-methyl group and the other ALA molecule to contribute the propionate side chain and the pyrrole nitrogen (Gibbs and Jordan, 1986) (Fig 1.4).

ALA dehydratase is one of the better-studied enzymes in the haem pathway and has been cloned and purified from a number of bacterial, avian and mammalian sources (Wetmur et al, 1986; Gibbs et al, 1985; Anderson et al, 1979; Bishop et al, 1986; Bishop et al, 1989). The human form of the enzyme has been mapped to chromosome 9Q34 (Potluri et al, 1987).

The interest in ALA dehydratase is partly owing to its clinical relevance in lead poisoning (Moore and Goldberg, 1985) and in hereditary tyrosinaemia (Sassa and Kappas, 1983), as well as the rarely described ALA dehydratase porphyria (Sassa, 1998).

A genetic polymorphism has been identified in exon 4 of the ALA dehydratase gene, which causes an amino acid substitution of asparagine for lysine. Twenty percent of the human population is heterozygous or homozygous for the asparagine allele, which may predispose individuals to lead toxicity (Battistuzzi et al, 1981; Wetmur et al, 1991; Astrin et al, 1987).

Compared to the rate-determining enzyme, ALA synthase, in the haem pathway – under physiological conditions, ALA dehydratase is abundantly present in mammalian cells; in liver there is 800 to 1000% more ALA dehydratase activity, than ALA synthase (Kappa and Sassa, 1995).

2 major classes of ALA dehydratase enzymes are present - the zinc and magnesium dependant ALA dehydratases (Frankenberg et al, 1999). The zinc dependant ALA dehydratases are found in mammals, yeasts and some bacteria (e.g. *E. coli*). The magnesium dependant ALA dehydratases are found in plants and other bacteria.

The avian and mammalian forms of the enzyme are octomers formed from 8 identical subunits of approximately 36kDa (Shemin et al, 1974). In the case of human ALA dehydratase the holoenzyme contains four catalytic sites and can be viewed as a tetramer of dimers with one active site per dimer. Each active site binds two molecules of ALA at two distinct positions, the A-site and P-site (Shoolingin-Jordan, 1998). The ALA molecule contributing the acetate group and the amino-methyl group of PBG binds at the A-site. The ALA contributing the propionate side chain and the pyrrolic nitrogen binds at the P-site. There is an ordered binding in which the keto group of the ALA contributing the propionate side chain forms a transient covalent bond with a conserved lysine (human Lys-252) in the P-site first. Once there is bound substrate at the P-site, with an available 5-amino group, binding of the second ALA molecule onto the enzyme at the A-site may occur. The amino-nitrogen is then incorporated into the pyrrole ring of PBG.

Binding of the second substrate at the A-site is dependent on the presence of a divalent metal ion (Zn^{2+} or Mg^{2+}), and removal of these divalent ions prevent binding at the A-site resulting in loss of activity but has no effect on ALA binding at the P-site (Norton et al, 1998). Thus in mammalian systems up to a maximum of eight Zn^{2+} ions can bind onto an ALA dehydratase octamer (Wu et al, 1974; Tsukamoto et al, 1980), four being required for catalysis (at the A-site) and four not. Although the binding of the latter four metal ions at the P-site may appear non-essential they probably play a role in conformational stabilisation of the enzyme (Hasnain et al, 1985). The two metal binding sites have been specifically identified on *E. coli* ALA dehydratase and are termed the alpha and beta sites (Spencer and Jordan, 1995).

The enzyme is inhibited by lead, which is thought to stoichiometrically displace zinc atoms from the enzyme (Gibson and Goldberg, 1970; Granick et al, 1973;

Finelli et al, 1975; Tsukamoto, 1980). This enzyme is also strongly inhibited by succinylacetone - a compound, which is structurally very similar to ALA, and tends to accumulate in hereditary tyrosinaemia (Sassa et al, 1981). Succinylacetone covalently binds to one of the active site lysine residues - thus not allowing the first ALA molecule to bind to the enzyme (Erskine et al, 1999).

Two tissue-specific forms of ALA dehydratase exist which are encoded by a single gene which contains separate erythroid and housekeeping promoters and can undergo alternative splicing (Kaya et al, 1994; Bishop et al, 1996). It has been proposed that this novel expression of erythroid-specific and housekeeping transcripts apparently evolved to ensure that there is enough supply of haem for high-level tissue-specific haemoglobin production (Bishop et al, 1996).

Successful expression systems exist for *E.coli*, *Saccharomyces cerevisiae* and *Pseudomonas aeruginosa* ALA dehydratase. Ultra-pure preparations of the recombinant enzyme have yielded the protein as a crystal, sometimes suitable for X-ray diffraction (Senior et al, 1996; 1997). The crystallisation and initial X-ray characterisation of the ALA dehydratases from *E. coli* and *Saccharomyces cerevisiae* at a resolution of 2Å have been reported (Erskine et al, 1997) as well as a more detailed structural analysis at 1.67Å for *Pseudomonas aeruginosa* ALA dehydratase (Frankenberg et al, 1999).

In all cases, the best crystals were obtained when these proteins were covalently bound to laevulinic acid. The X-ray structures have confirmed that ALA dehydratase is a homo-octamer with each of its subunits adopting a "TIM" barrel fold with an N-terminal arm of 30 amino acid residues (Erskine et al, 1999). The monomers form asymmetric dimers with their "arms" wrapped around each other, and four of these dimers interact to form octamers with their active sites located on the surface.

In the *E. coli* enzyme Lys-247 (equivalent of the essential Lys-252 at the P-site in human ALA dehydratase) forms Schiff-base link with the bound laevulinic acid at the active site. This is also the case in the yeast ALA dehydratase where X-ray analysis shows the formation of a Schiff-base with Lys-263 (also equivalent to human Lys-252) (Erskine et al, 1999₂).

In contrast, structural analysis of the magnesium containing *Pseudomonas aeruginosa* ALA dehydratase reveals that in each dimer the monomers differ from one another by having a “closed” or an “open” active site pocket (Frankenberg et al, 1999). No metal ions are found in the active site of both monomers, however a single well-defined and highly hydrated Mg^{2+} was identified in the “closed” form - about 14Å away from the active site lysine. Based on this information, a structure-based mechanism of action involving allosteric binding of Mg^{2+} at the active site with rate enhancement, has been proposed (Frankenberg et al, 1999).

B. Formation of the tetrapyrrole macrocycle

3. Biosynthesis of hydroxymethylbilane by PBG Deaminase [EC 4.3.1.8] (Hydroxymethylbilane synthase)

The next reaction is the polymerization of four PBG molecules to form the linear, unstable tetrapyrrole, hydroxymethylbilane, which is catalyzed by the enzyme PBG deaminase (Kappas and Sassa, 1995). In essence, the formation of hydroxymethylbilane is initiated in the cytosol, by the assembly of four PBG molecules, via a stepwise deamination and head-to-tail polymerization by this enzyme (3rd reaction, Fig 1.2).

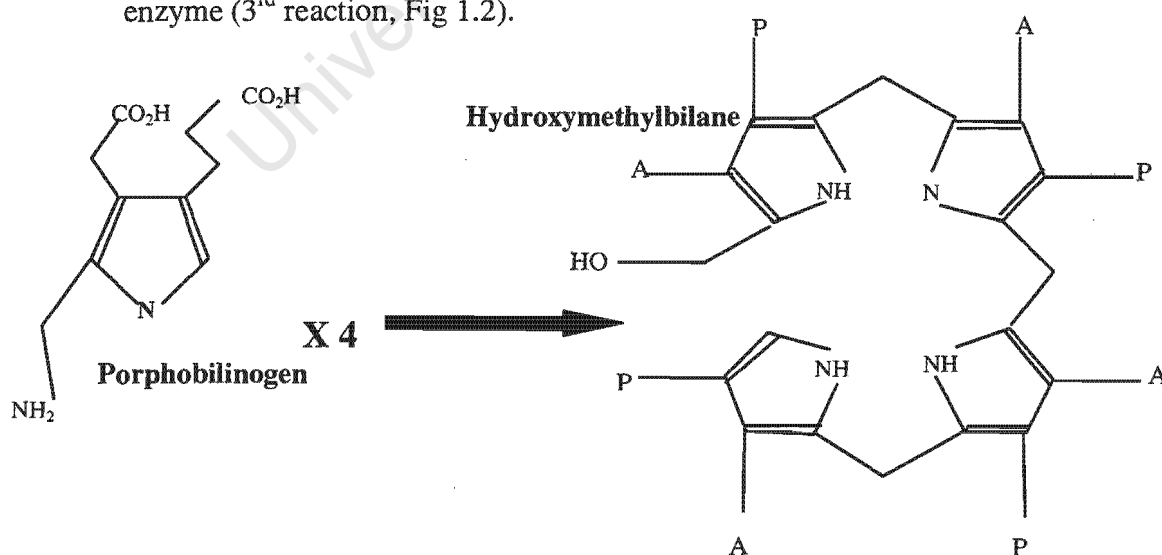


Fig 1.5 The polymerization of four ALA molecules to form an unstable linear tetrapyrrole, hydroxymethylbilane.

In the absence of the next enzyme, uroporphyrinogen III synthase, hydroxymethylbilane can be spontaneously cyclised to form the uroporphyrinogen I isomer which cannot undergo any further processing in the haem pathway. However the pair of enzymes, PBG deaminase and uroporphyrinogen III synthase work together, closely and concurrently. Because PBG deaminase is rate limiting in this pair of reactions, the enzymatic formation of the III series isomer is favored (Battersby, 1988).

PBG deaminase has been purified from a variety of pro- and eukaryotic sources (Jordan and Shemin, 1973; Anderson and Desnick, 1980; Williams et al, 1981; Corrigall et al, 1991). In humans, PBG deaminase is encoded for on the 11th chromosome at the position 11q23 (Wang et al, 1981). It is a cytosolic monomeric protein, with a molecular weight of 35 to 40 kDa (Jordan, 1990).

PBG deaminase is unique in that it contains a covalently attached dipyrromethane cofactor at the active site, which binds substrate molecules during the sequential assembly of the linear tetrapyrrole molecule (Jordan and Warren, 1987). The structure of the dipyrromethane cofactor and its sites of attachment to the enzyme have been characterised (Jordan et al, 1988; Jordan, 1990). It appears that initially the PBG deaminase apoenzyme catalyses the deamination and polymerisation of two molecules of PBG at its active site (Awan et al, 1997). The resultant dipyrrole is covalently linked via a thioether linkage to the enzyme through a conserved cysteine (*E. coli* Cys-242) (Jordan et al, 1988; Louie et al, 1996). This dipyrrolic cofactor then acts as a primer, which gets elongated in a stepwise mechanism, one PBG unit at a time, through enzyme intermediate complexes, "ES" (with one PBG attached); "ES2" (two PBGs attached); "ES3" (three PBGs attached), and finally "ES4" (four PBGs attached). The tetrapyrrole product, hydroxymethylbilane, is released by hydrolytic cleavage, from "ES4", regenerating the enzyme - leaving the dipyrromethane intact (Jordan, 1994; McNeil and Shoolinger-Jordan, 1998). Thus, the two proximal PBGs (ie. the dipyrromethane cofactor) remain covalently linked to the enzyme and are not turned over.

In mammals a single PBG deaminase gene exists - consisting of 15 exons extending over 10kb of DNA (Deybach and Puy, 1995). Two different transcripts, differing at their 5' ends, are produced from the single gene (Namba et al, 1991; Deybach and Puy, 1995). The first is a ubiquitous, "housekeeping" mRNA transcript produced in all cells in which exon 1 is spliced to exon 3. The second form is specific to erythroid cells and initiates by alternate splicing at exon 2 (Grandchamp et al, 1987). Exon 2 does not contain an AUG translation-initiating codon, and translation of the erythroid-specific mRNA is initiated at an AUG located in exon 3 (Chretien et al, 1988). Exon 1 contains an AUG, which is spliced into the same reading frame as the AUG in exon 3. Thus, translation of the "housekeeping" mRNA produces a protein that differs from the erythroid form by the absence of 17 amino acids (encoded by exon 1) at its N-terminus (Grandchamp et al, 1987).

Activation of the transcription of PBG deaminase is controlled by two separate promoters. The "housekeeping" promoter lies upstream of exon 1 and contains motifs commonly associated with "housekeeping" genes (Grandchamp et al, 1987; Chretien et al, 1988). The erythroid specific promoter lies in intron 2 and displays structural homology with the beta-globin gene promoters. It is well characterized and contains 3 classes of protein binding sites (GATA, NF-E2, and CACC), characteristic of erythroid promoters (Beaumont et al, 1989; Mignotte et al, 1989; Porcher et al, 1991). The housekeeping and erythroid promoters are independently regulated even though the housekeeping promoter contains the erythroid promoter in its transcript (Raich et al, 1989).

E. Coli PBG deaminase has been crystallized (Louie et al, 1992) and resolved to 1.76Å resolution (Louie et al, 1992; 1996). The high-resolution crystallization reveals a protein folded into three alpha/beta domains of approximately 100 amino acids each, linked by flexible strands. The flexible boundaries between the three domains, appear to allow the conformational changes necessary to accommodate each added PBG pyrrole while the tetrapyrrole, hydroxymethylbilane, is synthesized. Deamination of the PBG, and formation of the methene bridges occurs in the third domain, which contains the conserved cysteine residues and the covalently bound dipyrromethane cofactor. The

catalytic site is positioned in a deep cleft that occurs between the 1st and 2nd domains. Site-directed mutagenesis experiments have demonstrated that numerous salt bridges occur between cofactor acetate and propionate groups and arginine residues in the 1st and 2nd domains, which are important for enzyme activity (Jordan and Woodcock, 1991; Lander et al, 1991).

4. Closure of the tetrapyrrole ring by Uroporphyrinogen-III Synthase [EC 4.2.1.75] (Uroporphyrinogen Cosynthase)

Hydroxymethylbilane is then cyclized, with inversion of the D ring to form uroporphyrinogen III by uroporphyrinogen III synthase (Battersby et al, 1982₁, Battersby et al, 1982₂) (4th reaction, Fig 1.2). This inversion probably occurs via a chiral spiro intermediate (Leeper, 1994).

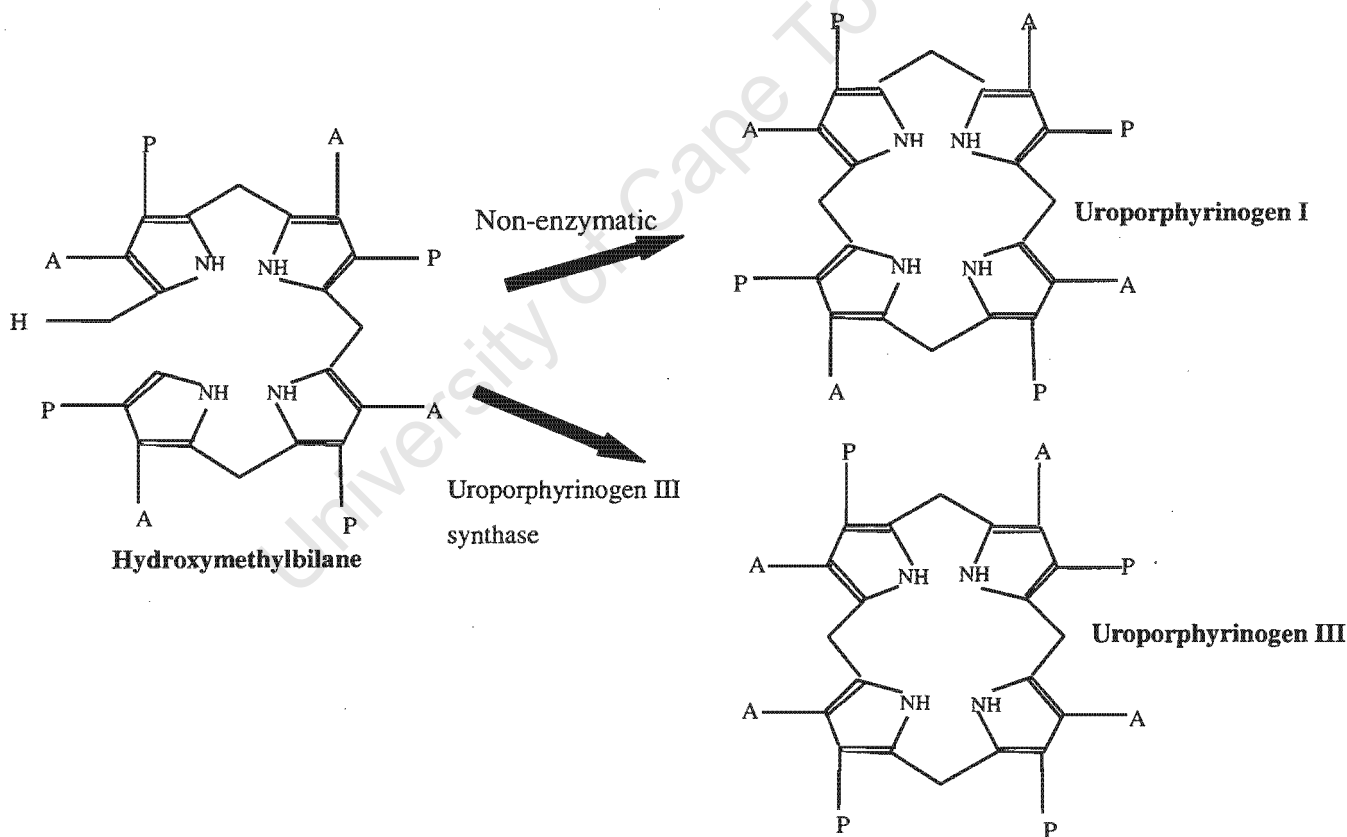


Fig 1.6 Formation of Uroporphyrinogen III, by the enzyme uroporphyrinogen III synthase and formation of Uroporphyrinogen I, by non-enzymatic closure of the ring.

Enzymatic formation of uroporphyrinogen III is rapid, which favors the formation of the III series isomer (as apposed to the non-enzymatic formation of the uroporphyrinogen I isomer). It has been shown in human erythrocytes that an excess of uroporphyrinogen synthase, relative to PBG deaminase, exists, which would favour formation of the uroporphyrinogen III isomer.

Considering the requirement for uroporphyrinogen cosynthase to act in concert with its "partner", PBG deaminase, and the fact that the two enzymes may be co-purified, it has been suggested that they may exist in a cytosolic complex (Tsai et al, 1987).

Uroporphyrin III synthase have been cloned from several bacteria and mammalian species (Stamford et al, 1995; Amillet and Labbe-Bois, 1995; Xu et al, 1995; Tsai et al, 1988; Jordan et al, 1988). Moreover it has been purified from a number of pro- and eukaryotic sources – including spinach, *Euglena gracilis*, *E.coli*, rat liver and human (Tsai et al, 1987₁; Tsai et al, 1987₂; Tsai et al, 1988; Kohashi et al, 1984; Smythe and Williams, 1988; Harts and Battersby, 1985, Alwan et al, 1989).

The human uroporphyrinogen cosynthase gene has been mapped to chromosome 10q25.3 (Astrin et al, 1991), and the cDNA expressed in *E. Coli* (Tsai et al, 1988). In both the human and mouse there are 5' and 3' untranslated regions and an open reading frame spanning 10 exons and encoding a polypeptide of 265 amino acids. The mouse gene shares an 80% nucleotide and 78% amino acid identity with that of the human gene (Xu et al, 1995).

All forms studied to date exist as monomeric subunits with molecular weights of around 30 000 Da (Jordan, 1989), which are extremely thermolabile. Because of this instability, the protein has not been well characterised. There is no evidence for a cofactor of any sort, although the enzyme is activated by sodium, potassium, magnesium and calcium ions, and inhibited by cadmium, copper, mercury and zinc ions. The human enzyme has an isoelectric point of 5.5, and a pH optimum of 7.4 (Desnick et al, 1998).

C. Modification of peripheral side chains

5. Biosynthesis of coproporphyrinogen-III by Uroporphyrinogen Decarboxylase [EC 4.1.1.37]

Following the formation of the tetrapyrrole ring, coproporphyrinogen is formed by the decarboxylation of the four acetate chains of uroporphyrinogen III, by the soluble cytoplasmic enzyme uroporphyrinogen decarboxylase. Both the I and the III isomers of uroporphyrinogen are decarboxylated, but the uroporphyrinogen III series isomer proceeds much more rapidly. The decarboxylation reaction commences on the asymmetric D ring and proceeds in a stepwise manner through rings A to C to give the heptacarboxylic, hexacarboxylic and pentacarboxylic intermediates (5th reaction, Fig1.2).

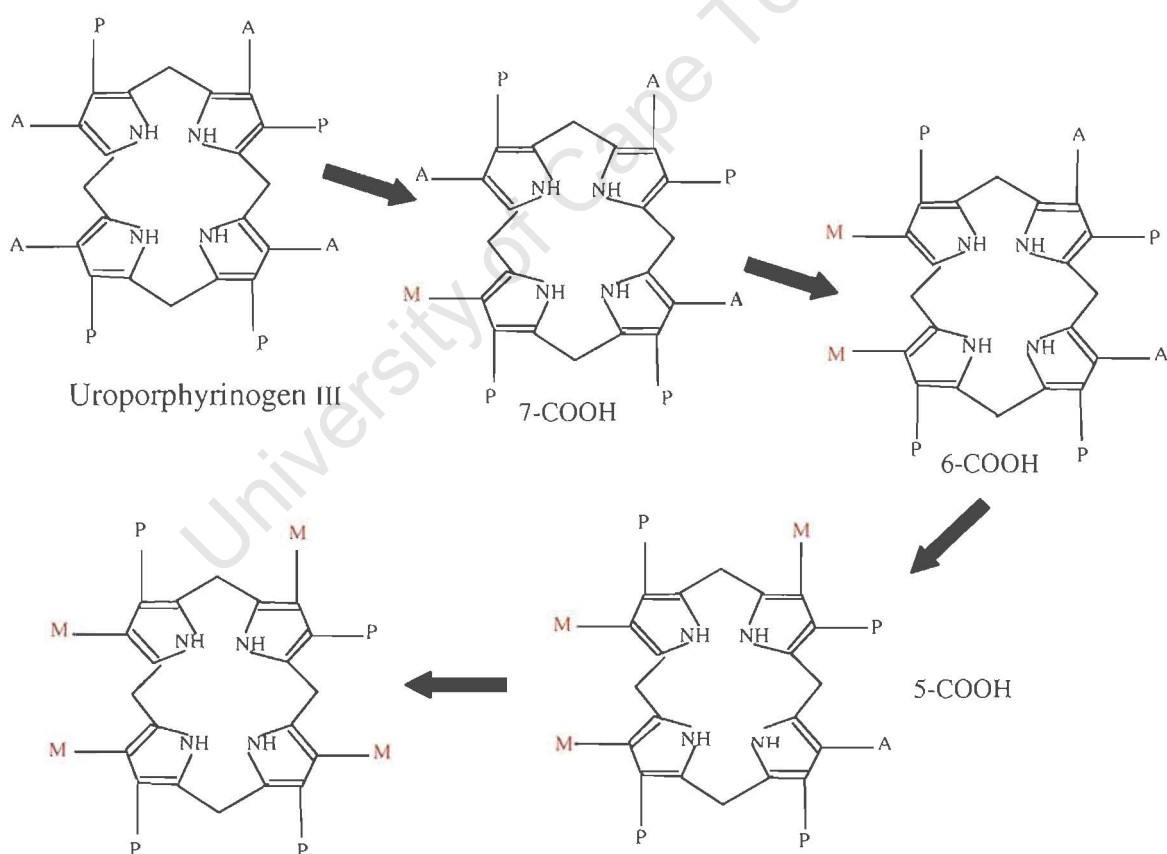


Fig 1.7 Decarboxylation of Uroporphyrinogen III including the hepta- (7-COOH), hexa- (6-COOH) and penta- (5-COOH) forms and the final product of uroporphyrinogen decarboxylase – coproporphyrinogen.

The intermediates are stable porphyrinogens that occur naturally, in detectable concentrations *in vivo*. Each intermediate acts as the substrate for further decarboxylation until the requisite coproporphyrinogen-III is formed. Both the series I and III uroporphyrinogen isomers formed, are suitable substrates for this enzyme, but the series III isomer is more rapidly decarboxylated.

Uroporphyrinogen decarboxylase has been purified from yeast (Felix et al, 1990), bovine liver (Straka et al, 1983), chick erythrocytes (Kawanashi, 1983) and human erythrocytes (de Verneil et al, 1983; Elder et al, 1983). This enzyme functions as a monomer, with a molecular mass of about 41kDa, and unlike most decarboxylases, does not appear to require a cofactor for enzymatic activity (Bernard and Akhtar, 1979). The chicken enzyme, on the other hand is reported to exist as a dimer composed of two 40 000 Da subunits (Kawanishi et al, 1983).

The cDNAs for the gene encoding this protein in humans and rat have been cloned, sequenced and characterised (Romeo et al, 1986; Romana et al, 1987a). The two uroporphyrinogen decarboxylase gene sequences are very similar with 85% and 90% homology at the DNA and protein levels, respectively. The cDNA for the mouse gene encoding this enzyme has 88% and 90% nucleotide and amino acid sequence identity, respectively, with the human enzyme (Wu et al, 1996). The isolated human uroporphyrinogen decarboxylase gene is made up of 10 exons and two transcriptional start sites were identified (Romana et al, 1987₂). The human gene encodes a 367 amino acid residues polypeptide (predicted molecular weight approximately 41 000 Da), is present as a single copy containing 10 exons within about 3 kb of DNA and has been mapped to chromosome 1p34 (de Vernueil et al, 1983; McLellen et al, 1984). Two transcriptional start sites separated by six nucleotides have been identified (Romana et al, 1987₂) but the same polyadenylation site is used in all tissues and it seems that both sites are used in the same proportion in both erythroid and nonerythroid cells. Two isoforms of this enzyme were identified in human erythrocytes, by Murkeji and Pimstone (1987).

Various inhibitor studies using sulphhydryl blockers or divalent metals such as copper, and mercury, in human uroporphyrinogen decarboxylase suggest that cysteine and histidine residues are important for enzyme activity especially free thiols and various conserved histidines, lysines and arginines (Batlle, 1986; Woods and Fowler, 1987; Elder, 1983; Straka, 1983, Whitby et al, 1998). The salt bridges that occur between the arginine residues of the enzyme and the acidic side chains of the pyrrole are involved in alignment and orientation of the substrate for catalysis (Billi de Catabbi, 1991). However, site-directed mutagenesis experiments indicate that no single cysteine is absolutely critical for the integrity of the catalytic site, as activity, in all cysteine mutants, was essentially maintained at a significant level. Three histidine mutants also retained significant enzyme activity but one (human H339N) has been identified as important in imparting isomer specificity (Wyckoff et al, 1996).

A recombinant human uroporphyrinogen decarboxylase, expressed with a histidine tag in *E. coli* for purification purposes, was crystallized and initial data collected at a 3.0Å resolution (Phillips et al, 1997; Laterriere et al, 1997). Subsequently, the crystal structure has been determined at 1.60Å resolution (Whitby et al, 1998).

The 40.8 kDa protein is comprised of a single domain containing an (beta/alpha) 8-barrel with a deep active site cleft formed by loops at the C-terminal ends of the barrel strands. Many conserved residues cluster at this cleft, including the invariant side chains of Arg37, Arg41 and His339, which probably function in substrate binding, and Asp86, Tyr164 and Ser219, which may function in either binding or catalysis. Uroporphyrinogen decarboxylase is a dimer – both in the crystallized form and when in solution. Assembly of the dimer juxtaposes the active site clefts of the monomers, suggesting a functionally important interaction between the catalytic centers.

6. Biosynthesis of protoporphyrinogen IX by Coproporphyrinogen Oxidase [EC 1.3.3.3]

At this point the synthesis of haem re-enters the mitochondria where coproporphyrinogen-III oxidase, is located in the intermembrane space and loosely associated with the inner mitochondrial membrane on the intermembrane space side (Medlock and Dailey, 1996; Martesek et al, 1997). Coproporphyrinogen-III catalyses the modification of the propionic side chains on the A and B rings of coproporphyrinogen-III to vinyl groups, by decarboxylation and oxidation (dehydrogenation) to form protoporphyrinogen-IX (6th reaction, Fig 1.2).

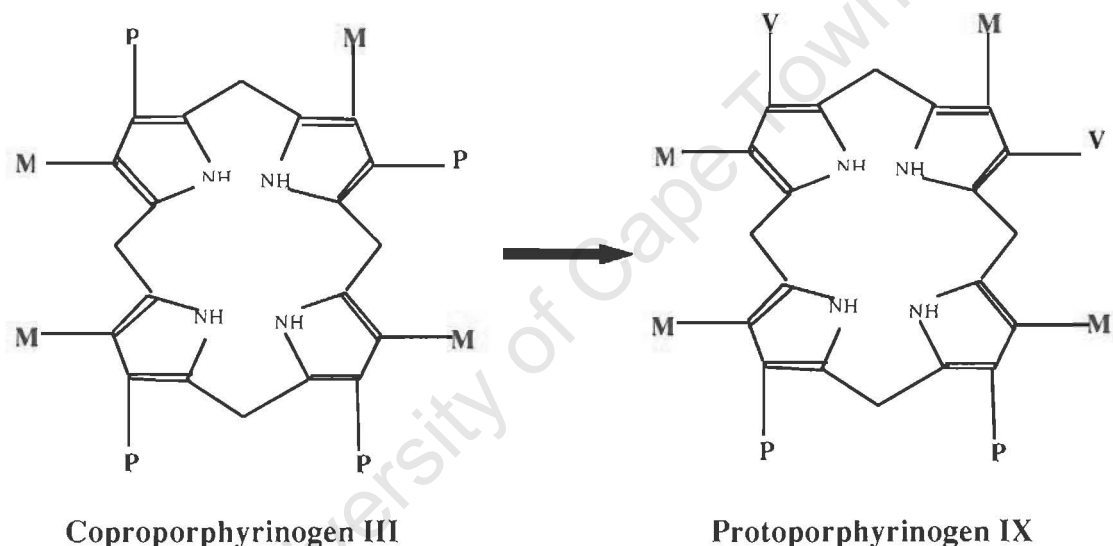


Fig 1.8 The chemical structures of coproporphyrinogen III and protoporphyrinogen IX. The oxidation of coproporphyrinogen III series, by coproporphyrinogen oxidase yields the porphyrinogen, protoporphyrinogen IX

Coproporphyrinogen oxidase does not accept the I and II isomer series of coproporphyrinogen, but does react with the III and IV series isomers (Sano and Granick, 1960; Porra and Falk, 1964; Battle et al, 1964).

In eukaryotes, this oxidative decarboxylation reaction requires molecular oxygen as the electron acceptor and generates two carbon dioxide molecules (Battle et al, 1964; Sano and Granick, 1961). The reaction commences with the decarboxylation of the 2-propionate and then proceeds to the 4-propionate. The mechanism probably involves a hydroxylation reaction that generates a β -hydroxypropionate intermediate, which is then decarboxylated and at least one protein tyrosine group(s) may be involved in this part of the catalytic mechanism (Sano, 1966; Yoshinaga and Sano, 1980).

In an alternative scheme, it has been suggested that a hydroxylation reaction does not take place, but the reaction proceeds via a hydride removal during the decarboxylation (Seehra et al, 1983). It is possible that both schemes may occur naturally depending on the nature of the organism (Dailey, 1990). Indeed, in some prokaryotes there appears to be two forms of coproporphyrinogen oxidase, based on their oxygen requirements. In the case of *Salmonella typhimurium*, two genes (the *hem N* gene and the *hem F* gene) encoding an oxygen-dependent and oxygen-independent coproporphyrinogen-III oxidase have been cloned and sequenced (Xu and Elliot, 1993; Xu and Elliot, 1994). The *hem N* gene is expressed under aerobic growing conditions and requires molecular oxygen as an electron acceptor, while the *hem F* anaerobic form of the enzyme does not require molecular oxygen, but does have a variety of cofactors.

Coproporphyrinogen oxidase has been purified from a number of sources including rat (Battle et al, 1965), bovine (Yoshinaga and Sano, 1980₁; Kohno et al, 1993) and mouse liver (Bogard et al, 1989) and *Saccharomyces cerevisiae* (Camadro et al, 1986). Although early studies reported molecular weights in the region of 70 – 80 000 Da (Battle et al, 1965; Yoshinaga and Sano, 1980₁), later studies indicate a dimeric protein consisting of approximately 35 000 Da molecular weight subunits (Camadro et al, 1986; Bogard et al, 1989; Kohno et al, 1993). cDNA data has confirmed this. It is probable that those studies reporting a higher molecular weight could have been the dimeric form of the enzyme.

The cDNA sequence of the human gene encoding coproporphyrinogen-III oxidase has been cloned, sequenced and characterised (Taketani et al, 1994; Martasek et al, 1994; Delfau-Larue et al, 1994; Medlock and Dailey, 1996).

Analysis of the cDNA and the cloned gene from a number of oxygen-dependent species as well as the N-terminal amino acid sequence from mouse liver has led workers to suggest that newly synthesised coproporphyrinogen-III oxidase has an N-terminal mitochondrial-targeting peptide, which is cleaved during transport into the mitochondria. Although the length of this leader sequence was initially proposed to be 31 amino acid residues in length (Kohno, 1993; Taketani, 1994) other workers have reported an unusually long leader sequence of 110 amino acids (Delfau-Larue et al, 1994; Martasek et al, 1994).

In humans, there appears to be a single copy of the gene with multiple transcriptional initiation sites. The human gene spans approximately 14 kilobases, and consists of seven exons and six introns (Delfau-Larue et al, 1994). This gene has been mapped to chromosome 3q12 of the human genome (Cacheux et al, 1994). Potential regulatory elements have been identified in the GC-rich promoter region (six Sp1, one CACCC and four GATA sites) and it is suggested that a single promoter may be differentially regulated in erythroid and non-erythroid tissue (Martasek et al, 1994, Taketani 1994). The gene contains two polyadenylation signals separated by 126 base pairs and it is possible that these two signals, differently utilised, may play a role in tissue-specific expression of coproporphyrinogen-III oxidase mRNA (Martasek et al, 1999). Coproporphyrinogen-III oxidase transcripts are induced during erythroid cell differentiation (Conder et al, 1991; Taketani et al, 1995).

The cDNA encoding human coproporphyrinogen oxidase gene was expressed in *E. coli* cells and purified to apparent homogeneity (Medlock and Dailey, 1996). Metal analysis of this purified protein by ultraviolet/visible spectroscopy, inductively coupled plasma atomic emission spectroscopy, and electron paramagnetic resonance spectroscopy revealed that, unlike reports in the mouse enzyme (Kohno, 1993) the human enzyme did not have a metal centre and there was no *in vitro* stimulation by either Fe²⁺ or Cu²⁺.

C. Oxidation of protoporphyrinogen IX and insertion of iron

7. Oxidation of protoporphyrinogen to protoporphyrin by Protoporphyrinogen Oxidase [EC 1.3.3.4]

The penultimate step in the haem biosynthetic pathway is the oxidation of protoporphyrinogen IX to protoporphyrin. This six-electron oxidation is catalyzed by protoporphyrinogen oxidase (7th reaction, Fig 1.2). Protoporphyrinogen oxidase is associated with the intermembrane space loosely associated with the inner mitochondrial membrane (Deybach, 1985).

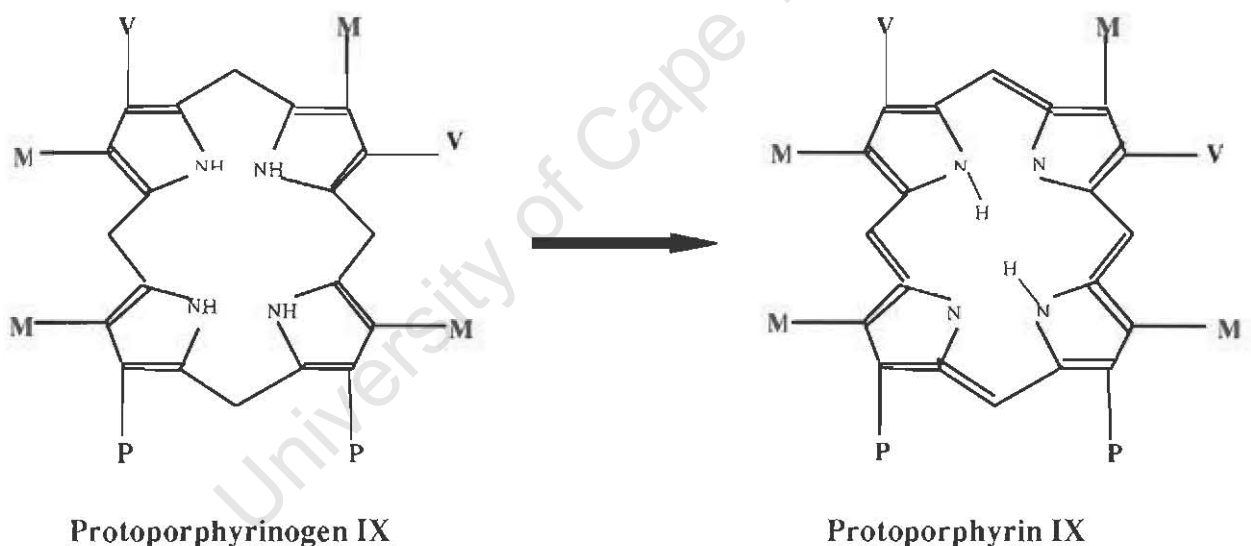


Fig 1.9 The chemical structures of **protoporphyrinogen IX** and **Protoporphyrin IX**. Protoporphyrinogen IX is oxidized, by the enzyme protoporphyrinogen oxidase to yield the porphyrin, protoporphyrin IX.

During the oxidation, the methylene bridges in protoporphyrinogen-IX are converted into methenyl bridges and protoporphyrin-IX results (Fig 1.8). The aerobic reaction utilizes molecular oxygen as the terminal electron acceptor. In prokaryotes, several alternative compounds such as nitrate, and fumarate are

utilised as the terminal electron acceptors in this reaction (Jacobs and Jacobs, 1975; 1976).

PPO has been cloned from a number of different sources, including the bacteria *Bacillus subtilis*, *Myxococcus Xanthus*, yeast (Camadro and Labbe, 1996), mouse (Dailey et al, 1995) and human (Nishimura et al, 1995). The human form of the enzyme has been localized to chromosome 1q23 (Roberts et al, 1995). The gene spans 5.5 Kb, including the 660bp of promoter region (Puy and Robreau, 1996). The enzyme is about 51kDa in size and consists of 477 amino acids. The signal sequence typically found on nuclear-encoded mitochondrial proteins is not found on PPO. The enzyme functions as a homodimer and requires FAD as a cofactor (Dailey and Dailey, 1996; Nishimura et al, 1995). During the cloning and characterisation of the *B. subtilis* cDNA sequence for PPO, Dailey et al (1994₁) identified the dinucleotide-binding domain in this PPO gene confirming association of this enzyme with flavins.

All PPO's catalyse the oxidation of protoporphyrinogen-IX into protoporphyrin-IX and many will (Jacobs and Jacobs, 1984₁; Dailey et al, 1994₁; Poulson, 1975; Dailey and Karr, 1987; Camadro et al, 1985) also oxidise the non-physiologically active, structurally similar dicarboxylic mesoporphyrinogen-IX. The *B. subtilis* enzyme is a unique exception to all the known PPO species in that, in addition to protoporphyrinogen-IX and mesoporphyrinogen-IX, it was shown to oxidise the coproporphyrinogen-III molecule (Hansson and Hederstedt, 1994; Dailey et al, 1994₁).

An interesting feature of protoporphyrinogen oxidase is the inhibition by several chemically unrelated herbicidal compounds, the most notable being the diphenyl ethers. Whilst eukaryotic protoporphyrinogen oxidases are strongly inhibited by such bicyclic compounds, these appear to have very little effect on the activity of prokaryotic enzymes such as those of *E. Coli*, *B. japonicum* (Jacobs et al, 1990) and *B. subtilis* (Dailey et al, 1994). However, once again the behaviour of the *M. xanthus* PPO, rules this out as a general prokaryotic property, because it was shown to be strongly inhibited by the diphenyl ethers (Dailey and Dailey, 1996₁).

Investigation of several PPO genes has revealed the lack of any identifiable membrane targeting signals in many of these proteins, despite finding intrinsic inner mitochondrial membrane proteins – suggesting as yet unidentified internal targeting sequences. However, a N-terminal leader sequence required for membrane targeting and translocation has been suggested in few of these proteins (Camadro et al, 1994; Narita et al, 1996; Lermontova et al, 1997).

8. Insertion of iron atom by ferrochelatase [EC 4.99.1.1]

The final step in the biosynthesis of haem is the insertion of a ferrous iron atom (Fe^{2+}) into protoporphyrin IX (Goldberg et al, 1956) (8th reaction, Fig 1.2). This is catalyzed by the enzyme ferrochelatase, which is an inner mitochondrial membrane protein (McKay et al, 1969; Jones and Jones, 1968; Harbin and Dailey, 1985).

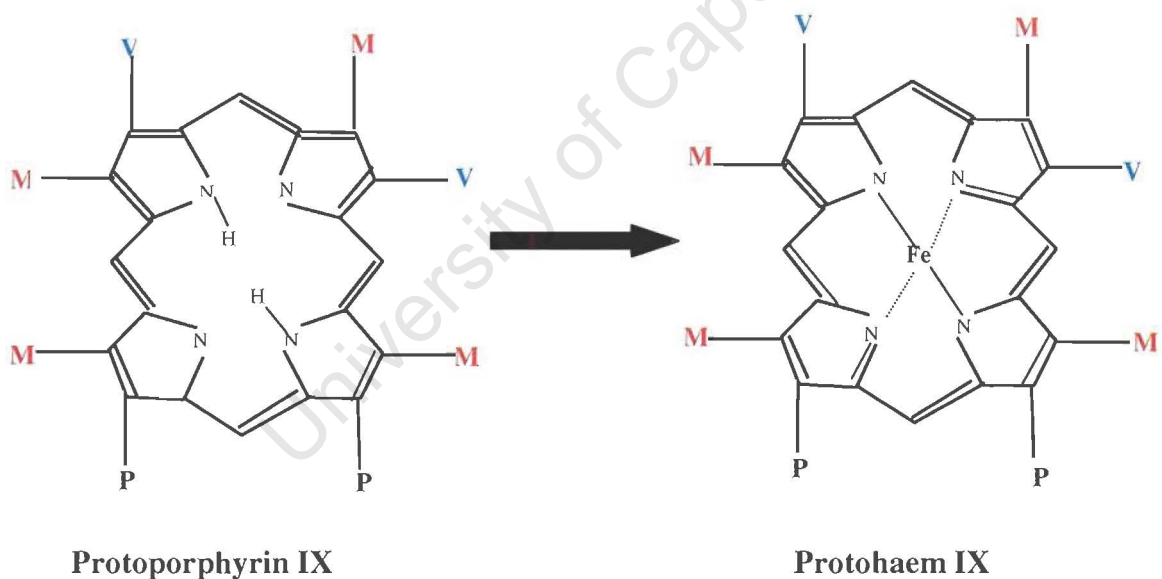


Fig 1.10 The chemical structures of protoporphyrin IX and protohaem IX. The iron atom is inserted by the enzyme ferrochelatase – the final enzyme of the haem biosynthetic pathway.

The enzyme was first purified from rat liver (Taketani and Tokunaga, 1981) and subsequently purified from bovine liver (Taketani and Tokunaga, 1982), chick

erythrocytes (Hanson and Dailey, 1984) and human liver (Matthews-Roth et al, 1987).

Ferrochelatase has also been cloned from various sources - including the bacteria *E.coli* (Miyamoto et al, 1991) *B subtilis* (Hansson and Hederstedt, 1992), *B japonicum* (Frustaci and O'Brien, 1992), yeast (Labbe-Bois, 1990), mouse (Taketani et al, 1990; Brenner and Frasier, 1991) and human (Nakahashi et al, 1990; Taketani et al, 1992). Enzymes from these sources exhibit similar properties including a subunit molecular weight of approximately 42 000 Da.

Initial characterisation of the mouse ferrochelatase gene facilitated cloning and sequencing of the human gene (Nakahashi et al, 1990). The human ferrochelatase gene was isolated from a placental cDNA library using a radio-labelled mouse cDNA fragment. This enzyme was synthesized as a 47 833 Da (423 amino acid residues) protein precursor which was modified into a smaller mature protein of 42 158 Da by cleavage of a putative leader sequence of 54 amino acid residues. Analysis of the primary sequence of this protein showed identities of 88% and 46% to the mouse and yeast ferrochelatases, respectively. Human ferrochelatase gene was subsequently mapped to chromosome 18q22 (Whitcombe et al, 1991; Taketani et al, 1992).

Analysis of the gene sequence reveals that human ferrochelatase consists of 11 exons with a minimum size of 45 Kb (Taketani et al, 1992).

The cloned mature forms of the human and mouse ferrochelatases have been expressed, purified and characterised (Dailey et al, 1994_{2, 3}). In this study the intriguing presence of a single labile iron-sulphur (2Fe-2S) cluster was demonstrated at the carboxyl end of the purified mature human ferrochelatase. By contrast, in the same study, sequence analysis of the prokaryotic, yeast, and plant ferrochelatase gene cDNAs revealed a lack of a similar putative binding site for the iron sulphur cluster.

Further investigations involving site-directed mutagenesis and spectroscopic characterisation of the human enzyme revealed that three cysteines at the carboxyl terminal; Cys-403, Cys-406 and Cys-411 (which are conserved in many of the known ferrochelatase sequences) are involved in the ligating the iron sulphur [2Fe-2S] cluster to the protein (Crouse et al, 1996). Another cysteine, Cys-196, has been identified as a fourth ligand (Sellers et al, 1998). The precise function of the iron-sulphur cluster is to be elucidated. However, its absence in bacterial and yeast ferrochelatases, suggests a regulatory role in the mammalian enzymes (Ferreira et al, 1994).

The active site is hydrophobic. Sulphydryl groups on the cysteine residues in the active site of the enzyme can be inactivated by reagents like arsenate or N-ethylmaleimide, prior to incubation of the enzyme with ferrous iron, but not afterwards. These vicinyl cysteines are required for iron binding, but not for binding of protoporphyrin (Dailey, 1984)

It is probable that the ferrous iron binds initially to the sulphydryl groups of the cysteine residues. Protoporphyrin binds after the iron. A protoporphyrin binding pocket, similar to those found in many haem-binding proteins is present. It appears that the protoporphyrin binding to the enzyme is mediated by arginine residues, which correctly align the protoporphyrin to allow insertion of the iron atom (Dailey and Fleming, 1986). This is followed by the relocation of two protons from pyrrole nitrogen's to the vicinyl cysteines, which enables the enzyme to repeat the catalytic cycle.

The murine and human ferrochelatase cDNA's have two polyadenylation signals in the 3' region. Two different sized ferrochelatase mRNA transcripts have been found in both human (Nakahashi et al, 1990) and mouse tissue (Brenner and Frasier, 1991).

The smaller mRNA transcript is produced by utilization of the 5' polyadenylation signal and this transcript is predominantly found in erythroid tissue. This is a more stable transcript and may contribute to the increased

requirement for haem in erythroid tissue. The larger, less stable transcript dominates in non-erythroid tissues (Chan et al, 1993).

The crystal structure of recombinant *B. subtilis* ferrochelatase, a water-soluble monomeric protein lacking any cofactor or [2Fe-2S] cluster, has been resolved to 1.9Å resolution by Al-Karadaghi et al (1997).

More recently the X-ray crystal structure of recombinant human ferrochelatase has been solved at 2.0 Å (Burden et al, 1999). The structure reveals that the enzyme is an 86kD homodimer that contains one [2Fe-2S] cluster per subunit. Each monomer contains 48% α helix and 14% β sheet structure and is folded into two similar domains in a fashion that typifies the periplasmic binding protein family. Two differences that exist between the two domains are - an additional 50 residues at the amino-terminal end that constitutes a portion of the active site, and a 30-residue addition at the carboxyl-terminus that participates in ligation of the [2Fe-2S] cluster and dimer stabilization. Each monomer contains an active site pocket whose entrance is composed of two hydrophobic lips.

In the homodimer, both active sites are present on the same molecular face and this surface is the largest hydrophobic region of the protein. A proposed function of this region is to serve as the site of membrane attachment. The result of such an organization is that both active sites are within the membrane proper and are in a position to accept the hydrophobic substrate – protoporphyrin - either from the hydrophobic milieu of the phospholipid bilayer or directly from the preceding pathway enzyme, protoporphyrinogen oxidase.

The active site pocket contains a majority of highly conserved residues. Key among these may be His₂₆₃. Substrate iron is probably inserted from the opposite side of the pocket from His₂₆₃. Residues involved in porphyrin macrocycle distortion remain to be unequivocally identified.

The porphyrias

Introduction

The porphyrias are a group of genetic or acquired diseases caused by partial defects in enzymes of the haem biosynthetic pathway. These enzyme defects result in partial blocking at specific steps in the pathway leading to accumulation of haem precursors generally prior to that stage of the pathway.

Under physiological circumstances, in normal individuals, due to the regulation and kinetics of the enzymes in the pathway, relatively little accumulation of intermediates occurs. However, in the porphyrias, haem precursors and/or porphyrin intermediates accumulate intra-cellularly and are thereafter excreted. Accumulation of specific haem-pathway intermediates is associated with specific enzyme deficiency, although biochemical expression of the disorder can vary considerably between individuals.

Many archaic and sometimes misleading names exist for the porphyric disorders. As biochemical knowledge and clinical expertise in the porphyria's developed, the classification was revised several times.

Gunter proposed the original classification of the porphyrias in 1911. Gunter is credited with being the first scientist in the field of porphyria to recognize that this was an inborn error of metabolism.

Slightly later classifications (in the 1950's and 1960's) were made according to in which tissue the disease was predominantly expressed. Owing to the great requirements that erythroid cells and hepatocytes have for haem, expression of the disease may be considered predominantly hepatic or erythroid, as determined by porphyrin accumulation in that particular tissue. Congenital porphyria was found to be mainly expressed in bone marrow – hence the

terminology porphyria erythropoetica, while in the remaining forms of porphyria, porphyrin over-expression appeared to be predominantly in the liver.

| Gunter (1911) | Waldenstrom (1937) | Schmidt et al (1954) | Waldenstrom (1957) | Watson (1960) | Goldberg & Rimington (1962) |
|------------------------------|--------------------------------------------------------------------------------------------------------------------------------|---------------------------------------|--------------------------------------------------------------------|-----------------------------------------------------------|------------------------------|
| Hepatoporphyria Acuta | Porphyria Acuta a) Latent b) Abdominal form c) Nervous form d) Classical form e) Comatose form commencing as b) | Intermittent Acute Type Mixed Type | Acute Intermittent Porphyria | Hereditary Acute Intermittent a) Manifest b) Latent | Acute Intermittent Porphyria |
| | | | | Hereditary Mixed or "Variegate" | |
| Hepatoporphyria Acute toxica | | | | Acquired | Acquired |
| | | | | Constitutional (PCT) | Hereditary |
| Hepatoporphyria chronica | Porphyria cutanea tarda | Cutanea Tarda Type | Porphyria Cutanea Tarda (PCT) a) Symptomatica b) Hereditaria | Hereditary Cutaneous | |
| Hepatoporphyria congenita | Porphyria Congenita | Congenital porphyria | Congenital Porphyria | Porphyria Erythropoietica (Recessive) | |

Table 1.1 Historical classifications of the porphyrias.

Current classification takes into account both the clinical presentation and the tissue in which the particular type of porphyria is predominantly expressed.

Clinical presentation of the particular porphyria also differs depending on which enzyme is defective. It is useful to divide the porphyria clinically into two main groups – the acute porphyrias and the non-acute porphyrias.

The acute porphyria's are that group in which an acute attack of porphyria can occur. This presents clinically as an acute neurovisceral crisis characterized by an ascending motor neuropathy and autonomic instability, associated with high levels of the precursors aminolevulinic acid and porphobilinogen in the plasma and urine. The acute attack will be discussed in further detail later in this section.

The accumulation of later porphyrins is characterized by a mutilating photosensitivity and skin fragility caused by the action of the sun on porphyrins, which have accumulated in the epidermis. Accumulation of aminolevulinic acid and porphobilinogen is not connected to the development of skin lesions.

| | Type of porphyria | Enzyme defect | Skin Lesions | Tissue Expression |
|------------------------------|-------------------------------|--------------------------------|---------------------|-----------------------------------|
| Acute Porphyria's | Acute Intermittent Porphyria | PBG deaminase | No Skin Lesions | Hepatic porphyria's |
| | Plumboporphyria | ALA dehydratase | Lesions | |
| | Hereditary coproporphyria | Coproporphyrinogen Oxidase | Skin Lesions | |
| | Variegate Porphyria | Protoporphyrinogen Oxidase | | |
| Non-acute Porphyria's | Familial | Uroporphyrinogen Decarboxylase | Skin Lesions | Erythropoietic Porphyria's |
| | Acquired | | | |
| | Erythropoietic protoporphyria | Ferrochelatase | | |
| | Congenital porphyria | Uroporphyrinogen Co- synthase | | |

Table 1.2 Classification of the types of porphyria according to clinical expression of the disease showing the correlation between clinical expressions with the affected enzyme.

As can be seen from the table 1.2, to date, porphyric disease because of a defect in hepatic ALA synthase has not yet been described. Theories exist as to the reason no defect in hepatic ALA synthase has been reported (May, 1995). These include suggestions that heterozygous defects of hepatic ALA synthase may not cause symptoms due to up-regulation of ALA synthase, and that perhaps homozygous mutations of ALA synthase might not be compatible with life. Indeed, a defect in the erythroid ALA synthase, which results in an X-linked sideroblastic anaemia has been described in many reports (Cox et al, 1992; Cotter et al, 1992).

It might be that a heterozygous mutation in hepatic ALA synthase does not result in clinical disease, due to the ability of ALA synthase to be induced. Furthermore it is possible that a homozygous defect in hepatic ALA synthase would cause a haem deficiency of such severity as to be incompatible with life.

The hepatic porphyrias

1. *The acute porphyrias*

The acute porphyrias are a family of diseases characterized biochemically by the accumulation of ALA and PBG (often transient) and clinically by a sudden potentially lethal presentation.

Attacks are usually precipitated by a variety of exogenous and endogenous factors like certain pharmaceuticals, fasting and steroid hormones (Kappas et al, 1989).

The acute attack is associated with overproduction of ALA and PBG (Kappas et al, 1989). The pathogenesis of the clinical presentation is not fully understood. However a double heterozygote PBG deaminase deficient mouse is now available, which may help elucidate some of the mechanisms involved (Lindberg et al, 1996). It is likely that the pathogenesis of the acute attack is

multi-factorial and many mechanisms are potentially involved without being mutually exclusive. The pathogenesis of the acute attack of porphyria will be discussed in Chapter 2, following a discussion about the regulation of the haem pathway.

The acute porphyria's can be divided into two main groups – those that present without skin lesions and those that can have skin lesions.

1. 1 Acute porphyria not associated with skin lesions

ALA dehydratase deficiency

Cause

Plumboporphyria (ALA-D deficiency porphyria) is due to an autosomal recessive defect of the second enzyme in the haem pathway, ALA dehydratase.

There are other conditions, which can result in decreased ALA dehydratase activity – hereditary tyrosinaemia and lead poisoning. Hereditary tyrosinaemia is a disease in which a genetic defect at the fumaryl-acetoacetase step in the degradation of tyrosine results in accumulation of succinyl acetone, (Lindblad et al, 1997), which is a potent inhibitor of ALA dehydratase. Neurological disturbances similar to those found in patients with ALAD deficiency porphyria, can be seen in patients with lead poisoning.

Incidence

ALA dehydratase deficiency porphyria is an extremely rare autosomal recessive disorder, resulting from a homozygous or compound heterozygous ALA dehydratase deficiency. This results in ALA dehydratase levels of <1% of normal. To date only individual case reports of the disease have been described (Sassa, 1998).

Presentation

About 40 % of patients suffering from hereditary tyrosinaemia suffer from acute attacks of porphyria. (Rank et al, 1991) and their acute attacks are managed the same as those of a patient with porphyria. To illustrate the extreme variation in presentation, Sassa (1998) discussed case reports of four patients, with differing presentations of plumboporphyria. All of these patients presented with an acute attack of porphyria. One subject had severe symptoms present from birth, and had a liver transplant aged 6. Two unrelated adolescent German males presented with acute attacks during adolescence. The fourth patient presented in his 60's with a mild attack of porphyria.

Treatment

The treatment of the acute attack of porphyria is discussed in the section dealing with acute intermittent porphyria. Patients suffering from severe frequent and recurrent acute attacks may require liver transplantation.

Acute Intermittent Porphyria (AIP)

Cause

This form of porphyria occurs as a result of an autosomal dominant defect in the third enzyme of the haem pathway, PBG deaminase (Grandchamp, 1998).

Incidence

The incidence of AIP is fairly rare and not everybody with a defect in the PBG deaminase has an acute attack of porphyria. A study looking at erythrocyte PBG deaminase deficiency in Finnish blood donors found decreased PBG deaminase activity in one donor per 500 donors (Mustajoki et al, 1992). Acute attacks of AIP are thought to occur in 1 to 2 persons per 100 000 members of the population. However there is an area in Northern Sweden where AIP is particularly prevalent and acute attacks occur in about 1 individual per 1000 of the population (Kappas et al, 1989).

Presentation

The majority of persons with a mutation in PBG deaminase, never develop clinical symptoms. It has been estimated from family studies that only 10 to 20% of persons with a mutation in PBG deaminase, suffer from clinical symptoms (Kappas et al, 1989). The majority of persons with an abnormal PBG deaminase gene, who suffer from acute attacks are women.

However, in patients who do develop symptoms, acute attacks present most commonly with abdominal pain, with associated nausea, vomiting and constipation. Other features of autonomic neuropathy are hypertension and tachycardia (Grandchamp, 1998).

Features of more severe acute attacks include a motor neuropathy – more commonly a peripheral neuropathy, but cranial nerve involvement can be present, resulting in bulbar palsy. The neuropathy can become severe enough so as to cause respiratory impairment and death. Convulsions, in part related to hyponatraemia, may be present. Without treatment, the patient can die.

Diagnosis

During an acute attack, elevated urinary excretion of ALA and PBG occurs. Immediate diagnosis of the acute attack, can be made using Erlich's reagent, which causes the urine to turn pink in the presence of porphobilinogen (Watson and Schwartz, 1941).

During the acute attack, diagnosis of AIP as opposed to another form of acute porphyria, is based on measurements of different porphyrins, in urine, plasma and stool (Bonkvosky and Barnard, 1998).

Previously measurement of PBG deaminase activity in erythrocytes was used to identify carriers of the disease. This did however result in incorrect diagnosis in up to 15 % of individuals, so this has largely been replaced by DNA analysis (Bonkovsky, 1998).

Treatment

One of the most important parts of managing patients with AIP, is prevention of the acute attack, by avoiding common precipitating factors. These include the avoidance of medication, known to precipitate acute attacks, and avoidance of caloric deprivation (Grandchamp, 1998). One aspect of management of the acute attack comprises supportive treatment – pain management, treatment of blood pressure and cardiac problems, intravenous glucose/calories, and respiratory support, if needed. Specific treatment to reverse the acute attack, consists of haem arginate infusions – which has been shown to decrease ALA synthase activity and lead to a normalization of ALA levels (Bonkovsky, 1971; Mustajoki et al, 1986).

In patients suffering from a severe, intractable acute attack, it is sometimes necessary to add infusions of tin protoporphyrin, or similar inhibitor of haem oxygenase to the treatment regimen (Dover et al, 1991). This is because, with repeated infusions of haem arginate, haem oxygenase, the enzyme responsible for degradation of haem can be induced (Cable et al, 1994).

1.2 Acute porphyria associated with skin lesions

Hereditary Coproporphyrria

Cause

Hereditary coproporphyrria (HC) occurs as a result of an autosomal dominant defect in the enzyme coproporphyrinogen oxidase (Berger and Goldberg, 1955).

Incidence

This form of porphyria is thought to be extremely rare – occurrence is much less frequent than AIP or VP. Reported incidence of AIP to VP to HC vary from 40:9:1(in Poland) to 2.4:0.75:1(in Israel) – as quoted in a review by Martasek (1998).

Presentation

70% of individuals suffering from HC never experience an acute attack of porphyria. The 30 % who suffer from acute attacks, present with similar symptoms to those described in the section discussing presentation of the acute attack in AIP. Once again, these patients are predominantly women. The commonest precipitating factor is administration of xenobiotics.

Jaundice can also be part of the presentation of the acute attack. It is thought that acute attacks are less severe, than in patients suffering from AIP – often the acute attack subsides after only one dose of haem arginate. However, deaths have occurred during the acute attack in patients with HC so careful observation and treatment are still necessary.

Photosensitivity, consisting mainly of bullous lesions on light exposed areas can also be present – and is particularly common, when jaundice occurs as part of the acute attack of porphyria.

A severe homozygous, or compound heterozygous form of the disease has been described (Grandchamp et al, 1977). This tends to present at a very young age – and presentations vary – with individuals presenting with severe hypertrichosis and skin pigmentation, haemolytic anaemia, hepatosplenomegaly. Acute attacks can (but do not necessarily) occur in these patients (Grandchamp, 1980). Activity in the homozygous/compound heterozygous patients with HC is reduced to between 2% and 10 % of normal.

Diagnosis

Diagnosis of the acute attack can be made as described in the section dealing with AIP. Once diagnosis of an acute porphyria is suspected definitive diagnosis of HC can be made by measurements of porphyrins in urine, stool and plasma. Measurements of urinary porphyrins show increases in uroporphyrin and coproporphyrin, faeces display marked increases in faecal coproporphyrin, together with more modest increases in uroporphyrin and protoporphyrin (Bonkovsky, 1998).

The diagnostic feature of HC is the presence of extremely high levels of coproporphyrinogen III in the faeces – which results in red fluorescence of the faeces when viewed under ultra-violet light (Martasek, 1998).

DNA analysis can be performed on family members to diagnose latent HC.

Treatment

Management of the acute attack of porphyria, is similar to the management of AIP, described in the previous section.

The best possible management of the skin problems, is sun avoidance. Commonly used sunscreens do not prevent photodermatitis as they only protect against the shorter UV rays – and it is the longer-length UV rays, which cause the photodermatitis found in porphyria. The only effective sun-creams are those containing zinc oxide or titanium dioxide.

Variegate Porphyria

Cause

Variegate porphyria (VP) is an autosomal dominant defect in the enzyme protoporphyrinogen oxidase (Deybach et al,1981; Siepker and Kramer, 1985).

Incidence

Worldwide, of the acute porphyria, VP probably has the largest numbers of patients, mainly due to an extra-ordinarily high incidence of the disease present in South Africans of Dutch descent. In South Africa alone, over 100 new cases are diagnosed every year (Hift et al, 1997). Cases have been reported worldwide.

Presentation

Patients often present with photodermatitis – blisters, skin erosions and eventually scarring, thickening, and hirsutism in sun-exposed regions. Hift et al (1997) report that 40% of their patients with VP present with skin lesions alone, a further 10 % present with skin lesions, but subsequently experience an acute

attack, and contrastingly only 9% of patients present initially with an acute attack of porphyria.

Acute attacks of porphyria can occur, but, in contrast to those experienced by AIP sufferers, these tend to be mainly precipitated by xenobiotics. This is similar to the experiences reported in patients with HC. It would therefore appear that the threshold for precipitation of the acute attack is not as low as in patients with AIP. When an acute attack does occur, the symptoms are similar to those found in patients with AIP.

There have been cases described of patients with a homozygous or double heterozygous abnormality in PPO. These patients present in early childhood with severe skin disease – even in non-sun exposed areas, brachydactyly, short stature, seizures, nystagmus. Half of the patients display signs of mental retardation. Rather inexplicably these patients do not appear to suffer from acute attacks of porphyria (Corrigall et al, 2000; Roberts et al, 1998; Frank et al, 1998; Roberts et al 1996; Hift et al, 1993)

Diagnosis

Previously diagnosis relied on porphyrin concentrations, measured in stool, urine and plasma. Typically, an elevated stool concentration of protoporphyrin, together with the presence of a pseudo 5-COOH-porphyrin together with elevated coproporphyrin is present. However, in latent sufferers, near-normal concentrations of protoporphyrin in the stool can make diagnosis difficult (Hift et al, 1997; Kirsch et al, 1998; Bonkovsky et al, 1998).

An easier spectrophotometric measurement of plasma, can reveal a fluorometric emission at 625nm using excitation light of 405nm, which is specific for VP. This is thought to be more sensitive than measurement of stool protoporphyrin.

The most accurate diagnosis, is screening of the PPO gene for mutations. Unfortunately as there are multiple possible mutations in the PPO, this is mainly of use in screening relatives of an affected individual, whose mutation is known.

Treatment

Management of the acute attack is as described in the section dealing with AIP. The most important aspect of management of VP is patient awareness and avoidance of precipitating factors – particularly xenobiotics, known to be porphyrinogenic.

The mainstay of treatment of skin manifestations is avoidance of sun exposure – staying out of the sun, protective clothing and use of barrier creams (zinc or titanium based creams), when exposed to sunlight.

2 The non-acute porphyrias

Cutaneous hepatic/porphyria cutanea tarda

Porphyria cutanea tarda (PCT) is caused by a decrease in activity of uroporphyrinogen decarboxylase. Unlike most of the other forms of porphyria, this is not a straightforward genetic problem. Indeed a minority of patients with PCT display a defect in the uroporphyrinogen decarboxylase gene (Elder, 1998).

The majority of patients display a decrease in uroporphyrinogen decarboxylase activity restricted to liver tissue, without an accompanying gene defect. In these individuals, PCT appears to be triggered by a variety of agents – most notably alcohol, hepatitis C, and oestrogen. Excess iron deposits in the liver, increased serum ferritin, and transferrin saturation may be present. In some patients a defect in a MHC (major histocompatibility complex) class I-like gene (the gene called the HFE gene - that found to be involved in haemochromatosis) can be found (Bonkovsky et al, 1998; Stuart et al, 1998; Bulaj et al, 2000).

Familial PCT is found in a minority of patients. The commoner form of familial PCT is an autosomal dominant defect in uroporphyrinogen decarboxylase, resulting in about 50% activity of the enzyme (Elder, 1998; Elder et al 1989). Clinical penetrance is low – less than 10%. A rarer form of a related disorder,

HEP (hepatoerythropoetic porphyria) occurs and in these patients uroporphyrinogen decarboxylase activity is less than 20 % of normal, in all tissues and patients have defects in both uroporphyrinogen genes (Roberts et al, 1995; Elder et al 1998). These gene defects are not identical to those found in the autosomal dominant form of the disease.

A fourth form of PCT is also described – namely toxic PCT, which can occur following exposure to halogenated aromatic hydrocarbons – for e.g. hexachlorobenzene and 2,3,7,8-tetrachlorodibenzo-p-dioxin. These result in inactivation of hepatic uroporphyrinogen decarboxylase. The most notable incidence of toxic PCT occurred in Turkey between 1956 and 1961, following hexachlorobenzene exposure (Cripps et al, 1984). Some patients continued to show evidence of PCT 20 years later.

Incidence

PCT has the highest prevalence of any of the porphyrias. Incidence of PCT has been reported to vary between 1:25 000/population in North America (Harber and Bickers, 1981) to >1:5000 in Czechoslovakia (Martasek et al, 1987). About 20% of cases are thought to be familial PCT (Elder, 1998).

Presentation

Patients with PCT present with skin disease, characterized by a mutilating photosensitive dermatitis. These skin lesions occur in light exposed areas and include extreme skin fragility, bullous lesions, scarring, facial hypertrichosis and hyperpigmentation.

Hepatoerythropoetic porphyria presents in early childhood with severe photosensitivity and skin lesions. The autosomal dominant form presents usually in early adulthood – perhaps at a slightly earlier age than sporadic PCT. Associated conditions, such as hepatitis C and excessive alcohol intake should be looked for.

Diagnosis

Diagnosis is made by measuring increased levels of uroporphyrin I and III and heptacarboxylic porphyrin in the urine, increased levels of plasma uroporphyrin and increased levels of heptacarboxylic porphyrin and isocoporphyrin in the stool. Levels of ALA and PBG are not increased in patients with PCT.

Treatment

In cases of familial (autosomal dominant) and sporadic PCT, therapy is based on depletion of hepatic iron stores, by phlebotomy – which leads to clinical and biochemical remission in most cases. In some patients, where phlebotomy is unsuitable, low dose oral chloroquine, helps mobilize uroporphyrin from the liver -in a uroporphyrin-chloroquine complex, which is secreted in the urine.

Phlebotomy is ineffective in patient's with HEP, therefore sun avoidance is the mainstay of treatment.

The Erythropoietic porphyrias

Congenital Erythropoietic porphyria

Cause

Congenital erythropoietic porphyria (CEP) occurs due to an autosomal recessive disorder of the enzyme, uroporphyrinogen III synthase (Kappas et al, 1995).

Incidence

This is an extremely rare form of porphyria and to date only about 300 cases have been described (Desnick et al, 1998).

Presentation

Presentation varies depending on the severity of the uroporphyrinogen III synthase deficiency. The severest cases may present at/before birth with

hydrops foetalis, due to severe haemolytic anaemia in utero. Other cases present in early childhood, with photosensitivity dermatitis and haemolytic anaemia, which varies in severity. The mildest cases may present only with skin lesions in adulthood. The more severe cases appear to have the lowest uroporphyrinogen III synthase activity, but exposure to ultraviolet light also plays a role in severity of clinical expression of disease.

Haemolytic anaemia is the result of porphyrin overproduction in the developing erythroblast, resulting in dysmorphic nuclei. Ineffective erythropoiesis as well as peripheral haemolysis are present.

The haemolytic anaemia presents with anaemia accompanied by features of haemolysis – including splenomegaly. Peripheral blood smear shows anisocytosis, poikilocytosis, polychromasia, basophilic stippling, and increased numbers of reticulocytes. Resultant splenomegaly adds to the anaemia and can result in thrombocytopenia and neutropenia.

The skin lesions typically present with increased fragility and blistering in sun-exposed areas, with associated thickening of skin, hypertrichosis of the face and extremities and areas of hypo- or hyperpigmentation. Scarring and secondary infection lead to deformities of nose, ears, eyelids and fingers. Urinary excretion of large amounts of porphyrin can manifest as pink to purple staining of diapers. Accumulation of porphyrins in the teeth can produce a reddish brown colour in natural light (erythrodontia) and fluorescence in long wave ultra-violet light.

Diagnosis

Uroporphyrin I and coproporphyrin I accumulate in bone marrow, erythrocytes and plasma. Increased levels of uroporphyrin I and coproporphyrin I can be measured in urine, and stools contain increased levels of coproporphyrin I, as well as the intermediate 7-, 6-, and 5-carboxylate porphyrins (Eriksen and Eriksen, 1997). Small increases in type III isomers can also be detected. ALA and PBG levels are not increased.

Treatment

Avoidance of sun exposure and careful management of even minor skin trauma is important, in reducing scarring and preventing deformity.

Blood transfusions can be therapeutic in mild cases, where erythropoiesis can be suppressed, and porphyrin production therefore decreased. At puberty, further suppression of erythropoiesis, using hydroxyurea, may be necessary (Guarini et al, 1994; Desnick et al, 1998).

Bone marrow transplant has been performed in a few cases, and results in decreased porphyrin levels and abrogation of the haemolytic anaemia and photosensitivity (Shaw et al, 2001; Harada et al, 2001; Tezcan et al, 1998; Thomas et al, 1996).

Erythropoietic protoporphyria

Cause:

Erythropoietic protoporphyria (EPP) is thought to result from an autosomal dominant defect in the enzyme ferrochelatase. However, more recently, it would appear, that more profound deficiency of ferrochelatase is present in patients with clinical disease, thus suggesting a second functional defect in the non-affected ferrochelatase gene (Gouya et al, 1999; Gouya et al 1996). Moreover, some patients with severe EPP have been shown to have double heterozygote mutations in both ferrochelatase genes (Rufenacht et al, 1998).

Incidence

EPP is a very rare form of porphyria. One study (Went and Klasen, 1984), in the Netherlands uncovered a total of 200 patients with EPP in 91 families. A review (Todd 1998), cited 24 different mutations published, in 27 unrelated families.

Presentation

Presentation is often in infancy with severe photosensitivity manifested by erythema, oedema when exposed to sunlight, for even short periods. Vesicles, bullae and skin fragility - common in other forms of porphyria, are uncommon.

Chronic skin changes include pigmentation and lichenification of the skin (particularly the hands), together with shallow pitted scars on the nose and cheeks with leathery pseudovesicles over the nose and hands.

A mild hypochromic microcytic anaemia may be present.

In some patients, abnormalities of the biliary tract and liver may be present (Gross et al, 1998; Doss and Frank, 1989). About 10 % of patients have gallstones (predominantly consisting of precipitated protoporphyrin). Mild increases in transaminases, alkaline and alkaline phosphatase and gamma-glutamyl transpeptidase occur in 20% of patients. Some of these patients may develop cirrhosis over time and in a few patients, disease progresses to liver failure (Gross et al, 1998).

In a minority of patients, a very severe, rapidly progressive liver failure, associated with increased photosensitivity and cholestasis can occur (Sarkany and Cox, 1995; Mion et al, 1992; Gross et al, 1998). This is accompanied by severe upper abdominal pain, splenomegaly and haemolysis. Without transplant, the clinical course is usually fulminant. In some of these patients, with severe end-stage disease with cholestasis, neurological manifestations, similar to those found in an acute attack of porphyria may occur (Rank et al, 1993). These manifestations also occur particularly after transplant surgery (Herbert et al, 1991). The pathophysiology has not yet been elucidated.

Diagnosis

Diagnosis is made by measurement of vastly increased levels of protoporphyrin in stool and erythrocytes (Bonkovsky and Barnard, 1998). ALA and PBG levels are not increased in EPP. Fluorescence can be detected in plasma, showing characteristic excitation maxima of 409 nm and emission maxima at 636 nm (de Salamanca et al, 1993).

Treatment.

Photosensitivity is treated by avoidance of exposure to visible light – including visible light of green and violet wavelength (in the 400nm region). Beta-

carotene has been used for treatment of the skin photosensitivity, but clinical efficacy in controlled trials has not been proven (Todd, 1994).

Blood transfusions and haematin infusions have been used to suppress erythropoiesis. Complete plasmapheresis has been used to decrease circulating protoporphyrin. Excretion of protoporphyrin in bile is promoted using oral charcoal and cholestyramine (Pimstone et al, 1987; Avner and Berekson, 1982; McCullough et al, 1988).

Fifteen liver transplants have been reported in patients with rapidly deteriorating liver functions. Gross et al (1998) have reported their experiences doing transplants on 8 patients with severe liver disease and EPP. EPP patients have unique problems, during and post liver transplant, including tissue damage, due to operating theatre lights (Bloomer et al, 1996). Patients are not cured of protoporphyria, as the erythroblasts still provide a source of excess protoporphyrin. Ideally bone marrow transplant, prior to liver transplant should be performed (Cox et al, 1998). As yet, this has not been performed, because the disease is not yet sufficiently well understood, to predict which patients might be at risk of fulminant liver failure, and therefore, the risks associated with bone marrow transplant are difficult to justify.

Perhaps promising for future therapy in patients with EPP is a recent report (Pawliuk et al, 1999) of the definitive cure of a mouse model of EPP using haematopoietic stem cells transduced with a polycistronic retrovirus expressing human ferrochelatase.

Summary

In this chapter we have looked at the complex pathway involved in the biosynthesis of haem. In eukaryotes, eight enzymes, four of which are mitochondrial are involved in the biosynthesis of the haem molecule.

Disorders related to each of the enzymes has been described. A defect in a particular enzyme leads to a distinct clinical picture.

We are studying ALA synthase, the rate-determining enzyme in the haem pathway. It would appear to play a major role in the regulation of haem biosynthesis. As yet, we have no explanation why induction of ALA synthase occurs in some forms of porphyria, but not in others.

In chapter 2 we will be looking at ALA synthase and the regulation of haem biosynthesis, and at possible pathogenetic mechanisms for the acute attack of porphyria.

University of Cape Town

Chapter Two

Literature Review: The role of ALAS in Haem Biosynthesis

As mentioned in the previous chapter, in animal cells the haem pathway proceeds with the condensation of succinyl CoA (from the citric acid cycle) and glycine to form ALA, by the enzyme ALA synthase. Early work by Shemin and co-workers (1945, 1955) was performed using both [¹⁵N] and [¹⁴C] labeled glycine. They established that the α -carbon and nitrogen, but not the carboxyl carbon are incorporated into haem. They then performed labeling experiments with [¹⁴C], and were able to demonstrate that the remaining carbon atoms in haem are derived from succinyl CoA.

The glycine and succinyl CoA condense to form the molecule 2-amino, 3-keto-adipic acid that is then decarboxylated to form ALA (Shemin and Russell, 1955). The [¹⁴C]-ALA that was chemically synthesized was proved to be incorporated into haem by whole cells (Shemin and Russel, 1953).

The molecular basis for the formation of ALA, is that glycine forms a stable Schiff-base carbanion linkage with the pyridoxal-5'-phosphate on the ALA synthase protein. The succinyl CoA has an electrophilic carbonyl group on the succinate, which reacts with the glycine molecule, forming the intermediate α -amino- β -keto-adipic acid, which is decarboxylated to form ALA (Ferreira et al, 1993).

ALA synthase, which catalyses the formation of ALA is the first committed enzyme in the haem pathway. It is a homo-dimer (Jordan, 1991), present in the mitochondrial matrix, loosely associated with the inner mitochondrial membrane (Scotto et al, 1983). Each sub-unit has a molecular weight of about 56kDa. Pyridoxal-5'-phosphate is required as a co-factor.

In mammalian systems two isoforms, encoded for on different chromosomes and differing in their regulation, have been cloned (Bishop, 1990). The erythroid isoform is only found in red blood cells, while the housekeeping or hepatic form is found in all other cells.

The hepatic or ubiquitous form was first cloned from livers of chick embryos (Borthwick et al, 1985), and subsequently the rat and human cDNA's were cloned (Yamamoto et al, 1988; Bishop, 1990). Erythroid ALA synthase was first cloned in chickens, and later from mice, human and rats (Riddle et al, 1989; Schoenhaut and Curtis, 1989; Bishop et al, 1990). In addition 2 isoforms of ALA synthase (HemA and HemT) were isolated from *Rhodobacter sphaeroides* (Bolt et al, 1999).

In humans the erythroid isoform is encoded for on the X chromosome and the hepatic form is encoded for on the 3rd chromosome (Bishop, 1990).

Amino-acid sequence alignment suggests the presence of a well-conserved carboxyl terminus and a less well conserved amino terminus with a high degree of homology between bacterial, yeast, avian and mammalian proteins. In eukaryotic cells the amino-terminus is not present in the mature mitochondrial enzyme and is likely to be a pre-sequence which directs the enzyme to the mitochondrion and which may also have a regulatory role (Urban-Grimal et al, 1986; Hayashi et al, 1976; Hayashi et al, 1983).

More recently, further detailed information about the reaction mechanism has been gained from studies on a murine erythroid form of ALA synthase, which was hyper-expressed and purified from *E.Coli* (Ferreira, 1993). In this model, the pyridoxal-5'-phosphate cofactor formed a Schiff-base linkage with an ϵ -amino group of a conserved lysine residue (Lys³¹³) in the enzyme (Ferreira, 1993; Neame and Dailey, 1993). When the conserved lysine was replaced with other amino acids (alanine, histidine or glycine) the cofactor still bound to the mutant enzymes non-covalently, but catalytic activity was abolished (Ferreira et al, 1995).

Further studies by Ferreira and coworkers (Ferreira et al, 1995) have revealed that a glycine-rich loop, GAGAGG is highly conserved between different species and a similar loop is found in many pyridoxal-5'-phosphate requiring enzymes. Site-directed mutants were constructed. In the functional mutants the 1st and 2nd glycine (G¹⁴² and G¹⁴⁴) residues could only be substituted with the amino acid, alanine. In addition, functional mutants all contained an arginine in position 149. The functional mutants showed decreased activity compared to the wild-type ALA synthase, in particular showing a decreased V_{max} (6-83fold lower) and generally showing an increased K_m for glycine (4-10 fold) and a slightly increased K_m for succinyl CoA (1.4 to 6 fold greater than in wild type ALA synthase).

In vivo studies were performed to generate heterodimers from catalytically inactive mutants of mouse erythroid ALA synthase. These were transformed into *E.Coli hemA*- strains, which require exogenous ALA or active ALA synthase for growth. Remarkably, a *hemA*- strain in which two catalytically inactive ALA synthase mutants (R149A and K313A) were co-expressed was able to grow – thus indicating the presence of catalytically active ALA synthase. This heterodimer was purified and the K_m values and enzyme activities were calculated, and ALA synthase activity, was measured. K_m values for the substrates were found to be similar to that found in wild type ALA synthase, and activity measured was 26% of that found in wild-type ALA synthase.

In addition, four catalytically inactive *Saccharomyces cerevisiae* ALA synthase mutants were studied. Once again, some of the mutant heterodimers exhibited enzymatic complementation (i.e. showed some activity when measured in tandem). Taken together, these experiments provided compelling evidence that the ALA synthase active site is located at the subunit interface and that catalytically essential residues were provided by each subunit (Tan and Ferreira, 1996).

Regulation of haem biosynthesis in higher vertebrates

All cells have a requirement for haem – to a greater or lesser extent. Demand for haem within a particular cell can vary greatly. For example in hepatocytes, sudden exposure to a xenobiotic or potential toxin can occur that requires an oxidation or a hydroxylation reaction for elimination of the substance. This would increase the requirement for a haem-containing cytochrome P-450 enzyme.

Haem in excess however, is potentially toxic to cells and when interacting with molecular oxygen it can catalyze oxygen radical formation, damaging proteins and lipids (Balla and Vercellotti et al, 1991; Muller-Eberhard and Fraig, 1993).

As the first committed step in the haem pathway is the formation of ALA by the ALA synthase and as this is the enzyme at lowest concentration in the haem biosynthetic pathway in both liver and erythroid cells (Bottomley and Muller-Eberhard, 1988), it is a likely site for regulation of the haem pathway.

In erythroid progenitor cells, the hormone erythropoietin is the primary stimulus for proliferation and differentiation of cells to form erythroblasts. With differentiation, there is a large increase in transcription and translation of the genes encoding enzymes in the haem pathway (Busfield et al, 1995). However the increase in ALA synthase is less than that in the other enzymes and in this situation ALA synthase continues to be rate determining.

In hepatocytes a variety of xenobiotics induce ALA synthase activity, which supplies the additional haem required by the xenobiotic induced cytochrome P-450's. However, the other enzymes in the haem pathway are not inducible, and do not appear to be rate limiting, even when ALA synthase activity is induced.

A comparison of housekeeping and erythroid ALA synthase sequences.

The hepatic or ubiquitous form was first cloned from drug-induced livers of chick embryos (Borthwick et al, 1985), and subsequently the rat and human cDNA's were cloned (Yamamoto et al, 1988; Bishop, 1990).

Erythroid ALA synthase was first cloned in chickens, and later from mice, human and rats (Riddle et al 1989; Schoenhaut and Curtis, 1989; Bishop et al, 1990). The erythroid form of ALA synthase has been purified from rat reticulocytes (Munakata, et al, 1993), while the murine form of erythroid ALA synthase has been hyper-expressed and purified in *E.coli* (Ferreira and Dailey, 1993).

The hepatic and erythroid ALA synthase isozymes display extensive amino acid homology in the C-terminus, as do the bacterial, avian, and other mammalian enzymes.

While the mitochondrial signal sequences from housekeeping ALA synthase are greater than 80% identical in chick, mouse, rat and human, they have little identity with the erythroid ALA synthase mitochondrial targeting sequences - about only 24% identity (Lathrop and Timko, 1993).

This difference between the two sequences probably reflects important regulatory mechanisms governing uptake of enzyme into the mitochondria, which differ in the two isoforms, and these are not yet completely understood.

Hepatic ALA synthase *** MESVRRCPFLSRVPQAFLOKAGK** SLLFYA
Erythroid ALA synthase MVTAAMLLQCCPVLARGPTSLLGKVVKTHQFLFGI

QNC**PK**MMEVGAKPAPRALSTAAVHY**Q**QIKETPPASEKD**K**TAKAKVQQTPDGSQQSP
GRCPILATQG*****LATQGPNC**S**QI*****HLKAT**K**AGGDS*****

DGTQLPSGHPLPATSQGTA SK**CP**FLAAQMNQRGSSVFC**K**ASL**KL**QEDVQEMNAVRK
*****SWAKGH**CP**FLSELDQDGKSKIV**Q**KAAP**KV**QEDV**K**AFK**T**DL*

EVAETSAG**PS***V**V**SVKTDGGDPSGL**L**KN**F***QDIMQ**K**Q**R**PERV**S**HLLQDN**L**PKSVST
*******PS**SLV**S**S*****L**R**KPFSGPQE**Q**EQI**S**GKV**T**HL**I**QNN**M**PG***N**YV

FQYDR**F**FE**K** **K**IDE**K**KNDHTY**R**V**F**K**T**V**N**RR **A**HIF**P**MADDY**S**DSLIT**K**K**Q**VS**V**WCS**N**
FS**Y**D**Q**FFR**D**K**I**ME**K**K**Q**DHTY**R**V**F**K**T**V**N**RWAD**A**Y**P**FA**Q**H**F**SEAS**V**ASK**D**VS**V**WCS**N**

DY**L**G**M**SR**H**PR**V**CG**A**VMD**T**L**K**Q**H**GAGAG**G**TR**N**IS**G**T**S**K**F**H**V**DLER**E**L**A**D**L**H**G**K**D**
DY**L**G**M**SR**H**P**Q**VL**Q**AT**Q**E**T**L**Q**R**H**GAGAG**G**TR**N**IS**G**T**S**K**F**H**V**E**L**E**Q**E**L**A**E** **L**H**Q**K**D**

AALL**F**SS**C**FB**V**AND**S**T**L**FT**L**AK**M**MP**G**CEI**Y**SD**S**GN**H**AS**M**I**Q**G**I**R**N**SR**V**P**K**Y**I**FR**H**N
SALL**F**SS**C**FB**V**AND**S**T**L**FT**L**AK**I**L**P**G**C**EI**Y**SD**A**GN**H**AS**M**I**Q**G**I**R**N**SG**A**AK**F**V**F**FR**H**N

DV**S**HL**R**ELL**Q**RS**D**PS**V**PK**I**V**A**F**E**T**V**H**S**MD**G**AV**C**PLE**E**L**C**D**V**A**H**E**F**GA**I**TF**V**DE**V**H
DPD**H**L**K**KL**L**E**K**SN**P**K**I**PK**I**V**A**F**E**T**V**H**S**MD**G**A**I**CP**L**E**E**L**C**D**V**SH**Q**Y**G**AL**T**F**V**DE**V**H

AV**G**LY**G**ARG**G**G**I**G**D**RD**G**V**M**PK**M**DI**S**GT**L**G**K**AF**G**CV**G**GY**I**AST**S**SL**I**DT**V**RS**Y**A
AV**G**LY**G**SR**G**AG**I**GER**D**G**I**M**H**K**I**DI**S**GT**L**G**K**AF**G**CV**G**GY**I**AST**R**DL**V**DM**V**RS**Y**A

AGF**I**TT**S**L**P**PM**L**LAG**A**LES**V**RI**L**K**G**A**E**GR**V**L**R**R**Q**H**Q**R**N**V**K**LM**R**Q**M**LM**D**AG**L**P
AGF**I**TT**S**L**P**PM**V**LS**G**ALES**V**RL**L**K**G**E**E**G**Q**AL**R**RA**H**Q**R**N**V**K**H**M**R**Q**L**LM**D**R**G**LP

VV**H**CP**S**HI**P**VR**V**AD**A**AK**N**TE**V**CE**L**MS**R**HN**I**Y**V**Q**A**IN**Y**PT**V**PR**G**E**L**L**R**I**A**PT**P**HH
IV**P**CP**S**HI**P**I**R**VG**N**AAL**N**SK**L**CD**L**LL**S**K**H**GI**Y**V**Q**AIN**Y**PT**V**PR**G**E**L**L**R**L**A**PS**P**HH

TP**Q**MM**N**Y**F**LEN**L**L**V**T**W**K**Q**V**G**LE**L**K**P**H**S**SA**E**C**N**FC**R**R**P**L**H**F**E**VM**S**ER**E**K**S**Y**F**S**G**L
SP**Q**MM**E**D**F**VE**K**LL**L**AW**T**AV**G**L**P**L**Q**D**V**SV**A**AC**N**FC**R**R**P**V**H**F**E**LM**S**E**W**ERS**Y**F**G**N**M**

SK**L*****V**S**A**Q**A**
GP**Q**Y**V**TT**Y**A

Fig 2.1 Alignment of the amino acid sequences of erythroid and hepatic ALA synthase. Hepatic and erythroid ALA synthase amino acid sequences are represented in 1 letter amino acid form, and presented aligned with the erythroid sequence below the hepatic. Homologous amino acids have been highlighted.

Studies looking at expression of both hepatic and erythroid ALA synthase, in murine erythroleukaemia cells have demonstrated differences in regulation of hepatic and erythroid ALA synthase (Fujita et al, 1991) that suggest the isozymes are under separate controls.

The proposed cleavage site of the amino-terminus of the housekeeping form of the enzyme has been deduced from the purified chicken mature and pre-enzyme forms of ALA synthase. Here a 56 amino acid pre-sequence is cleaved between 2 glutamine residues (Cox et al, 1991). The amino-terminus in erythroid cells is cleaved between a serine and glutamine residue (May BK, 1995). The mature housekeeping mitochondrial protein is therefore predicted to have a molecular weight of 65kDa and the erythroid mature protein, 60kDa.

The exon-intron organization has been determined for the chicken and rat hepatic and for the chicken, mouse and human erythroid isoforms of ALA synthase (Schoenhaut and Curtis, 1989; Maguire and Day; Yomogida et al, 1993; Lim et al, 1994; Conboy et al 1991).

The arrangement of introns and exons is conserved between erythroid and housekeeping genes –viz. exon 2 of the human form (exon 1 of chicken ALA synthase) corresponds to the mitochondrial signal sequence, while exons 5 to 11 (4-10 of chicken ALA synthase) corresponds to the catalytic domain of the enzyme. This implies the existence of a common ancestral gene that underwent duplication and translocation (May, 1995).

The regulation of erythroid ALA synthase

The production of haem and globin in erythroid cells is intimately associated with erythroid cell differentiation. Committed erythroid progenitor cells undergo differentiation and proliferation, (see Fig. 2.2 below). The end product of this is the anucleated mature erythrocyte circulating in the blood.

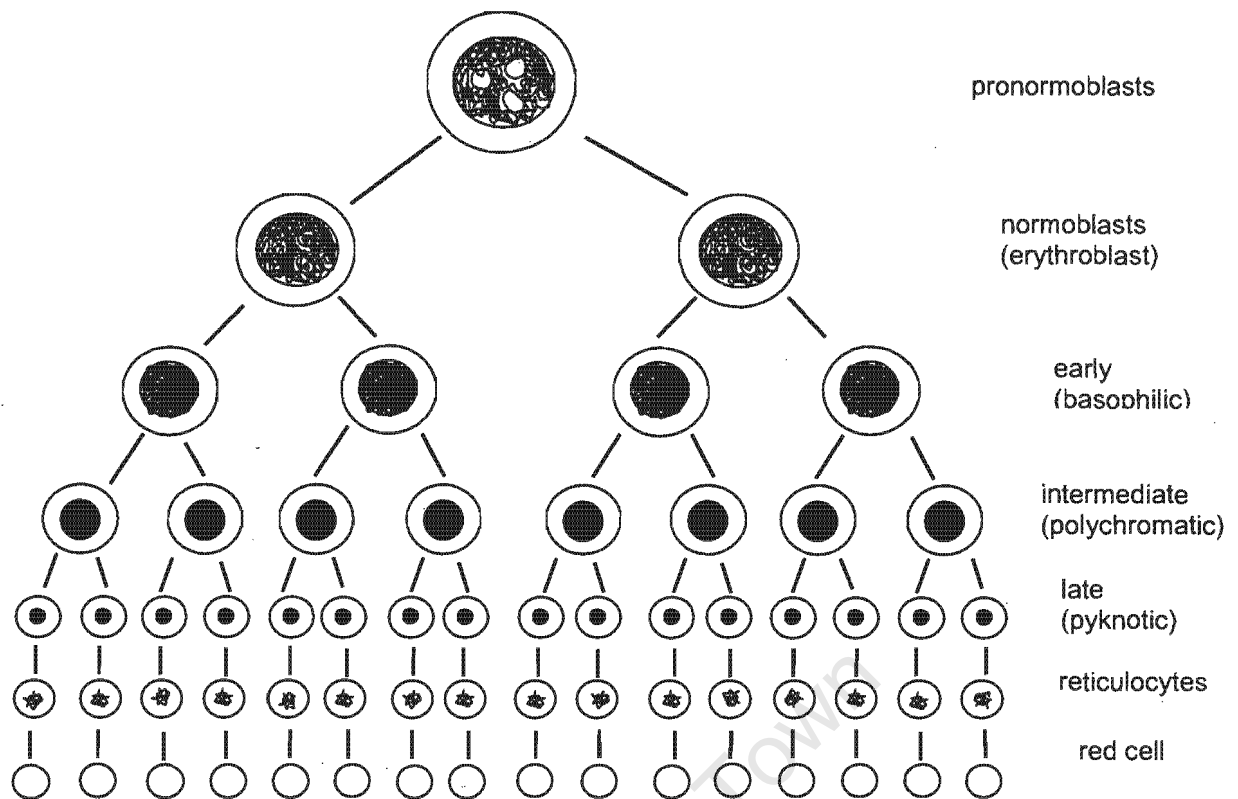


Fig 2.2 Diagram illustrating amplification and maturation sequences of the development of red blood cells from the pronormoblasts (Hoffbrand and Petit, 1984)

The process of erythropoiesis is stimulated by a haemopoetic growth factor, erythropoietin, which is specific for erythroid progenitor stem cells (Krantz, 1991). The earliest precursor cells, the burst forming unit erythroid cells (BFU's) differentiate and proliferate into the colony forming unit erythroid cells (CFU's), which are morphologically recognizable pro-normoblasts.

Expression of erythropoietin receptors commences in the BFU stage, reaches maximal amount in the CFU stages and thereafter declines (Broudy et al, 1991). The CFU proerythroblasts give rise to erythroblasts, in which maximal amounts of haemoglobin are produced. Following this, the nucleus of the cell is extruded.

However, the resulting reticulocytes continue to produce haemoglobin for a short while, after which time they lose the remaining ribosomes and mitochondria, and become mature circulating erythrocytes (May BK et al, 1995). The level of erythroid ALA synthase is markedly increased by the

presence of erythropoietin in the erythroblasts. Moreover, the erythroid ALA synthase promoter closely resembles the globin promoter - containing many of the same erythroid specific motifs (Cox et al, 1991).

Research work using JE2 and MEL cells has shown increases in transcription of most of the haem pathway genes during erythroid cell development (Fujita et al, 1991; Grandchamp et al, 1985; Kohno et al, 1993; Busfield et al, 1993). It is not yet established at which period during erythroid cell differentiation the transcription of haem biosynthetic genes is maximally increased, and whether or not the increased transcription is co-ordinated between enzymes in the biosynthetic pathway.

ALA dehydratase, while being encoded for on the same gene in erythroid and non-erythroid tissues, has separate housekeeping and erythroid specific promoters (Kaya et al, 1994). However the erythroid and hepatic isozymes are identical, the only difference occurring in the 5'untranslated region of the mRNA.

The third enzyme in the haem pathway, PBG deaminase, as previously mentioned in chapter one, exists in two different isozymes, which differ at the N-terminal sequence. The erythroid PBG deaminase mRNA contains erythroid specific promoters that are not present in the housekeeping form (Chretien et al, 1988; Mignotte et al, 1989₁).

The coproporphyrinogen oxidase and ferrochelatase genes appear to have promoter elements that contain both recognized erythroid and housekeeping motifs (Taketani et al, 1992).

Co-ordination of haem and globin synthesis with iron balance is also important to the erythroid cells. In addition to being potentially toxic, free iron is relatively insoluble and requires iron-binding proteins for its transportation and storage (May et al, 1995). Erythroid cells have the greatest requirement for iron in the body, accounting for 70% of total iron in the body - thus availability of sufficient iron and regulation of iron is important in haemoglobin synthesis.

In mammals, transferrin is the major iron-binding protein in serum and iron is delivered to cells as an iron-transferrin complex. Once intracellular, this iron is complexed with protoporphyrin, as haem and stored in ferritin shells (Klausner et al, 1993).

There are differences in regulation of iron homeostasis between erythroid and non-erythroid cells. In non-erythroid cells iron homeostasis is maintained by coordination between transferrin receptor and ferritin expression – in the presence of abundant iron, transferrin receptor levels decrease and ferritin levels increase, which results in a decrease in the uptake of intracellular iron, and promotes sequestering of excess intracellular iron. In iron shortage, the opposite occurs (Klausner et al, 1993; Theil, 1990). The mechanisms for this process are largely post-transcriptional, and are modulated by an iron-responsive-element (IRE). These are conserved sequences of 28 nucleotides that occur either in the 5' or 3' untranslated regions of the mRNA (Klausner et al, 1993).

The IRE forms a stable hairpin loop and is capable of interacting with a group of proteins called the iron-regulatory-element binding protein (IRE-BP). In the presence of low iron concentrations, the IRE-BP adopts a conformation that allows strong binding to an IRE.

This IRE is present in the 5'-untranslated region of the ferritin and the 3'-untranslated region of the transferrin mRNA. When bound to the 5' region of the ferritin mRNA, translation of ferritin is inhibited. When the IRE-BP binds to the IRE of the transferrin receptor mRNA, it prevents nuclease binding and increases the stability of the mRNA. This results in increased translation of the transferrin receptor protein (Klausner et al, 1993). One of the mechanisms thought to be operative is that in the presence of sufficient iron the IRE-BP is able to assemble an iron-sulfur cluster, which prevents binding to the IRE's (Hirling et al, 1991; Philpott et al, 1993).

In erythroid cell differentiation, an increase in transcription of transferrin receptors appears to be the predominant regulatory mechanism. The transferring

gene promoter contains an erythroid active element, that stimulates receptor gene transcription (Lok and Ponka, 2000). There is also evidence to suggest that there is increased transcription of the ferritin gene in addition to post-transcriptional regulation by iron. Moreover experiments performed using Friend erythro-leukaemia cells induced to erythroid differentiation (using DMSO), it was demonstrated that uptake of iron from transferrin limited and controlled haem synthesis (Laskey et al, 1986). Formation of haem in erythroid cells is therefore dependent on cellular availability of iron, and this is an important factor in the regulation of erythroid ALA synthase.

The 5'-untranslated region of erythroid ALA synthase consists almost entirely of an IRE structure similar to that found in the transferrin and ferritin mRNA's. This 52 nucleotide IRE is highly conserved in mouse, chick and human erythroid ALA synthase mRNA, and is not found in the housekeeping ALA synthase or any other haem biosynthetic enzyme mRNA. The binding of an IRE-BP inhibits translation of erythroid ALA synthase (Melefors et al, 1993; Gray and Hentze, 1994; Dandekar et al, 1991; Hentze and Caugham, 1987). In addition to the two specific RNA binding proteins, (IRP1 and 2) which have been described, it has been demonstrated that ferrochelatase, which contains an iron-sulfur cluster is able to exhibit IRE-BP activity and is able to bind to the IRE of erythroid ALA synthase (Ferriera, 1995).

A model has been proposed for the regulation of erythroid ALA synthase in differentiating erythroid cells (May, 1995). It suggests that, in response to erythropoietin, transcription of the erythroid ALA synthase gene and other genes of the haem biosynthetic pathway enzymes increase. Iron is transported into erythroid cells via the transferrin receptor and forms a pool of free and ferritin-bound iron. Erythroid cells appear unable to mobilize ferritin iron for haem synthesis and the presence of ferritin is probably to protect against toxicity of iron (Adams et al, 1993). Erythroid ALA synthase is translated if the level of free intra-cellular iron is sufficient to inhibit binding of the IRE-BP to the IRE of ALA synthase. When ALA synthase activity is increased, in keeping with the rate-limiting role of ALA synthase in the haem pathway, the production

of protoporphyrin is increased, and iron is inserted into the protoporphyrin molecule forming haem.

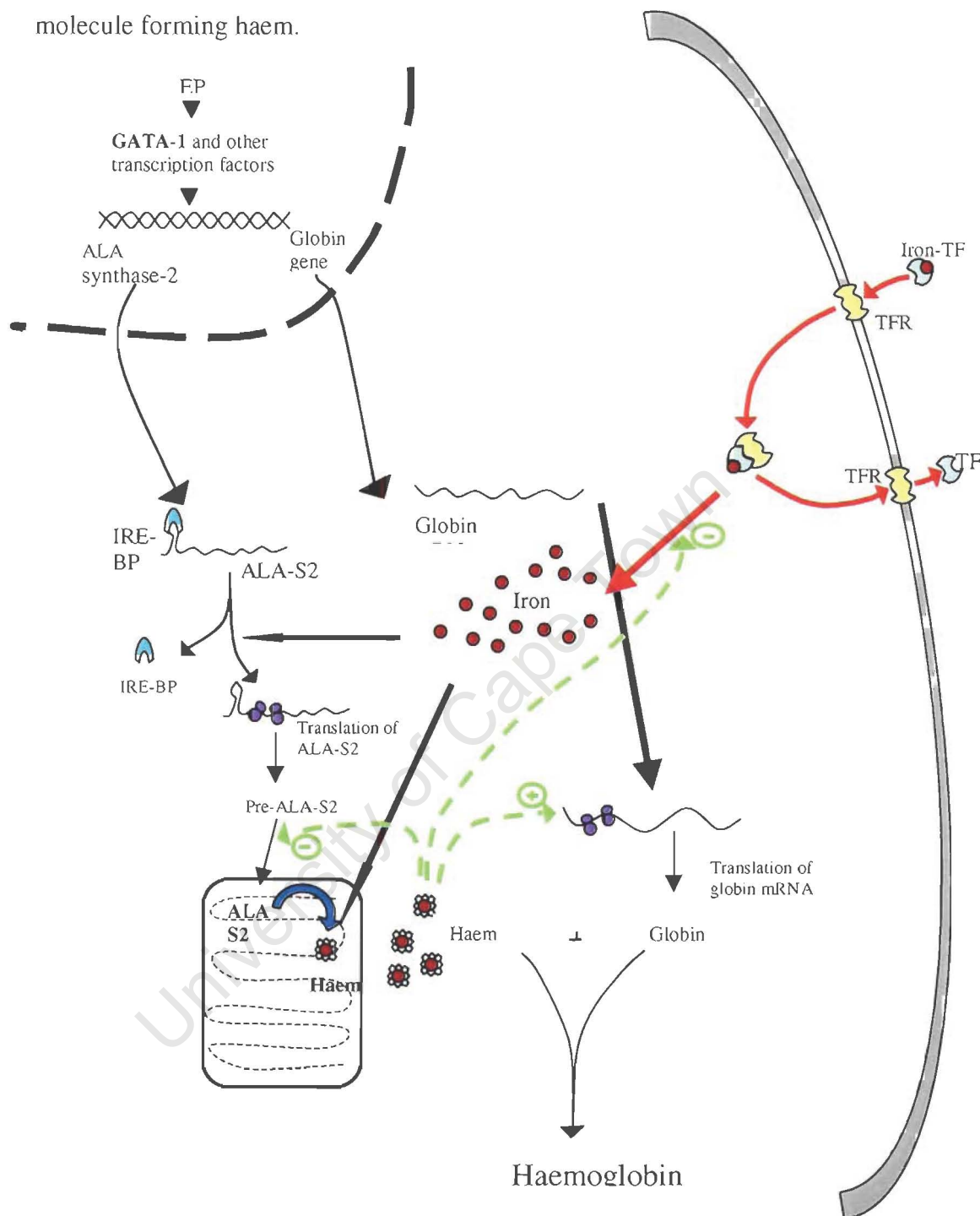


Fig 2.3 Proposed model for regulation of erythroid ALA synthase and globin mRNA in erythroid cells (May, 1995). The iron pool regulates translation of ALA-S2 via the iron-response element binding protein, while the cytosolic haem pool is proposed to act on translation of globin mRNA, while negatively regulating the synthesis of haem. The key to abbreviations used in the figure is as follows: ALA-S2 - Erythroid ALA synthase; TF- transferrin; TFR- transferrin receptor; IRE-BP – iron responsive element binding protein.

In states of iron deficiency, the regulation of erythroid ALA synthase activity ensures that large accumulations of protoporphyrin do not take place. In differentiating erythrocytes haem does not appear to have any effect on transcription or translation of erythroid ALA synthase. There is some evidence to suggest that haem can inhibit translocation of ALA synthase into the mitochondria (Lathrop and Timko, 1993), which may be of importance in co-ordinating haem and globin production.

The translation of globin genes is well co-ordinated with the supply of haem. In states of iron and hence haem deficiency, a haem regulated inhibitor kinase (HRI) in erythroid cells is activated and prevents translation of globin mRNA. In the presence of sufficient haem, HRI is inhibited, by binding of haem, which acts by catalyzing inter-subunit disulphide bond formation, resulting in dimer subunit inactivation.

The regulation of housekeeping ALA synthase

Housekeeping ALA synthase mRNA has been detected in small amounts in numerous rat tissues e.g. adrenal gland, heart, small intestine, brain and liver. Highest levels of ALA synthase mRNA occurs in adrenal gland, testis, liver and kidney. These results probably vary with the species, age, sex of the animal and with exposure to xenobiotics (Srivastava et al, 1993).

Regulatory sequences have been identified in the rat ALA synthase gene. These are present in the promoter region (up to -479 bp) and in the first intron of the ALA synthase gene. These include a TATA box and two motifs which are homologous to the binding site for the transcription factor, nuclear respiratory factor 1 (NRF-1), which is present in the promoter regions of many nuclear encoded mitochondrial proteins, particularly those concerned with oxidative phosphorylation (e.g. cytochrome c, γ -ATP synthase). This may indicate some coordination of mitochondrial haem supply with some of the respiratory chain subunits. Generally, housekeeping genes that contain this class of promoters are highly regulated, having tissue-specific promoters.

In contrast, the genes for ALA dehydratase, PBG deaminase, uroporphyrinogen-III decarboxylase, and ferrochelatase do not contain these promoters. Their promoters are GC rich, lack a TATA box and contain multiple Sp1 binding sites – which reinforces the evidence that these are differently regulated from the rate determining ALA synthase.

Haem regulates its own synthesis by controlling the amount of ALA synthase present using several mechanisms. These vary between species and may differ depending on the stimulus inducing ALA synthase.

The initial studies were performed in chick embryo livers cell cultures, using a variety of xenobiotics (Granick 1966; Whiting and Granick, 1976). These xenobiotics, which included AIA (allylisoisopropylacetamide) and DDC (3,5-diethoxycarbonyl-1,4-dihydrocollidine), resulted in increased ALA synthase activity. Metabolic labeling of protein and immuno-precipitation studies showed that the increase in enzyme activity was due to increased synthesis of ALA synthase protein and not due to activation of pre-formed protein. Moreover, Whiting and Granick (1976) found that there was an increase in immunologically detectable ALA synthase protein in the mitochondria, which was proportional to the increase in enzyme activity. It was also demonstrated that administration of haem prevented this increase in ALA synthase activity.

The induction of ALA synthase by xenobiotics was also noted to be tissue specific. In rats, AIA and Phenobarbital increased ALA synthase mRNA in liver and kidney (Srivastava et al, 1988), but not in other tissues.

Kurashima et al (1970) were the first to demonstrate that haem inhibited translocation of the ALA synthase pre-enzyme into the mitochondria. Ades (1983), performed metabolic labeling experiments using chicken embryo hepatocyte cultures and [S^{35}]-labeled methionine. He was able to confirm that haemin blocked the processing of precursor ALA synthase in AIA treated chicken embryo hepatocytes. Shortly afterwards, Srivastava et al (1983) were able to show that haemin prevented the transfer of the drug-induced ALA

synthase precursor into the mitochondria, and that this effect was specific for ALA synthase.

Other studies looking at the mechanism of xenobiotic induction and haemin repression of chick embryo ALA synthase, established that AIA increased the concentration of ALA synthase mRNA (Ades and Harpe, 1981) and that haemin decreased this mRNA concentration (Drew and Ades, 1986). When they studied ALA synthase mRNA while using α -amanitin to block transcription of ALA synthase, they noted that addition of haemin to the cell culture resulted in a decrease in the half-life of ALA synthase, and proposed that while the mechanism of AIA induction of ALA synthase mRNA appeared to be as a result of increased transcription of ALA synthase, haemin decreased the half-life of the mRNA.

As the chicken embryo ALA synthase mRNA does not contain (A+U)-rich sequences in the 3' untranslated region (like similarly regulated mRNA's where mRNA half-life is important in regulation of the protein), the effect of haemin on the mRNA stability is still being investigated (May et al, 1995). It was also observed that the addition of a translational blocker, cycloheximide to AIA treated chicken hepatocytes, resulted in further induction of ALA synthase mRNA (Ryan and Ades, 1989; Hamilton et al 1988). This effect was also seen with the translational inhibitor, ricin (Ryan and Ades, 1991). Hamilton (1988) proposed the existence of a labile repressor protein, which inhibited ALA synthase transcription.

However, when α -amanitin was added to hepatocyte cultures following AIA induction of ALA synthase, and cycloheximide was added several hours later, ALA synthase mRNA appeared to be increased compared to controls not containing cycloheximide. This led to the proposal that the stability of ALA synthase mRNA may be inhibited by binding of a labile protein. However, in contrast, nuclear run-off assays performed by Dogra et al (1993), using chick livers from embryo's treated with Phenobarbital and cycloheximide have established that the changes in ALA synthase mRNA appear to be

predominantly due to changes in the rate of transcription of the ALA synthase gene. The mechanism of drug induction of ALA synthase remains elusive, although it was recently found that a tyrosine kinase inhibitor prevented the induction of ALA synthase (Dogra and May, 1996).

It would appear that there are differences in the regulation of the avian and mammalian forms of ALA synthase. Studies performed in a rat hepatocyte system (Srivastava et al, 1988; Yamamoto et al, 1988) found that the regulation of ALA synthase by haemin appears to be at the transcriptional level, rather than at the level of mRNA stability. AIA and Phenobarbital also appeared to induce ALA synthase at transcriptional level. A study by Yamamoto et al (1983) using a cell free rabbit reticulate lysate system and polysomes from AIA treated rats, suggested that protein synthesis appeared to be inhibited by the addition of haemin, and that specifically, this effect appeared to be at the peptide elongation step.

Furthermore, as in the avian system, haemin inhibits translocation of the pre-ALA synthase into the mitochondria (Yamauchi et al, 1980). This regulation is mediated via the conserved haem- regulatory Cys-Pro motifs found in the amino-terminus of the enzyme (Lathrop and Timko, 1993).

Many of the xenobiotics that induce ALA synthase activity are inducers of one or more specific cytochrome P450's. The cytochrome P450s induced are those involved in oxidation or hydroxylation reactions in the smooth endoplasmic reticulum of hepatocytes. The induction of ALA synthase is postulated to occur in order to provide haem for the cytochrome p450. Many studies have been performed to try and deduce the mechanism for xenobiotic induction of ALA synthase and a variety of cytochrome P450's. These studies have also tried to see if the induction of the cytochrome P450 and ALA synthase are related.

When chick embryo's or rats are treated with xenobiotics e.g. Phenobarbital or AIA, the rate of transcription of ALA synthase is increased (Srivastava et al, 1988; Hansen et al 1989; Dogra et al, 1993). Haemin administration prevents the xenobiotic induction of ALA synthase activity. In the original studies in a

chick embryo system, (Hamilton et al, 1988), looked at the effect of Phenobarbital and AIA on ALA synthase and a Phenobarbital-inducible cytochrome P450 (CYP-PB).

The experiments showed rapid and simultaneous induction of the mRNA's for ALA synthase and CYP-PB. This did not agree with the previously proposed models in which the depletion of the haem pool by increased cytochrome P450 resulted in an induction of ALA synthase activity. Moreover treatment with cycloheximide did not prevent the induction of ALA synthase but resulted in even greater induction than was seen with xenobiotics alone. While haemin completely suppressed ALA synthase activity, mRNA amount was reduced only by 50%. Of note is that in the presence of cycloheximide, the repression of ALA synthase mRNA by haem was prevented.

Further studies by Hamilton, et al (1992) and Dogra, et al (1992) confirmed the increases in mRNA for ALA synthase and CYP450_{2H1/2} in chick embryo systems in the presence of Phenobarbital-like xenobiotics and inhibitors of protein synthesis. Transcription run-off assays (Dogra et al, 1992) showed that these changes in mRNA were predominantly due to changes in the rate of transcription of these genes. Furthermore, the fact that the induction can proceed with almost complete inhibition of protein synthesis points to the presence of a labile repressor protein, which may be involved in expression of these genes. Once again it was shown that xenobiotic induction of ALA synthase does not require the concomitant synthesis of a P450 apoprotein.

Studies looking at the effect of haemin on xenobiotic-induced ALA synthase activity have shown differences compared to the avian system. Haemin administration to rats can completely inhibit the xenobiotic induction of ALA synthase and this effect appears to be at the level of transcription of the gene (Srivastava et al, 1988).

Sinclair et al (1990) further examined the role of haem in regulation of ALA synthase and cytochrome P450's in rats using rat hepatocyte cultures. Phenobarbital increased the amount and activity of cytochrome P450 IIB1/2,

ALA synthase mRNA and ALA synthase activity. Treatment of the hepatocytes with succinyl acetone increased the mRNA for ALA synthase and several cytochrome P450's. However, while ALA synthase activity was increased after treatment of hepatocytes with succinyl acetone, the amount of various cytochrome p450 proteins was reduced, as was the cytochrome P450 activity. The decrease in cytochrome P450 protein may be due to the fact that haem appears to maintain the catalytically active structure of cytochrome P-450 and increases the efficiency of incorporation of cytochrome P450 into lipid membranes, by altering the secondary structure of the cytochrome P450 (Uvarov et al, 1990).

Although in Sinclair, et al's study (1990), the availability of haem was decreased after treatment of the hepatocytes with succinyl acetone, this did not have an effect on the xenobiotic induced induction of the cytochrome P450 transcription. Sinclair et al (1990) showed that induction of cytochrome P450 is independent of haem status in the intact rat hepatocyte. In addition, administration of inhibitors of haem biosynthesis (e.g. succinyl acetone) to rats, in the absence of xenobiotics only a small increase in ALA synthase transcription is observed, implying that there might be a xenobiotic-mediated transcription factor involved in induction of ALA synthase activity (May et al, 1995).

The induction of ALA synthase by xenobiotics is quite heterogenous. However, considerable progress is being made in elucidating the mechanisms of cytochrome P450 induction. Different cytochromes P450's are induced by different xenobiotics and the mechanisms of induction appear to differ as well (Waxman and Azaroff, 1992). For example, induction of the human cytochrome P450 1A2 by 3-methylcholanthrene appears to be mediated by stabilization of the mRNA and increased translation of the P450 1A2, while the induction of the 3A series of cytochrome P450's by macrolide antibiotics appears to involve protein stabilization. The induction of the P450 2B by phenobarbital in rat hepatocytes appears to be due to increased transcription of the corresponding genes. Other genes induced by phenobarbital e.g. epoxide hydrolase, NADPH: P450- reductase, glutathione S-transferase, fibrinogen beta-chain and gamma-

chain, apolipoprotein B (Fruch et al, 1997) - although induced at the level of transcription, appear to differ in response to phenobarbital, suggesting that different genes may be regulated quite differently in response to the same stimulus. The planar polyhalogenated or polycyclic aromatic hydrocarbons while inducing some of the cytochrome p450 isozymes result in uroporphyrinogen decarboxylase inhibition – which depletes the free haem pool (Marks, 1988).

Heterocyclic compounds similar to 3,5,-diethoxycarbonyl-1,4,-dihydro-2,4,6-trimethylpyridine, and compounds containing a terminal olefinic or acetylenic group, cause mechanism-based inactivation of cytochrome P-450, with resultant destruction of the haem moiety – increasing demand for haem (Marks et al, 1988).

Adding to the complexity of understanding the mechanisms of cytochrome P450 induction by xenobiotics are the studies looking at the effect of cycloheximide in induction of a variety of cytochrome P450's. In a rat hepatocyte system, cycloheximide appears to block the usual phenobarbital – induced accumulation of P4502B mRNA, but it appears to increase P4503A mRNA. As previously discussed, the regulation of cytochrome P450 in avian systems differs from that in mammalian systems. Although some progress has been made in looking at cytochrome P450 metabolism in humans, little has been conclusively proven about the regulation of cytochrome P450 and haem biosynthesis in humans. In addition to the ethical problems associated with obtaining human tissues, there are technical problems with long-term hepatocyte cultures (Ryan et al, 1993).

However over the last few years, there has been some progress at looking at cytochrome P450 vaccinia transfected hepatoma cell lines (Gonzalez, 1993). Moreover, progress has also been made at uncovering which cytochromeP450's are responsible for metabolism of which particular xenobiotics using hyper-expressed cytochrome P450's in lymphoblast cell lines (Crespi et al, 1991; Birkett et al, 1993; Crespi et al, 1993₁; Crespi et al, 1993₂).

In summary though, the important points are that haem biosynthesis is tightly regulated – partly owing to the potential for intracellular toxicity of excess haem (although the toxicity is counter-acted by induction of haem oxygenase and subsequent conversion of haem to bilirubin [May, 1995]) and to sudden needs for increased haem. Mechanisms of regulation of haem biosynthesis appear to differ in mammalian and avian livers as well as in different tissues in the same animal.

The role of ALA in the pathogenesis of the acute attack of porphyria

The acute porphyrias consist of the porphyria's mentioned in the previous chapter, together with the condition called hereditary tyrosinaemia – an inborn error of metabolism resulting in the accumulation of succinyl acetone, which inhibits the enzyme ALA dehydratase, which can have a presentation similar to plumboporphyria (ALA dehydratase deficiency porphyria) and lead poisoning, which can present with neurological symptoms similar to those found in plumboporphyria.

As previously mentioned, this group of porphyrias has the potential for presenting as an acute attack of porphyria. This refers to the life-threatening neurovisceral crises that intermittently occur and which are clinically manifest by a motor neuropathy (causing symmetrical weakness), autonomic instability (e.g. causing BP fluctuations, hypertension, tachycardia, abdominal pain), and sensory problems (e.g. parasthesia, dysasthesia). In addition, two of the acute forms of porphyria can present with skin lesion – viz. variegate porphyria and hereditary coproporphyria. The acute attack is always associated with increased levels of ALA and PBG in serum and urine.

Treatment is supportive plus the administration of haem, which leads to a decrease in ALA and PBG levels and improvement in symptoms. Supportive medical treatment may involve for e.g. ventilation if paralysis of respiratory

muscles occurs, treatment of metabolic disturbances like hyponatraemia, control of blood pressure fluctuations, carbohydrate supplementation.

Often attacks are precipitated by a variety of exogenous and endogenous factors e.g. xenobiotics like pharmaceutical medications, fasting, steroid hormones. According to Kirsch et al (1998) there are differences in the acute attack in patients with VP and AIP. In patients with VP males and females are equally likely to have an acute attack – in contrast to AIP in which the acute attack appears to be more common in young women. In addition, recurrence of an acute attack is much rarer in VP compared to AIP. Moreover in VP acute attacks are rarely, if ever seen in response to endogenous factors for e.g. secondary to menstrual cycle – indeed they are most commonly precipitated by xenobiotics. In terms of treatment of the acute attack, patients with AIP appear to need treatment with haem arginate with much greater frequency compared to patients with VP. Although the acute attack is associated with overproduction of ALA and PBG, the pathogenesis of the clinical presentation is not fully understood. It is likely that the pathogenesis of the acute attack is multi-factorial and many mechanisms are potentially involved without being mutually exclusive. Some of the proposed pathogenetic mechanisms will be discussed below.

Common pathological findings are patchy demyelination of peripheral nerves and axonal degeneration. Further findings are loss of neurons and chromatolysis of cells in the anterior horn of the spinal cord, as well as chromatolysis in neurons of brain stem nuclei – particularly the dorsal vagal nucleus and ganglia of the autonomic nervous system (Bonkovsky et al, 1982; Cavanagh and Mellick, 1965; Meyer et al, 1998).

Direct neurotoxicity of ALA

One proposed mechanism is direct neurotoxicity of ALA. Percy et al (1979) were able to show non-saturable uptake of ALA into primary cultures on neurons and glial cells. Although ALA administered to volunteers has not been associated with symptoms of acute porphyria (Dowdle et al, 1968), ALA

concentrations as low as 2×10^{-5} M caused reversible misfiring of electrically stimulated neurons in crayfish neuro-muscular preparations (Bonkovsky et al, 1982). In addition concentrations as low as 10^{-5} M caused the death of culture chick embryo neuronal and glial cells (Percy et al, 1981). A more recent study in 1998 (Abdul-Razzak and Bagust, 1998) demonstrated that ALA applied to rat spinal cord, in concentrations from 1 - 1000 μ M, resulted in decreased spontaneous activity in lumbar dorsal roots and decreased amplitude of the monosynaptic component on the ventral root reflex.

However these effects have not been demonstrated in human spinal cord neurons *in vitro* (Gorchein, 1989). Moreover *in vivo* studies in rodents have failed to produce any symptoms suggestive of an acute attack of porphyria (Edwards et al, 1984₁; Edwards et al, 1984₂). Percy and Shanley (1977) investigated CSF from 4 VP patients, during an acute attack. Levels of ALA in the CSF, were well below levels in plasma, and much lower than concentrations of ALA shown to exert effects *in vivo*.

Shanley et al (1975) were able to show uptake by rat brain of C_{14} -ALA, during intraventricular injection of ALA. Brain uptake of ALA following intraperitoneal or subcutaneous injection of C_{14} -ALA, even in nephrectomized rats which had sustained elevated blood levels of ALA, was extremely low. However in the rats receiving intraventricular injections of ALA, uptake of ALA was greater in the hypothalamus, than in other areas.

There have been numerous attempts to get an *in vitro* model, simulating the effects of an acute attack of porphyria. Some of the preliminary studies have looked specifically at the effects of ALA accumulation on sub-cellular elements (Monteiro et al, 1989; Balla et al 1991₁; Balla et al 1991₂; Hermes-Lima et al, 1992; Onuki et al, 1994; Oteiza et al, 1994). Monteiro et al (1989) were able to demonstrate that ALA auto-oxidizes, which resulted in the formation of free radicals.

In some of the *in vitro* models, some of the potential damaging effects of ALA demonstrated included inducing iron release from ferritin, with concomitant lipid peroxidation in liposomes (Oteiza et al, 1994), single strand breaks in plasmid DNA in the presence of ALA and Fe^{2+} ions, which was attenuated by the addition of anti-oxidant enzymes, metal chelators and HO^\cdot scavengers (Onuki et al, 1994); an increase in Ca^{2+} uptake with a resultant inhibitory effect on oxygen consumption of the mitochondria and an effect on trans-membrane potential of cortical syntaptosomes (Penatti et al, 1996). Neal et al 1997 were able to show that ALA accumulation in CHO (Chinese hamster ovary) cell culture resulted in inhibition of colony formation and decreased cell survival, as well as decreases in glutathione, glutathione disulfide and catalase – parameters indicative of oxidative stress.

Neurotransmitter interactions

Many studies were performed during the 1970's, and once again more recently looking at potential interactions of ALA with the neurotransmitters, GABA and L-glutamic acid. ALA displays structural similarity to both these neurotransmitters. *In vitro* reports looking at rat brain, subjected to exposure to ALA concentrations in the region of 10^{-4}M , showed that ALA inhibited the uptake and increased the efflux of GABA (Brennan and Cantrill, 1981). Na^+K^+ -ATPase was also inhibited – which is known to stimulate efflux of GABA. At lower ALA concentrations (10^{-6}M), ALA acted as a partial agonist of GABA by inhibiting the stimulated release of GABA from nerve endings (Brennan and Cantrill, 1981).

Muller and Snyder (1977) were able to show that ALA competed for the binding of GABA to synaptic GABA receptors in CNS membranes. Meyer et al (1998) made the point that in view of recent reports of two or more distinct GABA receptor systems, similar binding studies should be repeated – looking at binding of ALA to the different sub-classes of GABA receptors. More recently, Emmanuelli, et al (2001) reported that ALA inhibits the binding of [3H]Muscimol binding to both human and rat cerebral cortical membranes (in

an almost identical fashion) and plan further investigations using rat membranes.

Neuronal haem deficiency

Another mechanism proposed is that symptoms of the acute attack of porphyria may be related to neuronal haem deficiency. Little is known about the regulation of the haem pathway or of the regulation of ALA synthase in neural tissue. Decreased activity of hepatic cytochrome p450 enzymes has been shown in patients suffering from porphyria (Mustajoki et al, 1994). However there is no evidence of decreased hepatic p450 activity directly resulting in porphyric symptoms. However a deficiency in haem in neuronal tissues, could result in a decrease in cytochrome p450 activity which could have implications for cytochrome p450 metabolized neuro-active substances.

Another theory, about a more indirect effect of ALA on the CNS, is related to the presumed decrease in the activity of haem dependant enzyme - hepatic tryptophan dioxygenase (tryptophan pyrrolase) during an acute attack of porphyria. This is thought to lead to elevated plasma concentrations of tryptophan. Plasma concentrations of tryptophan are thought to largely determine CNS tryptophan concentration. 5-Hydroxytryptamine (5-HT) – an important neurotransmitter is synthesized from tryptophan, and thus an increase in brain tryptophan might well cause an increase in 5-HT – with increased serotonin effect explaining some of the CNS manifestations of acute porphyria. Litman and Correia (1983) demonstrated in rat models (with chemically induced porphyria) that tryptophan pyrrolase activity was impaired and that this was associated with elevated tryptophan and 5-HT turnover in the brain, which was reversed after the administration of haem. Bonkovsy et al (1991) and Price et al(1959) have shown increased excretion of tryptophan and 5-HT metabolites in the urine of patients with acute porphyria. Increased blood levels of tryptophan and 5-HT have also been demonstrated in patients with AIP, which can be reversed by infusion of haem arginate.

An increase in serotonin, can explain many of the features of the acute attack of porphyria – particularly the autonomic neuropathy associated with the acute attack of porphyria. However this does not explain the motor neuropathy or the seizures seen in patients having an acute attack of porphyria.

A double heterozygote PBG deaminase deficient mouse is now available, which may help elucidate some of the mechanisms involved (Lindberg et al, 1996). These mice are compound heterozygotes (denoted T1/T2[-/-]), which have only 30% of normal PBG deaminase activity. Although they appear to have normal porphyrin excretion, treatment with phenobarbital results in induction of hepatic ALA synthase and increased plasma and urinary ALA. In this model, a decrease in large diameter myelinated fibers has been shown, together with damage to intramuscular nerve bundles – findings similar to those in patients suffering from acute AIP. They also display electromyographic signs on neurogenic denervation and show symptoms of peripheral neuropathy. These findings are present in mice not treated with phenobarbital or showing increased excretion of ALA. However even with treatment of these mice with phenobarbital, the classical sign of abdominal pain associated with the acute attack of porphyria is not demonstrated. Presently studies of autonomic function in the compound heterozygous AIP mice are taking place, which should increase our understanding of the pathogenesis of the acute attack of porphyria.

Summary

Although relatively little is yet known about the regulation of haem biosynthesis in humans, it is clear from the animal models studied, that regulation of haem biosynthesis and ALA synthase activity in non-erythroid tissues is important to our understanding of porphyria. Obvious ethical constraints and technical problems limit our ability to study human hepatic ALA synthase. In the following chapters in this thesis we embark on a project in which we were able to make antibodies to ALA synthase and to embark on an immunohistochemical study of ALA synthase in different tissues.

Chapter Three

The production of antibodies to ALA synthase.

3.1 Introduction

Little is known about the regulation or tissue specific expression of ALA synthase in healthy humans or in individuals suffering from porphyria (see chapter 2). Although the tissue distribution of ALA synthase mRNA has been studied in rats (Srivastava et al, 1992) similar studies in humans have not been reported.

The human hepatic form of the enzyme has not yet been purified as technical problems have hampered research of the human hepatic form. Problems encountered include the minute quantities of ALA synthase produced under physiological conditions (9-11nmol/g in human liver), its highly hydrophobic nature and the short half-life of the enzyme – the human hepatic form has a half-life of approximately 30 minutes (personal communication DF Bishop).

Unlike mouse liver, which is easily homogenized for subcellular fractionation, homogenizing human liver requires many time consuming steps, which may include a collagenase digestion to obtain a smooth homogenate. The instability of the enzyme, its susceptibility to proteolytic breakdown and the hydrophobicity of the enzyme add to the technical difficulties in working with this enzyme. Moreover, there are ethical constraints associated with the use of fresh human liver.

These problems notwithstanding, the sequence of the human hepatic ALA synthase gene was published by Bishop (1990). The gene was cloned from a human foetal liver cDNA library using rat primers.

Much of the information available on ALA synthase has been obtained from studies investigating the enzyme regulation in AIA (allylisopropylacetamide) and DDC (3,5-dicarbethoxy-1,4-dihydrocollidine or 3,5-diethoxycarbonyl-1,4-dihydrocollidine) treated rats or chicken embryos.

Treatment with these compounds results in a chemical porphyria with a concomitant induction of ALA synthase. The mechanism for the induction of ALA synthase by AIA and DDC is poorly understood. This has been reviewed in detail in chapter 2.

On a sub-cellular level, the only form of ALA synthase, which has successfully been hyper-expressed and purified, is the mouse erythroid form of the enzyme (Ferreira and Dailey, 1993). These scientists were able to overcome the problems of poor solubility and instability, by expressing mouse erythroid ALA synthase under control of an alkaline phosphatase promoter, thus allowing the ALA synthase to be exported into the periplasmic space. In this expression system, traditionally, an alkaline phosphatase pre-sequence is present on the amino-terminus of the expressed protein and cleaved off as the protein enters the periplasmic space. However, only by removing this alkaline phosphatase pre-sequence, were they able to achieve the transportation of ALA synthase into the periplasmic space, with the enzyme in a processed and soluble form. Remarkably, the enzyme was active and retained physical and catalytic properties observed in mammalian tissue. Sufficient quantities of murine erythroid ALA synthase were obtained, to allow characterization of the physical and kinetic properties of this enzyme.

Aim

The objective of this work was to produce antibodies to human hepatic ALA synthase for immunocytochemical examining the distribution of the enzyme in human tissue. Information about this would be of help in understanding more about the pathogenesis of the acute attack in patients suffering from an acute porphyria, as at present, many theories exist about the pathogenesis of the acute attack and

whether there are specific macro and micro tissue environments in which ALAS is induced.

Background to experimental approach:

My initial attempts at hyper-expressing active full length ALA synthase in *E.coli* were unsuccessful. ALA synthase cDNA sub-cloned into pGEM (pGEM-ALA synthase) was used in these initial experiments. *E.coli* transformed with pGEM-ALA synthase was allowed to grow in culture broth, both at 37 °C and 28 °C. Once the cells had reached an A_{260} of 1.0, IPTG was added to the culture medium to induce production of the ALA synthase protein. On centrifugation, no cell pellet was obtained, despite shortening the IPTG induction period to 15 minutes, or reducing the amount of IPTG from the standard of 0.1 μ M to 0.01 μ M and 0.001 μ M.

Supernatants from the above-mentioned cultures contained >0.61mM ALA as determined by the Watson Schwartz test in the UCT porphyria lab, whereas supernatants from un-induced cultures contained no ALA detectable in a similar test - suggesting that little ALA synthase was present, prior to induction using IPTG. The absence of a cell pellet on centrifugation of the IPTG-induced ALA synthase containing cells, suggested massive cell lysis, probably a result of the toxicity of the ALA produced by ALA synthase. Indeed, 10 μ M concentrations of ALA (>50-fold less than was measured in our cultures), was sufficient to kill both neuronal and glial components of brain cell cultures in the chick embryo (Percy et al, 1981).

Further work in *E.coli* using full length ALA synthase was consequently abandoned in favour of work with smaller, possibly more manageable and expressible sequences of the ALA synthase protein.

We also considered that even if successful expression of ALA synthase had been achieved, the instability of the enzyme and its hydrophobicity, as described above would have made purification technically difficult.

The approach decided on, was to identify fragments of ALA synthase corresponding to areas of the protein likely to be of low hydrophobicity and containing a high proportion of exposed residues, by employing computer analysis of the primary amino acid sequence. Fragments chosen, were to be sub-cloned into a suitable expression system and hyper-expressed in *E.coli*, purified to homogeneity, and used for antibody production.

3.2 Materials and Methods

Materials

The PSORT software available on the Internet was accessed via the web site EXPASY. In addition the Profile fed neural network systems (PHD) from Heidelberg (PHDsec for secondary structure and PHDacc for solvent accessibility) were utilized, and accessed via the web site JPRED. Primer designer software for windows (Scientific and Educational software, version 2.0) was made use of for designing of the ALA synthase primers.

Methods

1. *Computer predictions on the hydrophobicity and other characteristics of ALA synthase*

Hydrophobicity predictions were performed based on hydrophobicity values assigned to each amino acid by Kyle and Doolittle (1982). Windows of 15 amino acids were chosen. The program relies on statistical calculations of local residue interactions around the secondary structural state of the central amino acid. The

linear weight variational model was used in which all amino acids in each window are given equal weighting.

Instability indices (Guruprasad et al, 1990) were calculated. Calculation of an instability index is based on statistical analysis of the amino acid sequence and calculating the occurrence of particular dipeptides, which are noted to occur in unstable proteins (Guruprasad et al, 1990). Glycosylated residues and intracellular protein location were also predicted (Nakai et al, 1996; Horten and Nakai, 1996; Horten and Nakai, 1997; Fujiwara et al, 1997).

Secondary structure and solvent accessibility were predicted using PHD software, after a Blast search (Altschul et al, 1990) and multiple sequence alignment had been performed (Barton et al, 1990). Multiple sequences alignments generate additional secondary structure predictions, which influence the final secondary structure prediction of the protein under investigation, and thereby improves accuracy to over 70% for individual residues.

2. Design of primers

Oligonucleotide primers were designed using Primer Design software and were synthesized by Gentest. These primers incorporated *EcoRI* and *BamHI* sites to facilitate sub-cloning.

3. PCR and cloning

Prof. DF Bishop (Mt Sinai School of Medicine, New York) kindly donated ALA synthase cDNA, which had been cloned into the *Hind III* and the *Eco RI* sites of the vector, pGEM (Promega). The vector pGEM is a circular *E.coli* cloning vector, 2870bp in size and contains the Ampicillin resistance gene and the prokaryotic *T7* and *Sp6* promoters.

The vector chosen for the expression of the amplified ALA synthase fragments was pGEX-2T. This plasmid is commercially available from Pharmaciae, and successful

by amino acid sequences, which are specific cleavage sites for thrombin on the amino terminus of the chosen protein. This *E.coli* expression vector, pGEX-2T, is a plasmid, 4948 base pairs in size, containing a *tac* promoter, a β -lactamase gene, and the *lacI^q* and *lacZ* operons. Expression of Sj26 is controlled by the *tac* promoter and inducible by IPTG.

Subcloning of heterogeneous sequences, downstream of the thrombin cleavage site is facilitated by the presence of a multiple cloning site recognized by *Bam* *HI*, *Eco* *RI* and *Sma* *I* restriction endonucleases.

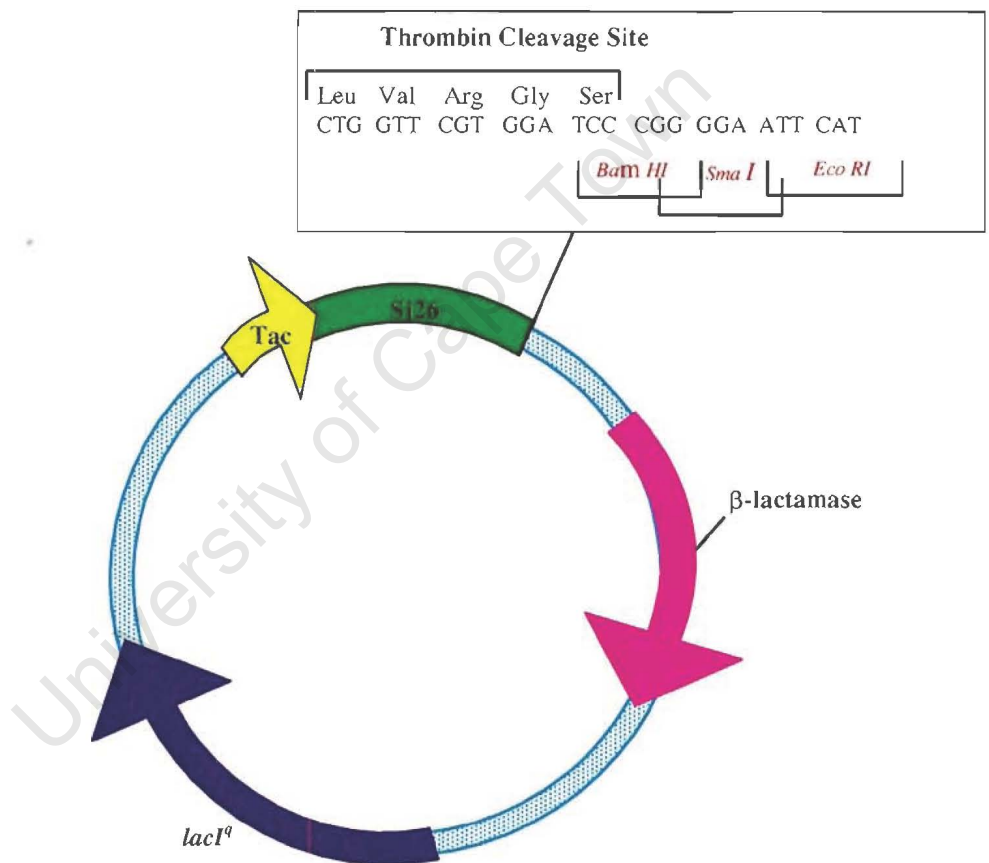


Fig 3.2.1 Structure of the pGEX-2T vector

Advantages of this system include the relative ease of fusion protein purification using a glutathione (GSH) affinity column, which relies on the affinity of

glutathione (GSH) - (covalently bound to agarose beads) towards the *Sj* GST. The purified fusion protein is then eluted from the column by the addition of 5 to 10 mM GSH. The *Sj* GST can be released from the foreign protein at the thrombin cleavage site, using thrombin.

Additional advantages stem from the fact that many GST fusion proteins remain soluble, in contrast to non-fused heterologous proteins expressed in *E.coli*, the latter being often denatured and consequently insoluble. Fusion proteins can usually be purified under non-denaturing conditions thus keeping the secondary structure and antigenicity intact (Smith & Johnson, 1988).

Although the *Sj* GST can be released, this is not absolutely necessary as the GST is small relative to other carrier proteins (e.g. β -galactosidase, protein A, and maltose binding protein). Immunological problems of non-specific antibody binding, typically associated with antibodies produced to protein A fusions are more likely to be absent (Smith, 1994). Cross-reactivity between antibodies to the *Schistosoma japonicum* GST and mammalian GST's has not been reported (personal communication, Pharmacia technical staff). Moreover, it is reported that the *Schistosoma japonicum* GST appears to enhance the immunogenicity of the antigen (Pharmacia technical bulletin, 1997).

The pGEM-ALAS plasmid, obtained from Prof. DF Bishop, was amplified in the XL1Blue strain of *E.coli* (see A 1.4) and re-extracted using ion-exchange chromatography (see A 1.2). This DNA was used as the template to amplify the four ALA synthase fragments, by PCR (see A 1.6).

The PCR products were subjected to restriction enzyme digestion, by *Bam*HI and *Eco*RI, followed by sub-cloning into the corresponding sites of pGEX-2T, as described in A 1.3.

The ligated pGEX-2T vectors (pGEX-2T-ALAS fragments 1 – 4) were transformed into the XL1Blue strain of *E.coli*, and grown overnight on ampicillin agar plates (see A 1.4). Colonies from the ampicillin agar plates were inoculated into ψ -broth (a nutrient rich *E.coli* culture broth - see A 2) containing ampicillin at a concentration of 100 μ g/ml. and allowed to grow overnight in a 37°C shaking incubator. These cultures were subjected to small-scale isolation (as described in A1.1) to obtain DNA for restriction enzyme mapping.

The plasmid DNA, obtained from the minipreps, was subjected to *Eco RI* and *Bam HI* digestion and separated using agarose gel electrophoresis (see A 1.5). Colonies that appeared to be correct on restriction enzyme mapping were selected for sequencing and larger scale preparations of DNA.

The ALA synthase fragments were released from the pGEX-2T constructs using *EcoRI* and *BamHI* restriction enzymes. These were sub-cloned into the pBluescript-SKII vector. These constructs were used for automatic sequencing to exclude PCR errors (see A 1.7).

4. Expression and purification of fusion proteins in *E.coli*

A single colony of *E.coli*, transformed with pGEX-2T-ALAS-fragment1 (pFP1), pGEX-2T-ALAS-fragment2 (pFP2), pGEX-2T-ALAS-fragment3 (pFP3), and pGEX-2T-ALAS-fragment4 (pFP4) was picked from an ampicillin agar plate and grown overnight in 25 ml of ampicillin ψ B (a rich *E.coli* culture broth containing tryptone, yeast, potassium chloride and magnesium sulphate - see A2), in an orbital shaker at 37°C.

This starter culture was diluted 1:20 into pre-warmed $\psi\beta$, containing ampicillin at 100 μ g/ml and grown in an orbital shaking incubator at 37°C to an OD₆₀₀ of 0.8. Fusion proteins were expressed for 3 hours after induction of the *tac* promoter by the addition of IPTG at a concentration of 100 μ mol/l.

After incubation on ice for 15 minutes the cells were harvested by centrifugation at 4000g. The supernatant was discarded and the cell pellet was washed in 50 ml PBS (phosphate buffered saline – see A2) with PMSF (0.1mM), before being stored dry at -80°C for purification of the protein the following day.

5. *Standard purification technique for Sj GST (Schistosoma japonicum GST) without fusion protein and soluble Sj GST fusion proteins*

The original method for purifying GST fusion proteins and Sj GST was described by Smith and Johnson (1988). The cell pellets of both the *E.coli* transformed with pGEX-2T and pFP1 - 4 obtained as described above, were thawed on ice and resuspended in 15 ml of PBS. The suspended cells were then disrupted by sonication on ice. The suspension was sonicated in short pulses (of 20 seconds) separated by cooling periods of 30 seconds to prevent over-heating of the cells. The cell suspension was sonicated for a total sonication time of 2 to 3 minutes, progressively becoming more translucent indicating cell disruption. Triton X-100 was added to a final concentration of 1% and the mixtures were centrifuged for 30 minutes at 12000g using a Beckman J21-C centrifuge. The supernatants were then decanted and placed on ice, whilst the cell pellets were resuspended in 10 ml of PBS containing 1% Triton X-100.

During the initial attempts at expression and purification of FP 1 – 4 (fusion proteins 1 – 4), the supernatants and pellets of the *E.coli* transformed with pGEXT-2T or pGEX-2T FP 1 - 4 (pFP 1 - 4) were assayed for GST activity using the pGEX-2T transformed *E.coli* as a positive control.

This extra step was indicated firstly to simultaneously screen for ability of the fusion protein to bind to GSH (glutathione) and therefore suitability for affinity purification and secondarily to confirm expression of the fusion protein. Moreover, the activity assay was useful to determine the solubility of the fusion proteins – i.e.

whether or not the expressed fusion protein was soluble and present in the supernatant, or insoluble and associated with the cell pellet.

In the pGEX-2T-transformed control cells, which were expressing Sj GST, GST was fully soluble (as shown in CDNB screening – see below) and thus purified by the standard technique described by Smith and Johnson (1988). The lysate was passed through an agarose GSH column, (pre-equilibrated with PBS) by gravity flow. The column was subsequently washed with 30 column volumes of PBS, and the Sj GST was eluted using 3 times 2 ml of 5 mM GSH (in PBS with 0.1mM PMSF).

6. *CDNB assays to screen for GST activity*

GST activity was measured using a modification of the CDNB (1-chloro-2,4-dinitrobenzene) assay (Mannervik and Danielson, 1998 – also see A 1.10). GST catalyses the conjugation of CDNB to glutathione (GSH), with the resultant conjugate displaying strong molar absorption, at 340nm.

A volume of 2.75ml KH_2PO_4 (0.1M); Na_2HPO_4 (0.1M); pH 6.5 – (see A2); 0.1ml of CDNB solution (30mM CDNB in 100% ethanol) and 0.15ml of reduced GST solution (20 mM reduced GSH in water) were combined in a quartz spectrophotometer cuvette to be used as a blank for the spectrophotometer (AR_B). A second quartz cuvette (AR_S) was prepared containing the above-mentioned reagents with the addition of 10 to 50 μl of protein lysate - either from the supernatant or pellet. A volume of PBS, equal to the volume of protein lysate was added to AR_B . The absorbencies of both the AR_B and the AR_S cuvettes were simultaneously read at A_{340} , at 0.5-second intervals for a period of one minute. The change in the A_{340} /min/ml can be calculated using the following formula:

$$\frac{[\text{AR}_S(\text{time}2) - \text{AR}_S(\text{time}1)] - [\text{AR}_B(\text{time}2) - \text{AR}_B(\text{time}1)]}{(\text{time}2 - \text{time}1)(\text{ml sample})}$$

The change in the A_{340} 's is used as a relative comparison of GST fusion protein content between two samples, as the activity of the GST moiety is often affected by the presence of the fusion protein, so activity may not accurately reflect the absolute amount of fusion protein present. Moreover, the solubilization of proteins from the cell pellets is not necessarily complete and therefore activity witnessed might also not reflect absolute amounts of fusion protein present.

7. Purification of insoluble Sj GST fusion proteins according to Frangioni and Van Neel

It was noted that all the GST activity of the fusion proteins was detected in the cell pellet, therefore a protocol applicable to the purification of insoluble fusion proteins, described by Frangioni and Van Neel (1993), was chosen for purification of FP 1 - 4.

This technique uses sarkosyl to solubilise the GST fusion protein from the membrane fraction of the bacteria. Frankel et al, (1991) postulate that extremely insoluble proteins co-aggregate with the bacterial outer membrane, during and shortly after lysis, and that sarkosyl, in the absence of divalent cations is effective at preventing this. Sarkosyl causes less denaturation than a variety of other commonly used agents (e.g. 8 M urea; 6 M guanidium; SDS).

The frozen cell pellet, obtained as described above was thawed on ice, before being resuspended in a volume of 15ml STE (150 mM Sodium; 10mM Tris HCL [pH 8.0]; 5mM EDTA; 0.1mM PMSF).

Lysozyme was added to the sample to a final concentration of 100 μ g/ml, and the sample was gently mixed before being incubated on ice for 15 minutes. Following the addition of DTT to a final concentration of 5mM, the sample was briefly vortexed and incubated on ice for a further 10 minutes. Sarkosyl was added to a final concentration of 1.5% and the sample was incubated on ice for 15 minutes,

During initial Western blots, which were used to screen the immunized rabbit serum for antibodies, primary antibody was applied to the nitrocellulose in the following dilutions: 1:500; 1:1000; 1:2000; 1:4000; 1:8000; 1:16000. Secondary antibody – goat anti-rabbit (Omnimed) was used at a dilution of 1: 2000.

ELISA's were also used to verify production of antibody to FP 3 in the immunized rabbits. ELISA's were performed as a modification of the indirect ELISA technique described in Current Protocols in Immunology (1995) – see A 1.16.

3.3 Results and Discussion

1. Computer predicted analyses

Computer based analyses of protein characteristics and predictions, using amino acid sequences, are of great benefit when attempting to study a protein, which has not been previously purified. Software using sequence analysis is readily available and continually updated and refined as more proteins are characterized (Nakai and Kanehisa, 1992; Horton and Nakai, 1996; Horton and Nakai, 1997).

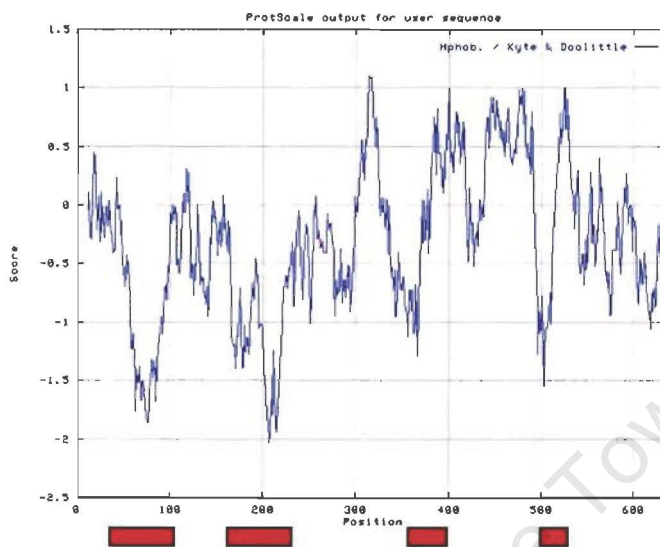


Fig 3.3.1 A hydrophobicity plot of the ALA synthase sequence

For this analysis, windows of 15 amino acids were chosen. The linear weight variational model was used, in which equal weighting is given to all amino acids within a window. A red bar indicates areas of hydrophobicity of less than -0.5 units. These correspond to areas of choice for the expression of fragments in *E.coli*.

The instability index of the pre-enzyme and the processed ALA synthase were calculated to be 45.49 and 43.17 respectively – values indicative of an unstable protein. (Proteins with an instability index of less than 40 are predicted to be stable where as those with values of greater than 40 are predicted to be unstable).

Table 3.3.1 below lists instability indices of several other haem pathway proteins as well as the index of cytochrome C oxidase.

| Protein | Instability index |
|--------------------------------|--------------------------|
| Processed ALA synthase (ALA-S) | 43.17 |
| Hydroxymethylbilane synthase | 39.60 |
| Uroporphyrinogen Decarboxylase | 49.88 |
| Coproporphyrinogen Oxidase | 58.15 |
| Protoporphyrinogen Oxidase | 48.71 |
| Ferrocheletase | 50.36 |
| Cytochrome C oxidase (Chain 1) | 28.97 |

Table 3.3.1 Instability indices of selected proteins

The half-life of the ALA synthase mitochondrial protein was estimated to be 0.8 hours in reticulocytes *in vivo*, (which approximates the reported half-life of 30 minutes). The predicted half-life of the protein in yeast is 10 minutes. Only two serine residues are predicted to be favourable for glycosylation. The localization of the ALA synthase protein was predicted to be in the mitochondrial matrix – which correlates with the immuno-localization study in rats (Rohde et al, 1990)

Secondary structure predictions were performed, using multiple aligned sequences – to improve accuracy. Furthermore, after independent predictions of α -helices and β -sheets based only on the primary amino acid sequence, a further secondary structure was computed giving consideration to potential competition between the α -helices and β -sheets. It was desirable for sequences chosen for hyper-expression to contain some regions where secondary structure was predicted to be linear - in the event that the hyper-expressed protein was obtained only in the denatured form. Peptide mapping using poly-clonal antibodies to certain proteins has shown that many of the antibodies formed are directed against linear peptides, rather than to areas of α -helices or β -sheeting in the protein (Craig et al, 1998). Therefore, as it was not known whether or not our purified fragments would be obtained in a denatured form, some linear peptides within the chosen sequence were desirable. Below is the predicted secondary of ALA synthase amino acid sequence.

| | | | | |
|--------------------------|---------------------------|---------------------------|--------------------------|--------------------------|
| ***** MESVVRRCPF | **αααααα LSRVPQAF LQ | αα***** KAGKSLLFYA | ***** QNCPKMMEVG | ***** AKPAPRALST |
| ***** AAVHYQQIKE | *****ααα TPPASEKDKT | ααααα***** AKAKVQQT PD | ***** GSQQSPDGTQ | ***** LPSGHPLPAT |
| *****αα SQGTASKCPF | αααααα** LAAQMNQRGS | βββαααααα SVFCKASLEL | αααααααα QEDVQEMNAV | αααααα*** RKEVAETSAG |
| **ββββββ* PSVVSVKTDG | *****ααααα GDPSGL LKNF | ααααα***α QDIMQKQRPE | ααααααα** RVSHLLQDNL | ***ββββββ PKSVSTFQYD |
| αααααα*** RFFEKKID EK | *****ββββ KNDHTYRVFK | βββ***** TVNRRAHIFP | ***** MADDYSDSLI | **ββββββ* TKKQVSVWCS |
| ***** NDYLGMSRHP | ββββααααα RVCGAVMDTL | ααα***** KQHGAGAGGT | *****ααα RNISGTSKFH | ααααααααα VDLERELADL |
| α*****ββββ HGKDAALLFS | βββββ*αααα SCFVANDSTL | αααααα*** FTLAKMMPGC | βββ*****αα EIYSDSGNHA | ααααααα** SMIQGIRNSR |
| ***ββββαα VPKYIFRHND | ααααααααα VSHLRELLQR | ***** SDPSVPKIVA | ***** FETVHSM DGA | ****αααααα VCPLEELCDV |
| αααββββββ AHEFGAITFV | ***** DEVHAVGLYG | ***** ARGGGIGDRD | ***** GVMPKMDII | ***** SGLTGKAFGC |
| ***** VGGYIASTSS | ααααααααα LIDTVRSYAA | *βββββ**** GFIFTTSLPP | **ααααααα PMLLAGALES | ααααα**ααα VRILKSAEGR |
| ααααααααα VLRRQHQRNV | αααααβββ*** KLMRQMLMDA | ***βββββ*** GLPVVHCPSH | ββββββαααα IIPVRVADAA | ααααααααα KNTEVCDEL M |
| αα**ββββββ SRHNIYVQAI | ββββααααα NYLTVPRGEE | ααααα***** LLRIAPTPHH | **ααααααα TPQMMNYFLE | α*****βββ NLLVTWKQVG |
| ββββ***** LELKP HSSAE | *****βββ CNFCRRPLHF | ββββ***** EVM SEREKS Y | ***** FSGLSKLVSA | **** QSTP |

Fig 3.3.2 Predicted secondary structure of ALA synthase The predicted secondary structure of this sequence is indicated above the amino acid sequence, using α for predicted α-helices and β for predicted β-sheeting, and * for linear areas.

Computer predictions of accessible/exposed residues were also performed using the profile fed neural network systems software, which predicts accessible residues in the sequence of choice, after performing multiple sequence alignments and analyses of several ALA synthase sequences of prokaryotic and eukaryotic origins. Structure predictions on a single amino acid sequence are reported to have a 65% chance of being correct (for each residue) (Frishman and Argos, 1996). When structure predictions are performed following multiple sequence alignments and following calculations on the individual structure of each sequence, it is claimed that the predictions have a better than 70 % chance of being accurate (Rost et al, 1993; Rost et al, 1994a; Rost et al, 1994b). In the figure below, the results of this computer based analysis is shown.

| | | | |
|-------------|------------|--------------|------------|
| MESVRRCPF | LSRVPQAFLO | KAGKSLLFYA | QNCPKMMEVG |
| AKPAPRALST | AAVHYQQIKE | TPPASEKDKT | AKAKVQQTPD |
| GSQQSPDGTQ | LPSGHPLPAT | SQGTASKCPF | LAAQMNQRGS |
| SVFCKASLEL | QEDVQEMNAV | RKEVAETSAG | PSVVSVKTDG |
| GDPSGLLKNF | QDIMQKQRPE | RVSHLLQDNL | PKSVSTFQYD |
| RFFEKKIDEK | KNDHTYRVFK | TVNRRAHIFP | MADDYSDSLI |
| TKKQVSVWCS | NDYLGMSRHP | RVCGAVMDTL | KQHGAGAGGT |
| RNISGTSKFH | VDLERELADL | HGKDAALLFS | SCFVANDSTL |
| FTLAKMMPGC | EIYSDSGNHA | SMIQGI RNSR | VPKYIFRHND |
| VSHLRELLQR | SDPSVPKIVA | FETVHSM DGA | VCPLEELCDV |
| AHEFGAITFV | DEVHAVGLYG | ARGGGIGDRD | GVMPKMDII |
| SGTLGKAFGC | VGGYIASTSS | LIDTVRSYAA | GFIFTTSLPP |
| PMLLAGALES | VRILKSAEGR | VLRRQHQRNV | KLMRQMLMDA |
| GLPVVHCP SH | IIPVRVADAA | KNTEVCDELM | SRHNIYVQAI |
| NYLTVPRGEE | LLRIAPPHH | TPQMMNYFLE | NLLVTWKQVG |
| LELKP HSSAE | CNFCRRPLHF | EVM SERE KSY | FSGLSKLVSA |
| QSTP | | | |

Fig 3.3.3 Sequence of ALA synthase showing predicted accessible residues. The ALA synthase amino acid sequence is represented in 1 letter form, indicating amino acids that are likely to be exposed(X) and those that are not, indicated either in black (X) or blue (X) and predicted to be submerged or not defined residues, respectively.

2. ALA synthase fragments chosen for expression in *E. coli*

Fragments for expression in *E. coli* were chosen after the above mentioned computer based analysis of the ALA synthase gene and its deduced amino acid sequence. The choice of fragments was primarily influenced by the results of the computer based analysis, but other factors determining the final selection of the fragments were suitability for design of primers for PCR and the occurrence of *Bam* *HI* restriction enzyme sequences within the ALA synthase gene sequence.

The first segment chosen was 55 amino acids in length and corresponds to the pre-sequence of the enzyme. Despite this part of the ALA synthase sequence being non-optional in terms of hydrophilicity, the pre-sequence was chosen for generation of antibodies to facilitate future studies comparing amounts of pre-enzyme and processed enzyme produced. As so little is known about the processing of ALA synthase and the regulation thereof, it is probable that the additional information obtained from these antibodies would be interesting and relevant to future studies involving the regulation of ALA synthase.

The second fragment chosen corresponds to an area proximal to the N-terminus of the mature protein, and is 66 amino acids in length. A large proportion of this region was predicted on the Kyle and Doolittle (1990) hydrophobicity scale to have hydrophobicity values of between -0.5 and -2.0 units. This area corresponds to one of the least hydrophobic regions of ALA synthase. Moreover over 50% of the residues in this region of the protein are predicted to be exposed residues.





The third fragment was chosen from a central area in the protein and is 295 amino acids long. Hydrophilic areas are present at the beginning and end of this fragment. Although the centre of the fragment contains several hydrophobic residues and peptides predicted to be in α -helical and β -sheet conformation, the initial and terminal thirds contain predominantly peptides predicted to be in linear conformation. At 295 amino acids, this fragment is somewhat longer than the

others. We wished to include a longer fragment - so while hydrophobic and secondary structure conditions appeared slightly less favourable than perhaps with the shorter fragments, more epitopes are available for polyclonal antibody production.

The last fragment was 116 amino acids long and is close to the carboxy-terminus of the protein. This area of the protein was reasonably hydrophilic – with hydrophobicity predictions reaching -1.0 at the beginning of the fragment.

Below, the amino acid sequence of ALA synthase with the 4 fragments, which were chosen for hyper-expression in *E.coli* and for subsequent antibody production, shown in colour.

MESVVRRCPF¹LSRVPQAF²LQKAGK³SLLFYAQNCPK⁴MMEVGAKPAPRALSTAAVHYQQI
KETPPASEKDKTAKAKVQQTPDGSQQSPDGTQLPSGHPLPATSQGTASKCPFLAAQM
NQRGSSVFCKASLELQEDVQEMNAVRKEVAETSAGPSVSVKTDGGDPSGLLKNFQD
IMQKQRPERVSHLLQDNLPKSVSTFQYDRFFEKKIDEKKN³DHTYRVFKTVNRRAHIFPM
ADDYSDSLITKKQVSVWCSNDYLGMSRHRVCGAVMDTLKQHGAGAGGTRNISGTSK
FHVDLERELADLHGKDAALLFSSCFVANDSTLFTLAKMMPGCEIYSDSGNHASMIQGIR
NSRVPKYIFRHNDVSHLRELLQRSDPSVPKIVAFETVHSMDGAVCPLEELCDVAHEFGA
ITFVDEVHAVGLYGARGGGIGDRDGVMPKMDIISGTLGKAFGCVGGYIASTSSLIDTVRS
YAAGFIFTTSLPPMLLAGALESVRILKSAEGRVLR³RQHQRNVKLM⁴RQMLMDAGLPVVH
CPSHIIPVRVADAAKNTEVCDELMSRHNIYVQAINYLTVPRGEELLRIAPTPHHTPQMMN
YFLENLLVTWKQVGLLELKP³HSSAECNFCRRPLHFEVMSEREKSYFSGLSKLVSAQ*

Fig. 3.3.4 Amino acid sequence of ALA synthase displaying the fragments chosen for expression and purification in *E.coli*. The 4 ALA synthase fragments are indicated in colour as shown in this legend. Fragment 1 -  ; fragment 2 -  ; fragment 3 -  and fragment 4 - 

3. PCR and cloning

The primers use for amplification of the ALA synthase fragments are shown below.

| | Nucleotide residues | Amino acid residues | Forward primer | Reverse primer |
|----|---------------------|---------------------|--------------------------|---------------------------|
| 1 | 1 – 167 | 1 - 56 | TGAGGATCCATGGAGAGTGTGTC | ATGGAATTCCTGGTAGTGTACTGCT |
| 2. | 236 – 435 | 78 - 145 | CTGATGGATCCAGCAGAGTCCA | GAGGAATTCAGCAACCTCTTTCCT |
| 3 | 534 – 1435 | 178 - 478 | ATGGGATCCCAGAAAGAGTGTC | CTGGAATTCGAGAGGTGGTGAAG |
| 4 | 1527 –1875 | 509 - 625 | CTAGGATCCCTCCATGAGACAGAT | CTGGAATTCTCTCTTTCACTCATC |

Table 3.3.2 The primers for amplification of the ALA synthase fragments

The red and blue shaded nucleotides represent the *Bam* HI and *Eco* RI restriction enzyme sites respectively.

All four fragments of ALA synthase were amplified using the primers designed and products corresponding to the expected sizes of 179 bp, 199 bp, 865 bp and 349 bp were obtained. An agarose gel showing all 4 PCR products is shown in Fig 3.3.5.

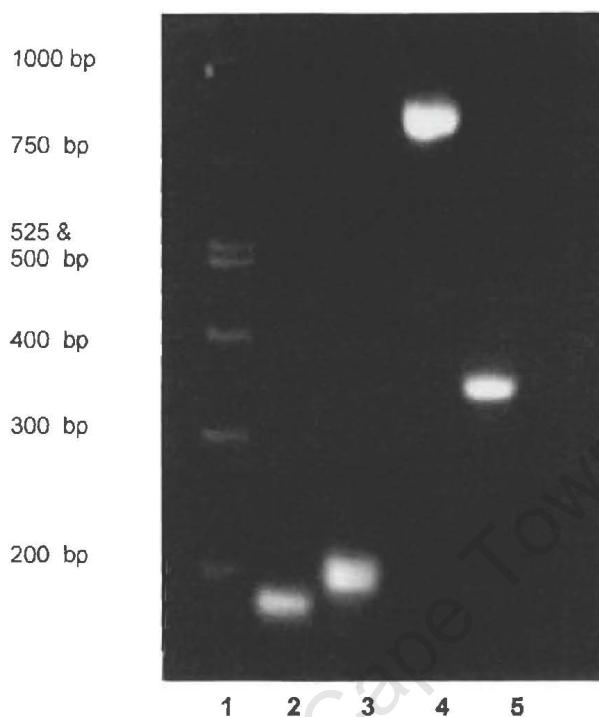


Fig 3.3.5 PCR amplification of the 4 fragments of the ALA synthase gene
 The four PCR products were electrophoresed on a 2% agarose gel and stained with ethidium bromide. Lane 1 corresponds to a DNA low molecular weight marker. The molecular weights of the marker bands are indicated on the left of the agarose gel. Fragments 1 to 4 are shown in lanes 2 to 5, respectively.

To minimise the problems of ALA synthase instability and hydrophobicity the fragments of ALA synthase were to be expressed as *Schistosoma japonicum* glutathione transferase (GST) fusion proteins.

Each PCR products was ligated into pGEX-2T. An electrophoresis of the *Bam* *HI* and *Eco* *RI* restriction enzyme digestions of plasmid preparations obtained is shown in Fig 3.3.6. The ALA synthase PCR products were sequenced using automated sequencing, and no Taq DNA polymerase errors were detected. The results of the automated sequencing are shown in A 4.

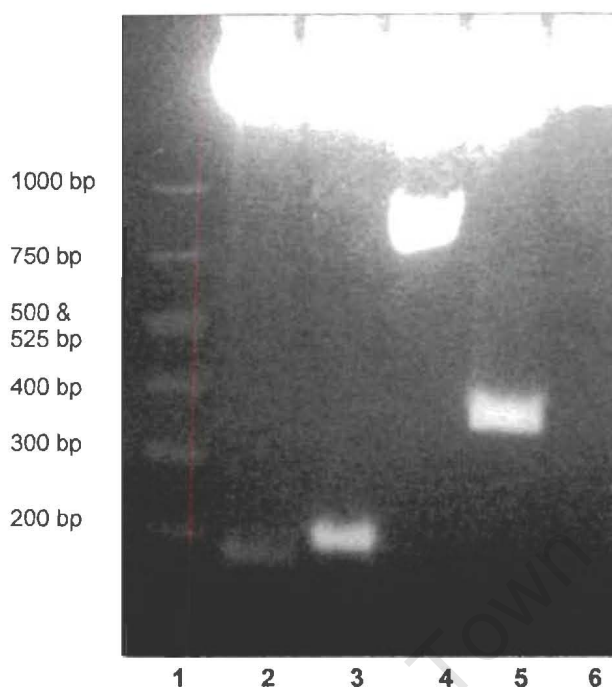


Fig 3.3.6 The purified plasmid preparations pFP1; pFP2; pFP3; pFP4 subjected to a *Bam* *HI* and *Eco* *RI* restriction enzyme analysis. The products of this restriction enzyme digestion have been electrophoresed on a 2% agarose gel and stained with ethidium bromide. Lane 1 corresponds to molecular weight markers. The molecular weights of the marker bands are indicated on the left of the agarose gel. Lanes 2 to 5, correspond to the restriction enzyme digest of pFP1 to pFP4, respectively. The lane 6 contains undigested pGEX-2T.

4. Expression and purification of fusion proteins in *E.coli*

The fusion proteins from all 4 fragments were expressed in *E.coli*. These were purified using affinity chromatography. The predicted size of *Sj* GST is 28kDa, while the predicted sizes of FP 1-4 are 35kDa, 35 kDa, 57kDa and 40kDa respectively.

Despite expressing ALA synthase as a fusion protein with *Sj* GST, the ALA synthase fusion proteins were insoluble and associated with the cell pellet and were unsuitable for the purification procedure described by Smith and Johnson (1998).

We therefore had to modify the purification procedure, using a method specifically designed for insoluble GST fusion proteins, described by Frangioni and van Neel (1993).

All of the purified ALAS fusion proteins, except that of fragment one, were smaller than expected size. The fusion proteins 2 and 4 (FP2 and FP4) were virtually the same size as the *Sj* GST.

The purified fragment 3-fusion protein appeared as 3 bands – the biggest band being about 40kDa in size (compared to the expected size of 57kDa), which corresponded to an ALA synthase fragment of about 12kDa (see Fig 3.3.7 below).

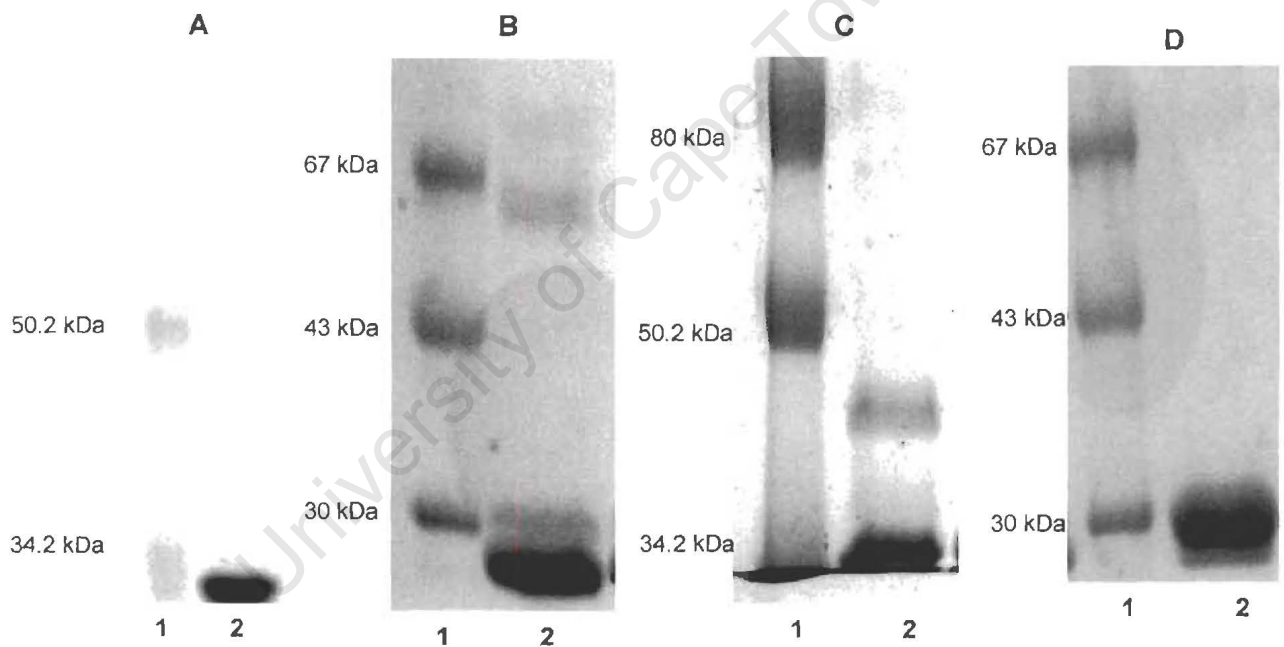


Fig 3.3.7 The purified fusion proteins 1 to 4

These were electrophoresed on 10 % SDS PAGE gels and stained using Coumassie blue. The first lanes of all the panels are SDS-PAGE molecular weight markers. The sizes of the molecular weight markers are indicated to the left of each gel. Lane 2 of all the SDS-PAGE gels "A" to "D" correspond to the purified fusion proteins FP1 to FP4 respectively.

Initially the problem was thought to be one of degradation. However the use of protease inhibitors, PMSF, leupeptin, pepstatin and EDTA did not increase the size of the fusion proteins. We queried whether this might be due to degradation taking place prior to lysis of the *E.coli*. Therefore growth and induction of the fusion proteins was attempted in the BL21 strain of *E.coli* (a protease deficient strain obtained from Pharmacia) using a variety of growing conditions, including low temperatures and short IPTG induction times, but this did not improve the attenuated protein size.

While the problem appeared to be one of degradation, is possible that it could have been another problem - perhaps one of transcription or translation.

Difficulty in expression of mitochondrial proteins in *E.coli* has been well described (Ferreira and Pederson, 1992). Ferreira and Pederson studied the expression of the liver mitochondrial phosphate transporter (H⁺/Pi symporter) in *E.coli*. Expression was not obtained using a variety of different plasmid expression systems, or by attempting to produce the protein as a fusion with the usually successfully expressed either the alpha or beta ATP synthase subunits. Successful expression was obtained only once the carboxy-terminus was truncated and the gene fused to a cDNA fragment derived from the ATP synthase alpha subunit gene.

Further experiments demonstrated that the molecular basis for *E. Coli's* inability to express the complete liver H⁺/Pi transporter was not related to transcriptional problems, or cellular toxicity. *In vitro* transcription-translation assays revealed that the problem with expression of full-length H⁺/Pi symporter was due to translational problems – associated with prokaryotic ribosomes. When eukaryotic ribosomes were present, full-length H⁺/Pi symporter was expressed.

We therefore concluded that this (rather than degradation) might be a cause of the production of truncated ALA synthase fusion proteins, but as no *in vitro* transcription-translation assays were performed, we were unable to verify this.

Moreover it is possible that the truncated purified fusion proteins could be as a result of both degradation and translation problems.

5. Western blotting

Western blots were performed to verify that the purified proteins eluted from the columns were indeed *Schistosoma japonicum* GST fusion proteins. Using a polyclonal rabbit anti-*Schistosoma japonicum* GST antibody at a dilution of 1:1000, bands corresponding in size to the purified fusion proteins were visualized on the Western Blot.

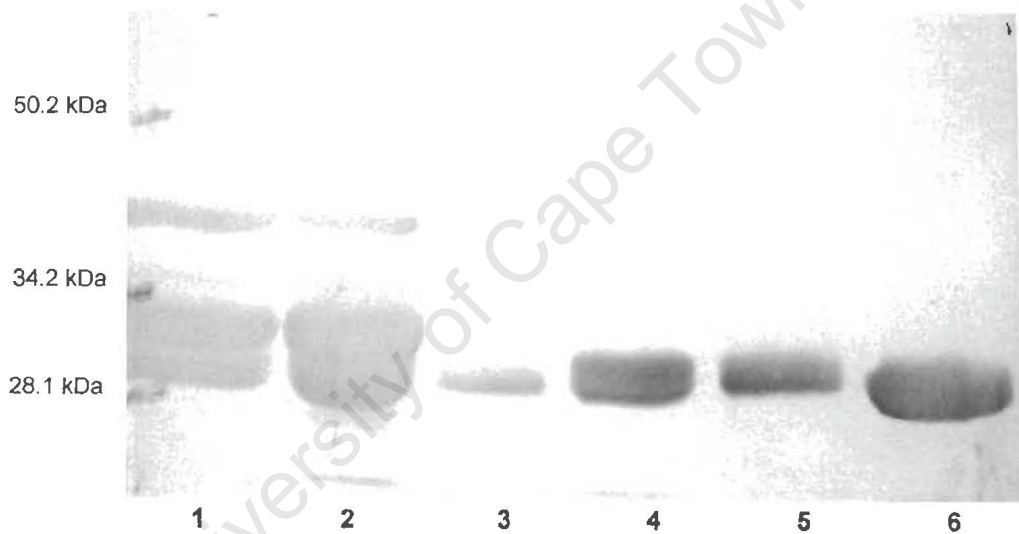


Fig 3.3.8 Western blots performed using anti *Schistosoma japonicum* GST antibodies. In lanes 1 and 2 FP 3(fusion protein 3 – i.e. fragment 3) is present. Lane 3 contains FP 2(fusion protein 2), lane 4 contains FP 4(fusion protein 4), lane 5 contains FP 1(fusion protein 1) and lane 6 contains *Sj* GST.

6. Production of antibodies to ALA synthase fragment 3

We were unable to obtain Thrombin cleavage of FP1 or FP3 under standard conditions (enzyme to substrate concentration of 10u/mg fusion protein, room temperature and a time period of 22 hours.) This may be related to the folding of the fusion protein obscuring the thrombin cleavage site, or to denaturation of the thrombin in detergent.

When the thrombin digest was allowed to proceed at 37°C for a period of 24 hours complete degradation of the ALA synthase fragment occurred. We therefore elected to make use of the whole fusion protein for antibody production.

As yield of the FP1 were low, and the fragment small in relation to the size of the *Sj* GST, we decided to concentrate efforts in obtaining antibodies to FP3, the fusion protein that contained an ALA synthase fragment 12 kDa in size. FP3 was considered liable to contain enough ALA synthase epitopes for successful polyclonal protein production in rabbits.

Bulk purifications of FP 3 were prepared and this was used to inoculate rabbits. Ten immunizations were performed. Maximum antibody titres against FP3 were obtained after the 9th and 10th immunizations.

Positive reactions were obtained at dilutions of 1:25600 and 1:1600 when tested with ELISA's and Western blotting, respectively. (See Fig 3.3.9 and 3.3.10).

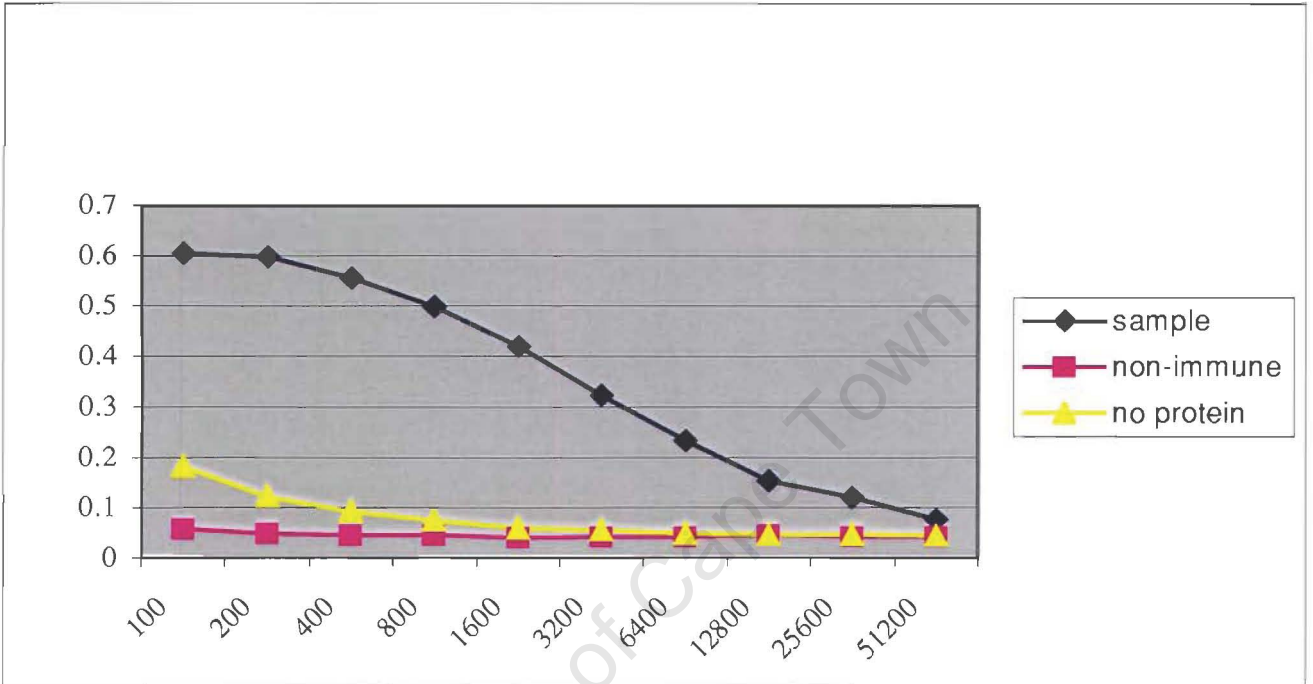


Fig 3.3.9 Elisa performed to test antisera from a rabbit immunized with FP 3

Two background signal controls were included - the “non-immune” (using non-immunized rabbit serum) and “no protein” (in which the ELISA wells were not coated with protein). The Y-axis represents the absorbency readings (OD 540) obtained on the ELISA microtitre plate reader. The X-axis represents the serum dilutions.

Figure 3.3.10 displays Western blots of FP 3, using serum from a rabbit previously immunized with FP3, and “non-immune” rabbit serum.

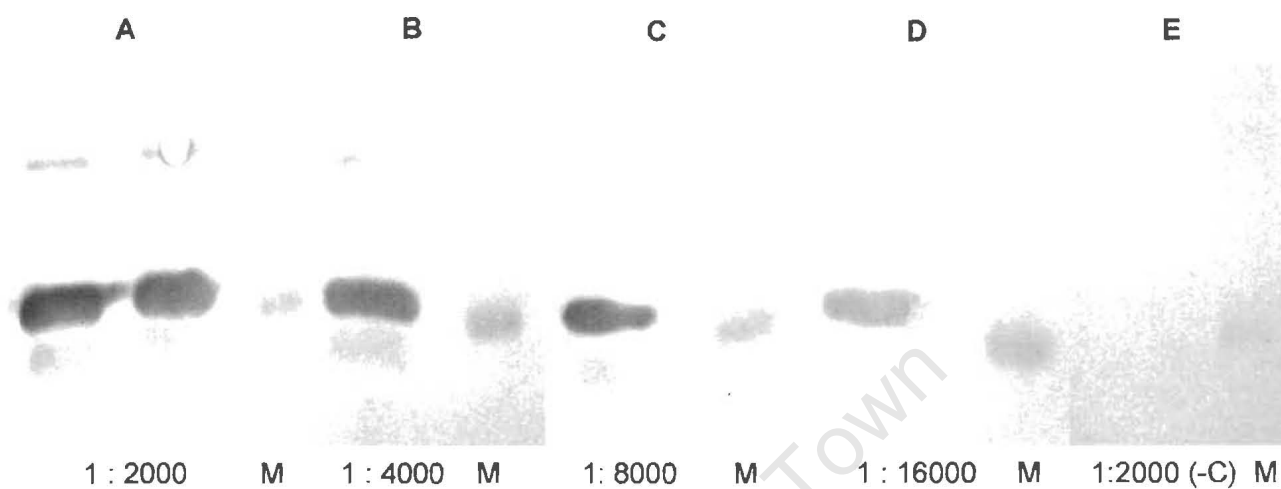


Fig 3.3.10 Western blotting of purified FP 3

Panels A to D show Western blots performed using immunized rabbit sera at dilutions of 1:200, 1:4000, 1:8000 and 1:16000 respectively. Panel E was performed using non-immune rabbit serum at a dilution of 1:2000. The lanes marked M contain a pre-stained molecular weight marker of 30 kDa.

Summary

Research is being hampered due to the small quantities and highly hydrophobic nature of the mitochondrial matrix enzyme, ALA synthase. Murine erythroid ALA synthase is currently the only form of ALA synthase to be successfully hyper-expressed in *E.coli*.

In this work, secondary structure analysis was performed on the human, hepatic ALA synthase amino acid sequence. Fragments predicted to be less hydrophobic, and containing a high proportion of exposed residues were selected for hyper-

expression in *E.coli*. These fragments were sub-cloned into the *E.coli* expression vector, pGEX-2T, which expresses foreign proteins as *Schistosoma japonicum* fusion proteins. A 12-kDa fragment of human hepatic ALA synthase was successfully expressed in *E.coli*, as a fusion protein, and purified to homogeneity. Rabbits were inoculated with the purified fusion protein, and antibodies were raised to the fusion protein. The fusion protein proved to be highly immunogenic in rabbits, with antibodies positive to a titre of 1:25600 (using ELISA).

The next two chapters involve the detailed characterization of the antibody.

University of Cape Town

Chapter Four

Characterisation of the Antibody Produced to the GST-Fragment 3 Fusion Protein

4.1 Introduction

Our decision to proceed with immunization of rabbits with the entire fusion protein complex was based on two considerations: We were unable to separate the *Schistosoma* GST from the fragment 3 using thrombin. Secondly, Smith et al (1986) reported that despite a 42% homology between the *Schistosoma japonicum* (*Sj*) GST and Rat Yb1 isozyme (which is most similar to the human μ GST isozyme), no immunological cross-reactivity had been observed between the *Sj* GST and any rat isozymes. Furthermore, according to the manufacturers of the *Sj* GST fusion protein (Pharmacia) there is no immunological cross-reactivity between *Sj*GST and human GST – although they were unable to produce any evidence for this observation.

Extensive literature reviews did not mention any potential for cross-reactivity, but as the antibody was to be used for immuno-cytochemical studies in humans it was important to prove that there was not immunological cross-reactivity with human GST – particularly μ GST and that antibodies were present to the ALA synthase portion of the fragment.

In order to show cross-reactivity to ALA synthase we needed to generate a control with full-length processed ALA synthase, without *Schistosoma* GST being present. Because of the problems we experienced trying to express full length ALA synthase in *E.Coli*, we decided to express ALA synthase in a eukaryotic system.

Neal et al 1997 were able to show that ALA accumulation in CHO (Chinese

hamster ovary) cell culture resulted in inhibition of colony formation and decreased cell survival. To minimize toxicity as a result of ALA formation, the mitochondrial-directing region would be removed, hopefully preventing import into the mitochondria and hence preventing substrate access, but still allowing the mature enzyme to be expressed.

Immunocytochemical studies could then be performed on the transfected cells to confirm cross-reactivity with ALA synthase. When COS cells were tested for immunological reactivity with FP3 none was visible, so this was chosen as a suitable eukaryotic system for transfection experiments involving human ALA synthase.

4.2 Materials and Methods

Materials

Primer designer software for windows (Scientific and Educational software version 2.0) was made use of for designing of the ALA synthase primers.

Human liver was obtained from 2 male cadavers in their early thirties. Ethics committee approval for removal of liver tissue was obtained. Both victims died instantly after being shot and a specimen of liver was obtained within 12 hours of death. The tissue was stored at -80°C until required.

Methods

1. Cytosolic preparation of human liver

Preparation of cytosol (and subsequent purification) took place at 4°C . The liver was cut into small pieces and placed in homogenization buffer (see A2) to make a 30% weight/volume homogenate.

Initial homogenization was performed using an Ultra-turrex homogenizer (Janke and Kunkel, Germany), using 20 second bursts of homogenization, followed by 20 seconds of incubation on ice. Final homogenization was performed using a motorized Potter-Elvehjem glass-teflon homogenizer.

The homogenate was centrifuged in a bucket handle rotor at 24 000g for a period of 1 hour in a Beckman J21-C centrifuge. The supernatant layer was removed and re-centrifuged at 100 000g for 2 hours in a Beckman L8-70M ultracentrifuge, and subsequently filtered through a 0.22 μ m Millipore filter.

The cytosol so obtained was tested for the presence of μ -GST using double immunodiffusion.

2. Double immunodiffusion to test for the presence of human μ GST

This was performed according to the method described by Ouchterlony (1958). The detailed method is available in A 1.19. Antiserum to human μ GST (kindly produced by Ann Corrigan, in rabbits) was used to test for the presence of μ GST in the liver cytosol obtained.

Agar plates were made as described in A1.19. Four mm holes were punched into the agar in a rosette pattern (namely 6 holes surrounding a central hole).

In 2 of the rosettes, 10 μ l of antiserum to μ GST was pipetted into the central well, while in the peripheral wells of each rosette, either 10 μ l of cytosol from liver "A" or liver "B" was pipetted in doubling dilutions.

In a further 2 of rosettes 10 μ l of cytosol preparation from either liver "A" or "B" was pipetted into the central well – in one of the rosettes, cytosol from liver "A" was used, while in the other rosette, cytosol from liver "B" was used with 10 μ l of

antiserum to μ GST being pipetted into the peripheral wells in doubling dilutions.

Diffusion between cytosol and antiserum was allowed to take place for 48 hours as described in A 1.19. The plates were washed in normal saline for 72 hours to remove unprecipitated protein, followed by a 4-hour wash in double distilled water, before being stained for 2 hours in amido-black. The gels were then destained using 5% acetic acid.

3. Human GST purification

These were purified using a hexyl-GSH affinity column according to the method described by Guthenberg and Mannervik (1979). The principle is similar to that used in the purification of the *Sj* GST fusion proteins – relying on the affinity of the GST for the glutathione for binding to the column followed by elution using an excess of glutathione.

A volume of 10ml hexyl-GSH sepharose was used per 50ml of cytosol. The column was equilibrated with equilibration buffer as described in A2. Cytosol was applied to the column at a flow rate of 17,5ml/hour. The column was washed overnight with equilibration buffer, until the OD_{280nm} of the eluant was identical to that of the equilibration buffer.

The column was subsequently washed with equilibration buffer containing 0.2M NaCl to remove non-specifically bound proteins, after which the GST mixture was eluted using 5 mm Hexyl-GSH Solution (described in A2). The detailed method is seen in A 1.20.

4. Western blots

These were performed according to the method described by Towbin (1979) as described in detail in A1.13 and in Chapter 3.

For both blots, the human GST mixture and purified FP 3 were run on a gel as

described in A 1.12. The initial blot used the antibody to human μ GST at a concentration of 1:2000 as primary antibody, while in the next blot the primary antibody used was that generated to FP3, at a concentration of 1:2000.

5. Construction of the His-ALA-synthase-EGFP and cloning strategies

As described in chapter 3, full-length human hepatic ALA synthase cDNA was obtained from Prof. DF Bishop, Mt Sinai, New York. This was provided as an insert sub-cloned into the *Hind III* and *Eco RI* sites of the pGEM vector and referred to as pGEM-ALA synthase (pGEM-ALAS).

The vector chosen for eukaryotic expression of ALA synthase was the eukaryotic expression vector, pEGFP-N1. This 4651 bp circular vector was obtained from Clontek and expresses proteins as amino terminal fusion protein with EGFP (Enhanced Green Florescent Protein). EGFP is a red shifted variant of the protein GFP, which fluoresces when excited by light at wavelength 488nm, and emits light at a wavelength of 507 nm.

One is thus able to screen colonies for successful expression of protein, using a fluorescent microscope, set at 488nm, and cells expressing the EGFP fusion are visible as green fluorescing cells.

For propagation of the vector in *E.coli*, the vector contains a pUC-19 derived origin of replication and a kanamycin/neomycin resistance cassette, allowing selection, using kanamycin. For eukaryotic cell expression, a CMV early promoter and SV 40 polyadenylation signal is present. The neomycin (kanamycin) resistance cassette contains the SV40 early promoter and Herpes Simplex thymidine kinase, which allows selection of stably transfected cells using G418 (an antibiotic similar to neomycin, which is toxic to COS cells in the absence of the neomycin resistance cassette).

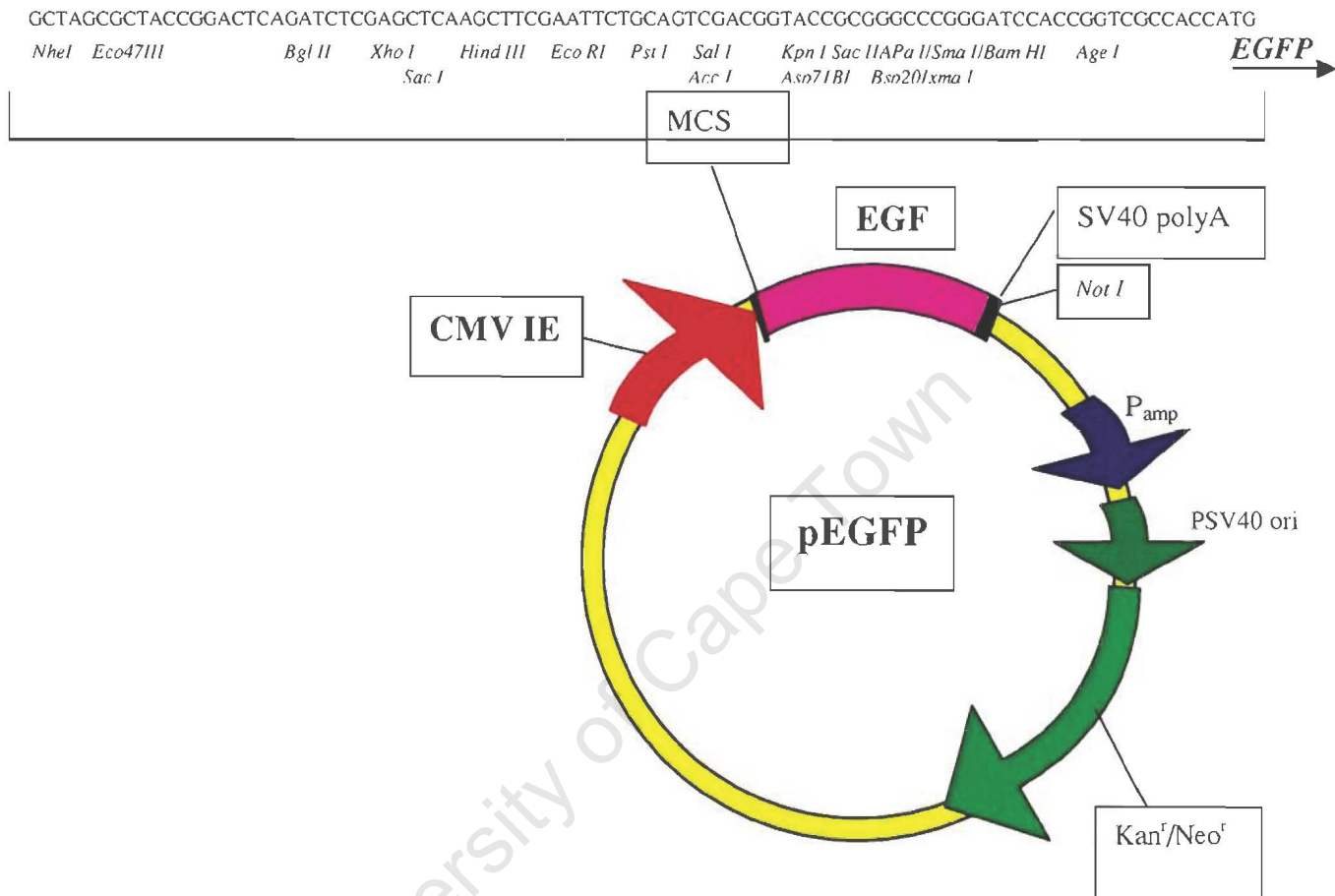


Fig 4.2.1 The structure of pEGFP. CMV IE refers to the intermediate early promoter of CMV. The multiple cloning site (MCS) of pEGFP is illustrated and genes cloned into this area are expressed as fusions to the amino terminus of EGFP as there is no intervening stop codon.

To attempt to decrease the potential toxicity of active ALA synthase, the mitochondrial directing region was removed, in the hope that the enzyme would not be imported into the mitochondrion, and would therefore not have the substrate

1997 and chapter 2 page 71), the mitochondrial directing region was removed, in the hope that the enzyme would not be imported into the mitochondrion, and would therefore not have the substrate access necessary to produce ALA.

Furthermore we decided to introduce a histidine tag at the amino terminus of ALA synthase. If expression in eukaryotic cells was highly successful we wished to attempt purification and further characterization of ALA synthase, and a histidine tag would be a useful tool for purification using a Nickel column.

Primers were designed, using Primer Design software, corresponding to the first 400bp of ALA synthase. The forward primer contained the sequence for an 8 amino acid histidine tag, together with the sequence for the *Eco RI* restriction enzyme, to facilitate cloning.

The sequences of the forward and reverse primers are as follows:

| | Position | Sequence |
|-----------------------|----------|-------------------------------------------------------------------|
| Forward Primer | 151 | 5'-GCCGAATTCATGCATCACCACCACCAT CACCATCAC-GCAGCAGTACACTACCAA-3' |
| Reverse Primer | 511 | 5'-GGAAGTTCTTCAGCAGTCCA-3' |

Table 4.2.1 Primers for amplification of the ALA synthase fragment. The red shaded nucleotides represent the *Bam HI* restriction enzyme site.

The figure below describes how the pEGFP-ALA synthase construct was produced.

access necessary to produce ALA.

Furthermore we decided to introduce a histidine tag at the amino terminus of ALA synthase. If expression in eukaryotic cells was highly successful we wished to attempt purification and further characterization of ALA synthase, and a histidine tag would be a useful tool for purification using a Nickel column.

Primers were designed, using Primer Design software, corresponding to the first 400bp of ALA synthase. The forward primer contained the sequence for an 8 amino acid histidine tag, together with the sequence for the *Eco RI* restriction enzyme, to facilitate cloning.

The sequences of the forward and reverse primers are as follows:

| | Position | Sequence |
|-----------------------|----------|-------------------------------------------------------------------|
| Forward Primer | 151 | 5'-GCCGAATTCATGCATCACCACCACCAT CACCATCAC-GCAGCAGTACACTACCAA-3' |
| Reverse Primer | 511 | 5'-GGAAGTTCTTCAGCAGTCCA-3' |

Table 4.2.1 Primers for amplification of the ALA synthase fragment. The red shaded nucleotides represent the *Bam HI* restriction enzyme site.

PGEM-ALA synthase was used as the template for the PCR reaction. PCR was performed according to the method described in A.1.6. The annealing temperature used was 52°C. The amplified product was 410 bp in length and contained a unique *BsmI* site at position 417 bp, which was employed in creating the new construct. This fragment was subjected to RE Digestion, first with *EcoRI*, then followed by *BsmI* as described in A1.3. This yielded a DNA fragment 266 bp in size.

The pGEM-ALA synthase construct was subjected to restriction enzyme digestion with *BsmI* and *EcoRI*, yielding a fragment 1678 bp in size.

These digested fragments of ALA synthase were resolved on a 1.5 % agarose gel, run at 80V (see A 1.5). The appropriate band were then excised from the gel and purified using a DNA extraction kit (Biorad). The purified DNA was then resuspended in water and an aliquot of this DNA was run on a gel to check the quantity.

These fragments were sub-cloned into a suitable cloning vector - *pBluescript-SK* to facilitate sequencing. *PBluescript* is a high copy number, *E.coli* phagemid, 2961 bp in size and is supplied by Strategene. It was initially derived from pUC19, and contains the *lacZ* transcription gene, and *T3* and *T7* promoters.

PBluescript-SK was subjected to restriction enzyme digestion with *EcoRI*. This was followed by treatment with Alkaline Phosphatase as described in A 1.3 to prevent re-annealing of the pBluescript DNA.

The 266 bp and 1678 bp fragments of ALA synthase were together ligated into *pBluescript* at a ratio of 2:1 (insert to vector) as described in A1.3. The ligation mixture was transformed into the *E.coli* strain, XL-1 Blue, which had been rendered competent by the RbCl₂ method described in A 1.4.

These were plated for selection on 100µg/ml ψB-agar plates (A2). Viable colonies were selected and grown up in 5 ml of ψB, for small-scale isolation of plasmid DNA (see A1.1). Restriction enzyme digestion and subsequent agarose gel electrophoresis was performed to verify correct insertion of the ALA synthase cDNA.

Following appropriate culture and large-scale isolation of DNA (A 1.2), the

modified ALA synthase was sequenced by automated sequencing using primers designed to the *T3* and *T7* promoters, in order to exclude any errors in the sequence.

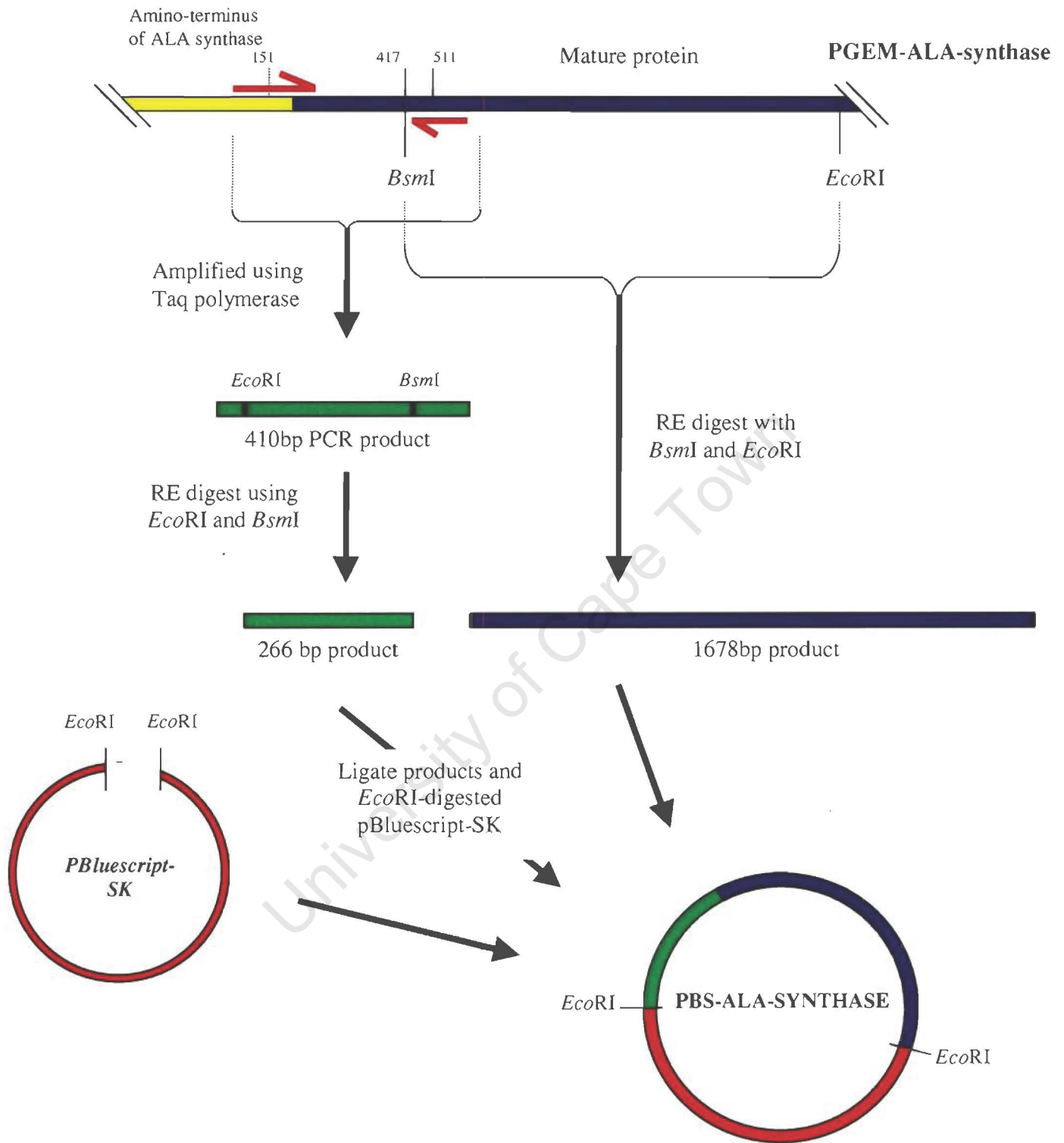
PEGFP-ALA synthase was constructed as follows: The ALA synthase-pBluescript construct was digested with *StuI*. A unique *StuI* site is present in the ALA synthase sequence, close to the stop codon. This was followed by restriction enzyme digestion using *EcoRI* to release the 5' end of the ALA synthase sequence, from pBluescript. This 1944 bp fragment was resolved on a 1% agarose gel (see A 1.5) followed by purification of the DNA from the gel using a Biorad – kit.

PEGFP was subjected to RE digestion using *EcoRI* and *SmaI* - both are unique restriction enzyme sites present in the multiple cloning site of pEGFP. This DNA was cleaned using a DNA Clean-up Kit, obtained from Roche Molecular Biologicals, used according to manufacturer's instructions.

The pEGFP and the his-ALAS were ligated at a ration of 2:1 (insert to vector) as described in A 1.3. As previously described, the ligation mixture was transformed into competent XL1-Blue and plated for selection on kanamycin- $\psi\beta$ plates (see A2). Viable colonies were grown in ψ broth and DNA was isolated as described in A1.1. DNA from these colonies was subjected to RE digestion and the products were resolved on agarose gel to confirm identity of the clones.

The cloning strategy is presented in schematic form in Fig. 4.2.2 below.

Bulk DNA preparations (μg quantities) of a correct clone were processed according to the method described in A 1.2, for use with COS cell transfections.



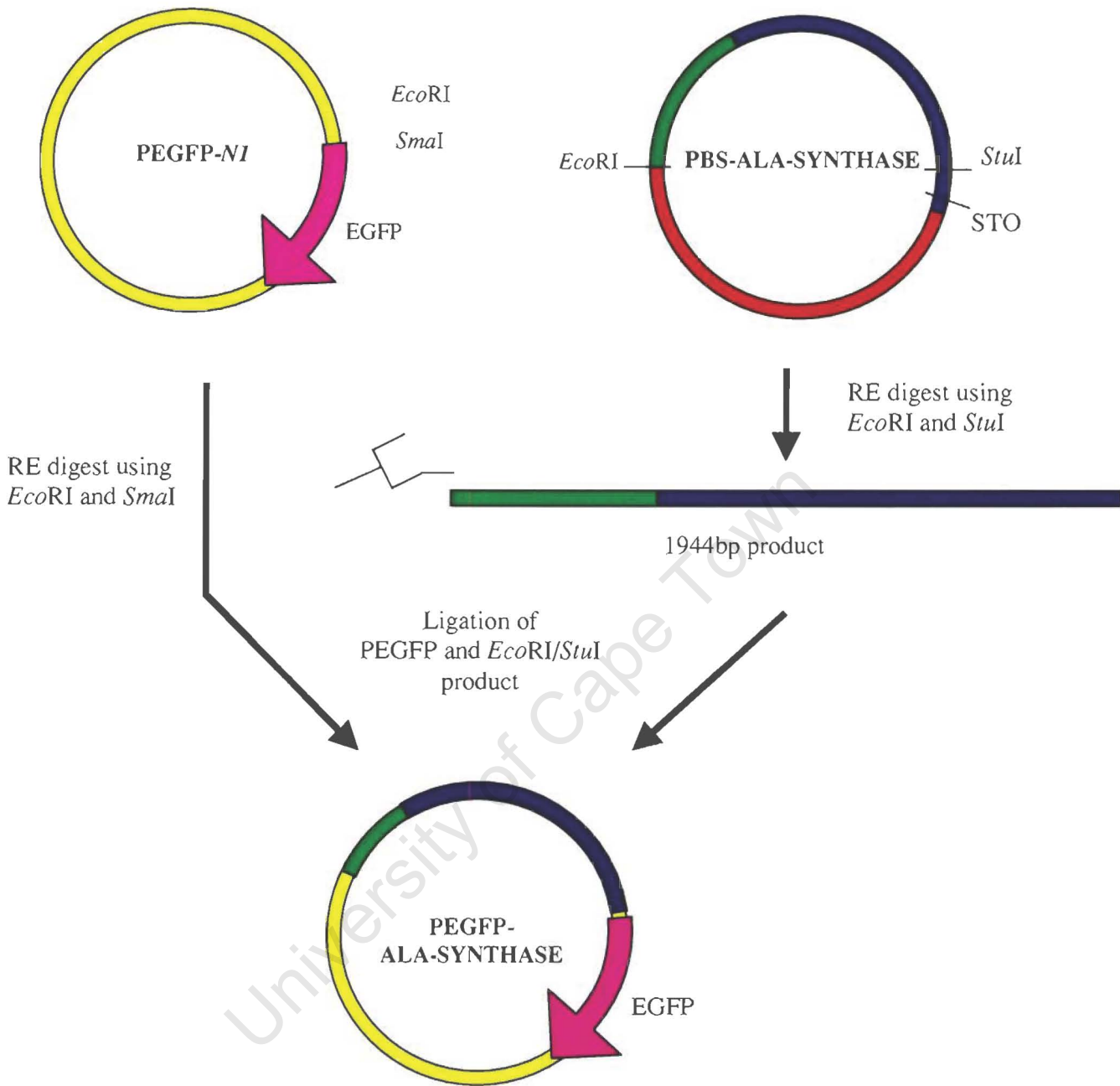


Fig 4.2.2. The cloning strategy for sub-cloning the processed ALA synthase into the Eukaryotic expression vector, pEGFP, is illustrated in schematic form.

6. *COS cell transfections with DEAE-DEXTRAN*

COS cells were grown as described in A 1.17 and transfected using DEAE Dextran (see A 1.18).

Briefly, COS cells were plated onto 2 chambered microscope slides that had been treated with Poly-L-Lysine. After overnight incubation at 37 °C and 5% CO₂, the cells were incubated in the DEAE dextran with DNA (3mg DEAE dextran and 2.5 µg DNA per well).

Sample slides included either pEGFP DNA or ALAS-EGFP DNA in the DEAE dextran, while negative controls contained no DNA. After 4 to 5 hours of incubation with DEAE dextran, the COS cells were subjected to a 1 hour chloroquine shock, followed by a 2 minute DMSO shock.

The cells were incubated in DMEM/FCS (as described in A 1.18) overnight at 37°C. The following morning the cells were incubated at room temperature for 4 hours to increase fluorescence of the EGF protein.

These cells were fixed by incubation of the slide in 100% methanol for a period of 5 minutes followed by air-drying for 30 minutes. After the chambered apparatus was removed from the microscope slides, they were cover-slipped using the water-soluble mounting medium, glycergel.

7. *Visualization of EGFP using fluorescent microscope*

The fluorescent microscope was set as for visualizing FITC labelled proteins. The excitation wave-length of the microscope was 480 nm – close enough to the excitation maximum for EGFP (488nm).

Cells that were expressing EGF protein would fluoresce green under microscopy. Non-transfected cells were included in this experiment as a negative control to exclude auto-fluorescence.

8. Immunocytochemistry of transfected COS cells

COS cells were transfected and treated as described above up until, and including the methanol fixation step. Chambers of cells of a microscope slide were transfected with pEGFP or with pEGFP-his-ALA synthase (pEGFP-his-ALAS).

A negative control experiment was performed on pEGFP and pEGFP-his-ALAS transfected cells using non-immune rabbit serum as primary antibody. The samples (COS cells transfected with both pEGFP and pEGFP-his-ALAS) were treated in an identical fashion to the negative controls, instead using immune rabbit serum, from the rabbit immunized to FP3.

Automated immunostaining was performed using the DAKO Techmate-500. All solutions used were standardized DAKO solutions specifically for use with the Techmate-500. After several wash steps (using DAKO wash solution) the slides were blocked using 1:20 dilution of non-immune goat serum with DAKO antibody diluent.

Primary antisera was applied at a dilution of 1:1000 to the cells and allowed to incubate for 25 minutes. The secondary antibody used was biotin labeled goat anti-rabbit. Thereafter streptavidin labeled HRP (Horse radish peroxidase) was applied. DAB (Di-amino-benzidine) was used for visualization.

A positive result would result in brown staining of the cytoplasm of the cells. Finally the nuclei of the cells were stained using haematoxylin.

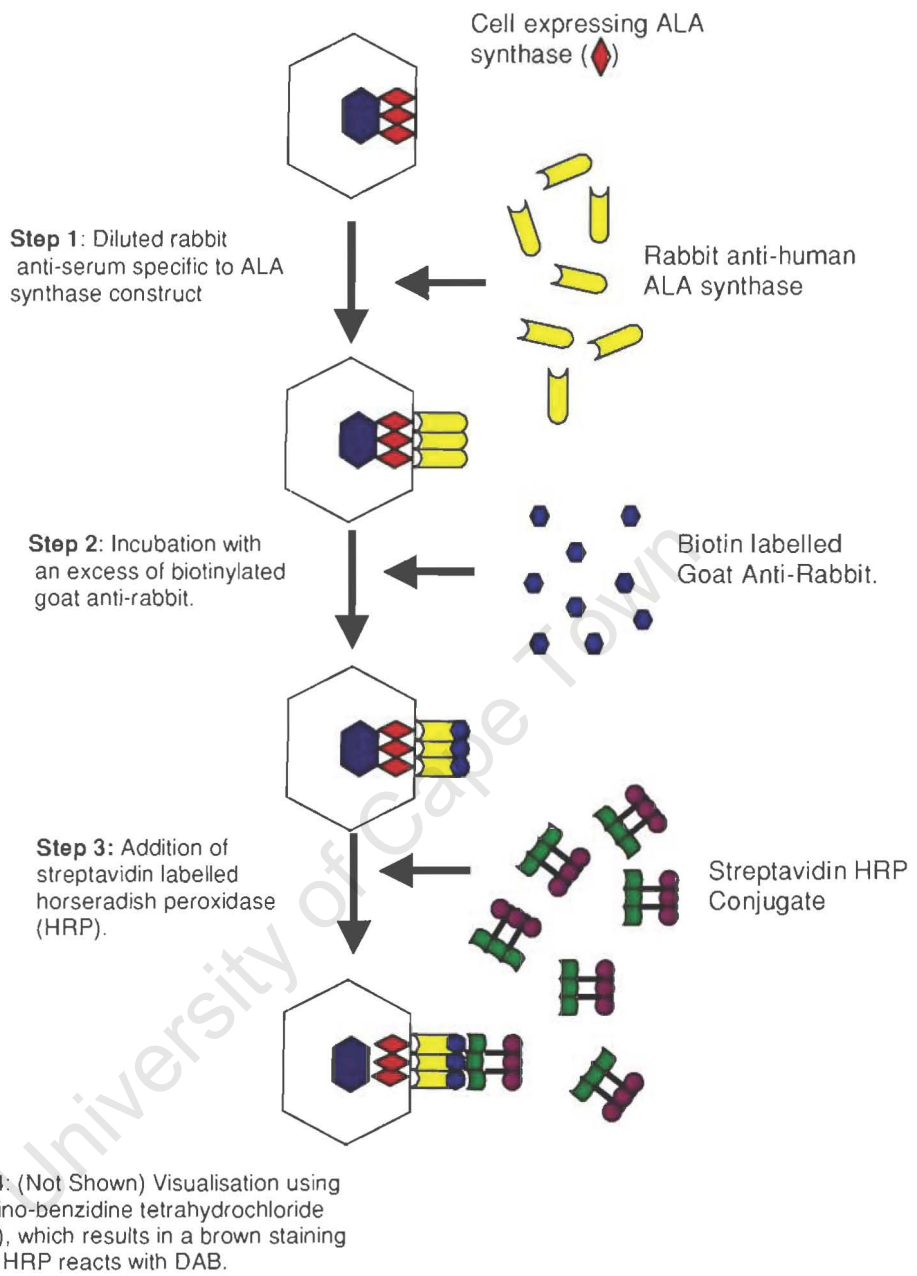


Fig 4.2.3 Schematic representation of the HRP-Streptavidin-Biotin Anti-rabbit Immune complex method.

4.3 Results and discussion:

1. Double immunodiffusion to test for the presence of human μ GST

Only 40% of human liver contains μ GST, therefore we needed to ensure that this was present in the cytosol of the liver that we would be using. Cytosol was prepared from 2 human livers, designated A and B. Cytosol from liver A did not contain μ GST as is demonstrated in the double immunodiffusion below, which was checking for precipitation of rabbit antihuman μ GST.

The liver B cytosol contained μ GST as demonstrated in the double immunodiffusions shown below, and was therefore ideal to verify lack of cross-reactivity between μ GST and *Schistosoma japonicum* GST.

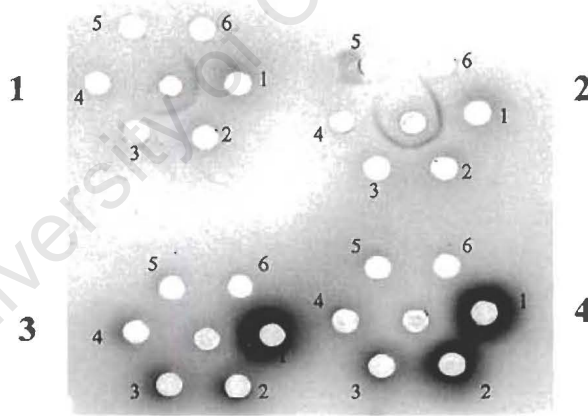


Fig 4.3.1 Immunodiffusion, showing in the rosettes labeled “a” and “b”, the cross-reactivity of rabbit anti-human μ GST (central well) and cytosol from liver “B”(peripheral wells). In peripheral well “1”, neat liver cytosol from liver ‘B’ is present. In wells 2 to 6, doubling dilutions of cytosol from liver “B” is present. In the immunodiffusions in rosettes “3” and “4”, the lack of cross-reactivity of rabbit anti-human μ GST antibody (central well) to cytosol from liver “A” is shown.

2. Human hepatic GST purification

GST purification was performed on cytosol from liver B using a h-GSH affinity column as described in A 1.20. The purified product consisted of a mixture of human GST's, including μ GST. This was tested for cross reactivity to the anti-sera to the fusion protein as described below.

3. Western blotting

There was no immunological cross-reactivity demonstrated between human GST's (including μ GST) and the anti-sera to FP3, using Western blotting, as is shown in the figure below. In addition the FP3 does not cross-react with polyclonal antibodies to μ GST.

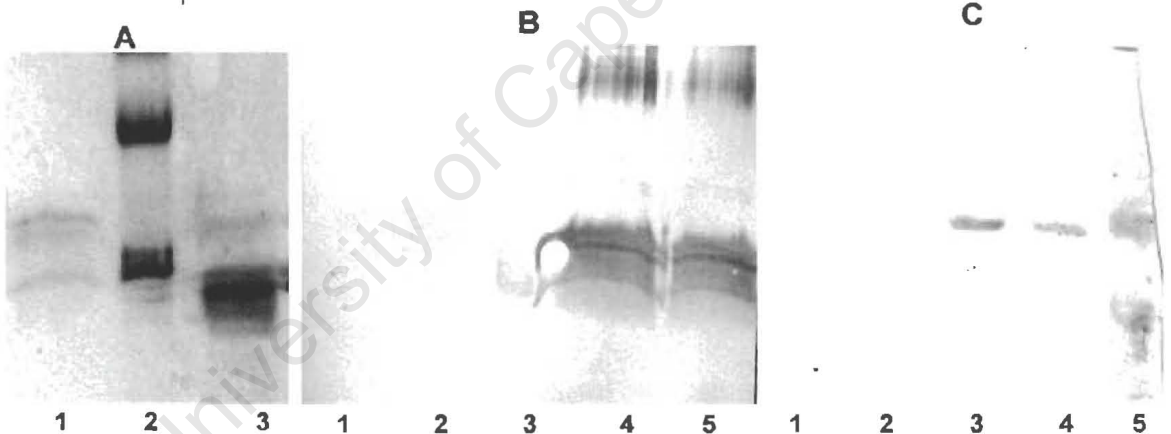


Fig 4.3.2 SDS polyacrylamide gel(10%) of lig 3 and human GST and Western blots of human GST and FP 3, using antibody to *Shistosoma japonicum* (B) and to μ GST(C).

- SDS polyacrylamide gel (10%) showing in lanes 1, 2 and 3, purified FP3, molecular weight markers and purified human GST mixture, respectively.
- Western blot using antibody to *Shistosoma japonicum* GST (*Sj*GST). Human GST (lanes 1 to 2), molecular weight markers (lane 3) and *Sj*GST(lanes 4 to 5) are present. No cross reactivity to human GST's is visible.
- Western blot using antibody to human μ GST. *Sj* GST (lanes 1 to 2), human GST(lanes 3 to 4) and molecular weight markers (lane 5) are present. The *Sj*GST does not immunologically react with the rabbit anti-human μ GST.

The result confirms that antibodies to *Shistosoma japonicum* GST do not cross-react with antibodies to human GST's and suggests that the anti-sera is cross-reacting to human ALA synthase, rather than human GST. While we were convinced that the antibody we had raised was not only directed at the GST portion of the fusion protein it was possible that the antibody was not reacting to the ALA synthase portion either, but to some unknown contaminant. Hence in next experiment definitive proof is provided of the immuno-reactivity between human hepatic ALA synthase and anti-sera to the fusion protein.

4. Construction of the His-ALA-synthase-EGFP

The Histidine tag-*BsmI* product was successfully amplified using PCR and a product conforming to the expected size of 417 bp was obtained. Following restriction enzyme digest with *EcoRI* and *BsmI* a product conforming to the expected size of 266bp was obtained. This is illustrated in figure 4.3.3 below.

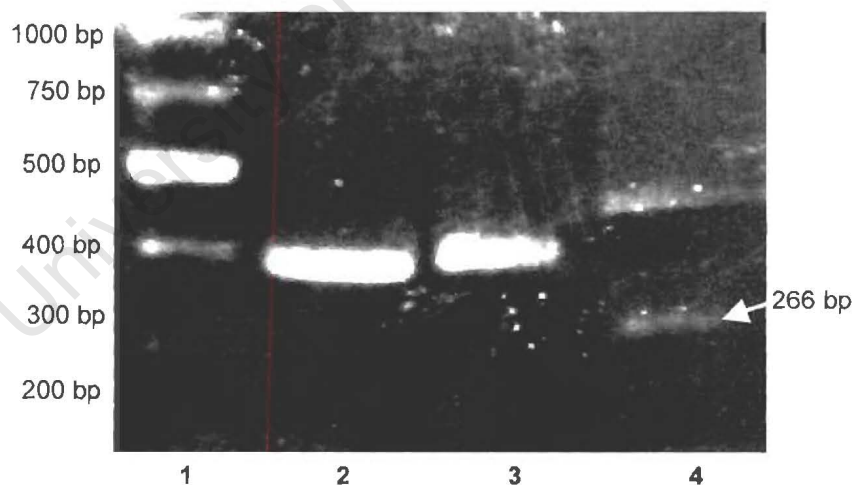


Fig 4.3.3 PCR amplification, followed by *EcoRI* and *BsmI* digest of the His-ALA S fragment electrophoresed on a 2% agarose gel and stained with ethidium bromide. Lane 1 corresponds to a DNA molecular weight marker. Lane 2, 3 and 4 contains *EcoRI* digest of the PCR product, the undigested PCR product, and the incomplete *BsmI* digest of Lane 2

respectively – the lower band corresponding to the 266 bp product used in creation of a histidine-tagged processed ALA synthase product.

After digesting pGEM-ALA S using *BsmI* and *EcoRI* a product of 1678 bp was obtained. This 1678 bp product and the 266bp PCR product were ligated to one another and into the *EcoRI* site of pBluescript (see figure 4.3.4 below). The his-tagged processed ALA synthase was successfully constructed and sub-cloned into *P-Bluescript*.

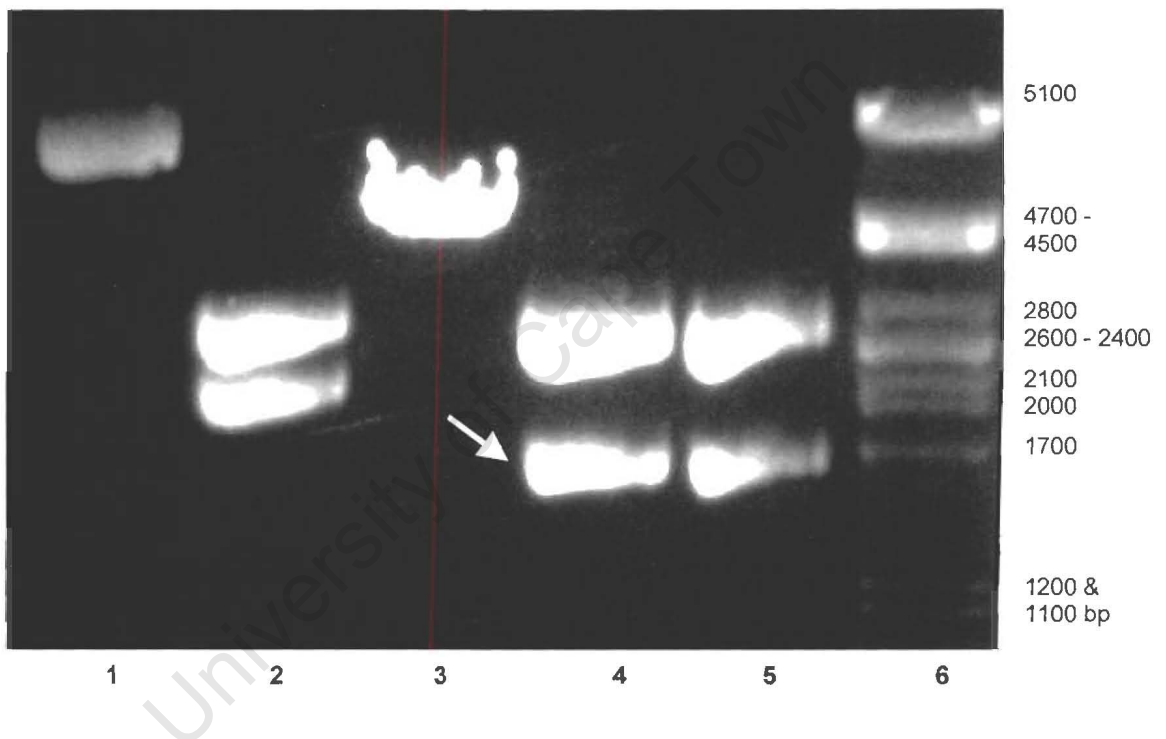


Fig 4.3.4 The purified plasmid preparation of pGEM ALA S has been subjected to an *EcoRI* and *BsmI* restriction enzyme digestion. The products of the restriction enzyme digest have been electrophoresed on a 1% agarose gel and stained with ethidium bromide. Lane 6 corresponds to the molecular weight markers. Lane 1 contains uncut pGEM ALA synthase, lane 2 contains an *EcoRI* digest of pGEM ALA synthase, lane 3 a *BsmI* digest of pGEM ALA synthase, while lanes 4 and 5 contain *BsmI* and *EcoRI* digestions of pGEM ALA synthase. An arrow indicates the expected product, of 1678 bp.

Automated sequencing using the T3 and T7 promoters revealed no errors in the ALA synthase insert. After releasing the histidine tagged ALA synthase insert from pBluescript, it was sub-cloned into the *EcoRI* and *SmaI* sites of pEGFP. An agarose gel showing a *NotI EcoRI* digest of the pEGFP –his-ALA synthase construct is shown in figure 4.3.5.

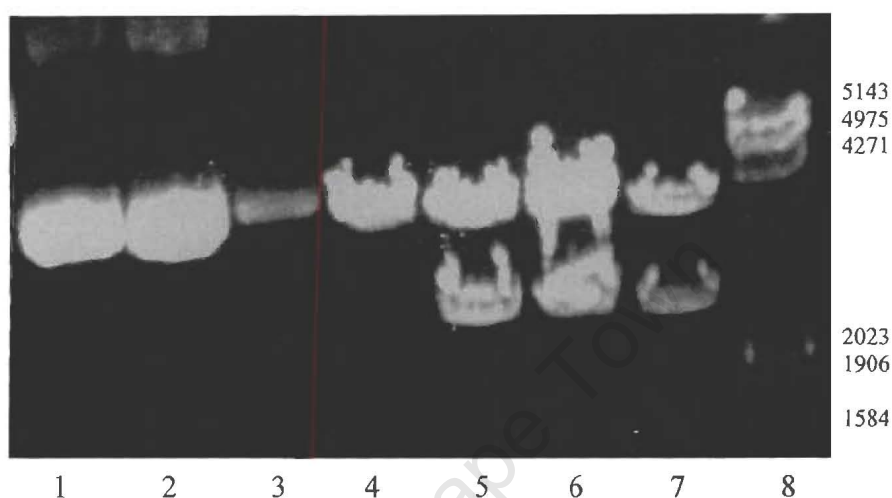


Fig 4.3.5 Purified plasmid preparations of pEGFP and pEGFP-ALAS, and *EcoRI* and *NotI* restriction enzyme analysis of these plasmids. Products of the plasmid purifications and restriction enzyme digestion have been electrophoresed on a 1 % agarose gel and stained with ethidium bromide. Lane 8 corresponds to molecular weight markers. Lane 1 corresponds to uncut pEGFP, lanes 2 to 4 correspond to uncut pEGFP-ALAS, lanes 5 to 7 correspond to *EcoRI* and *NotI* digests of pEGFP-ALAS. The size of the bands in lanes 5 to 7 correlate well, with the expected sizes of 3929bp and 2715 bp.

5. COS cell transfections

COS cells were transfected using DEAE dextran method. The following morning, live cells were present – although there were only half the number of cells on the microscope slide containing the pEGFP-his-ALAS transfected cells compared to the pEGFP transfected cells, and the cells subjected to the transfection step, using no DNA. Moreover the cells containing the his-ALA synthase construct died rapidly over the next 24 hours and 48 hours after transfection, so that very few live cells remained. In contrast, 48 hours after transfection the pEGFP transfected cells increased in density, suggesting

as a positive control to establish specificity of my antibody to ALA synthase, further use of this technique requiring bulk preparations of ALA synthase (for e.g. to characterize ALA synthase further) would not be possible.

The transfected COS cells were to be used 24 hours after transfection for fluorescent microscopy and immunocytochemistry.

6. Fluorescent microscopy

The cells were visualized under a fluorescent microscope. It appeared that the cells had been successfully transfected, as seen by green fluorescence of cells transfected with the pEGFP construct and cells transfected with the pEGFP-his-ALA Synthase construct. Fig 3.2.5 shows a photograph of transfected cells expressing pEGFP. The control cells – viz. those subjected to the transfection proceedings, which had no DNA added did not show any green fluorescence, thus proving that the fluorescence seen was not auto fluorescence. Photographs showing the fluorescence in the pEGFP-ALAS transfected COS cells can be seen in figure 4.3.6.

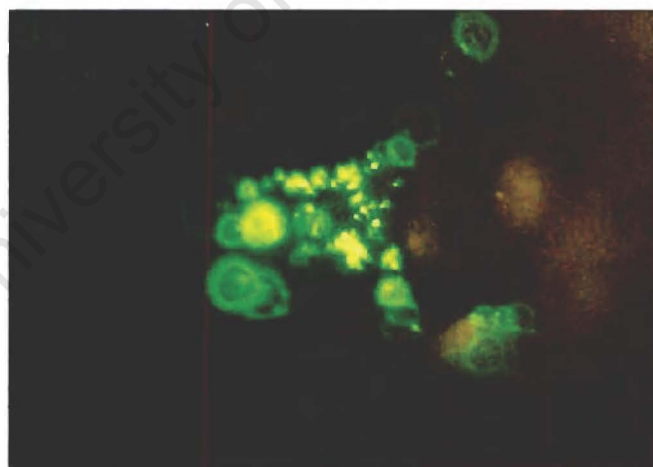


Fig 4.3.6: Fluorescent microscopy of COS cells transfected with pEGFP-ALAS. A high-powered (1000X) enlargement of the COS cells, as visualized under light 400nm wavelength. The green fluorescence indicates the presence of EGFP. No photograph of untransfected cells visualized at 400nm light is present, as this appeared to be a dark visual field, which could not be photographed.

under light 400nm wavelength. The green fluorescence indicates the presence of EGFP. No photograph of untransfected cells visualized at 400nm light is present, as this appeared to be a dark visual field, which could not be photographed.

7. Immunocytochemistry

The immunocytochemistry was performed as described in the methods section. The cells transfected with the pEGFP construct alone, showed no immunostaining, following incubation with ALA-synthase antisera and with negative control rabbit sera. The cells containing the pEGFP-his-ALA synthase construct showed no immunostaining with the non-immune control sera. This can be seen in the figure below.

When immunocytochemistry was performed on the pEGFP-his-ALA synthase transfected cells using antisera obtained from rabbits immunized with fusion fragment 3, brown staining was visible throughout the cells – indicating that the ALA synthase construct was recognized by antibodies to the fusion protein fragment 3.

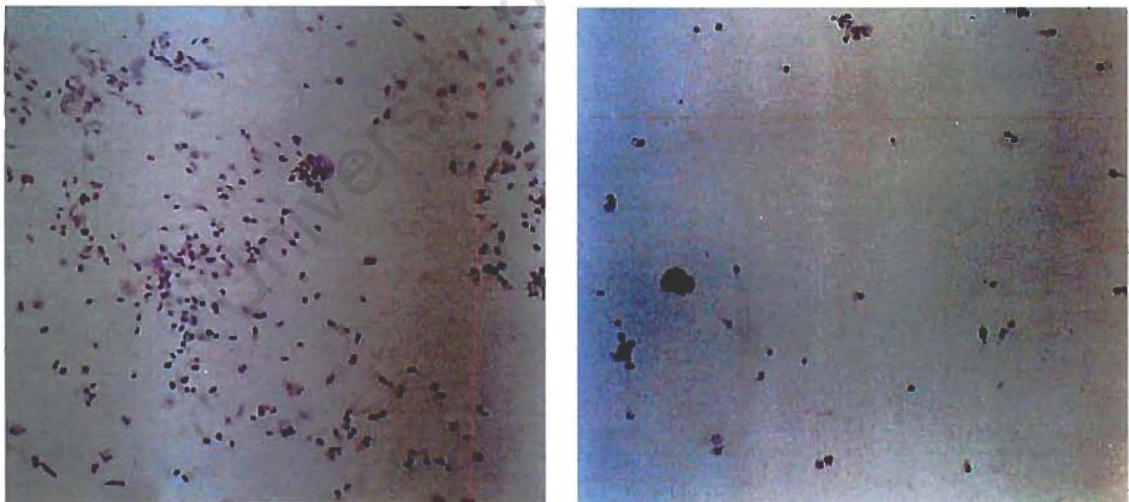


Fig 4.3.7 Immunostaining of COS cells with non-immunized rabbit serum visualized at 100 times magnification. COS cells transfected with pEGFP(left) or pEGFP-his-ALAS (right) were subjected to immunocytochemistry, using non-immune rabbit serum. No immunostaining, (visualized as brown staining of the cytosol) is present.

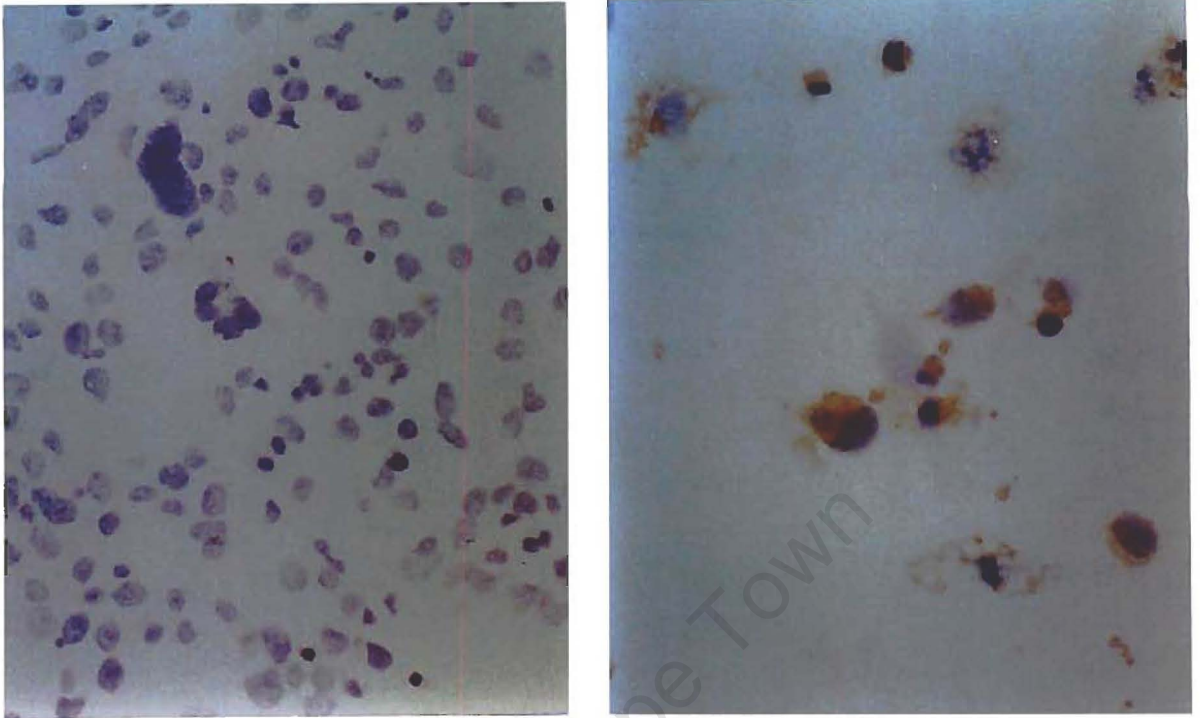


Fig 4.3.8 Immunostaining of COS cells using anti-sera to FP3 visualized at 400 times magnification. COS cells transfected with pEGFP(left) or pEGFP-his-ALAS(right) were immunostained using antisera to FP3. The COS cells transfected with pEGFP (left) show no immunostaining. The COS cells transfected with pEGFP-his-ALAS (right) shows positive staining as indicated by the brown pigment in the cytoplasm of these cells.

Thus we are satisfied that staining obtained in human tissue indicates cross-reactivity between the ALA synthase protein and the antisera to FP3.

Summary

Having produced a polyclonal antibody to FP3 (fusion protein 3 – the *Schistosoma japonicum*-GST-ALA synthase fusion protein) as described in the previous chapter, we undertook to characterise firstly in order to establish that there was no immunological cross-reactivity between any possible *Schistosoma* GST antibody and human GST as this would render the antibody unsuitable for human ALAS immunocytochemical studies.

cross-reactivity between any possible *Schistosoma* GST antibody and human GST as this would render the antibody unsuitable for human ALAS immunocytochemical studies.

Western blotting was performed using a human GST mixture that included μ GST and showed no cross-reactivity with the antisera to the fusion protein (FP3). Furthermore antibodies to μ GST showed no cross-reactivity to the fusion protein.

Secondly, given the absence of suitable positive control system it was also important to prove cross-reactivity of the antisera to human ALA synthase.

To prove cross-reactivity of the FP3 antibodies to ALA synthase, ALA synthase was transiently transfected into COS cells, using DEAE dextran. The antisera to FP3 cross-reacted with the ALA synthase transfected COS cells, but no cross-reactivity to non-transfected COS cells was present, thus proving that the antisera recognized ALA synthase.

In the next chapter, we will be performing immunocytochemistry on a variety of different human tissues to look at the tissue distribution of ALA synthase.

Chapter Five

Further characterization of antibody

5.1 Introduction

Another possible cross reaction of the antibody to the 100 amino acid fragment of human hepatic ALA synthase (F3- fragment 3), described in the previous chapters, is with the erythroid isoform of ALA synthase. In this chapter we set out to examine this potential cross-reactivity and further, to establish whether or not there is cross reactivity with rat hepatic ALA synthase.

There is an amino acid sequence homology of 59% between corresponding areas in F3 and the published human erythroid ALA synthase sequence. Fig 5.1.1 illustrates this.

| | | | |
|-------------|------------|-------------|------------|
| PERVSHLLQD | NLPKSVSTFQ | YDRFFEKKID | EKKNDHTYRV |
| SGKVTHLIQN | NMPG-NYVFS | YDQFFRDKIM | EKKQDHTYRV |
| FKTVNRRRAHI | FPMADDYSDS | LITKKQVSVW | CSNDYLGMSR |
| FKTVNRWADA | YPFAQHSEA | SVASKDVS VW | CSNDYLGMSR |
| HPRVCGAVMD | TLKQHGAGAG | hepatic | |
| HPQVLQATQE | TLQRHGAGAG | erythroid | |

Fig 5.1.1 The fragment of ALA synthase (F3) to which antibodies were generated is aligned with the corresponding area of erythroid ALA synthase. The homologous amino acids are shown in red. The homologous amino acids correspond to 59% of the sequence.

The applications of the antibody would be altered should there be cross-reactivity between the hepatic and erythroid isoforms. We considered that foetal liver, with its erythroid precursors in the hepatic sinusoids, which are known to have high levels of erythroid ALA synthase, could be used to check for cross reactivity to the erythroid ALA synthase. To maximise the chances of

immunostaining in erythroid precursor cells we decided to use multiple samples from different stages of gestation.

Furthermore we considered that should the antibody generated to human ALA synthase cross-react with rat ALA synthase, this could open up many new research applications, as the ethical constraints associated with the use of human tissue are not present. It is easier to control for diet, age, sex, xenobiotic usage in tissue studies performed on rats, although the limitations of a rat model, as discussed in chapter 2 are well described. The homology between rat hepatic ALA synthase and human hepatic ALA synthase in the region to which the antisera was generated is about 90%.

| | | | |
|---------------------|---------------------|---------------------|---------------------|
| PERVSHLLQD | NLPK S VSTFQ | YD R FFEKKID | EKKNDHTYRV |
| PERVSHLLQD | NLPK V VSTFQ | YD H FFEKKID | EKKNDHTYRV |
| FKTVNRR A HI | FPMADDY S DS | LIT K KQVSVW | C SN DYLGMSR |
| FKTVNRR A QI | FPMADDY T DS | LIT N NQVSVW | S SN DYLGMSR |
| HPRVCGAV M D | TLKQHGAGAG | Human | |
| HPRVCGAV I E | TVKQHGAGAG | Rat | |

Fig 5.1.2 The fragment of ALA synthase (F3) to which antibodies were generated is aligned with the corresponding area of rat ALA synthase. Residues that are different between the two species are indicated in red. The homologous amino acids, indicated in black correspond to 90% of the sequence.

5.2 Materials and Methods

Materials

Foetal liver was obtained from archived paraffin sections of foetal liver obtained at time of post-mortems. Care was taken to select blocks where minimal autolysis was present. Haematoxylin and Eosin sections showed the presence of

erythroid precursors in the hepatic sinusoids. Liver was obtained from 8 foetuses between 14 and 25 weeks of gestation.

Rat liver was obtained from discarded rat liver at the microsurgery unit of our Medical School. This was fixed in 10% formalin and made into a paraffin block according to standard protocols.

Method

1. Processing of foetal liver samples and immunocytochemistry

Paraffin sections 0.4 μm in thickness were cut from paraffin blocks of foetal human liver and mounted onto glass slides. Sample slides (which were to be incubated in anti-sera to FP3 - fusion protein 3) as well as a negative control slide (which were to be incubated in non-immune rabbit serum) were cut from 8 foetal liver samples.

These slides were then incubated in 4 successive baths of xylol (at room temperature) to remove paraffin wax from the specimens, over a period of 20 minutes. They were then washed twice in absolute ethanol, to remove the xylol. This was followed by two washes in 96% ethanol, which was soluble in water. Finally the slides were washed in distilled water.

Antigen retrieval was achieved by microwaving the slides. The slides were placed in a plastic slide holder (DAKO) in a citrate-containing antigen retrieval buffer (DAKO). The microscope slides were then microwaved on maximum power for a period of 10 minutes. The slides were allowed to stand in the hot citrate buffer for 20 minutes.

These slides were briefly washed in distilled water, followed by loading onto the DAKO Techmate 500, for immunocytochemistry. The immunocytochemistry technique is described in chapter 4, performed by the Techmate 500 automated immunostainer.

After the staining and visualization procedures are completed as outlined in 4.2, the slides were incubated in several baths of 96% ethanol for 2 to 3 minutes, followed by 2 absolute ethanol washes. The slides were incubated in xylol, and mounted using Entillen (Sarchem)- a xylol soluble mounting medium.

The slides were examined under light microscopy, by an independent, blinded histopathologist. Staining was graded as follows:

1. No staining – i.e. no brown hue was visible in cytoplasm
2. Mild staining – a faint brown blush was visible in cytoplasm.
3. Moderate staining – a darker brown pigment was visible in the cell cytoplasm.
4. Strong staining – a dark brown pigment was visible in cell cytoplasm.

2. Processing of rat liver samples and immunocytochemistry

The method used for preparing slides and immunostaining is as described above. Negative controls were performed using non-immune rabbit serum as previously described and sample slides were treated in the identical fashion, using immune rabbit serum in place of the non-immune serum.

5.3 Results and discussion

1. Immunocytochemistry of foetal livers

In all the negative control slides, no immunostaining was visible.

In the sample slides faint to moderate immunostaining (visible as a brown tint in the cytosol of hepatocytes) was visible in the foetal hepatocytes, indicating that hepatic ALA synthase was being detected. This acted as an internal positive control. However, the very distinctive erythroid precursors, which were present in the hepatic sinusoids did not stain for ALA synthase.

A photograph of a sample slide, as well as a negative control slide, are shown in the figure below.

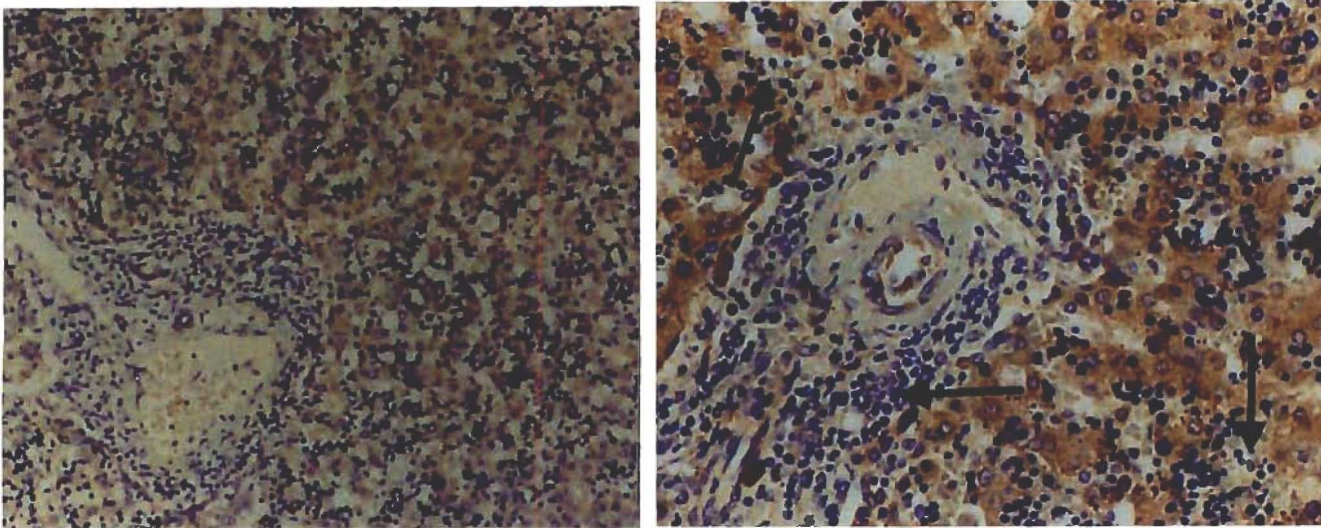


Fig 5.3.1 Immunostaining for ALA synthase in foetal liver. To the left a negative control specimen is present. On the right a sample is present, stained with antibody to ALA synthase. This shows brown staining in the cytoplasm of hepatocytes, indicating the presence of ALA synthase. No staining is visible in the erythroid precursor cells, present in the hepatic sinusoids, which are indicated by the arrow.

Details of the results of the foetal liver immunocytochemistry are presented in the table below.

| Cell Type | Negative controls | Samples | | | |
|----------------------|--------------------------|--------------------|----------------------|--------------------------|------------------------|
| | | No Staining | Weak Staining | Moderate Staining | Strong Staining |
| Hepatocytes | 8 | 1 | 2 | 5 | 0 |
| Bile Ducts | 8 | 3 | 5 | 0 | 0 |
| Erythroid Precursors | 8 | 8 | 0 | 0 | 0 |
| Myeloid Precursors | 8 | 8 | 0 | 0 | 0 |

Table 5.3.1 Immunocytochemistry results of all foetal liver samples analyzed.

We are therefore certain that the anti-sera generated to the fusion protein cross-reacts immunologically with human hepatic ALA synthase, but not with human erythroid ALA synthase.

2. Immunocytochemistry of rat liver

No immunostaining was detected in the negative control slides of rat liver.

Cross-reactivity between the anti-sera to human hepatic ALA synthase and to rat ALA synthase was detected, as can be seen in the photographs in the figure below.

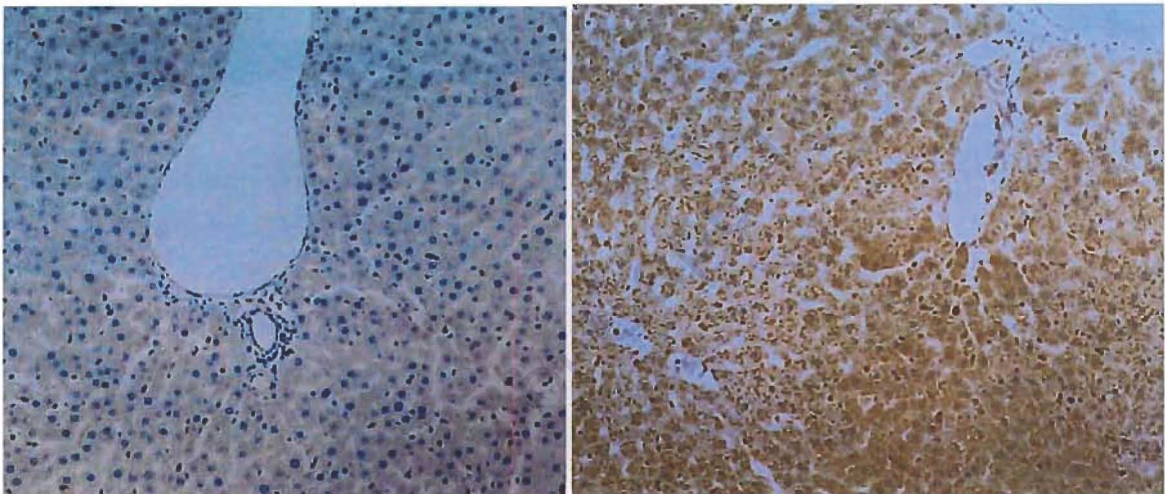


Fig 5.3.2. Immunocytochemistry of rat liver, using antisera to human ALA synthase. To the left a negative control specimen is present . To the right a sample of rat liver was immunostained using anti-sera to FP3 as the primary antibody. Staining is indicated by the brown colour in the cytosol of hepatocytes.

Hence, perhaps predictably, we conclude that the anti-sera generated to the fusion protein cross-reacts with rat hepatic ALA synthase.

Conclusion

The antibody to human hepatic ALA synthase fragment F3 does not cross-react with human erythroid ALA synthase, but it does cross-react with rat hepatic ALA synthase.

Summary

The antibody to FP3 was shown to cross-react with human hepatic ALA synthase, as shown in chapter 4. In this chapter, the antibody is further characterized by assessing cross-reactivity to erythroid ALA synthase and rat hepatic ALA synthase. Sequence alignment between the human hepatic ALA synthase fragment (F3) displayed 59% and 90 % homology to the human erythroid and rat hepatic ALA synthase amino acid sequences, respectively.

Immunocytochemistry revealed no cross-reactivity with erythroid precursor cells (which are known to produce high levels of erythroid ALA synthase) in human foetal liver sinusoids, thus indicating no cross-reactivity to erythroid ALA synthase. However there was immunological cross-reactivity of the FP3-antibody to rat hepatic ALA synthase.

Having characterized the antibody to human hepatic ALA synthase fragment 3 we set about using this antibody to examine tissue cross-reactivity to ALA synthase in a variety of human tissues. This is described in the next Chapter.

Chapter Six

Immunohistological examination of ALA synthase in human tissue

6.1 Introduction

As previously discussed in the literature review, little is known about the differences in regulation of ALA synthase in different tissues – or indeed its tissue distribution in humans. Currently, the most informative studies of ALA synthase tissue distribution have been from mRNA studies in rats (Srivastava et al, 1992). This study detected ALA synthase mRNA in small amounts in numerous rat tissues e.g. adrenal gland, heart, small intestine, brain and liver. The highest level of ALA synthase mRNA was found in adrenal gland, testis, liver and kidney.

The lack of information on ALA synthase distribution in human tissue is probably as a result of the ethical constraint associated with the use of human tissue, together with the technical difficulty in assaying small amounts of labile mRNA, or extremely low concentrations of ALA synthase protein. The difficulty in working with human ALA synthase has been discussed previously in this dissertation.

As has been detailed in the previous chapters, to overcome the technical difficulties in working with the ALA synthase protein itself (difficult to quantitatively assay, short half life, susceptible to proteolytic breakdown), we elected to make antibodies to ALA synthase and perform immunohistological examination of human tissues. This should allow examination of paraffin sections of human tissue at a microscopic level. The objectives of this section of work are therefore to examine in which human tissues ALA synthase is present and also to identify in which particular cells in a tissue ALA synthase could be detected, using immunohistochemical techniques.

6.2 Subjects and methods

Subjects

Surgical material, in the form of paraffin blocks was obtained from the archives of the pathology department at Groote Schuur hospital. Permission to use archived material was obtained from the head of the Pathology Department. In addition, tissue was obtained from 4 post-mortem examinations of previously healthy individuals in their mid thirties, who died immediately after violent trauma, for which ethical approval (Rec/Ref 031/99) was obtained from the UCT Ethics committee. Due to poor availability of specimens from some organs (as we relied on surgical removal of healthy tissue, which was difficult to obtain – and more so in particular tissues – like testis, kidney, and ovary) as well as variable preservation of tissue (poorly preserved tissue did not stain), surgical specimen numbers varied from 3 to 8 for each tissue examined.

The organs studied were liver, adrenal, kidney, ovary, testis, oesophagus, stomach, small intestine, colon, myocardium, lung, in surgical specimens and in the post-mortem specimens, liver, adrenal, kidney, ovary/testis, myocardium, lung, brain and skeletal muscle. (In the post mortem specimens, autolysis in the intestinal specimens was too severe to make immunocytochemistry of any use.) The tissue from both the post mortems and the surgical specimens had been fixed in buffered formalin and later embedded in paraffin wax.

Methods

The immunocytochemical technique used is that described in Chapters 4 and 5. The diagram of the immunocytochemistry method is repeated below for the convenience of the reader.

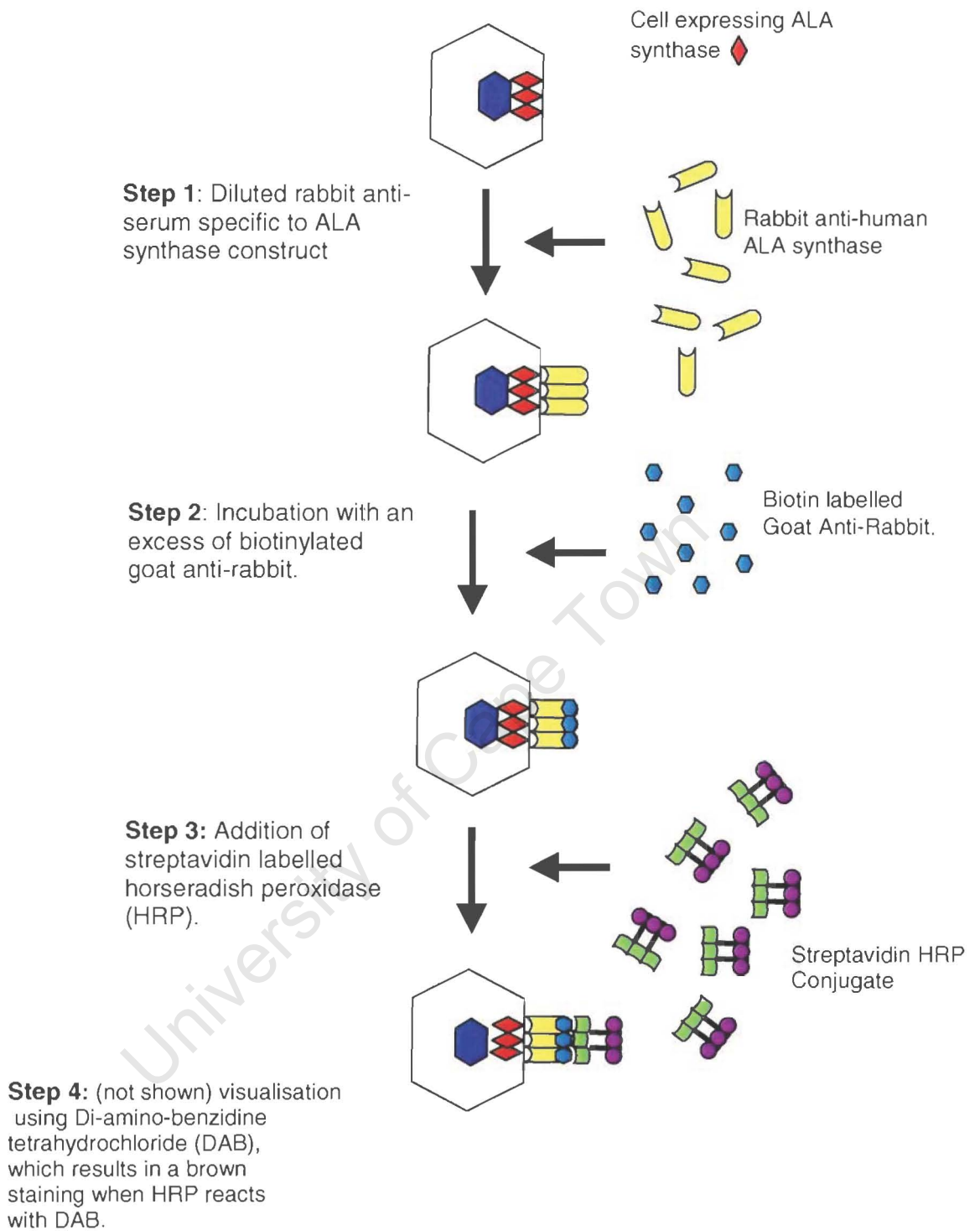


Fig 6.2.1 Schematic representation of the HRP-Streptavidin-Biotin anti-rabbit immune complex method

Primary antiserum was used at a dilution of 1: 500. All steps took place at room temperature. The non-immune control serum was obtained from non-immunized rabbits.

Optimisation of immunocytochemistry techniques

In optimising the immunocytochemistry technique the following adaptations were investigated:

- Immunocytochemistry at 37 °C – some antibodies bind preferentially to antigen at 37 °C – however this did not enhance antibody binding with our antisera and background staining was increased.
- When using formalin fixed and paraffin embedded tissues, some cross-linking of antigen occurs - hence different methods of antigen retrieval were tried. A variety of techniques have been developed to over-come this cross-linking and these have increased the range of antibodies which can be used in formalin fixed/paraffin embedded tissue – viz. trypsin digestion of tissue sections, pressure-cooking and micro waving (Leong, 1993; Cattoretti et al 1994; Bankfalvi et al 1995; Cuevas et al 1995). Depending on the antibody used, different antigen retrieval methods can be used to optimise staining. The micro waving and pressure-cooking methods can be applied for varying lengths of time, using a variety of solutions to immerse the slides during the procedure – for example citrate buffer, glycine buffer, urea or a standard saline buffer.

No immunostaining in human liver was present using FP3 antisera, when no antigen retrieval was used. All three of the above-mentioned methods of antigen retrieval were tried. Immunostaining was very poor, using trypsinization of the tissues. While pressure-cooking for 2 minutes gave the strongest signal, background was unacceptably increased, hence microwaving was chosen as the method of antigen retrieval. The disadvantages of using microwaving as the antigen retrieval system are that the time period is increased, and only a few specimens at a time (a maximum of 20) can be microwaved. The standard DAKO

citrate buffer and DAKO slide holder were used for antigen retrieval. The slides were microwaved for 10 minutes at maximum power in a 650W microwave oven and then allowed to stand in the warm buffer for a period of 20 minutes.

All immunostaining was performed using a DAKO Techmate⁵⁰⁰ immunostainer. The standard DAKO buffers supplied for use with the immunostainer were used. Less expensive, but less sensitive manual immunocytochemistry was also attempted, using a similar HRP (Horseradish peroxidase)-secondary antibody, but poor staining was achieved using this method. The low quantities of ALA synthase present required amplification of the signal, using the DAKO kit – in which several biotin molecules were bound to one secondary antibody, therefore allowing several HRP-streptavidin molecules to bind and amplifying the signal.

Stained sections were viewed using a microscope, by three independent observers, including one trained histopathologist (Dr. Philip Kaye) and results were averaged. The microscope was an Olympus and images were captured using an Olympus camera. Staining was graded as follows:

- 0 *No staining* – i.e. no different control sections and no brown hue was visible in cytoplasm
- 1- *Mild staining* – a faint brown blush was visible in cytoplasm.
- 2- *Moderate staining* – a darker brown pigment was visible in the cell cytoplasm.
- 3- *Strong staining* – a dark brown pigment was visible in cell cytoplasm.

6.3 Results and discussion

While some non-specific background staining was present, this was to be expected using an unpurified antibody (whole rabbit serum), and was taken into account

during interpretation of results. Moreover, the non-specific background staining was predominantly found in mucin containing cells.

Other control experiments performed included omission of primary antisera in the control slides. A faint background blush of staining was present – indicating the presence of endogenous tissue peroxidase. Although the automated immunostaining incorporates a step designed to block endogenous peroxidase reacting, some background was still visible. An additional manual blocking step – which involved incubating the slides in 3% methanol for 20 minutes made minimal improvement to the background staining. This is a well-described problem using the peroxidase method of immunocytochemistry (Kuhlmann and Peschke, 1986).

I was unable to perform controls involving blocking of antibody in immune serum, using purified antigen - FP3 (fusion protein 3), as the purified FP3 obtained was always at concentrations too low for blocking of antibody binding (the concentration of purified FP3 was in $\mu\text{g/ml}$ quantities, rather than in mg/ml). As previously discussed in chapter 3, it was not possible to concentrate FP3 using dialysis or an Amicon filter, as FP3 would adhere to the dialysis tubing, or to the filter.

ALA synthase was demonstrable in liver, adrenal, kidney, myocardium, testis, ovary, brain, anterior pituitary and lung.

Liver

Ten surgical specimens of liver plus four post-mortem specimens were examined, and the results are as follows:

| | Number of samples and staining intensity (n=14) | | |
|------------------|--------------------------------------------------------|--------------------------|------------------------|
| Cell Type | Weak staining | Moderate staining | Strong staining |
| Hepatocytes | 2 | 7 | 5 |
| Bile Ducts | 6 | 0 | 0 |
| Other cells | 0 | 0 | 0 |

Table 6.3.1 Staining intensity in resected and post-mortem liver specimens.

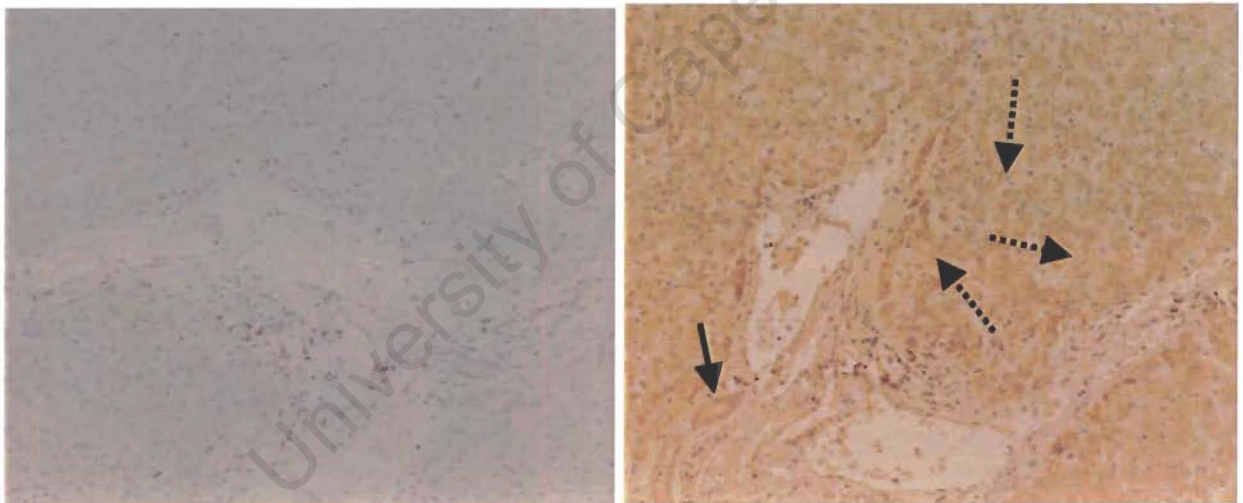


Fig 6.3.1.a Typical immunohistological examination of a surgical liver specimen using antisera to ALA synthase, viewed at 100 times magnification. On the left a negative control sample is featured, showing no non-specific staining. The photograph on the right shows moderate to strong staining in hepatocytes (indicated by dashed arrows) and weak staining in bile ducts (indicated by bold arrows).

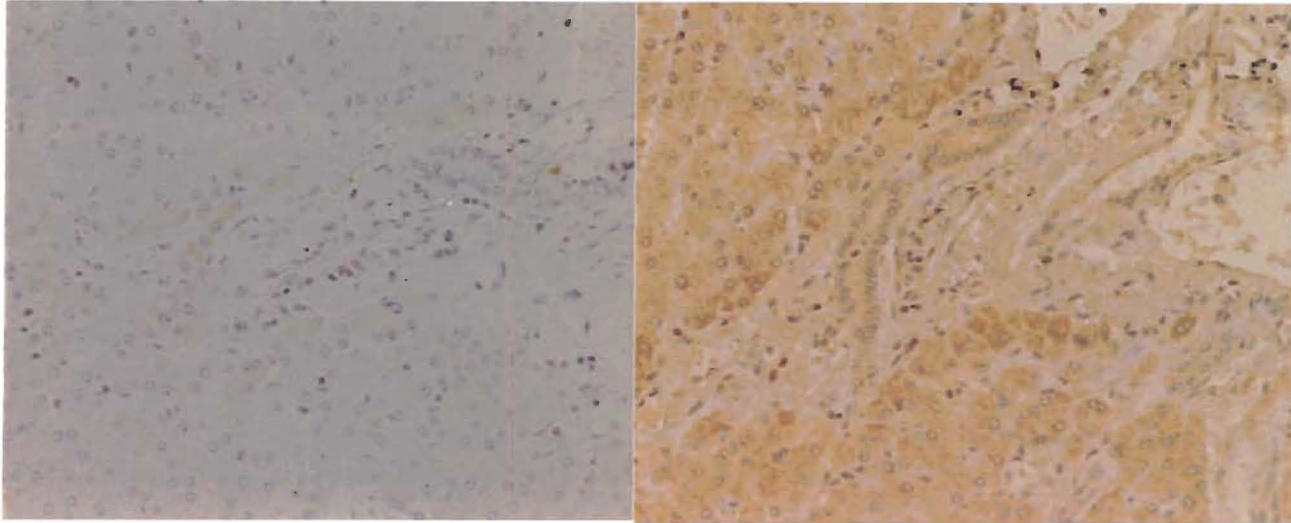


Fig. 6.3.1.b Typical immunohistological examination of a surgical liver specimen using antisera to ALA synthase, viewed at 200 times magnification. On the left, a negative control sample is present. On the right, moderate to strong staining for ALA synthase is visible in hepatocytes, with some weak to moderate staining in the bile ducts.

The liver – the largest internal organ plays important and complex roles in absorption of hormones, nutrients and toxins from blood, detoxification by conjugation and oxidation (a haem dependent mechanism), deamination of excess amino acids and urea synthesis, storage of glycogen and various vitamins, endocrine secretion of multiple blood proteins (from albumin, lipoproteins, to clotting proteins and growth factors). Hepatocytes are metabolically active cells, with abundant mitochondria, and given their multiple oxidative reactions and peroxidations (that require haem containing enzymes to catalyse these reactions – such as cytochrome P450's, peroxidases and catalases) obviously create a high haem demand. Therefore the moderate to strong staining obtained was to be expected.

Adrenal gland

Six surgical specimens were examined. In some of the negative control specimens, a faint blush of brown was noted in the adrenal cortex generally. This was significantly different from staining in the samples. Adrenal medulla was only present in 2 of the surgical specimens although it was present in all of the post-

mortem specimens. The adrenal medulla staining appeared to be in the ganglion cells.

| | Number of samples and staining intensity (n=10) | | |
|-----------------------|--------------------------------------------------------|--------------------------|------------------------|
| Cell Type | Weak staining | Moderate staining | Strong staining |
| Zona Fasciculata | 1 | 1 | 2 |
| Zona Reticularis | 1 | 4 | 3 |
| Zona Glomerulosa | 2 | 1 | 0 |
| Adrenal Medulla (n=6) | 0 | 6 | 0 |

Table 6.3.2 Staining intensity in surgical adrenal specimens.

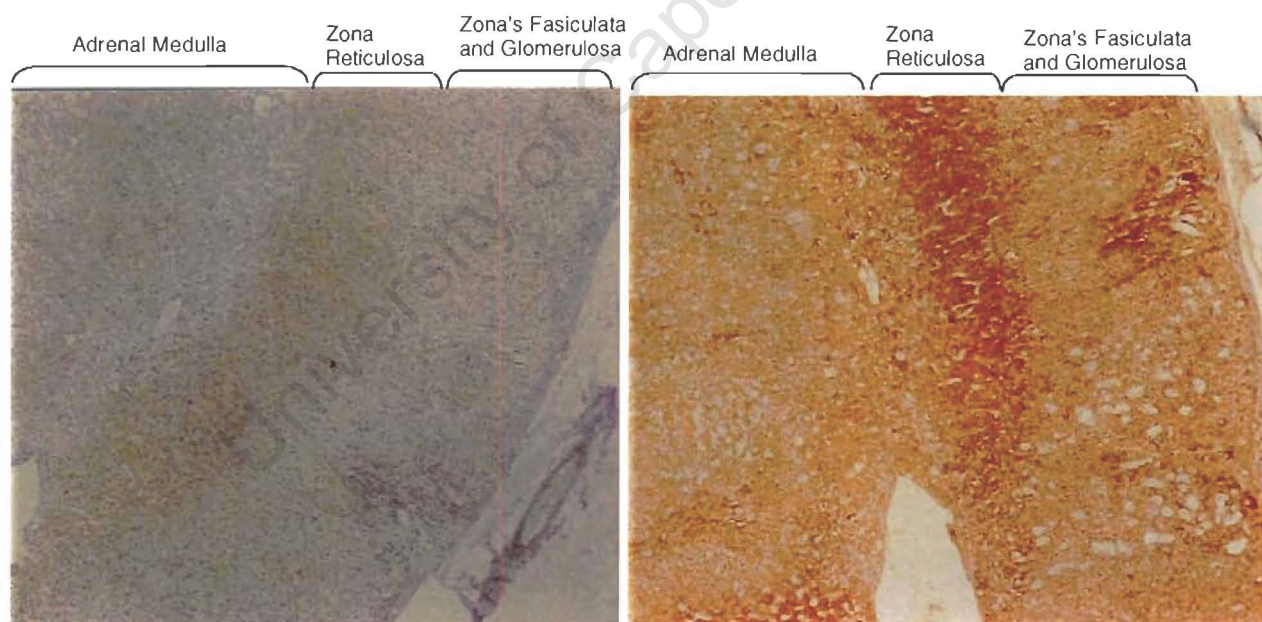


Fig 6.3.2.a Adrenal gland at 40X magnification. Cortex indicated by brackets with labels corresponding to Zona Glomerulosa, Zona Reticularis and Zona Fasciculata. The adrenal medulla is indicated as well. The negative control sample is on the left. Moderate staining is present in the Zona's Glomerulosa and Fasciculata of the adrenal cortex as well as the adrenal medulla. Strong staining is present in the zona reticulosa.

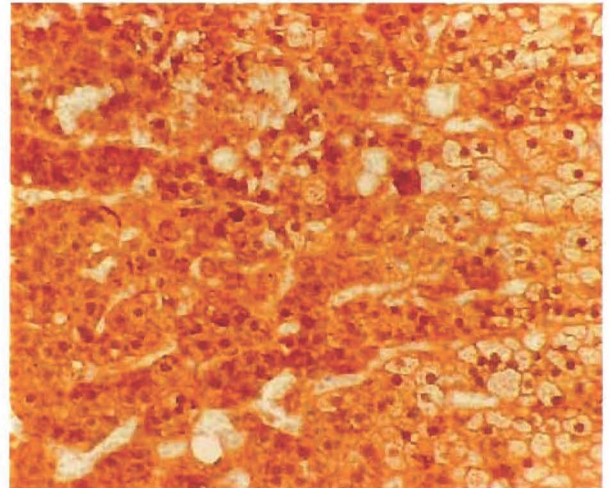
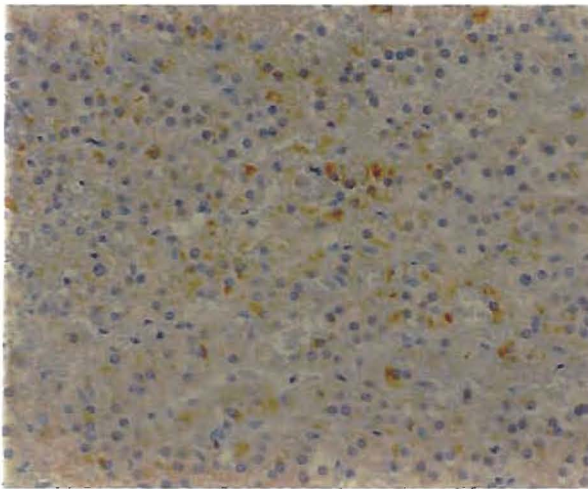


Fig 6.3.2.b The zona reticularis of the adrenal cortex at 200 times magnification. The negative control is shown on the left, with the sample, stained using antibody to ALA synthase is shown below. This sample shows a strongly positive stain for ALA synthase

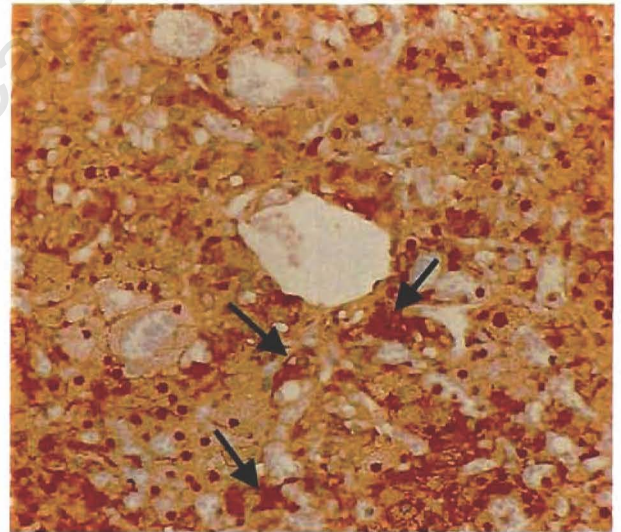
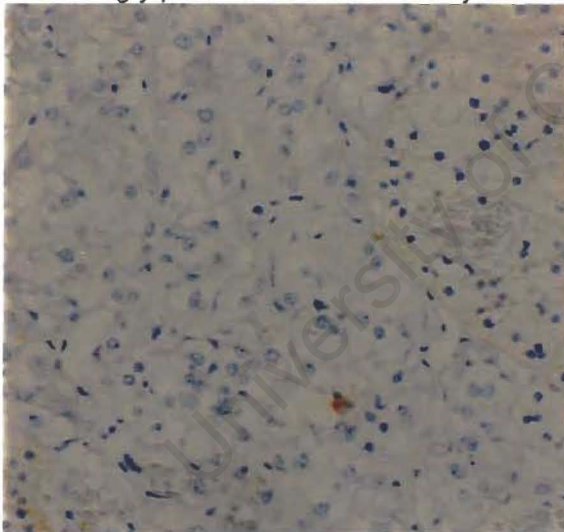


Fig 6.3.2.c Adrenal medulla at 200X magnification. The negative control is at the left, with the sample on the right, stained using antibody to ALA synthase. A solid arrow indicates the triangular neural ganglion cells, which stain strongly for ALA synthase.

The adrenal cortex shows moderate to strong staining in the zona reticulosa – an area functionally associated with the production of small amounts of sex steroids (notably oestrogen and progesterone) as well as androgenic steroids. Some of the

enzymes involved in the synthesis of these hormones include the haem-containing cytochrome b5 and P450c17 (Yanase et al, 1998). The zona glomerulosa and fasciculata, involved in production of mineralocorticoid and glucocorticoid respectively, show variable staining for ALA synthase.

The neural ganglion cells of the adrenal medulla – which produce adrenaline and nor-adrenaline, also stain for ALA synthase. The biosynthesis of catecholamines essentially involves hydroxylation, followed by decarboxylation of tyrosine – with its associated haem requirement (Gornall et al, 1986). Moreover, metabolism of catecholamines is determined by two enzyme systems – the catecholamine orthomethyltransferase (COMT) or the monoamine oxidase(MOA) systems(Gornall et al, 1986).

Kidney

Four surgical and four post mortem kidney samples were examined immunohistologically. There was weak, patchy staining in the tubular cells of some of the negative control samples. A control experiment, performed without the use of primary antibody showed this was due to incomplete blocking of endogenous peroxidase activity in the kidney samples.

| <i>Staining intensity and specimen number (n=8)</i> | | | |
|------------------------------------------------------------|----------------------|--------------------------|------------------------|
| Cell Type | Weak Staining | Moderate Staining | Strong Staining |
| PCT | 2 | 2 | 4 |
| DCT | 7 | 0 | 0 |
| Glomeruli | 0 | 0 | 0 |

Table 6.3.3 Staining intensity in surgical and post mortem kidney specimens

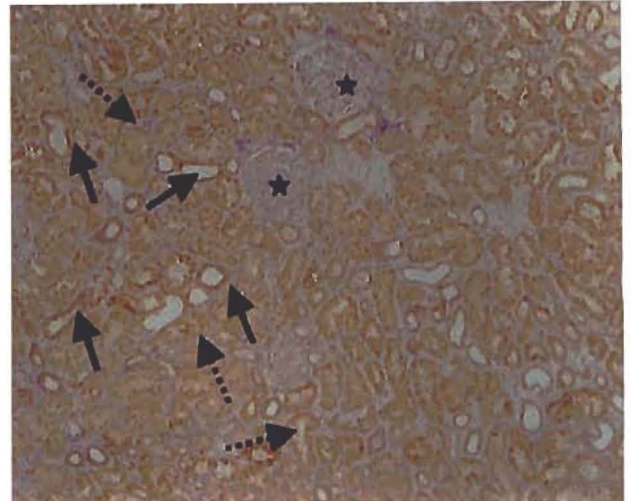
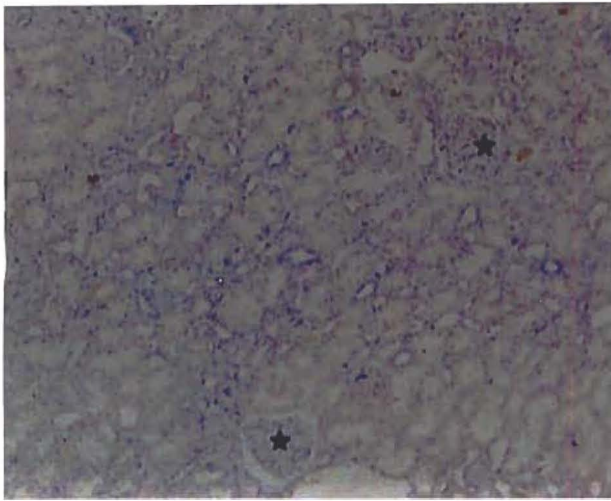


Fig 6.3.3.a Staining of kidney for ALA synthase at 40 times magnification. A control sample is present on the left. Strong staining is present in the proximal convoluted tubules (PCT's)- indicated by a solid arrow and moderate staining in the distal convoluted tubules (DCT's) -indicated by a broken arrow. The glomeruli do not stain for ALA synthase (indicated by an asterisk).

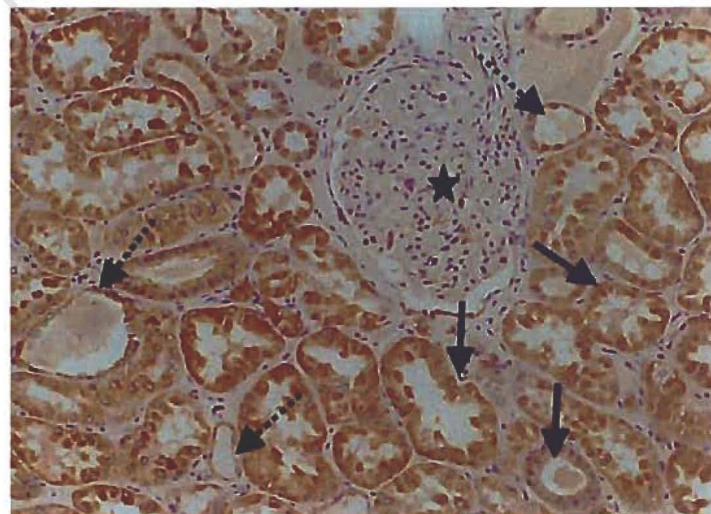
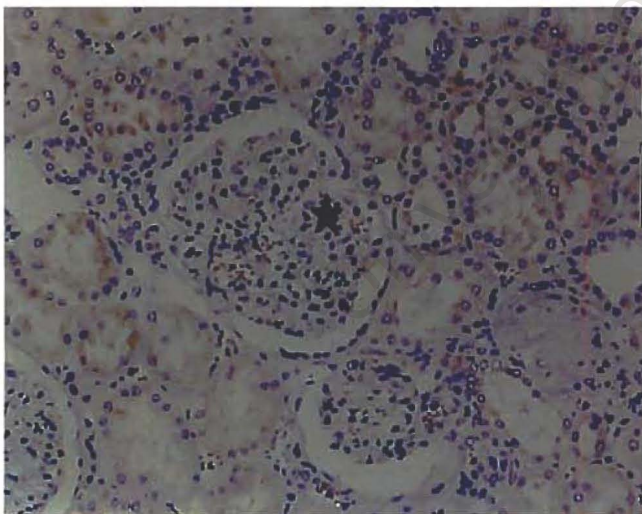


Fig 6.3.3.b Histological staining of kidney for ALA synthase at 100 times magnification. A control sample is present on the left. Strong staining is present in the proximal convoluted tubules (indicated by a solid arrow) and moderate staining in the distal convoluted tubules (indicated by a broken arrow).

The proximal convoluted tubular cells are metabolically active cells, with abundant mitochondria and highly specialized apical and basolateral surfaces. Here water, glucose, amino acids, sodium and phosphate are actively re-absorbed in processes tied to a sodium-potassium adenosine-tri-phosphate (ATP)-ase. The staining for ALA synthase seems to be explainable by the high oxidative activity.

Ovary

Six surgical ovarian samples and two post-mortem samples were examined. Owing to the small number of samples the results of the surgical and PM samples are presented together in one graph. Unfortunately most of the ovary samples that I was able to obtain were post-menopausal (including one of the post mortem ovaries examined from a woman in the mid thirties) – and these showed only staining in the Leydig cells. Of the four pre-menopausal specimens examined, there was staining in granulosa cells, and thecal luteal cells – cells not present in the post-menopausal samples.

| Cell Type | <i>Staining intensity and specimen number (n=8)</i> | | |
|-----------------------------|-----------------------------------------------------|-------------------|-----------------|
| | Weak Staining | Moderate Staining | Strong Staining |
| Leydig cells | 2 | 3 | 1 |
| Steroid cells (n=3) | 1 | 2 | 0 |
| Granulosa cells (n=3) | 2 | 1 | 0 |
| Follicular Epithelium (n=4) | 4 | 0 | 0 |

Table 6.3.4 Staining intensity in ovary samples

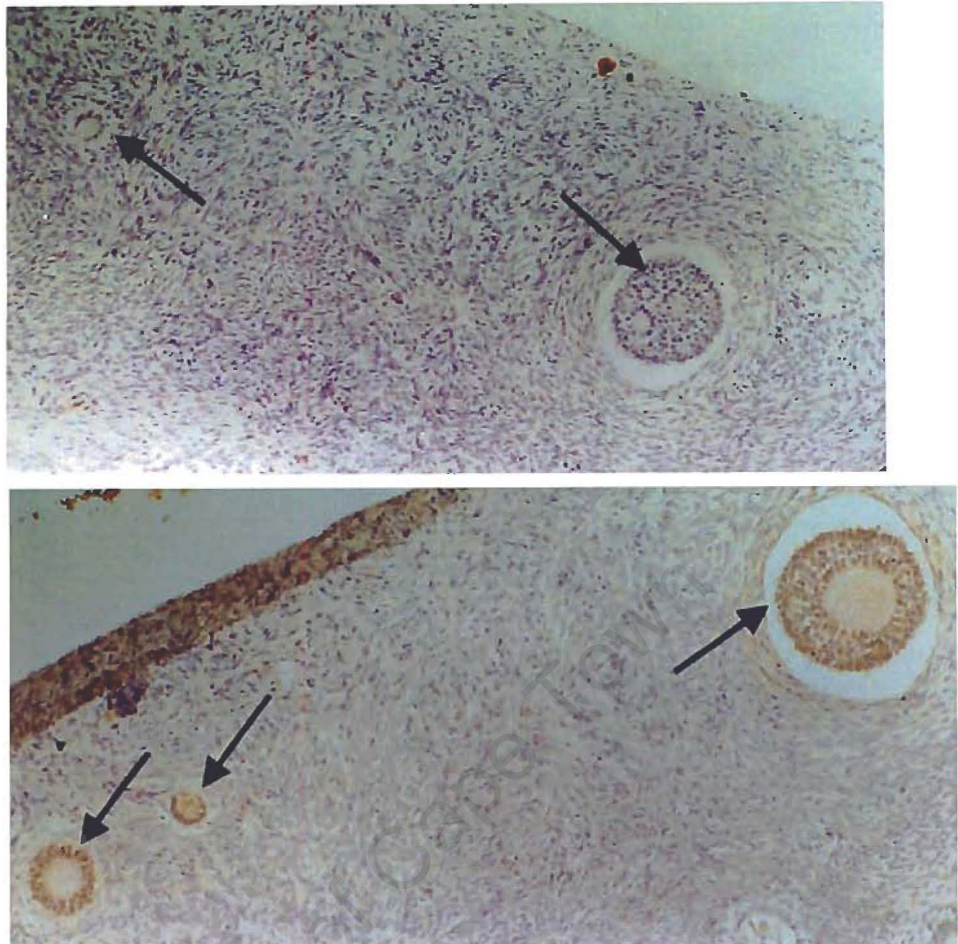


Fig 6.3.4 Typical immunohistological staining for ALA synthase in premenopausal resected ovary. On the top, a photograph of a negative control sample is present. On the bottom, a photograph of a surgical specimen of ovary, stained for ALA synthase is present. Solid arrows indicate follicles, at different stages of development. These show moderate staining for ALA synthase.

The staining of steroidogenic cells in ovary could be predicted from what is known about steroidogenesis in the ovary. These reactions involve haem-containing cytochrome p450 enzymes as well as the haem containing microsomal epoxide hydrolase (Hattori N et al, 2000) and are thus likely to create a demand for haem, which is reflected in the staining patterns.

Testis

Three surgical and two post mortem testes were stained for ALA synthase.

| Cell Type | Staining intensity and Specimen number (n=5) | | |
|-----------------------------|----------------------------------------------|-------------------|-----------------|
| | Weak Staining | Moderate Staining | Strong Staining |
| Epididymis (n=2) | 2 | 0 | 0 |
| Early Primary Spermatocytes | 1 | 1 | 0 |
| Late Primary Spermatocytes | 2 | 3 | 0 |
| Late Spermatids | 2 | 1 | 2 |
| Sertoli Cells | 0 | 0 | 0 |
| Leydig Cells | 4 | 1 | 0 |

Table 6.3.5 Staining intensity in testis specimens

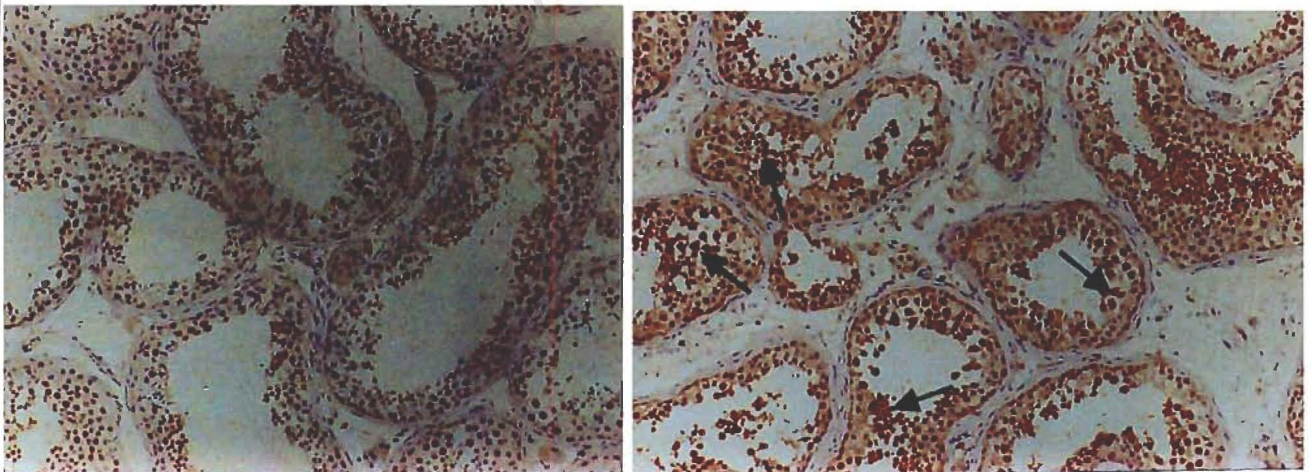


Fig 6.3.5.a Photograph of immunohistological examination of testis using antibody to hepatic ALA synthase at 100 times magnification. On the right a negative control slide is present. On the left, staining is visible for ALA synthase in the late spermatids (marked with a solid arrow).

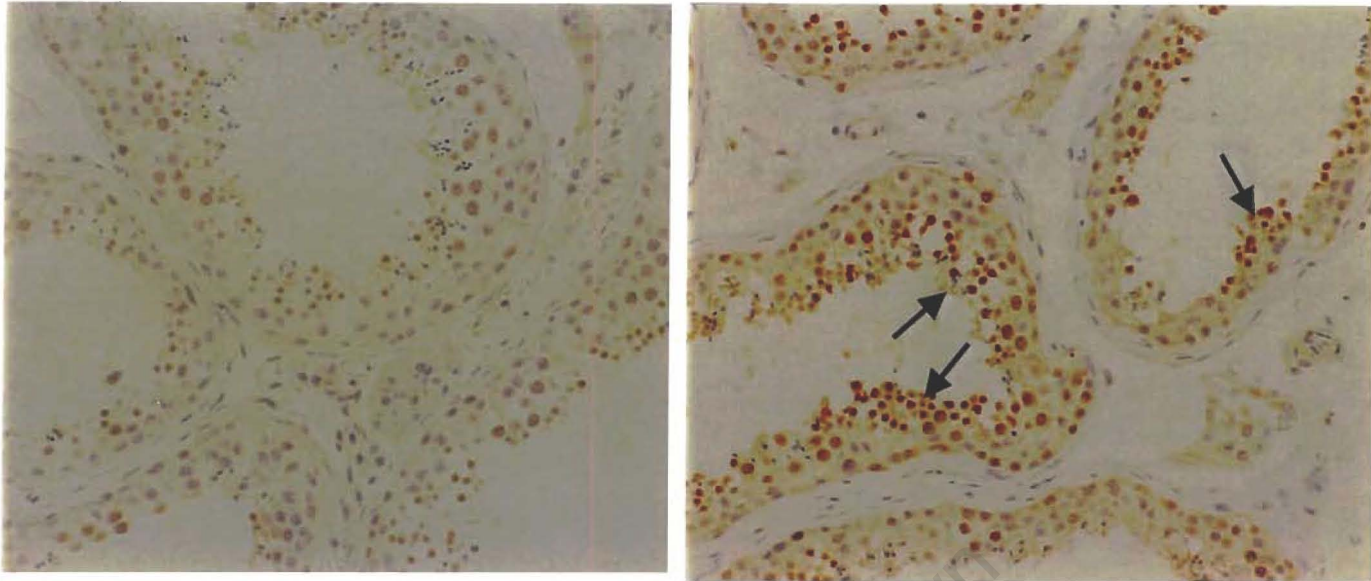


Fig 6.3.5.b Photograph of immunohistological examination of testis using antibody to hepatic ALA synthase at 200 times magnification. On the left a negative control slide is present. On the right, staining is visible for ALA synthase in the late spermatids (marked with a solid arrow).

Brain/Cerebrum

Only 4 post mortem samples were available for immunohistological examination. In the negative control samples no staining was visible.

| | <i>Staining intensity and Sample number (n=4)</i> | | |
|------------------|----------------------------------------------------------|--------------------------|------------------------|
| Cell Type | Weak staining | Moderate Staining | Strong Staining |
| Neurones | 0 | 0 | 4 |
| Glial cells | 0 | 0 | 0 |

Table 6.3.6 Staining intensity of brain using antibody to ALA synthase.

Previous work by Srivastava et al (1992) measured very little ALA synthase mRNA in brain. However they measured ALA synthase in whole brains and given that the supportive glial tissue outnumbers the neurones at a ratio of between 10

and 1 and up to 100:1 it is not surprising that little ALA synthase was measured. In the neurones staining was visible in the neuropiles as well as in the cell body. This probably reflects the presence of mitochondria involved in energy generations for transportation of secretory vesicles. This strong staining of neurones has implications for theories regarding the pathogenesis of the acute attack of porphyria, as these cells are clearly active in haem production. It would suggest that neuronal haem deficiency, as well as neurotoxicity of ALA might well play a role in the pathogenesis of the acute attack of porphyria.

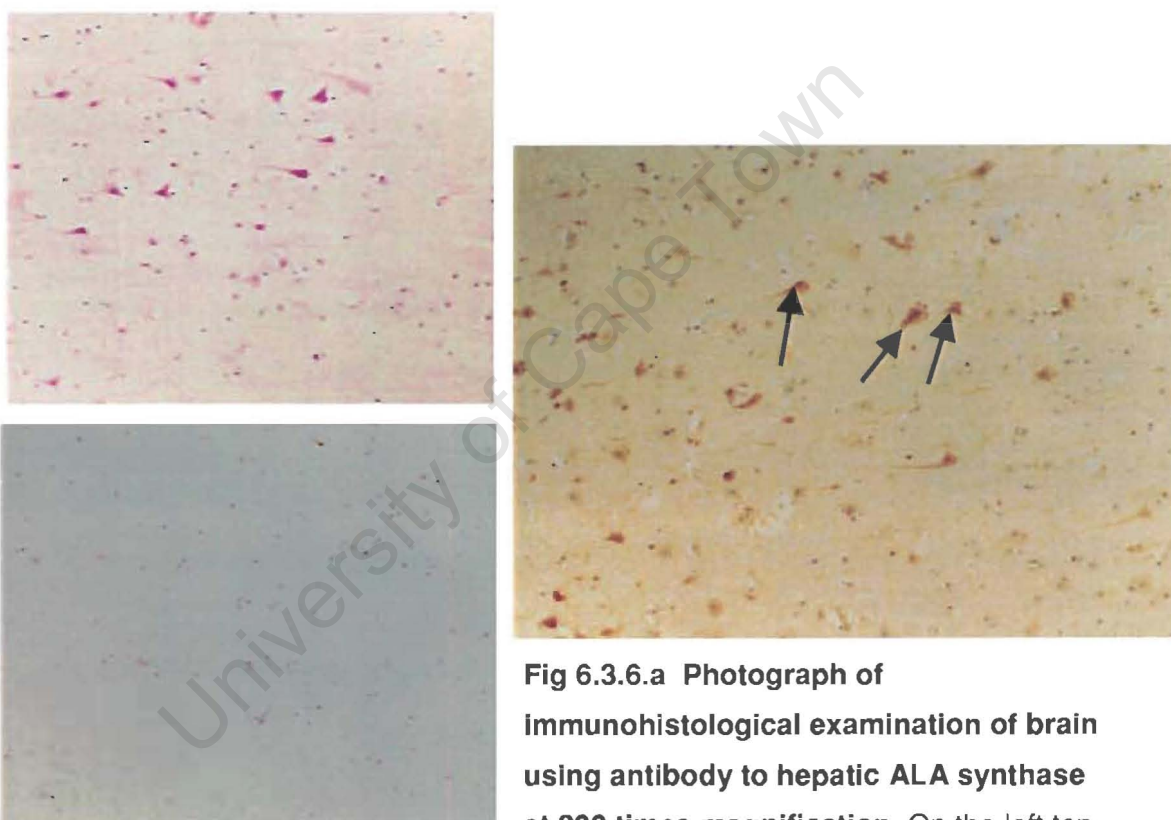


Fig 6.3.6.a Photograph of immunohistological examination of brain using antibody to hepatic ALA synthase at 200 times magnification. On the left top

photograph, an Haematoxylin and Eosin photograph is present showing neurones staining pink. Below, left, a negative control slide is present. To the right, staining is visible for ALA synthase in the neurones (marked with a solid arrow).

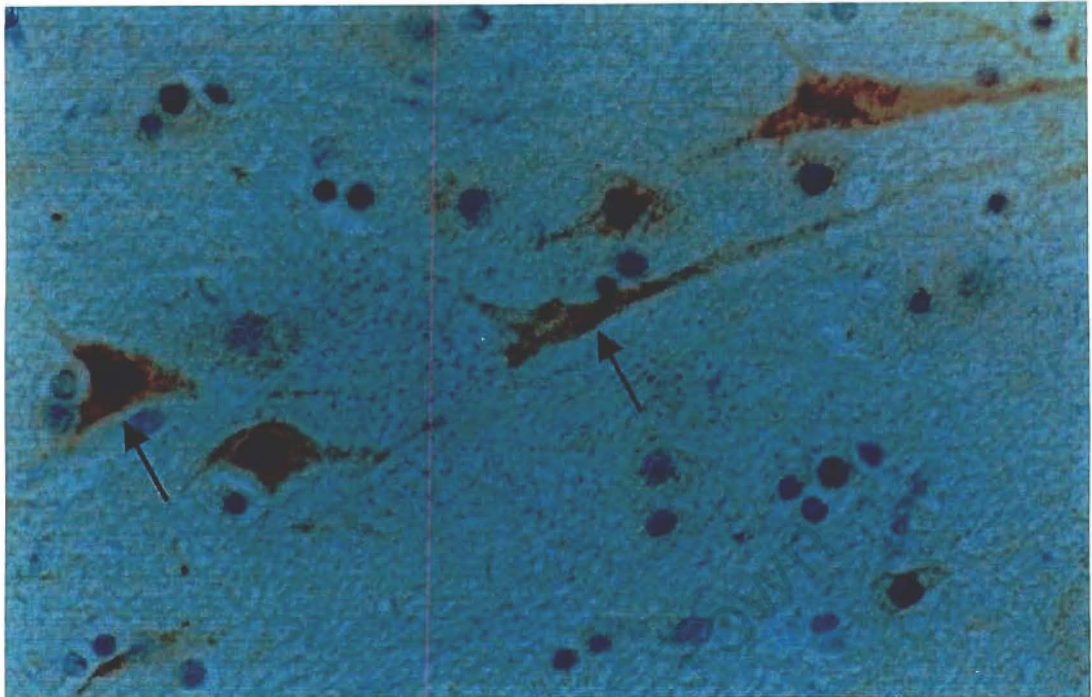


Fig 6.3.6.b A typical immunohistological examination of post mortem brain tissue using antibodies to ALA synthase. This photograph is looking at brain at 400 times magnification (under oil immersion). Bold arrows indicate neurones. Note the strong staining for ALA synthase – not only in the cell body of the neurones, but also in the dendrites and axonal processes.

Anterior pituitary

Only 2 samples of anterior pituitary, from 2 of the post mortem subjects, were available for immunohistological examination. In the samples, strong staining was present in some anterior pituitary cells – this probably represented a particular sub-population of anterior pituitary cells, but without further specialized antibody tests we are unable to say which particular cell type these are (for e.g. gonadotrophes, lactotrophes, growth hormone producing cells). There is some evidence of cytochrome P450 3A5 being present in the growth hormone containing cells (Murray et al 1995), which is thought to play a role in regulating growth hormone secretion and it is possible that these cells are staining for ALA synthase.

Photographs of an anterior pituitary specimen follow, together with the negative controls.

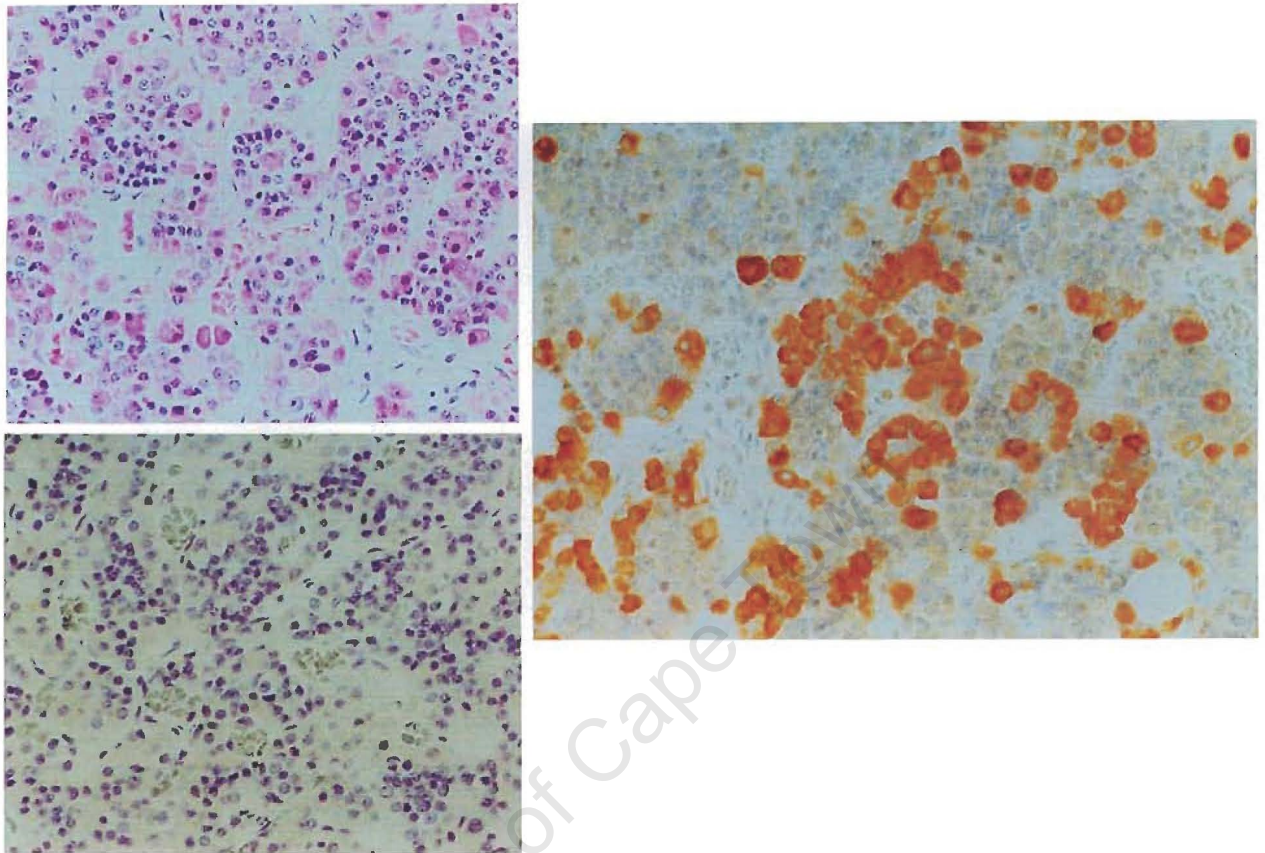


Fig 6.3.7 Immunohistological examination of post-mortem anterior pituitary specimen at 200 times magnification. Above, left a Haematoxylin and Eosin stain is present. Below left, a negative control is present. To the right, the sample was stained using antibodies to ALA synthase, and shows checkerboard staining of cells.

Oesophagus

Nine resected oesophageal specimens were examined for the presence of ALA synthase. Weak to moderate staining for ALA synthase was detected. Only two of the specimens contained oesophageal glands and these had non-specific staining in the mucinous glands, so mucinous glands were not listed in the table of results.

| Cell Type | <i>Staining intensity and sample number (n=9)</i> | | |
|-------------------------------------------|---------------------------------------------------|-------------------|-----------------|
| | Weak staining | Moderate Staining | Strong Staining |
| Functional squamous epithelium. | 2 | 3 | 0 |
| Prickle cell layer of squamous epithelium | 1 | 4 | 1 |
| Basal cell layer of squamous epithelium | 0 | 0 | 0 |
| Smooth muscle | 5 | 1 | 0 |
| Acinar glands | 1 | 0 | 0 |

Table 6.3.7 Staining intensity of oesophagus using antibody to ALA synthase

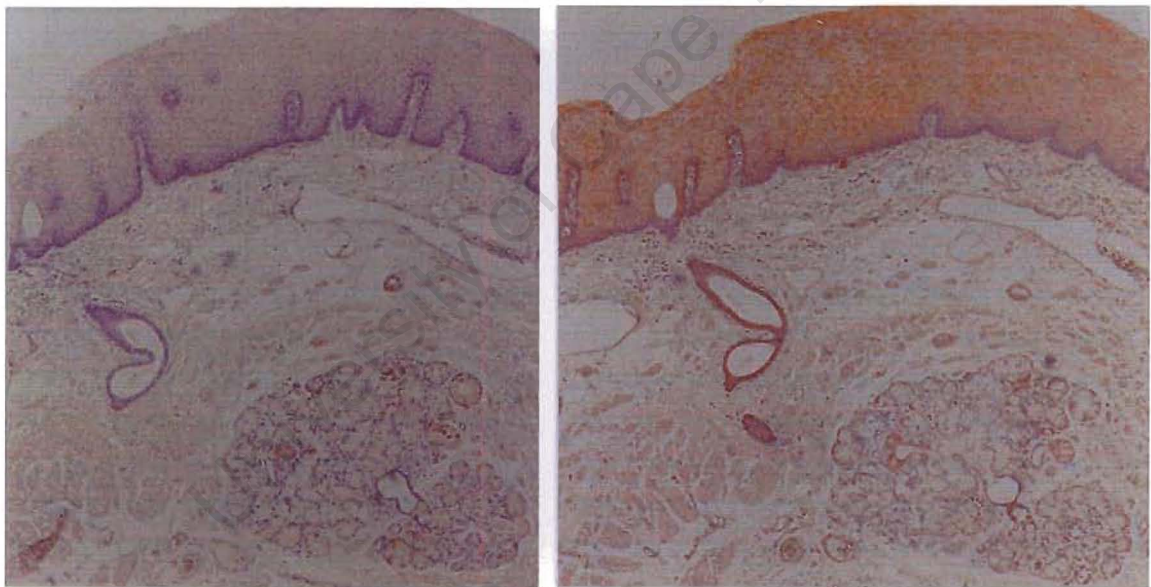


Fig 6.3.8.a Immunohistological examination of a specimen of resected oesophagus at 40 times magnification. To the left, a negative control specimen is present. On the right is oesophagus stained with antibody to ALA synthase. Only weak staining is present in the smooth muscle, acinus glands and functional layer of epithelium.

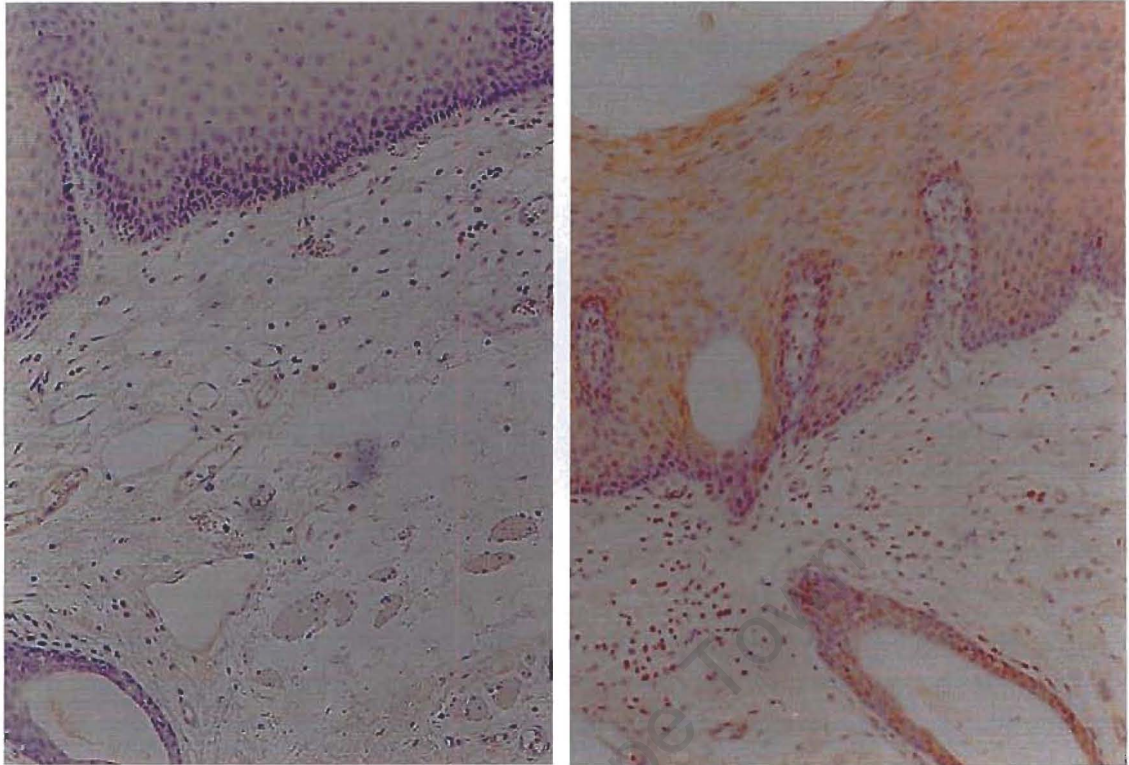


Fig 6.3.8.b Immunohistological examination of a specimen of resected oesophagus at 100 times magnification. Above a negative control specimen is. Below, oesophagus is stained with antibody to ALA synthase showing staining is present in the functional layer of epithelium.

Oesophageal squamous epithelium can be divided into three layers – the basal , prickle and functional cell layers. The prickle and functional cell layers consisted of progressively flatter glycogen-rich cells. The mature oesophageal epithelium – from the more metabolically active, mature functional layer stains positive for ALA synthase – as opposed to the basal layer of cells – which are actively dividing cells that are not functional.

Gopalakrishnan R et al (1999) demonstrated using western blots and RT-PCR, that cytochrome p450's are present in oesophageal muscosa – although in quite small amounts. Furthermore, Lechevrel et al (1999) were able to demonstrate that a wide range of cytochrome p450's were detectable using immunoblot and RT-PCR – thus

range of cytochrome p450's were detectable using immunoblot and RT-PCR – thus indicating a possible role in oesophageal metabolism of xenobiotics. No immunocytochemistry was performed in either study; therefore comparison with the specific staining for ALA synthase in the functional layer of oesophageal mucosa is not possible. However one would expect cytochrome P450's to be expressed in the functional layer of the oesophageal mucosa – which correlates with our staining for ALA synthase.

Stomach

Little immunohistological staining for ALA synthase was demonstrated, other than in the gastric glands. The results are summarized below.

| Cell Type | Staining intensity and sample number (n=6) | | |
|----------------|---------------------------------------------------|-------------------|-----------------|
| | Weak staining | Moderate staining | Strong staining |
| Alveolar cells | 2 | 0 | 0 |
| Fundic glands | 1 | 4 | 0 |
| Gastric mucosa | 0 | 0 | 0 |
| Other | 0 | 0 | 0 |

Table 6.3.8 Staining intensity of stomach using antibody to ALA synthase.

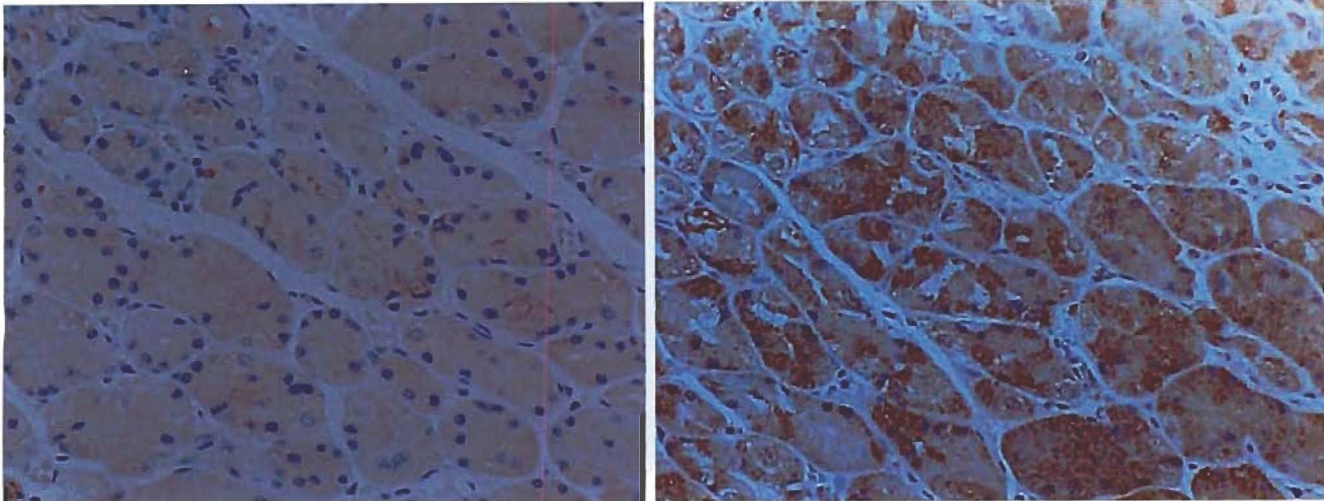


Fig 6.3.9 Immunohistological examination of resected stomach using antibody to ALA synthase. On the left, a negative control specimen is present. On the right, stomach is stained with antibody to ALA synthase, showing moderate staining in the parietal cells of the fundic glands only.

The fundic glands are straight, tightly packed glands with pits that occupy less and a quarter of the mucosal thickness. The basal cells are predominantly pepsinogen secreting “chief” cells; while towards the surface parietal cells predominate. The parietal glands produce neutral and acidic mucin, which protects the stomach epithelium from acid. The parietal cells have large numbers of mitochondria, with a high oxidative capacity, which produce the ATP needed for the hydrogen/potassium ATP-ase (proton pump) needed for the production of HCl (hydrochloric acid).

Small intestine and pancreas

Seven specimens of small intestine were examined for immunohistologically detectable levels of ALA synthase. Six of these specimens were resected from the terminal ileum and demonstrated no staining for ALA synthase. The only specimen obtained from duodenum showed weak staining in the crypts of Luberkhun. This sample is shown in the figure below.

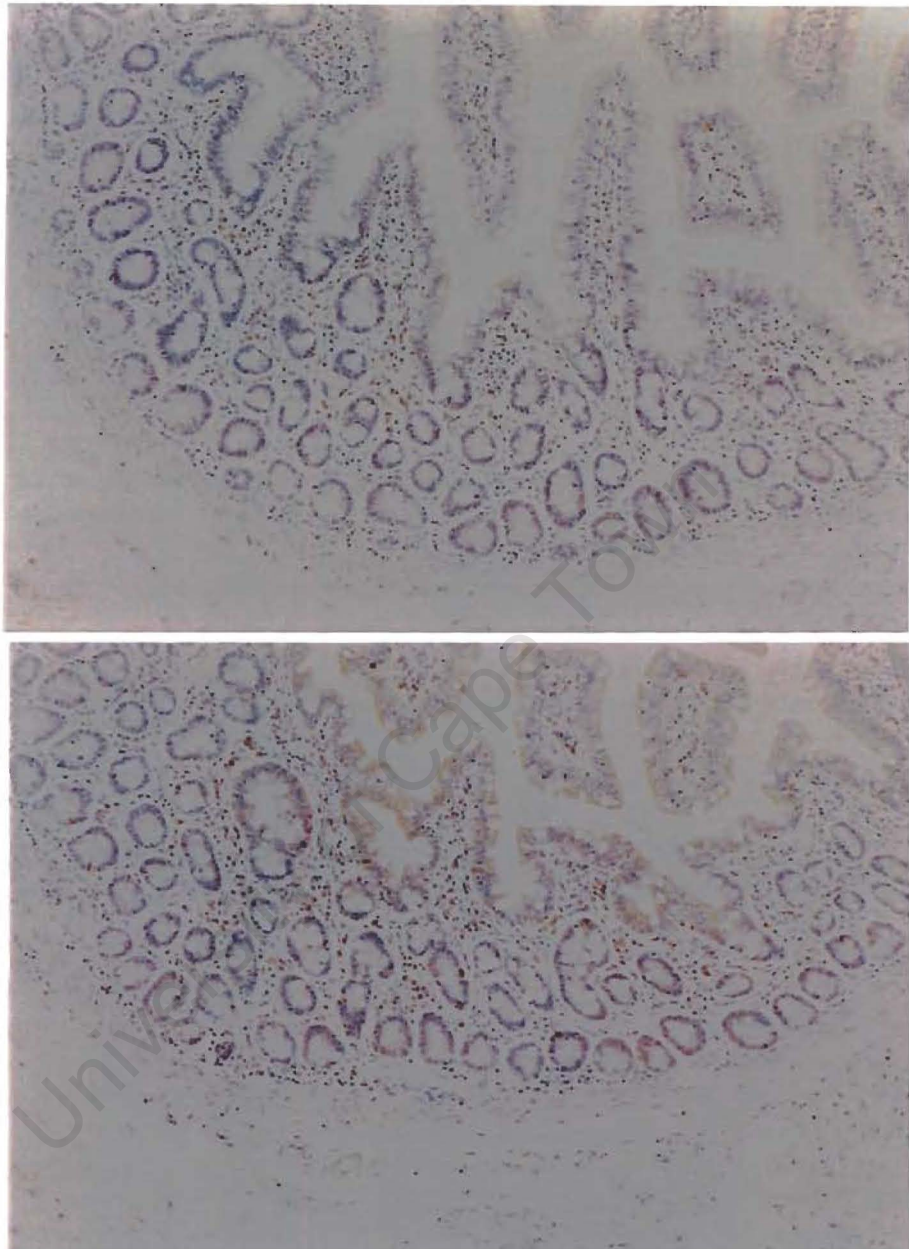


Fig 6.3.10 Immunohistological examination of duodenum using antibody to ALA synthase. Above, a photograph of the negative control specimen is present. Below, duodenum has been stained using antibody to ALA synthase. Staining is visible in the crypts of Luberkhun.

In the pathology archives only extremely abnormal pancreas, resected from patients with chronic pancreatitis was available, and this was not suitable for this study.

duodenal specimen. In this sample strong staining for ALA synthase was demonstrated in the islet cells. This is shown in the figure below.

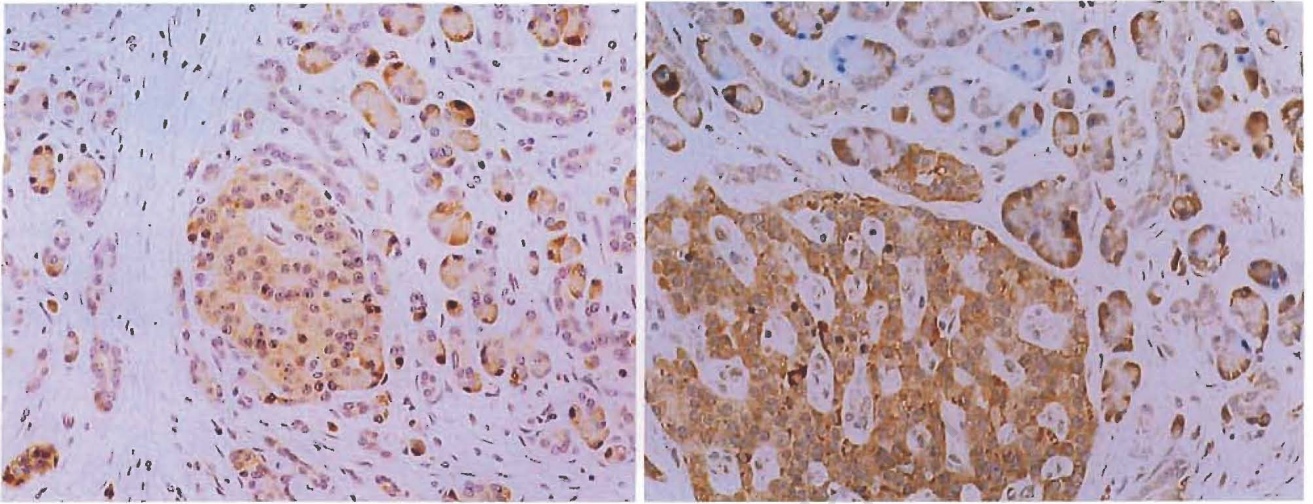


Fig 6.3.11 Immunohistological examination of pancreas using antibody to ALA synthase. On the left, a negative control sample of ALA synthase is present. On the right, pancreas has been stained using an antibody to ALA synthase demonstrating strong staining in the islet cells.

Given that our staining in all tissues followed an extremely consistent pattern, although there is only one sample it is worth noting that pancreatic acinar cells – which did not stain for ALA synthase, is amongst the most metabolically active cells in the body with extremely high rates of protein synthesis (personal communication from M Berman). The Beta islet cells however stained moderately positive for ALA synthase.

Colon

Six samples of colon were examined immunohistologically for ALA synthase. Five of the six samples demonstrated moderate staining in endocrine cells in the crypts and some weak staining in smooth muscle. No other staining for ALA synthase was present.

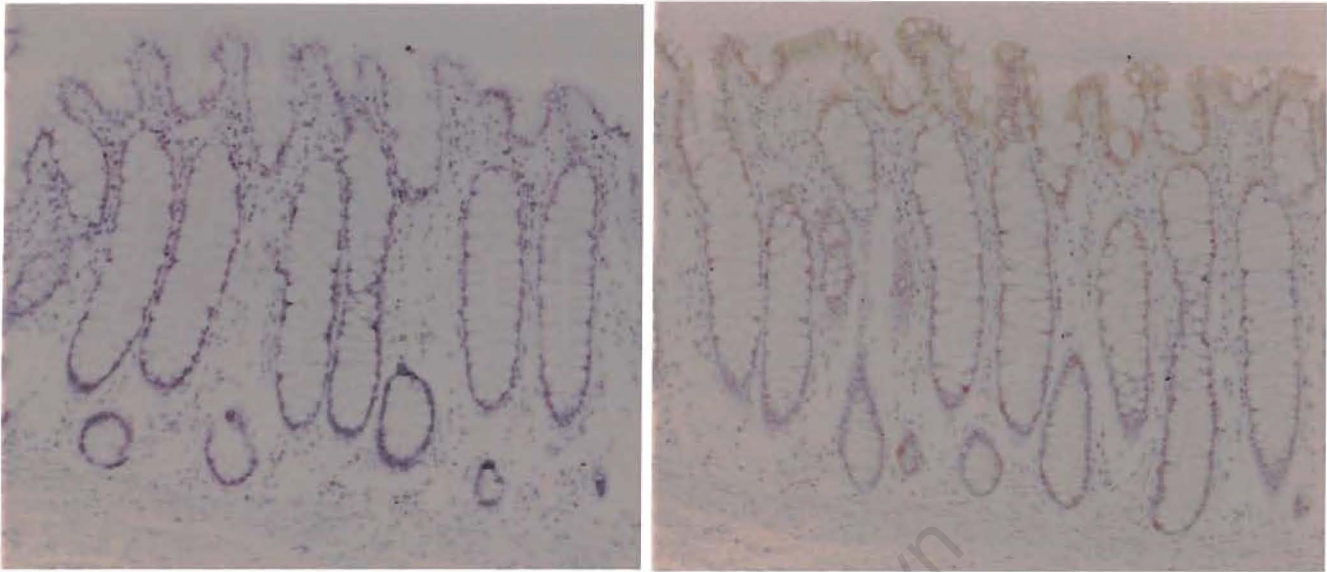


Fig 6.3.12.a Immunohistological examination of colon using antibody to ALA synthase at 100 times magnification. A negative control specimen is present on the left. To the right, weak staining is demonstrated in the endocrine cells in the crypts.

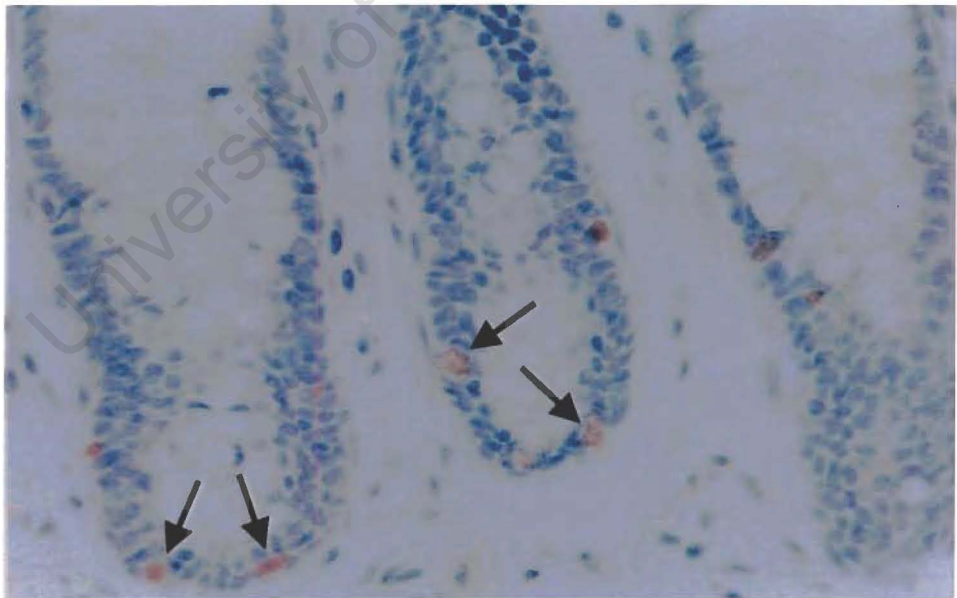


Fig 6.3.12.b Immunohistological examination of colon using antibody to ALA synthase at 200 times magnification, demonstrating the staining of endocrine cells in the crypts.

Skeletal muscle

Skeletal muscle samples were only obtained from the 4 post-mortem examinations. These samples showed checkerboard-staining patterns with some muscle fibres staining moderately strongly for ALA synthase. This indicates that a particular subgroup of muscle fibres is staining – probably the type I muscle fibres (aerobic muscle fibres).

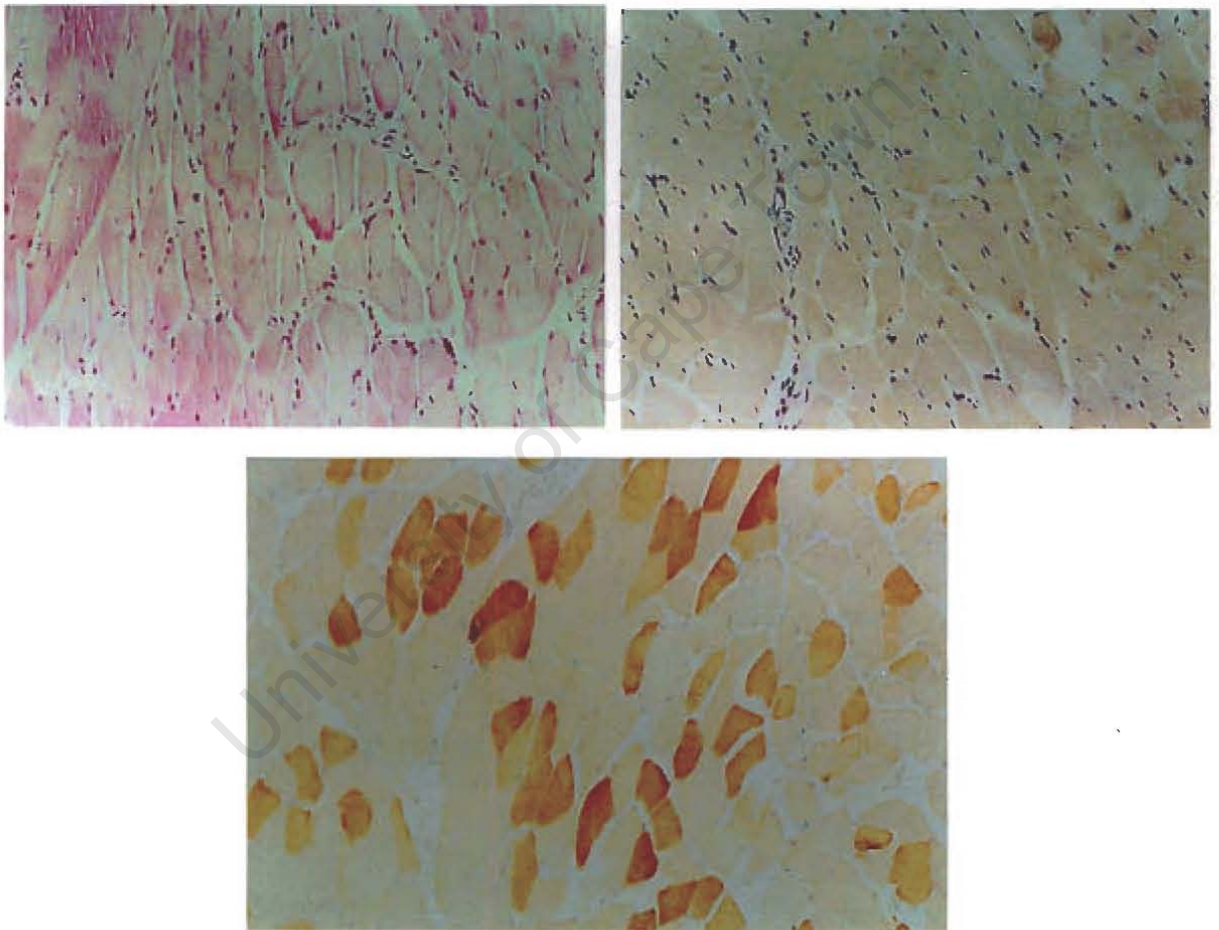


Fig 6.3.13 Immunohistological examination of skeletal muscle using antibody to ALA synthase at 100 times magnification. Above, on the left is an H and E, with a negative control specimen to the right. Below, moderately strong staining is demonstrated in some muscle fibres forming a checkerboard pattern.

The type I fibres have a larger mitochondrial content and depend on aerobic respiration. These fibres also have large quantities of myoglobin necessary for oxygen storage. In contrast the type II muscle fibres have much fewer mitochondria, little myoglobin but are rich in glycogen and glycolytic enzymes and are capable of rapid metabolism of glucose –to the lactate stage – for short intense and sporadic bursts of activity.

To confirm which muscle fibre might be staining, co-staining with antibodies to ATPase or to NADPH-TR would have been necessary. However, it is likely that the Type I fibre's with their high myoglobin and mitochondrial content, and oxidative demands are likely to contain more ALA synthase and one can assume that the staining present is likely to be in this sub-group of muscle fibre.

Lung

Several surgical and 4 post mortem lung specimens were examined immunohistologically for the presence of ALA synthase. Only two of the samples contained bronchial glands and in the acinus glandular cells stained moderately to strongly for ALA synthase. The bronchial brush border epithelium was weakly positive for ALA synthase. These cells are highly active cells requiring energy to produce motile cilia and contain large numbers of mitochondria towards the apices of the cells.

Immunohistochemical examination of lung tissue using anti-sera to cytochrome P450 (Kivisto KT, 1995; Raunio H et al 1999) enzymes demonstrates strong staining for cytochrome P450's in seromucous glands and some staining in ciliated and cuboidal bronchial epithelium.

| | Staining intensity and sample number (n=11) | | |
|---------------------------------------|----------------------------------------------------|--------------------------|------------------------|
| Cell Type | Weak staining | Moderate staining | Strong staining |
| Alveolar cells | 6 | 0 | 0 |
| Bronchial glands (acinar cells) (n=2) | 0 | 1 | 1 |
| Bronchial epithelium | 8 | 2 | 0 |
| Other | 0 | 0 | 0 |

Table 6.3.9 Staining intensity of lung using antibody to ALA synthase.

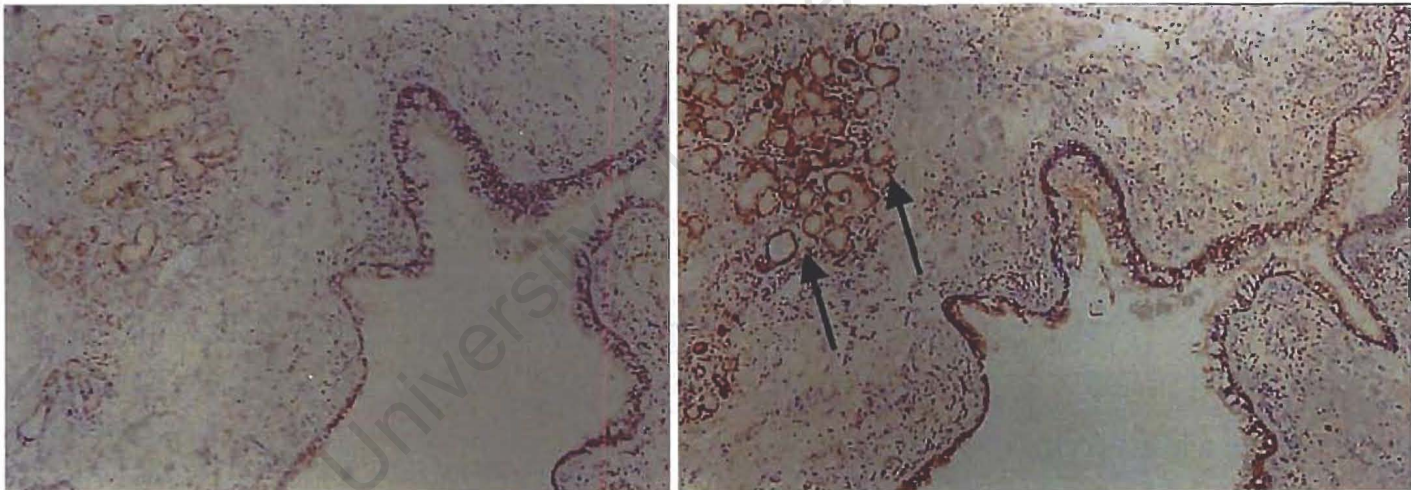


Fig 6.3.14.a Immunohistological examination of lung using antibody to ALA synthase at 40 times magnification. This sample contains bronchial glands(indicated by an arrow) showing moderate staining for ALA synthase. Note the weak staining in the brush border cells of the bronchial epithelium.

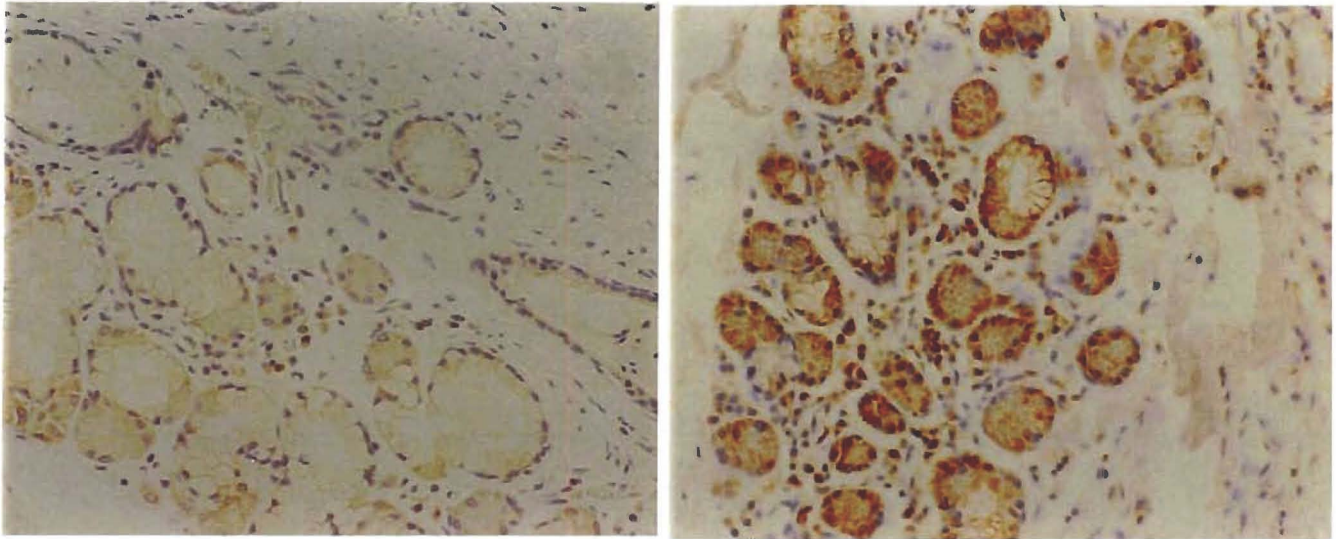


Fig 6.3.14.b Immunohistological examination of lung using antibody to ALA synthase at 100 times magnification. To the left a negative control sample is present. On the right, the sample contains bronchial glands showing moderate staining for ALA synthase.

Myocardium

Five myocardial biopsies were examined immunohistologically for ALA synthase.

| <i>Staining intensity and sample number (n=5)</i> | | | |
|----------------------------------------------------------|----------------------|--------------------------|------------------------|
| Cell Type | Weak staining | Moderate staining | Strong staining |
| Myocardial cells | 0 | 2 | 1 |

Table 6.3.10 Staining intensity of myocardium using antibody to ALA synthase.

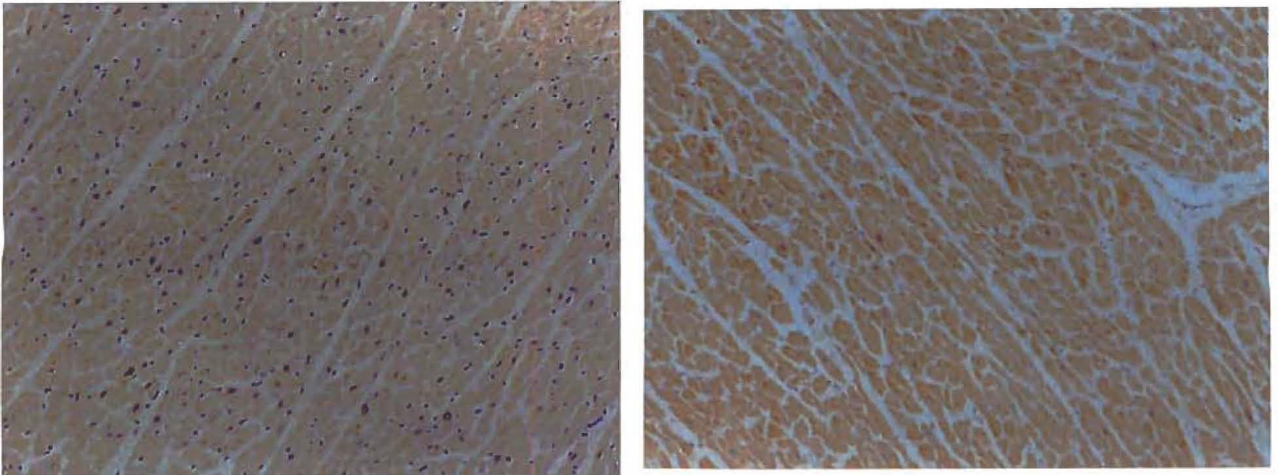


Fig 6.3.14.a Immunohistological examination of cardiac muscle using antibody to ALA synthase at a magnification of 100 times. To the left a negative control is present, while on the right, moderately strong staining is demonstrated in the muscle cells.

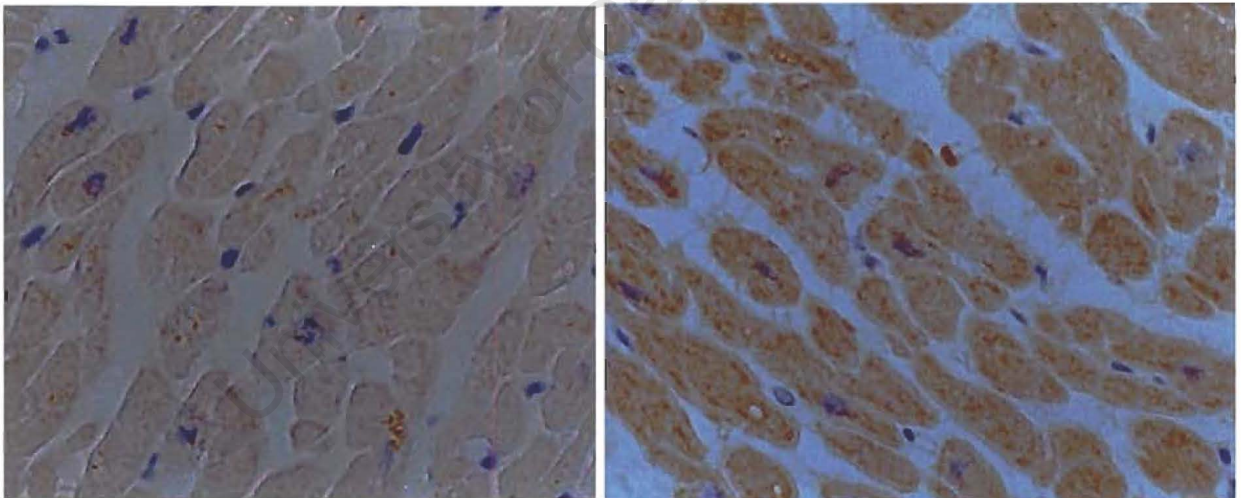


Fig 6.3.15.b Immunohistological examination of cardiac muscle using antibody to ALA synthase at a magnification of 400 times. As previously, a negative control is present on the left, while staining for ALA synthase is demonstrated in the right sample.

Myocardial cells are involuntary striated muscle cells, which contain many mitochondria and have a high oxygen demand. From this one could extrapolate a demand for haem and thus moderately strong staining for ALA synthase.

Summary of staining in all tissues

| Tissue | Cell Type |
|---------------------------|-----------------------------------------------------------------------------------------------------------------------------------------------|
| Liver | Hepatocytes – moderate to strong staining Bile ducts – none to weak staining. |
| Adrenal gland | Zona reticularis – moderate to strong staining Zona Glomerulosa – weak to moderate staining Adrenal medulla- staining in ganglion cells |
| Kidney | PCT- moderate to strong staining DCT- weak staining |
| Ovary | Staining in follicular epithelium |
| Testis | Staining in late spermatids |
| Neurones | Strong staining in neurones – including axons and dendrites |
| Anterior pituitary | Checkerboard staining in anterior pituitary cells. |
| Oesophagus | Weak to moderate staining in the functional layer of oesophageal mucosa, and in oesophageal glands. |
| Small intestine | Weak staining in the crypts of Luberkhun. |
| Colon | Moderate staining in endocrine cells. |
| Lung | Weak staining in bronchiolar epithelium, and moderate staining in bronchial glands. |
| Myocardial cells | Moderately strong staining in myocytes |
| Skeletal muscle | Moderate staining in type I muscle cells |

Table 6.3.11 Table showing summary of immunostaining in all tissues for ALA synthase.

The pattern of staining is presumed to represent the haem requirements of particular tissues.

As we have been studying human hepatic ALA synthase, our discussion does not take into account the high levels of erythroid ALA synthase present in developing erythroid cells, which accounts for about 85% of total haem production in the human body (May, 1995).

Haem containing proteins (as discussed in chapter 1) include NADH reductase, cytochrome reductase and cytochrome oxidase – all important electron carriers in the respiratory chain. Thus in tissues with large numbers of mitochondria, in which there are high metabolic requirements for ATP one would expect staining for ALA synthase.

However to state this alone as the reason for staining is rather too simplistic. I would like to suggest that over and above this, certain tissues (like liver, kidney, skeletal muscle) have specific requirements for haem to be incorporated into specific haem containing enzymes, which might not be simply proportional to mitochondrial number - leading to the highest levels of ALA synthase expression.

For example our strongest staining was obtained in liver. Although liver is metabolically very active, it is certainly not the most active tissue in the body, suggesting additional factors - such as a higher proportional amount of haem containing enzymes (such as the cytochrome p450's) that increase the specific haem requirement as a bigger determinant of ALA synthase presence. Liver with its multiple oxidative reactions and peroxidations (that require haem containing enzymes to catalyse these reactions) has a high requirement for haem and hence the strong staining.

Furthermore, in the anterior pituitary, all the cells are very active metabolically. However the staining for ALA synthase suggest variables in cellular expression amongst different cell types. This would suggest an additional haem requirement in the synthesis of some of the enzymes secreted by some of the pituitary cells (possibly as discussed above, the growth hormone secreting cells).

These results represent some insight into ALA synthase tissue distribution. While Srivastava's (1992) mRNA studies show similar ALA synthase distribution in rats (highest levels of hepatic ALA synthase being found in liver, testis, adrenal cortex, and myocardium), the immunocytochemistry shows the actual cell type containing ALA synthase. The advantage of this specificity using immunocytochemistry is for example, the high levels of ALA synthase detected in neurones – which perhaps was not apparent in the mRNA studies due to the “dilution effect” caused by the undetectable levels of ALA synthase in glial cells and other supporting tissue found in brain.

Disadvantages are the variation of staining between different samples. Although ALA synthase levels may vary between individuals depending on age, sex and diet (Srivastava, 1992) the variation seen using immunocytochemistry may represent time differences in fixing and processing of tissue.

Highly autolytic tissue yielded no staining for ALA synthase – even using liver. Therefore all immunocytochemistry using autolytic tissue was discounted in looking at these results.

Unfortunately due to the ethical constraints associated with using human tissue, optimum sample number (considered to be a minimum of 8 – personal communication – Corrigan, 1998), consistency in age and sex of patient was not possible – therefore limiting the conclusions that can be drawn using this study.

However, this immunohistological examination is the first in human tissue and sheds new light on the distribution of ALA synthase in human tissue.

Summary

An antibody was developed to human hepatic ALA synthase. In this work, human tissue was examined, immunocytochemically, for the presence of detectable quantities of ALA synthase. There was some inter-individual variation between tissue samples from the same organs; reproducible patterns of staining did emerge. We were able to show that ALA synthase is present in hepatocytes in moderate amounts, and in variable amounts in particular cells in different organs – for example - zona reticulosa in the adrenal gland, steroid secreting cells in the ovary, late primary spermatocytes in the testis, endocrine cells in the colon, myocytes in the myocardium, and some myocytes in skeletal muscle, some cells in the anterior pituitary, and in neurones in the brain. Thus for the first time not only the tissue distribution of ALA synthase is shown, but also which cells in a particular tissue express the enzyme most strongly.

One area this study does not address is the potential inducibility of the ALA synthase in each of these tissues. In the next chapter we will be discussing an immunocytochemical examination of a post mortem examination of a patient with acute intermittent porphyria who died during an acute attack of porphyria.

Immunohistological examination of ALA synthase in human tissue from a patient who died during an acute attack of AIP

7.1 Introduction

In this chapter we present an immunohistochemical examination for ALA synthase in several tissues from a patient (HK) who died as a result of prolonged, severe, recurrent acute attacks of acute intermittent porphyria (AIP).

HK first presented to a hospital in a state of flaccid quadraparesis and respiratory failure. This followed several bouts of acute abdominal pain over the preceding months. Her mother had died from a similar problem – which had never been diagnosed. A diagnosis of AIP was made after porphyrin analysis of urine, plasma and blood. It took several months for her to regain sufficient muscle strength to breathe spontaneously.

Following this, she continued to have acute attacks of porphyria at approximately 3 weekly intervals. However, the frequency and duration of these attacks increased until she was almost permanently confined to hospital. Several attacks were of sufficient severity to require admission to ICU for ventilation. She also required frequent early treatment with haem arginate and other supportive care. Unfortunately her response to haem arginate became less with time, with incomplete resolution of symptoms and shorter duration of response. Tin protoporphyrin was added to the treatment regime and appeared to have a better response of longer duration (with the effects lasting up to 3 to 4 weeks). Prophylactic administration of haem arginate did not appear to have any effect on preventing future attacks. Other treatments tried were parenteral administration of

GnRH agonist, which, although it caused persistent amenorrhoea, did not alter her clinical course.

Ongoing acute attacks continued for a further 5 years. Her clinical treatment was further complicated by tuberculosis – given the porphyrinogenicity of most anti-tuberculosis drugs choice of treatment was difficult. Initially she was treated with streptomycin and ethambutol, but unfortunately relapsed. She appeared to respond well to a nine-month course of streptomycin, ethambutol and amoxicillin-clavulinate.

Finally her condition deteriorated to the point that she was constantly in pain, despite ongoing treatment with massive doses of pethidine. Haem arginate, even with tin protoporphyrin, failed to clear her symptoms although it appeared to prevent a worsening to the point of paralysis (due to neuropathy). Finally, following a series of discussions between patient, medical and nursing staff, chaplain and ethicist, a decision was taken to scale down the intensity of therapy. No further haem arginate was given, and she died, well sedated, from respiratory failure.

The post-mortem showed a thin, small lady with obvious muscle wasting. Her heart, liver and kidneys were small. The liver was a dark slate grey colour. The kidneys were small, with thinned renal cortex.

Limited conclusions can be drawn from an immunohistochemical examination of one patient. Unfortunately, paraffin blocks from many other patients suffering from acute porphyria who died from a variety of conditions (and had previously given permission for further research to be undertaken), were destroyed in a fire.

Nevertheless, some insight into possible tissue differences in the inducibility of ALA synthase were deemed to be sufficiently interesting, for inclusion of this case report into this thesis.

7.2 Materials and methods

Materials

Surgical material, from patient HK, in the form of paraffin blocks, was obtained from the archives of the pathology department at Groote Schuur hospital. Permission to use archived material was obtained from the head of the pathology department.

Methods

The immunocytochemical technique used is that described in Chapters 4, 5 and 6.

7.3 Results and discussion

Liver

Macroscopically the liver appeared small (weighing 1042g – normal 1400-1600g), and appeared to be a dark, blue-grey colour. When cut it was slightly congested and very pigmented.

Histology showed no cirrhosis or fatty change. However examination of the liver was complicated by the presence of pigmented granules in the hepatocytes. This pigment appeared to be cytosolic, and was fairly clumped and refractile. It is demonstrated in the H and E stain of HK's liver below.

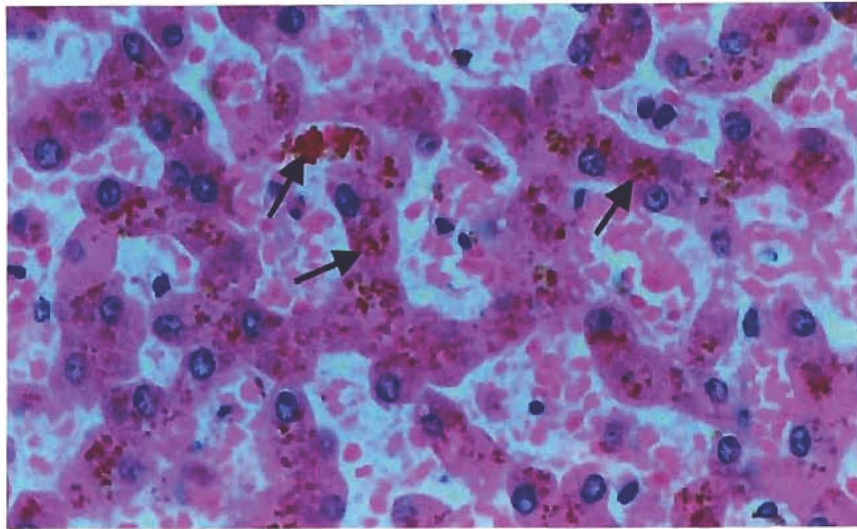


Fig 7.3.1. An H & E (haematoxylin and eosin) stained section of HK's liver viewed at 400 times magnification. Some of the pigmented granules, visible in the hepatocytes are indicated by an arrow.

Most of this pigment, stained positive for iron, as is shown in the perl's stain for iron, below. All iron stains as a blue-green colour.

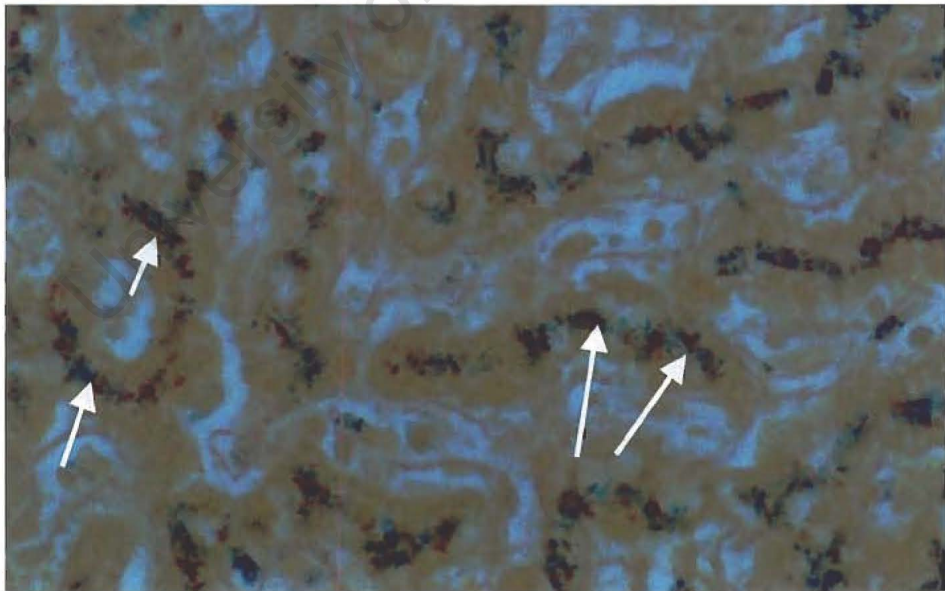


Fig 7.3.2 A Perl's stain of HK's liver viewed at 400 times magnification. The iron containing area's stain a greenish colour and some are indicated by arrows. Note the peri-cannicular arrangement of the iron pigment.

However, some pigment, (a small minority) which was less refractile than the iron pigment, was present and did not stain for copper, bile or porphyrin pigment. It is possible that this pigment could have been tin (due to her treatment with tin protoporphyrin) or lipofuscin.

Biempica et al, (1974) reviewed four liver biopsies in patient who suffered from acute intermittent porphyria as well as one biopsy obtained from a patient who died from AIP.

This was prior to the availability of haem arginate or tin protoporphyrin. They described several features found in biopsies from patients with AIP – including iron overload and the presence of lipofuscin granules – with larger areas of ferritin-like particles than that found in normal livers. In the one PM biopsy they studied, these particles were a prominent feature in all hepatocytes.

The pigment, a darker shade of brown than the immunohistochemical peroxidase stain does make interpreting the results more difficult. Unfortunately the water soluble Fast-red stain diffused throughout the liver sample, and was even more difficult to interpret. Because the negative control is shown with the sample, we are confidently able to interpret very strong staining for ALA synthase in hepatocytes, with weak to moderate staining in bile ducts.

The staining for ALA synthase in HK's liver was strongly positive in hepatocytes, and moderately positive in bile ducts.

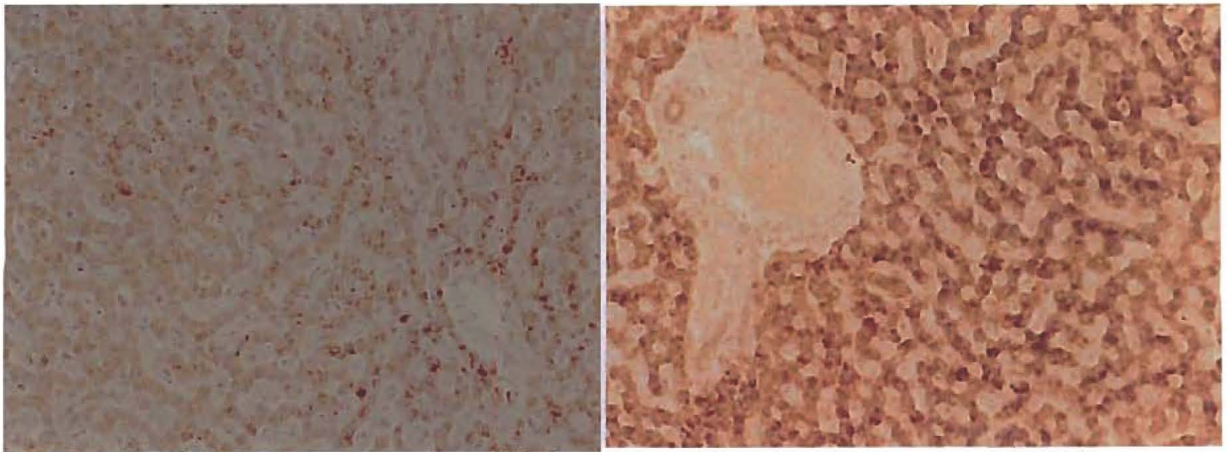


Fig 7.3.3 a Liver viewed at 100 times magnification from patient HK. The specimen on the left is a negative control sample, which shows pigmented granules in many hepatocytes. The specimen on the right is a one stained with antibody to ALA synthase. Strong staining for ALA synthase is present in hepatocytes, with moderately strong staining in bile ducts.

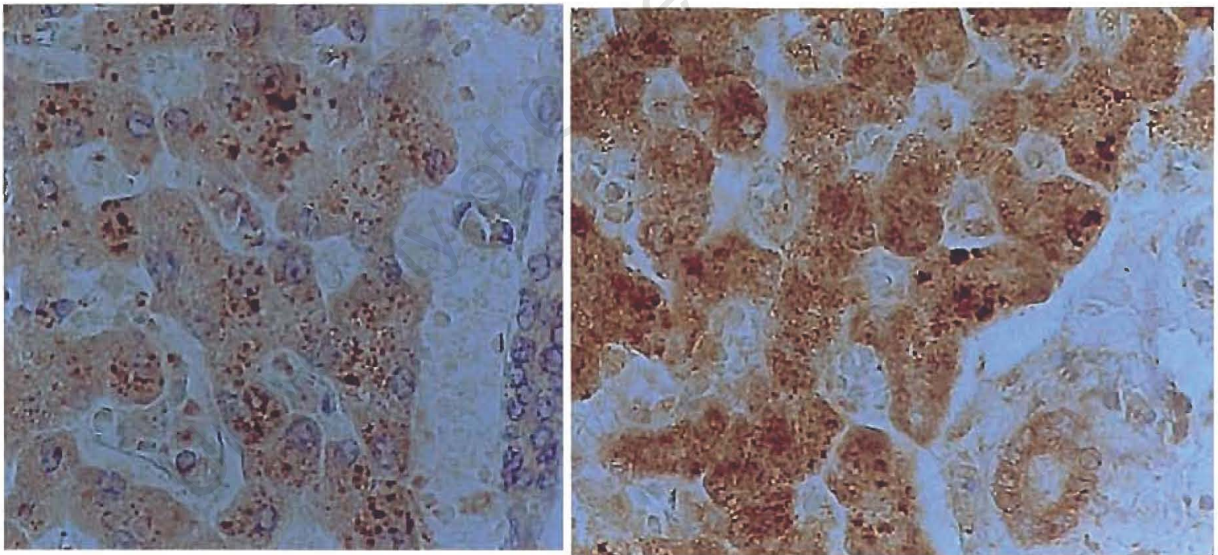


Fig 7.3.3.b Liver viewed at 400 times magnification from patient HK. The specimen on the right is a one stained with antibody to ALA synthase. Strong staining for ALA synthase is present in hepatocytes, with moderate staining in bile ducts.

Adrenal gland

Histologically the adrenal glands appeared normal. Staining for ALA synthase in the adrenal gland was very similar to that obtained in the standard surgical

specimens except the strong staining in the zona reticularis, appeared darker than the most strongly positive adrenal specimens in chapter 6. Strong staining for ALA synthase was also present in the ganglion cells of the adrenal medulla.

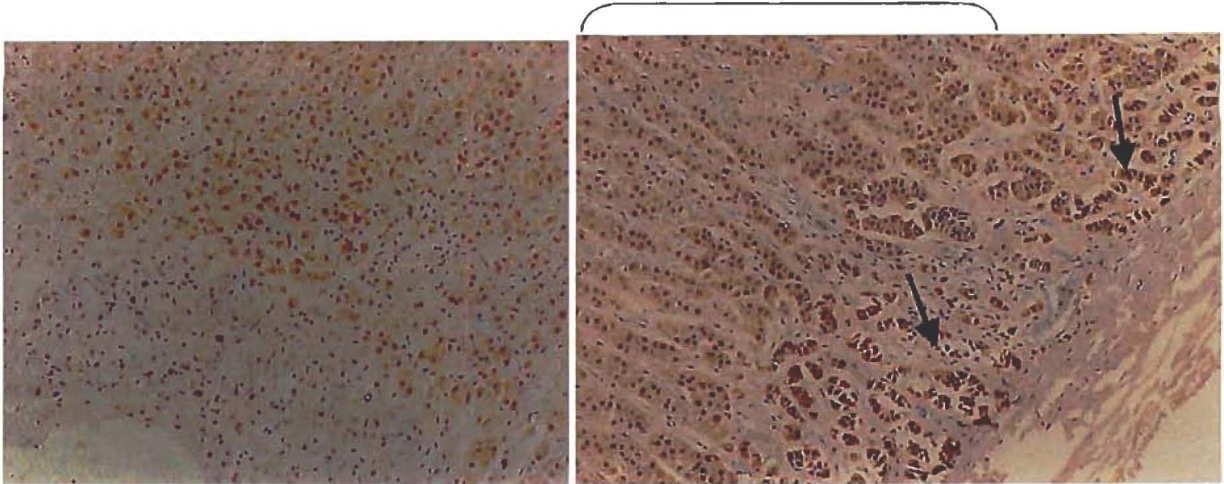


Fig 7.3.4.a. Adrenal cortex viewed at 100 times magnification. On the left a negative control specimen is present. On the right, there is strong staining in the zona reticularis, (some cells being indicated by a bold arrow) and moderate staining in the zona's fasciculata and glomerularis (indicated by a bracket).

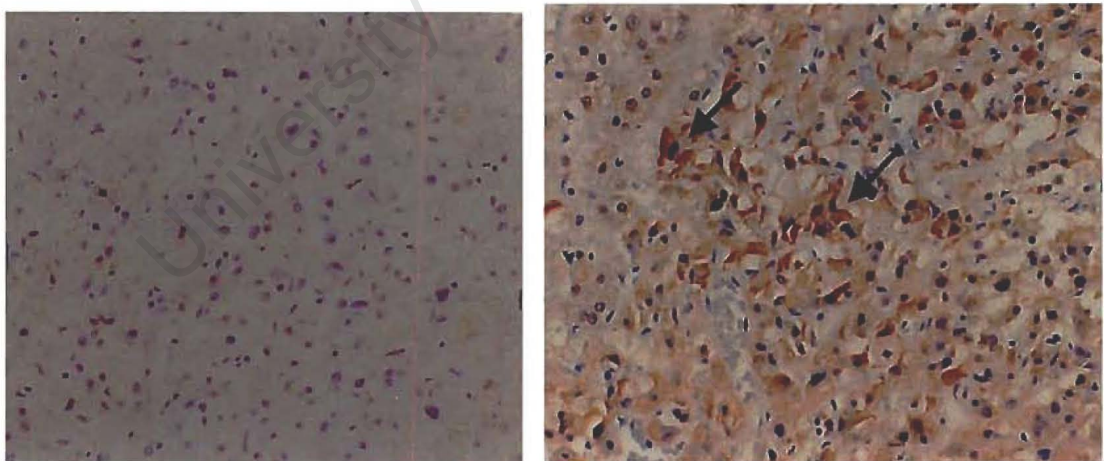


Fig 7.3.4.b Adrenal medulla viewed at 100 times magnification. To the left, a negative control specimen is present. On the right, the ganglion cells staining strongly for ALA synthase are indicated by an arrow.

Kidney

Both kidneys were small, with thinned cortices. The left and right kidney's weighed 75g and 79g respectively (normal 115 to 220g). There was no dilatation of the calyceal system. Histologically there was evidence of chronic pyelonephritis with focal areas of sclerosed glomeruli, tubular casts and interstitial inflammation. The staining for ALA synthase obtained in kidney is virtually identical to that obtained in our surgical biopsy specimens.

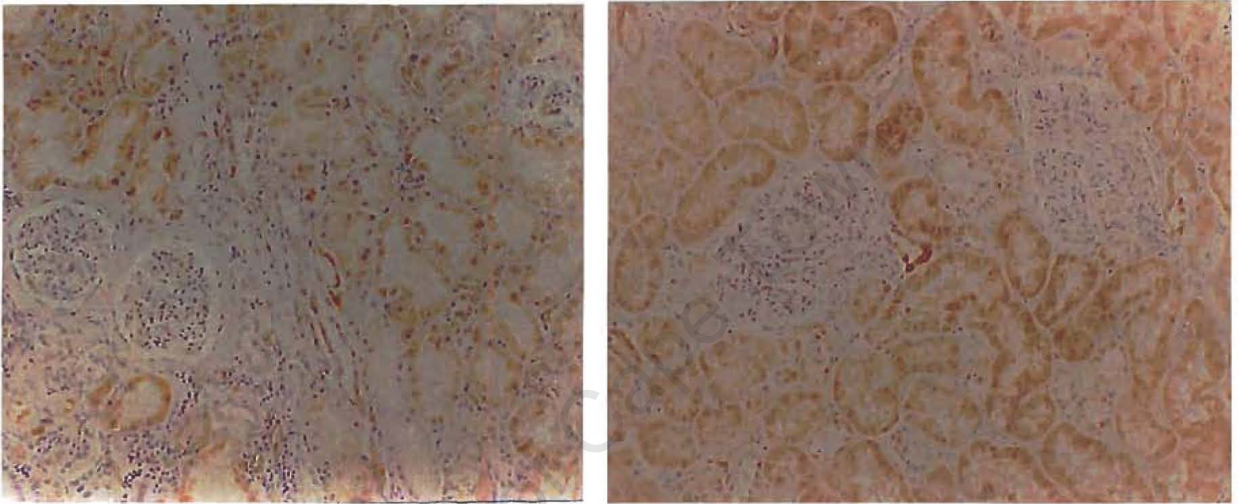


Fig 7.3.5.a Kidney viewed at 100 times magnification. To the left, a negative control specimen is present. Moderately strong staining for ALA synthase is present in the proximal convoluted tubules (PCT's).

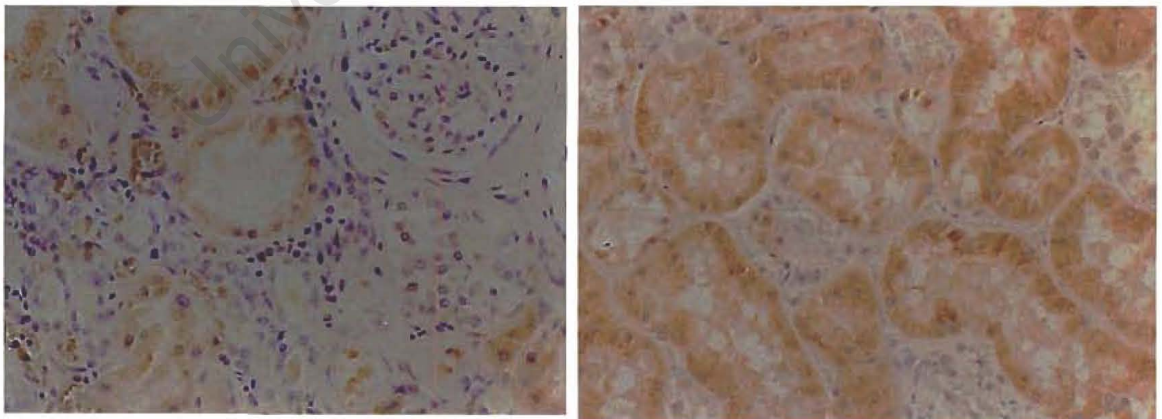


Fig 7.3.5.b Kidney viewed at 200 times magnification. To the left, a negative control specimen is present. Moderately strong staining for ALA synthase is present in the PCT's.

Myocardium

On macroscopic examination the heart appeared normal. Histology was unremarkable, except for iron deposits in supporting cells. Staining for ALA synthase was similar to that obtained in the surgical specimens, although once again it appeared to stain slightly darker for ALA synthase than the most strongly positive surgical specimen's.

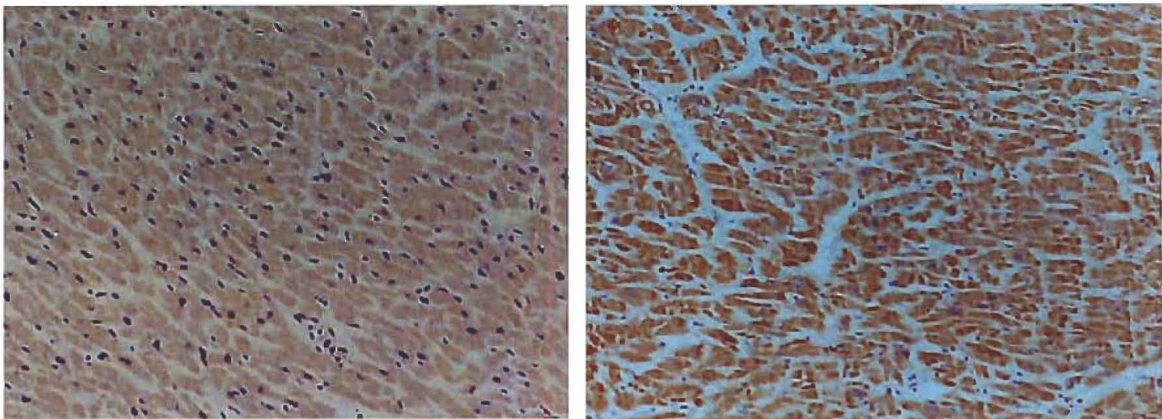


Fig 7.3.6 Myocardium of HK viewed at 100 times magnification. To the left, a negative control is present. To the right, moderate staining for ALA synthase is demonstrated in myocardial cells.

Skeletal muscle

Myocytes demonstrated either weak or strong staining for ALA synthase. The checkerboard pattern seen in non-porphyric samples (from chapter 6) was not seen – instead whole muscle bundles stained either weakly or strongly (fibre-type grouping). This pattern is commonly seen when staining for fibre types (e.g. stains for NADPH) in patients with peripheral neuropathy. The severe peripheral neuropathy that HK had would be an explanation for this staining pattern.

The explanation for this fibre-type grouping pattern is that as peripheral nerves are damaged and die the muscle fibres are re-innervated by sprouting of newly grown axons and endplates. Unlike the random (hence checkerboard) distribution of type 1 and 2 fibres which occur during normal development (and which are determined by

the type of innervating nerve fibre), patches of muscle fibres are all re-innervated by sprouting from the same nerve fibre growing in resulting in grouping of fibre types.

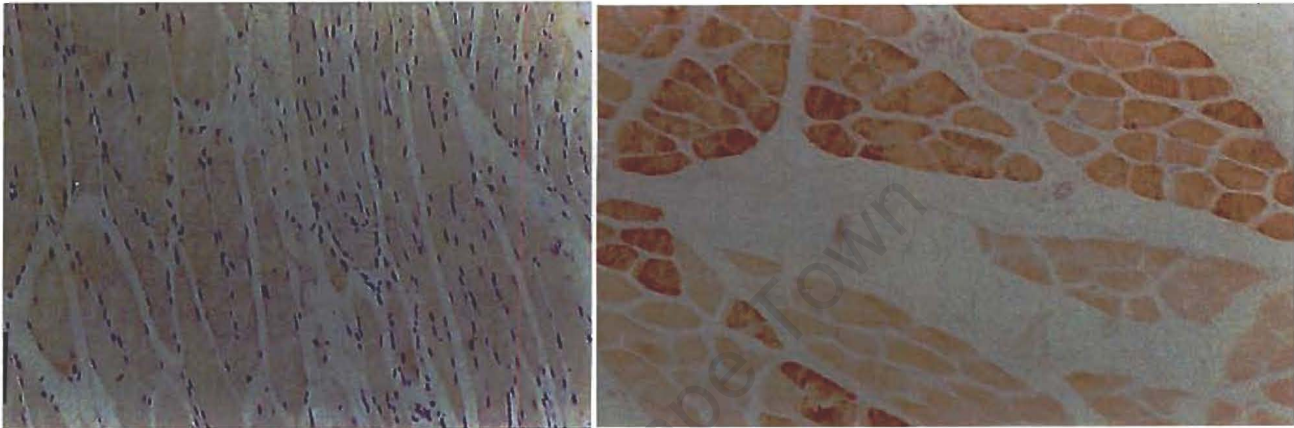


Figure 7.3.7 Skeletal muscle from HK viewed at 100 times magnification. Above a negative control sample is present. Below the sample stained for ALA synthase is present demonstrating variable staining for ALA synthase – although, unlike the other specimens from Fig. 6.3., no checkerboard pattern is present. The staining for whole muscle fibre bundles is probably indicative of the severe peripheral neuropathy that HK suffered from.

Anterior pituitary

Unfortunately no brain samples were available for immunocytochemistry, which is regrettable given its possible involvement in the pathogenesis of the acute attack.

However anterior pituitary had been sampled and demonstrated staining remarkably similar to that found in non-porphyrin individuals.

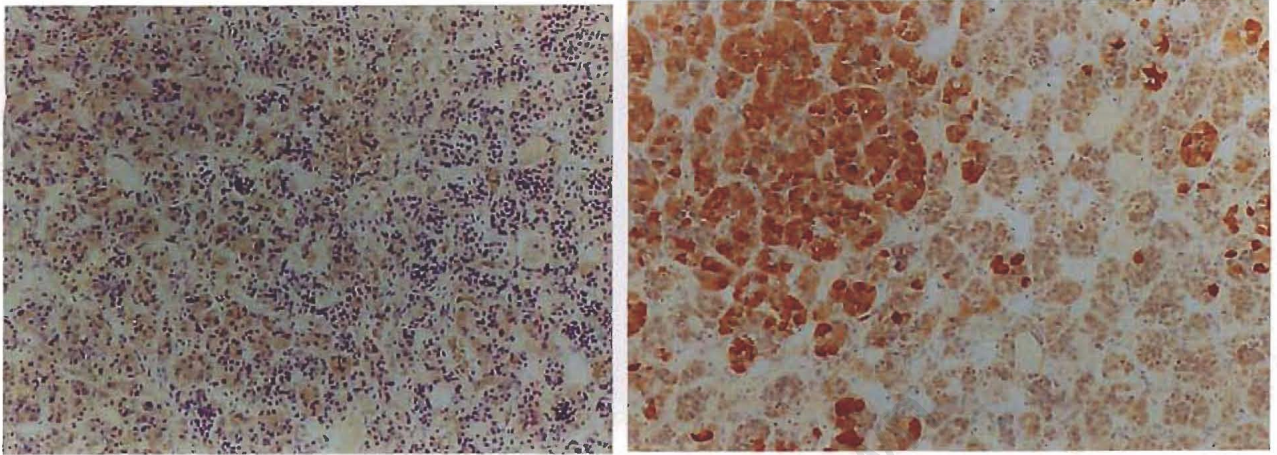


Fig 7.3.8 Anterior pituitary viewed at 100 times magnification. To the left a negative control is present. On the right, a checkerboard pattern of staining for ALA synthase is demonstrated.

Summary

In this chapter we looked at immuno-staining for ALA synthase in a young women, with severe Acute Intermittent Porphyria, who died during an acute attack of porphyria.

The liver samples, showed evidence of iron overload and stained strongly for ALA synthase. Strong staining for ALA synthase was also demonstrated in the proximal convoluted tubules of the kidney, zona reticulosa of the adrenal medulla, and myocardium. The staining in the kidney was as strong as that seen in the most strongly positive surgical specimens. The staining in adrenal gland and myocardium was slightly darker than that seen in the most strongly positive surgical specimens – implying high levels of ALA synthase.

Myocytes – probably Type Ia- stained strongly for ALA synthase, although not in the usual checkerboard fashion, but in a pattern characteristically seen with peripheral neuropathy.

Further conclusions from this study cannot be drawn and further case studies on porphyric subjects unfortunate to die either from acute porphyria or other causes would be helpful.

University of Cape Town

Chapter Eight

Final comments and future studies

ALA synthase, the first enzyme in the haem pathway can be induced, in acute porphyria, and thereby appears to play an important role in the acute attack of porphyria. Unfortunately the nature of the ALA synthase protein (mitochondrial matrix, hydrophobic and sensitivity to proteases) has made studying this enzyme technically difficult.

This project marked an important step in our characterization of human hepatic ALA synthase. We were able to produce an antibody to human hepatic ALA synthase. Expression of full-length enzyme did not prove possible, so a fragment of the protein was expressed in *E.Coli* as a fusion with *Shistosoma japonicum* glutathione transferase and purified on a hexyl-glutathione column. Antibodies were produced in rabbits, which recognized human and rat hepatic ALA synthase – but not human erythroid ALA synthase.

The antibody was suitable for use in immunocytochemistry – thus allowing us to examine the human tissue – and indeed cellular distribution of ALA synthase. ALA synthase was detected in hepatocytes, proximal convoluted tubule cells in the kidney, zona reticularis in the adrenal gland, myocytes, myocardium, bronchial glands of the lung, oesophageal epithelium, endocrine glands of the colon, anterior pituitary cells and neurones. Very little ALA synthase was detected in stomach and small intestine.

The apparent high concentrations of ALA synthase in neurones (including dendrites and axons), has not been documented previously. This result lends weight to the theories about the acute attack of porphyria being related to neuronal haem deficiency or direct neurotoxicity of ALA. Previously it was thought that there was very little ALA present in the CNS due to the low concentrations measured in

cerebro-spinal fluid. The amount of ALA potentially present in neurones has never been determined. This work suggests that the amount of ALA potentially present in neurones is significant, as judged by the amount of immunoreactive ALA synthase present in surgical brain tissue specimens. It is therefore clear that further research on the role of ALA synthase in neuronal functioning, both under physiological circumstances and more specifically in the acute attack of porphyria, is indicated.

The case study of patient HK, who died from porphyria, showed strong staining for ALA synthase in liver, kidney and adrenal gland. While it is intriguing to observe that the levels of ALA synthase were apparently induced to a high degree in the porphyric case, further case studies would be necessary before meaningful comparisons can be made.

However, one of the factors hampering further research into ALA synthase is the lack of a suitable expression system, for ALA synthase - which limits characterization of the human hepatic isoform of the enzyme. All of the prokaryotic expression systems that we tried were unsuccessful, and the eukaryotic expression system in COS cells was just adequate to use as a positive control for our antibody. As it would be of great value to be able to produce ALA synthase protein for study purpose, in expression systems, we would suggest further work using alternative systems. Some of these that could be tried include baculovirus expression systems, using insect cells or silkworm larvae (Murakami et al 2001).

Another important area of future research is investigation into the regulatory sequences of the human hepatic enzyme. Once regulation of ALA synthase is understood, both under physiological circumstances and in acute porphyria, the potential exists for specific therapies designed to prevent the induction of ALA synthase, and perhaps altering the course of the acute attack in severely affected individuals with acute porphyria.

APPENDIX 1

STANDARD METHODS

A 1.1 Small-scale isolation of plasmid DNA.

Plasmid DNA was extracted by an adaptation of the Ish-Horowicz and Burke (1981) method as described in the Short Protocols of Molecular Biology. Five ml of ψ BROTH (a nutrient rich *E.Coli* culture broth - see Addendum A2.), containing the appropriate antibiotic selection pressure was inoculated with *E.Coli* and incubated overnight, in a shaking incubator at 37°C. Two ml of culture was pelleted in an eppendorf microfuge for 1 minute. The supernatant was aspirated and discarded and the cells were resuspended in 100 μ l of GTE (see Addendum A.2). This was allowed to stand at room temperature for 2 minutes. Two hundred μ l of fresh 0.1M NaOH, 1% SDS was added to the sample and this was incubated on ice for 5 minutes. One hundred and fifty μ l of KAc (see Addendum A2) was added and the sample was incubated on ice for a further 5 minutes. This was then centrifuged in an eppendorf microfuge for 5 minutes. Four hundred μ l of the supernatant was aspirated and transferred to a clean eppendorf. Eight hundred μ l of 100% ethanol was added and the sample was allowed to stand at room temperature for 2 minutes, before being spun in the Eppendorf microfuge for 10 minutes, to precipitate the DNA. The DNA was washed in 1ml of 70% ethanol and briefly dried, before being resuspended in 20 μ l of TE (see Addendum A2), containing 1 μ l of 10 mg/ml RNase A.

A 1.2 Large-scale isolation of plasmid DNA

Plasmid DNA was extracted using ion exchange chromatography. The column were from Qiagen Plasmid Midi kit and used according to the manufacturers instructions. The protocol is based on a modified alkaline lysis procedure, followed by the binding of plasmid DNA to an anion-exchange resin. Impurities are removed using medium salt washes. The plasmid is eluted under high salt conditions and precipitated using isopropyl alcohol.

A 1.3 Restriction endonuclease digestion and DNA ligation reactions

The methods used are adaptations of those described by Maniatis et al, 1990. Up to 5µg DNA was digested in a total volume of 20µl, containing 3 - 5µl of restriction endonuclease per µg DNA and appropriate enzyme buffer as supplied by the manufacturer (Boehringer Manneheim). Reactions were incubated at the suggested temperatures for periods of 1 to 3 hours.

Ligation reactions were performed overnight at 10° C in a total volume of 20µl of ligation buffer supplied by the manufacturer (Promega) and 1 µl of T4 DNA ligase. The total concentration of DNA in the vector-insert ligation mixture was 15 pmol. The vector and insert DNA were present in a molar ratio of 1:2 per ligation reaction. To control for ligase activity, 5 pmol of single cut plasmid DNA was included as a positive control. When ligations were performed using a single-cut ligation, the vector was subjected to dephosphorylation using calf intestinal Alkaline Phosphatase, used according to the manufacturer's instructions.

A 1.4 Preparation and transformation of competent *E.Coli* cells

A modification of the Rubidium Chloride method described by Maniatis et al (1982) was used for the preparation of competent *E.Coli* cells. One colony of *E.Coli* was picked from a fresh agar plate and inoculated into 10 ml of ψB (See Addendum A2) and incubated overnight in a shaking incubator at 37° C. The following morning 5-ml of the overnight culture was inoculated into 100ml of pre-warmed ψB in a conical flask and incubated in a shaking incubator at 37°C for 1.5 to 2.5 hours, until the OD₅₅₀ reached 0.35. The culture was then decanted into two 50ml centrifuge tubes and chilled on ice for 15 minutes, before being centrifuged in a JA-20 rotor (Beckman) at 2500rpm for 5 minutes at 4° C. The supernatants were aspirated and discarded and each pellet was gently resuspended in 10.5ml ice-cold TFB1 (see A 2), pooled and incubated on ice for 90 minutes. Cells were then centrifuged at 2500 rpm in a JA -20 rotor at 4°C.

The supernatant was once again aspirated and discarded and the cells were gently resuspended in 3.5ml ice-cold TFB2 (see A 2). One hundred μl aliquots of cells were aliquotted into eppendorf tubes. The cells were then competent and could either be used immediately for transformation, or could be flash-frozen in liquid nitrogen and stored at -80°C where cells remained competent for several months for transformation at a later stage. Once frozen, competent cells were thawed on ice for 10 minutes. Fresh competent cells were ready for immediate use. Up to 10ng of DNA in 10 μl of dd (double distilled) H_2O , or 10 μl of a ligation mixture was added to a 100 μl aliquot of competent cells and incubated on ice for 30 minutes. The cells were subjected to a heat shock at 42°C for 2 minutes, followed by quickly returning the cells to ice for a period of 5 minutes. Four hundred μl of ψB was added to each sample, which was then incubated at 37°C for 45 minutes. Up to 100 μl of sample was plated onto a ψB agar plate (see A2) containing the appropriate selective antibiotic. To prevent spurious results the following control samples were included: competent cells with no plasmid DNA and competent cells with 1 pg to 1ng of uncut plasmid DNA, to assess transformation efficiency. Cells prepared and transformed in this manner had a transformation efficiency of approximately 10^6 colonies per μg of DNA.

A 1.5 DNA agarose gel electrophoresis

DNA fragments were separated using horizontal gel electrophoresis systems. Agarose in a TBE/EthBR Buffer (see A2) was used in concentrations varying between 0.75% and 2%, depending of the DNA fragment sizes. Samples were loaded into agarose gel wells with a 10% final volume of DNA sample loading buffer (see A2). DNA bands were visualised using a UV transilluminator (254 nm) and photographed using a Polaroid camera and 667 photographic film.

Standard DNA fragment sizes were obtained by digesting λDNA with either *Pst I*, or *Eco RI* and *Hind III*, restriction enzymes (see A2). For fragments smaller than 1000 bp(base pairs), a 100 bp ladder (Promega) was used. The DNA fragments were sized by comparison to a standard curve obtained by the calculating the log molecular mass of known DNA fragment sizes versus their relative mobilities.

A 1.6 PCR

PCR's were performed in using TAQ DNA Polymerase, (Boehringer Manneheim) in PCR buffer (with pre-added magnesium) according to the manufacturers instructions. dNTP's were used at a concentration of 200 μ M of each dNTP/100 μ l reaction. Primers (synthesised by Genosys) were used at a concentration of 25-pmol/100 μ l reaction. Concentrations of template varied between 100pg and 1 ng of plasmid DNA. Annealing temperatures varied depending on the primers that were being used.

A 1.7 DNA Sequencing

DNA sequencing was achieved in both directions using the di-deoxy chain termination Method (Sanger, 1977). A modified T4 DNA polymerase, Sequenase Version 2 T7 Polymerase (US Biochemical Corporation) was used. Fluorescent labelled sequencing primers directed to the T3 and T7 promoters were used. Sequencing was performed using an automatic sequencer (Pharmacia) and ALF express software (Pharmacia) was used to analyse the sequence.

A 1.8 Production of hexyl-GSH

This procedure was performed at room temperature, according to the method described by Vince, *et al* (1971). Two ml of reduced GSH was prepared to a concentration of 2mm. Thereafter 2ml of a 2N solution of NaOH was added to the GSH solution. Ethanol is added, one drop at a time, using a pasteur pipette, until cloud point is reached (usually after a total volume of 10ml was reached). One-iodohexane is slowly added to the solution over a period of 30 minutes to give a final concentration of 2mm hexane. This was covered with parafilm and stirred overnight. The pH is reduced to 3.5 by drop-wise addition of 47% of hydrogen Iodide. The solution was then incubated at 4°C for 4 hours. The solids were then removed by filtration and washed with 20ml of distilled water and dissolved in a minimum volume of water at 90°C. This was allowed to crystallize by the addition an equal volume of 100% ethanol and stored at -20°C overnight and the crystals are allowed to dry between pieces of Whatman filter paper.

The hexyl-glutathione is stored in a desiccator at -20° . Purity of the hexyl-glutathione was not verified.

A 1.9 Production of Hexyl-GSH affinity column

This was prepared according to the method described by Simons and Vander Jagt (1981). Six grams of epoxy-sepharose 4B was rehydrated in dd (double distilled) H_2O before being washed on a scintered glass filter with 800ml dd H_2O . 12 ml of hexyl-GSH ligand solution (see A2) was added to the epoxy-sepharose. This was gently shaken for 30 hours at 30° C. The coupled gel was then washed with 200 ml of dd H_2O , and the remaining active groups were blocked, by allowing the gel to stand in 1M ethanolamine, for 4 hours. The gel was then washed on a scintered glass funnel with 200ml of NaOH/ $NaHCO_3$ buffer (see A2) followed by 200ml of Borate buffer (see A2), 200ml of Acetate buffer and 400ml of dd H_2O . The column was then washed with 100ml of STE (see Addendum A2) and stored at 4° C in STE containing 0.1-% Sodium azide.

A 1.10 CDNB Assay to check for GST expression

This was a modification of the method described by Mannervik and Danielson (1988). Protein lysate was prepared as for protein purification (see in chapter 3) 2.75ml GST assay buffer (see A2), 0.1ml of CDNB solution (see A2) and 0.15ml of reduced GST solution (see A2) were combined in a quartz spectrophotometer cuvette to be used as a blank for the spectrophotometer. A second quartz cuvette containing the above-mentioned reagents with the addition of 10 to 50 μ l of protein lysate was prepared. The absorbency readings of both the blank and the sample cuvettes were simultaneously read at A_{340nm} , at 0.5 second intervals for a period of one minute. The activity was calculated by the change in absorbency in the blank subtracted from the change in absorbency of the sample, multiplied by 31.35, divided by the time in minutes. The result is expressed as the μ mol formed/min/mgprotein.

A 1.11 Protein Determination

Protein determination was performed using a Biocinchoninic acid kit obtained from Boeringer Manneheim, used according to manufacturers instructions.

Reagent for protein determination was prepared by adding 1 volume of Copper(II)Sulphate pentahydrate 4% solution to 50 parts of Biocinchoninic acid solution (containing biocinchoninic acid, sodium carbonate, sodium tartrate, sodium bicarbonate in 0.1N NaOH, pH 11.25). Two ml of reagent was used for each protein concentration calculation.

A rough estimate of protein concentration in the sample is established by doing an absorbancy reading at OD₂₆₀ nm.

A standard curve for calculations of protein concentration was prepared by adding increasing concentrations of BSA (1 mg/ml diluted with H₂O to give a total volume of 100µl volume) to 2 ml of biocinchoninic acid solution. Protein sample whose protein concentration had previously been roughly estimated is diluted as appropriate to ensure that the concentration is likely to fall within the range of the BSA protein concentrations is added to 2 ml of the biocinchoninic acid solution at the same time as the standard samples are prepared. After briefly vortexing each sample, the samples are incubated in a 37°C water bath for 30 minutes and allowed to return to room temperature. Absorbancy is read at 562 nm.

The absorbancy readings of the samples with known concentration of protein (i.e. the BSA samples) are plotted onto a graph. The y-axis represents the known concentration of protein, and the x-axis represents the absorbancy reading. The absorbancy of the unknown protein is read by plotting this onto the graph.

A 1.12 SDS Page gels

SDS polyacrylamide gels were run according to the method described by Laemelli (1972) and O' Farrell (1975). Acrylamide concentrations varied between 10 and 12%. Gels were run using the Biorad minigel apparatus as well as a larger piece of apparatus,

kindly made by one of the university technical staff. Acrylamide gel mix, separating and stacking gel buffers were prepared as described in A2. Separating and stacking gels were prepared as described (A 2) and allowed to polymerise. Protein samples were heated to 100°C in 1 times reducing solubilization solution (A2) for 3 minutes prior to being loaded in the sample wells.

Gels were allowed to run in SDS running buffer (A2) until the dye front was 2mm from the end of the gel. Gels were stained using Coumassie staining solution (A2) for 1 to 2 hours and thereafter placed in Destain solution (Addendum A2) until protein bands were clearly visualised. Rainbow molecular weight markers (Amersham) or Biorad prestained markers or Pharmaciae (non prestained markers) were used and proteins were sized by comparison to a standard curve obtained by the log molecular mass of the protein markers versus their relative mobility's.

A 1.13 Western blotting

A modification of Western blotting as described by Towbin *et al* (1979) was used to blot proteins onto nitrocellulose membranes. Both the tank system and the horizontal semi-dry blotting systems were used as described in Current Protocols in Immunology.

After SDS page gels had been run as described in A 1.12, gels were incubated in transblotting buffer (25 mM Tris, 192 mM glycine, 20% methanol). Filter paper and nitrocellulose membrane (Hybond C) were also immersed in transblotting buffer, until completely moistened.

Thereafter the gel was applied to the nitrocellulose membrane, after being sandwiched between several layers of filter paper. This was placed in a gel transfer chamber, with the gel being placed closest to the negative electrode. The gel is run at 300mA for one hour.

Once blotting onto the nitrocellulose membrane had been completed, the membrane was blocked in TBS/Tween/skim milk (A2) for 45 minutes. Primary antibody was added to fresh blocking buffer in dilutions ranging between 1:1000 and 1:5000. The

membrane was incubated in the primary antibody solution for 45 minutes. After the membrane had been washed in at least 3 washes of blocking buffer, secondary antibody (HRP Goat anti-rabbit obtained from Omnimed) was diluted 1:500 in blocking buffer and incubated with the membrane for 45 minutes. The membrane was then washed - twice with blocking buffer and three times with TBS-Tween (see A2) and a further 3 times with TBS.

The blot was developed using 4-chloro-1-naphthol solution (A2) in the dark for a period of 2 to 5 minutes (until the bands were clearly visualised.)

A 1.14 Preparation of Antigen for Antibody production in rabbits

Ten to 15 μg of purified protein that had been purified as previously described in chapter 3 was loaded onto each well of a 20 by 20 cm SDS page gel, prepared as described in A 1.13. After the gel had run, it was blotted onto nitrocellulose membrane as described in A 1.15. The proteins on the nitrocellulose membrane were stained in TCA Coumassie solution (A2) for 1 to 2 minutes and then destained in Destain buffer. The nitrocellulose membrane was then washed in ddH₂O and allowed to dry between 2 sheets of blotting paper. Approximately 100 μg of the appropriate protein band was then excised and solubilised by vortexing in 1 ml of DMSO, immediately prior to injection of antigen into rabbits.

A 1.15 Polyclonal antibody production in rabbits

The protocol for immunisation of rabbits is an adaptation of that described in Current protocols in Immunology (1995). The rabbits were initially inoculated with 1ml of antigen, prepared as described in A 1.14, combined with 1 ml of complete Freund's adjuvant, into multiple subcutaneous sites. The inoculation was repeated after a 21-day interval - this time using incomplete instead of complete Freund's adjuvant, and at 10-day intervals following the second inoculum until antibody responses were detected. A trial pre-immunisation bleed took place before the first inoculation and every inoculation following the third inoculation, until the desired antibody response was achieved. This was usually obtained after the 5th or 6th inoculation. Rabbits were then

maintained for a maximum of 20-ml ear bleeds, which took place every four weeks. Antibody response was tested using Western blotting (as described in A 1.13) and ELISA's (as described in A 1.16)

A 1.16 ELISA

ELISA's were performed as a modification of the indirect ELISA technique described in Current Protocols in Immunology (1995), supplement 2. Two to ten µg of purified protein was applied in a maximum volume of 50 µl per well of the ELISA microtitre plate and allowed to dry overnight at 37° C. One hundred µl of 80% methanol was applied to each well for a period of 15 minutes, in order to fix the protein. The wells were then blocked for 45 minutes using blocking buffer (see A 2). 50 µl of Primary antibody diluted in blocking buffer was applied at dilutions varying between 1: 1000 to 1: 32000. The wells were then washed 4 times with blocking buffer and twice with TBS-Tween. Fifty µl of the secondary antibody, diluted in blocking buffer, in concentrations varying between 1:2000 and 1:10 000 was applied to each well for a period of 45 minutes. The wells were then washed as described above, with 2 additional washes with TBS, and the ELISA was then developed using 100 µl of α-phenyldiamine in citrate buffer, and H₂O₂ (see A2), for a period of 10 to 30 minutes, in the dark. The reaction was stopped by adding 50µl/well of 2.5M H₂SO₄. The ELISA was read on a microplate reader at 540nm.

A 1.17 Maintenance of COS cells

COS cells were cultured according to the method described in Current Protocols in Molecular Biology (1997- section 9.2.1-9.2.10).

The cells were cultured in DMEM (Sigma or GIBCO) containing L-Glutamine and 10% heat inactivated foetal calf serum (FCS). Foetal calf serum (GIBCO) was heat inactivated by incubating it for 30 minutes at 56°C.

Prior to plating of cells onto the standard TC Plates or chambered microscope slides,

the plates were coated using Poly-L-Lysine. Poly-L-lysine stock was prepared as described in A2. A volume of 250 µl/well of a 12 well plate or per well on microscope slides. This was allowed to stand at 37°C for 10 to 15 minutes. The wells were washed several times using PBS. These were allowed to dry before cells were plated.

Cells were diluted to 50 000 cells/ml media before being plated. 12 ml of media was used per T75 Flask. The cells were incubated at 37 °C incubator (an autoflow, water – jacketed CO₂ incubator, with the CO₂ set at 5%).

The media was changed every 24 hours and the cells were allowed to grow to a confluence of 80 %. Once confluency was achieved, the cells were lifted using Trypsin/EDTA (see A2).

The TC flask was washed using HBS. Thereafter 5 ml of Trypsin/EDTA was applied to the cells. This was allowed to incubate at 37 °C for 3 to 5 minutes. The flask was checked every minute under the dissecting microscope and once the cells were rounded the flask was vigorously tapped to aid lifting of the cells. The trypsin reaction was stopped by the addition of 2 ml DMEM/FCS. This suspension was spun at 1000g for a minute and the supernatant was aspirated and discarded. The cells were resuspended in 5ml of DMEM/FCS. These were counted using a Coulter counter.

Cells were then diluted to the appropriate dilution before being plated.

A 1.18 DEAE Dextran transient transfections of COS cells.

Unless otherwise stated all incubation steps take place in an autoflow water jacketed 37° C incubator with the CO₂ concentration set at 5%.

For transfections of COS cells onto microscope slides, the two-chambered microscope slides were coated in poly-D-lysine (Sigma) – diluted 1:40. The slides were washed four times, using PBS. COS cells, which had been trypsinized as described in A1.17 were diluted to 100 000 cells/ml. Approximately 250 000 cells (in a volume of 2.5 ml) were placed in each well of the microscope slide and allowed to grow overnight at 37°

C in 5% CO₂.

The media was then aspirated from the wells and the cells were washed several times with HEPES/DMEM (see A2). A volume of 0.6ml of the HEPES/DEAE dextran/DNA solution (containing 1/10 volume of HBS/DEAE dextran – see A2 and 9/10 DMEM together with 2.5µg of DNA) was added to each well of the microscope slide and allowed to incubate at 37°C (5% CO₂) for 4 to 5 hours.

The DEAE dextran/DNA solution was carefully aspirated from the cells and 1 ml of freshly prepared chloroquine solution was added to each well (200µM Chloroquine in DMEM). The cells were incubated for a further hour at 37°C, followed by careful washing using HEPES/DMEM.

The final stage in the transfection was a DMSO shock. Ten percent DMSO (1ml) was added to each well and gently aspirated within 2 minutes of being applied to the cells. The cells were then washed with HEPES/DMEM. The cells were then incubated for 24 to 48 hours in DMEM/HEPES/10%FCS.

A1.19 Double immunodiffusion

A 1.2% solution of Agar Noble was dissolved in potassium phosphate buffer (0.15M NaCl; 0.05M sodium phosphate; 0.1% Sodium azide, pH7.4), with heating and using constant stirring to prevent boiling. Molten agar was poured onto a pre-warmed, ethanol cleaned glass plate, which had been placed on a horizontal platform. This was allowed to set for 30 minutes, before being stored at 4° C, covered until needed.

4 mm wells were punched in the agar in a rosette pattern. Several rosettes were punched into agar. In 2 of the rosettes, 10 µl of antiserum to µGST was pipetted into the central well. 10 µl of cytosol from each one of the liver cytosol preparations was pipetted into all of the peripheral wells in doubling dilutions.

In 2 of the rosettes 10µl of cytosol preparations was pipetted into the central well. 10 µl of antiserum to µGST was pipetted into the peripheral wells in doubling dilutions. The

plates were stored in a horizontal position for 48 hours at 25°C to allow diffusion of cytosol and antiserum. The plates were then washed in several changes of Saline (0.9% NaCl, 0.1% Sodium azide) for 72 hours to remove unprecipitated protein. The plates were then washed in double distilled water for 4 hours, before being stained for 2 hours in Amido black (0.2% amido black / 5% acetic acid.) The gels are then destained using 5% acetic acid.

A1.20 Human GST purification.

These were purified using a hexyl-GST affinity column according to the method described by Guthenberg and Mannervik (1979).

A volume of 10ml h-GSH sepharose was used per 50ml of cytosol. The column was equilibrated with 0.2mM DET, 0.01M Tris HCl. The cytosol was then applied to the column at a flow rate of 17.5ml/hour. The column was then washed overnight with equilibration buffer, until the OD₂₈₀ of the eluant was the same as equilibration buffer. The column was then washed with equilibration buffer containing 0.2M NaCl to remove non-specifically bound proteins, after which the GST mixture was eluted using 5 mM Hexyl-GSH (As described in A2.). A total volume of 15 ml hexyl-GSH buffer was applied to the column - 2ml at a time and allowed to empty by gravity flow.

The fractions were analysed for protein content in a spectrophotometer at an OD₂₈₀ and fractions containing protein were pooled and stored at -20°C until needed.

A.21. Watson-Swartz test for presence of ALA

Two ml of solution containing ALA (e.g. cell culture supernatant) is mixed with 1 ml of ethyl-acetoacetate and incubated at 100°C for 10 minutes. After the mixture has been allowed to cool to room temperature an aliquot is removed and added to an equal volume of Ehrlich's aldehyde. If ALA is present the colour changes to a bright pink colour.

APPENDIX 2

Standard buffers and media

Amido-Black stain for double immunodiffusion

| | |
|-------------|------|
| Amido black | 0.2% |
| Acetic acid | 5% |

CDNB buffer

| | |
|------|----------------------|
| CDNB | 30mM in 100% ethanol |
|------|----------------------|

DNA sample loading buffer/Stop buffer

| | |
|------------------|-----------------------------|
| Bromophenol blue | 0.25% (w/v) |
| Glycerol | 50% (v/v) |
| EDTA | 100mM (final concentration) |

Equilibration buffer for human GST purification

| | |
|----------|-------|
| DET | 0.2mM |
| TrisH Cl | 0.01M |

GSH buffer

| | |
|--------------|----------------|
| GSH(reduced) | 20mM in water. |
|--------------|----------------|

GST assay buffer

| | |
|--------------------------------------------------------------------------|------|
| KH_2PO_4 | 0.1M |
| Na_2HPO_4 | 0.1M |
| pH KH_2PO_4 to 6.5 using the Na_2HPO_4 . | |

GTE (pH 8.0)

| | |
|---------|-------|
| Glucose | 50mM |
| Tris | 25 mM |
| EDTA | 10mM |

Hepes Buffered Saline (HBS):

| | |
|----------------------------------|--------|
| NaCl | 137 mM |
| KCl | 5 mM |
| NaH ₂ PO ₄ | 0.7 mM |
| Hepes | 21 mM |

Hepes/DMEM

| | |
|------|------|
| DMEM | 50ml |
| HBS | 1ml |

HBS/DEAE dextran (3 mg/l):

| | |
|-------------------|-------|
| DEAE dextran: | 60 mg |
| HBS: | 20 ml |
| Filter sterilise. | |

Hexyl-Glutathione affinity column solutions

Ligand buffer (pH10.6)

| | |
|--------------------|------|
| Hexyl-GSH | 94mg |
| NaHCO ₃ | 0.1M |
| NaOH | 0.1M |

NaHCO₃ /NaOH buffer(pH10.6)

| | |
|--------------------|------|
| NaHCO ₃ | 0.1M |
| NaOH | 0.1M |

Borate buffer(pH 8.0)

| | |
|---------------|------|
| Sodium Borate | 0.1M |
| NaCl | 0.5M |

Acetate buffer(pH4.0)

| | |
|-----------------|------|
| Sodium Acetate | 0.1M |
| Sodium Chloride | 0.5M |

Hexyl-Glutathione column regenerating buffers

High PH regenerating buffer(pH8.5)

| | |
|----------|------|
| Tris HCl | 0.1M |
| NaCl | 0.5M |

Low PH regenerating buffer(pH4.5)

| | |
|------------|------|
| Na acetate | 0.1M |
| NaCl | 0.5M |

Alternate with 5-column volume washes of high and low PH regenerating buffers 3 times, followed by re-equilibration of column with STE

Hexyl-Glutathione Elution Buffer for purification of Sj GST fusion proteins.

Hexyl-GSH final concentration of 5 mM
For 50ml final volume proceed as follows:
Make up 12ml solution of the following:

| | |
|-------------------------------------|------------|
| NaCl | 0.2M |
| Tris HCl (pH7.8) | 0.05M |
| DTE | 2mM |
| N-octyl Glucoside | 1g |
| TritonX-100 | 25 μ l |
| Distilled water to volume of 12 ml. | |

Add hexyl-GSH and mix using the aid of a mortar and pestle.
Using Pasteur pipette add 10 drops of Tris HCl (pH8.8) 1M.
Add STE to final volume of 50ml.

Homogenization buffer for human liver cytosol preparation

| | |
|------------------|--------|
| DET | 0.2mM |
| PMSF | 0.57mM |
| Tris HCL(pH 7.8) | 0.01M |

KOAC(Potassium acetate) solution(pH 7.4)

| | |
|---------------------|---------|
| Potassium acetate | 29.44g |
| Glacial acetic acid | 11.5ml |
| Distilled water | 88.5 ml |

λ DNA molecular weight markers

20 μ l DNA (200 g/ l)
22 μ l ddH₂ O
5 μ l RE buffer

3 μ l Restriction enzyme

Incubated at 37°C for 2 hours. 20 μ l of Stop buffer added Stored at 4°C.

7 μ l loaded/well on Agarose gels

NaOH/SDS Solution

| | |
|------|---------|
| NaOH | 0.2M |
| SDS | 1%(w/v) |

Poly-D-Lysine stock:

| | |
|----------------------|--------|
| Poly-D-Lysine: | 1.5 ml |
| Dd H ₂ O: | 60 ml |

Potassium phosphate buffer for double immunodiffusion (pH 7.4)

| | |
|------------------|-------|
| Sodium Chloride | 0.15M |
| Sodium Phosphate | 0.05M |
| Sodium Azide, | 0.1% |

PMSF Stock

| | |
|------|---------------|
| PMSF | 100mM in DMSO |
|------|---------------|

SDS page solutions

Amps

| | |
|----------------------|----------|
| Ammonium Persulphate | 10%(w/v) |
| make fresh | |

Acrylamide Solution (30%)

| | |
|-----------------|----------------------------|
| Acrylamide | 29.2g |
| Bis-acrylamide | 0.8g |
| Distilled water | to a final volume of 100ml |

Coumassie stain

| | |
|-----------------------|-------------|
| Distilled water | 500ml |
| Methanol | 400ml |
| Glacial Acetic Acid | 100ml |
| Coumassie | 0.3 % (w/v) |
| Filter prior to usage | |

Destain

| | |
|---------------------|-------|
| Distilled water | 500ml |
| Ethanol | 400ml |
| Glacial Acetic Acid | 100ml |

Reducing Sample loading buffer

| | |
|------------------|---------|
| Tris HCl pH 6.8 | 0.0625M |
| SDS | 2% |
| Glycerol | 10% |
| Mercaptoethanol | 5% |
| Bromophenol Blue | 0.001% |

Separating gel buffer (pH8.8)

| | |
|----------|--------|
| Tris HCl | 1.125M |
| SDS | 0.3% |

Separating gel final mix

| | |
|-----------------------|-----------|
| For a 10% SDS gel | |
| Acrylamide stock | 3.3ml |
| Separating gel buffer | 2.5ml |
| Distilled water | 4.15ml |
| Amps | 0.1ml |
| TEMED | 7 μ l |

Stacking gel buffer (pH 6.8)

| | |
|----------|--------|
| Tris HCl | 0.375M |
| SDS | 0.3% |

Stacking gel final mix

| | |
|---------------------|------------|
| Acrylamide Stock | 1.3ml |
| Distilled Water | 6.1ml |
| Stacking gel buffer | 2.5ml |
| Amps | 0.3ml |
| TEMED | 10 μ l |

STE(pH8.0)

| | |
|----------|-------|
| NaCl | 150mM |
| Tris HCl | 10mM |
| EDTA | 1mM |

STE/PMSF

| | |
|--------------|-----------------------------|
| STE as above | |
| PMSF | 0.1mM (final concentration) |

TBE buffer (pH 8.0)

| | |
|------------|--------|
| Tris HCl | 89 mM |
| Boric Acid | 89 mM |
| EDTA | 2.5 mM |

TBE/Ethidium Bromide

TBE as above
Ethidium Bromide Final concentration 6µg/ml

ψ Broth

| | |
|--------------------------------------|------------|
| Bacto-tryptone | 2%(w/v) |
| Bacto-Yeast | 0.5%(w/v) |
| MgSO ₄ .7H ₂ O | 0.4% (w/v) |
| KCl | 10mM |

ψB Agar

| | |
|---------------|-----------|
| ψB - as above | |
| Bacto-Agar | 1.5%(w/v) |

TE Buffer (pH8.0)

| | |
|----------|------|
| Tris HCl | 10mM |
| EDTA | 1mM |

TFB1

| | |
|--------------------------------------|----------|
| RbCl | 100mM |
| MnCl ₂ .4H ₂ O | 50mM |
| KOAc | 30mM |
| CaCl ₂ .2H ₂ O | 10mM |
| Glycerol | 15%(v/v) |

pH 5.8 using glacial acetic acid. Filter sterilize

TFB2

| | |
|--------------------------------------|----------|
| MOPS(pH7.0) | 10mM |
| RbCl | 10mM |
| CaCl ₂ .2H ₂ O | 75mM |
| Glycerol | 15%(v/v) |

APPENDIX 3

References

- Abbes, A; Labbe-Bois R** (1993) Structure-function studies of yeast ferrochelatase. Identification and functional analysis of amino acid substitutions that increase V_{max} and the K_M for both substrates. *J Biol Chem.* 268(12): 8541-6.
- Abdul-Razzak R, Bagust J** (1998) Effects of delta-aminolaevulinic acid upon electrical activity of rat spinal cord in vivo. *Neurosci Lett* 252(3): 175 -8
- Adams, PA, Thumser AE** (1993) Haem-peptide-protein interactions: Part 5. The haem undecapeptide microperoxidase-11 ($Fe_3+MP-11$)/human serum albumin (HSA) reaction in aqueous methanolic solution. A simple system demonstrating the effect of hydrophobicity on ligand release from a ligand-protein complex. *J Inorg Biochem* 50(1): 1-7.
- Ades IZ, Harpe KG** (1982) Isolation of the mature subunits of delta-aminolaevulinate synthase from embryonic chick liver. *Biochem J* 205(2): 257 - 263
- Ades IZ** (1982) Biogenesis of mitochondrial proteins: regulation of maturation of δ -aminolevulinate synthase by hemin. *Biochem. Biophys. Res. Comm.* 110: 42-47
- Ades IZ** (1983) Biogenesis of mitochondrial proteins regulation of maturation of delta-aminolevulinate synthase by hemin. *Biochem Biophys Res Commun* 110 (1): 42 - 47
- Ades IZ, Harpe KG, Stevens TM** (1983) Biogenesis of mitochondrial proteins. Regulation of production of delta-aminolaevulinate synthase by haemin in embryonic-chick liver. *Biochem J* 214 (3): 967-974
- Ades IZ, Stevens TM, Drew PD** (1987) Biogenesis of embryonic chick liver delta-aminolevulinate synthase: regulation of the level of mRNA by hemin. *Arch Biochem Biophys* 253 (2): 297 - 304

Ades IZ, Stevens TM (1988) Maturation of embryonic chick liver delta-aminolevulinic synthase: precursor pools and regulation by intra-cellularly produced heme. *Int J Biochem* 20(9): 959 - 964

Aizencang GI, Bishop DF et al (2000) Uroporphyrinogen III synthase. An alternative promoter controls erythroid-specific expression in the murine gene. *J Biol Chem*. 275(4): 2295-304.

Akhtar M (1994) The modification of acetate and propionate side chains during the biosynthesis of heme and chlorophylls: mechanistic and stereochemical studies. *Ciba Found. Symp.* 180: 131-131

Al-Karadaghi S, Hansson M et al (1997) Crystal structure of ferrochelatase: the terminal enzyme in heme biosynthesis. *Structure*. Vol 5(11): 1501-10.

Alwan AF, Mgbeje BIA, Jordan PM (1989) Purification and properties of uroporphyrinogen III synthase (co-synthase) from an overproducing recombinant strain of *E. Coli* K12. *Biochem. J* 264: 397 - 402

Alwan SJ, Siligardi G et al (1997) Reconstitution of the holoenzyme form of *Escherichia coli* porphobilinogen deaminase from apoenzyme with porphobilinogen and preuroporphyrinogen: a study using circular dichroism spectroscopy. *Biochemistry*. 36(30): 9273-82.

Amillet JM, Labbe-Bios R (1995) Isolation of the gene HEM4 encoding uroporphyrinogen III synthase in *Saccharomyces cerevisiae* *Yeast* 11 (5): 419 - 24

Anderson PM, Desnick RJ (1979) Purification and properties of δ -aminolevulinic dehydratase from human erythrocytes. *J. Biol. Chem.* 254: 6924 - 6030

Anderson PM, Desnick RJ (1980) Purification and properties of uroporphyrinogen I synthase from human erythrocytes. Identification of stable enzyme-substrate intermediates. *J Biol. Chem* 225: 1993 - 1999

Astrin KH, Bishop DF et al (1987) δ -aminolevulinic acid dehydratase isozymes and lead toxicity. *Ann NY Acad. Sci.* 514: 23 – 29

Astrin KH, Warner CA et al (1991) Regional assignment of the human uroporphyrinogen III synthase gene to chromosome 10q25.2 – q26.3 *Hum. Genet* 87:18 – 22

Bachmair A, Finley D, Varshavsky A (1986) In vivo half-life of a protein is a function of its amino-terminal residue. *Science* 234(4773): 179-86

Balla G , Vercellotti GM et al (1991) Exposure of endothelial cells to free heme potentiates damage mediated by granulocytes and toxic oxygen species. *Lab Invest* 64(5): 648 – 655.

Balla G, Jacobs HS et al (1991) Hemin: a possible physiological mediator of low density lipoprotein oxidation and endothelial injury. *Arterioscler Thromb* 11(6): 1700-11

Bankfalvi A, Navabi H, et al (1995) Wet autoclave pretreatment for antigen retrieval in diagnostic immunohistochemistry. *Hum Exp Toxicol* 14(5): 465-6

Battle AM, de Salamanca RE, et al (1986) Photodynamic inactivation of red cell uroporphyrinogen decarboxylase by porphyrins. *Int J Biochem* 12 (2):143-7

Battersby AR, Fookes CJR et al (1982₁) Biosynthesis of porphyrins and related macrocycles. Part 18. proof by spectroscopy and synthesis than unrearranged hydroxymethylbilane is the product from deaminase and substrated for cosynthase in the biosynthesis of ourporphyrinogen III. *J Chem Soc Perkin Trans* 1: 2427 –2444. As quoted by **Desnick R, et al** (1998). Molecular genetics of Congenial erythropoietic porphyria. *Semin in Liv Dis* 18; 1:77 – 84

Battersby AR, Fookes CJR et al (1982₂) Diosynthesis of porphyrins and related macrocycles. Part 17. Chemical and enzymatic transformation of isomeric

aminomethylbilanes into uroporphyrinogens: Proof that unrearranged bilianes are the preferred enzymatic substrate and detection of a transient intermediate. *J Chem Soc Perkin Trans 1*:2413 –2426– as quoted by **Desnick R, et al** (1998). Molecular genetics of Congenital erythropoietic porphyria. *Semin in Liv Dis* 18; 1:77 – 84

Battersby AR, Fookes CJR, Pandey PS (1983) Linear tetrapyrrole intermediates for biosynthesis of the natural porphyrins. Experiments with modified substrates. *Tetrahedron* 39: 1919 - 1926

Battistuzzi G, Petrucci R et al (1981) δ -aminolevulinate dehydratase: a new genetic polymorphism in man. *Ann. Hum. Genet.* 45: 223 – 229

Baumstark, F. (1874). Zwei pathologische harnfarbstoffe. *Pflugers Arch. Gest. Physiol.* 9: 568-584.

Beale and Weinstein, (1990) Tetrapyrrole metabolism in photosynthetic organisms - in "*Biosynthesis of haem and chlorophylls*" p. 287 Ed Dailey, H, McGraw-Hill Inc. US

Berger H & Goldberg A (1955) Hereditary coproporphyria. *Br Med J* 2: 85 – 88, as seen in **Martasek P** (1998). Hereditary coproporphyria. *Semin. In Liver Dis* 18 (1) 25 - 32

Beri R, Chandra R (1993) Chemistry and biology of haem. *Drug Metab Rev*, 25: 49-152

Bernard GF, Akhtar M (1979) Stereochemical and mechanistic studies on the decarboxylation of uroporphyrinogen III in haem biosynthesis. *JCS Perkin I* 1979 2354-2360

Bevan DR Bodlander P, Shemin D (1980) Mechanism of porphobilinogen synthase. Requirement of Zn^{2+} for enzyme activity. *J Biol. Chem* 255: 2030 – 2035

Bhasker CR, Burgiel G et al (1993) The putative iron-responsive element in the human erythroid 5-aminolevulinic synthase mRNA mediates translational control. *J Biol. Chem.* 268: 12699 - 12705

Biempica, L; Kosower, N, et al (1974) Hepatic porphyria's: cytochemical and ultrastructural studies of liver in acute intermittent porphyria and porphyria cutanea tarda. *Arch Path* 98 (4) 336 - 343

Billi de Catabbi S, S. Rios de Molina MdC, et al (1991) Studies on the active centre of rat liver porphyrinogen carboxylase. In vivo effect of hexachlorobenzene. *Int J Biochem* 23: 675 – 679

Bishop DF (1990) Two different genes encode δ -aminolevulinic synthase in humans: nucleotide sequences of cDNAs for the housekeeping and erythroid genes. *Nucleic Acids Res.* 18: 7187 - 7188

Bishop TR, Hodes ZI et al (1989) Cloning and sequence of mouse erythroid δ -aminolevulinic dehydratase cDNA. *Nucleic Acids Res.* 17: 1775

Bishop TR, Frelin LP, Boyer SH (1986) Nucleotide sequence of rat liver δ -aminolevulinic acid dehydratase cDNA. *Nucleic Acids Res.* 14: 10115

Bishop TR, Miller MW et al (1996) Genetic regulation of delta-aminolevulinic dehydratase during erythropoiesis. *Nucleic Acids Res* 24(13):2511-8

Birkett DJ, Mackenzie PI (1993) In Vitro approaches can predict human drug metabolism *TIPS* 14: 292 - 4

Bogard M, Camadro J-M et al (1989) Purification and properties of mouse liver coproporphyrinogen oxidase. *Eur. J Biochem.* 181: 417 – 421

Bogorad L (1955). *Science* 121: 878-879.

- Bolt EL, et al** (1999) Characterization of the rhodobacter sphaeroides 5-aminolaevulinic acid synthase isoenzymes, HemA and HemT, isolated from recombinant Escherichia Coli. *Eur. J Biochem.* 265(1): 290 – 299
- Bonkovsky HL, Tschudy DP et al** (1971) Repression of the overproduction of porphyrin precursors in acute intermittent porphyria by intravenous haematin. *Proc Natl Acad Sci USA* 68: 2725 - 2729
- Bonkovsky HL, Schady W** (1982) Neurologic manifestation of acute porphyria. *Semin Liver Dis* 2: 108-124
- Bonkovsky HL, Healey JF, et al** (1991) Intravenous heme-albumin in acute intermittent porphyria: evidence for repletion of hepatic hemoproteins and regulatory heme pool. *Am J Gastroenterol* 86: 1050-1056
- Bonkovsky HL, Poh-Fitzpatrick M, et al** (1998) Porphyria cutanea tarda, hepatitis C, and HFE gene mutations in North America. *Hepatology* 27:1661-9
- Bonkovsky HL and Barnard G** (1998) Diagnosis of Porphyria Syndromes: A practical approach in the era of molecular biology. *Seminars in Liver disease* 18(1): 57 – 65
- Borthwick IA, Srivastava G, et al** (1982) Purification of 5-aminolevulinate synthase from liver mitochondria of chick embryo. *Eur. J Biochem.* 129:615 - 620
- Borthwick IA, Srivastava G et al** (1985) Complete nucleotide sequence of hepatic 5-aminolevulinate synthase precursor. *Eur. J. Biochem.* 150: 481 - 484
- Bottomley SS, Muller-Eberhard U** (1988) Pathophysiology of heme synthesis. *Semin hematol* 25 (4):282 - 302
- Braidotti G, Borthwick IA, May BK** (1993) Identification of regulatory sequences in the gene for 5-aminolevulinate synthase from rat. *J Biol. Chem.* 268: 1109 – 1117

Brennan MJ, Cantrill RC (1979) The effects of delta-aminolaevulinic acid on the uptake and efflux of amino acid neurotransmitters in rat brain synaptosomes. *J Neurochem* 33(3) 721-5

Brennan MJ, Cantrill RC (1981) Delta-Aminolaevulinic acid and amino acid neurotransmitters. *Mol Cell Biochem* 38 Spec No(Pt 1):49-58

Broudy VC, Lin N, et al (1991) Erythropoietin receptor characteristics on primary human erythroid cells. *Blood* 77(12):2583-90

Brown RW, Chirala R (1994) Utility of microwave-citrate antigen retrieval in diagnostic immunohistochemistry. *J Pathol* 173(4):371-9

Brownlie PD, Lambert R et al (1994) The three-dimensional structures of mutants of porphobilinogen deaminase: toward an understanding of the structural basis of acute intermittent porphyria. *Protein Sci* 3(10): 1644-1650

Brun A, Steen H, Sandberg S (1996) Erythropoietic protoporphyria: two populations of reticulocytes, with and without protoporphyrin. *Eur J Clin Invest* 26(4):270 – 278

Bulaj ZJ, Phillips JD, et al (2000) Hemochromatosis genes and other factors contributing to the pathogenesis of porphyria cutanea tarda. *Blood*. 95:1565-71

Burden AI, Wu C et al (1999) Human ferrochelatase: crystallization, characterization of the [2Fe-2S] cluster and determination that the enzyme is a homodimer. *Biochim Biophys Acta*. 1435(1-2):191-7.

Busfield SJ et al (1993₁) Retrovirally-produced erythropoietin effectively induces differentiation and proliferation of J2E erythroid cells. *Growth Factors* 9(2): 87- 97

Busfield SJ et al (1993₂) Erythropoietin induced ultrastructural alterations to J2E cells and loss of proliferative capacity with terminal differentiation. *Growth Factors* 9(4): 317 – 328.

Busfield SJ et al (1995) Erythropoietin exerts transcriptional and translational control over globin synthesis in J2E cells. *Cell Growth Differ* 6(4) 429-437

Cable EE, Pepe JA et al (1994) Differential effects of metalloporphyrins on messenger RNA levels of δ -aminolevulinic synthase and heme oxygenase. *J Clin. Invest.* 94: 649 - 654

Cacheux V, Martasek P et al (1994) Localization of the human coproporphyrinogen oxidase gene to chromosome band 3q12. *Hum Genet.* 94(5):557-9.

Camadro J-M, Chambon H, et al (1986) Purification and some properties of coproporphyrinogen oxidase from the yeast *Saccharomyces cerevisiae*. *Eur. J Biochem.* 156: 579 – 587

Camadro JM, Abraham NG , Levere RD (1985) Kinetic properties of the membrane-bound liver mitochondrial protoporphyrinogen oxidase. *Arch Biochem Biophys.* 242(1):206-12

Camadro JM, Thome F et al (1994) Purification and properties of protoporphyrinogen oxidase from the yeast *Saccharomyces cerevisiae*. Mitochondrial location and evidence for a precursor form of the protein. *J Biol Chem.* 269(51):32085-91.

Carvalho H, Bechara EJH, et al (1997) Haem precursor δ -aminolaevulinic acid induces activation of the cytosolic iron regulatory protein 1. *Biochem J* 328: 827 - 832

Cattoretti G, Pileri S, et al (1994) Antigen unmasking on formalin-fixed, paraffin-embedded tissue sections. *J Pathol* 174(3): 223-8

Celier C, Cresteil T (1991) Control of cytochromes P450 expression in guinea rat liver: implications of the intracellular heme pool. *Arch. Biochem. Biophys.* 290: 407 - 410

Chretien S, Dubart A , Beaupain D et al (1988) Alternative transcription and splicing of the human porphobilinogen deaminase gene result either in tissue-specific or in housekeeping expression. *Proc. Natl. Acad. Sci. USA* 85: 6 - 10

Cookson GH, Rimington C (1954). Porphobilinogen. *Biochem. J.* 57: 476-484.

Conboy JG, Chan JY, Chasis JA et al (1991) Tissue- and development-specific alternative RNA splicing regulates expression of multiple isoforms of erythroid membrane protein 4.1. *J Biol Chem* 266(13):8273-80.

Conder LH, Woodard SI, Dailey HA (1991) Multiple mechanisms for the regulation of haem synthesis during erythroid cell differentiation. Possible role for coproporphyrinogen oxidase. *Biochem J.* 275 (Pt 2):321-6.

Corrigall AV, Meissner PN, Kirsch RE (1991) Purification of human erythrocyte porphobilinogen deaminase. *S. Afr. Med. J* 80 : 294 - 296

Corrigall AV, Siziba KB et al (1998) Purification of and kinetic studies on a cloned protoporphyrinogen oxidase from the aerobic bacterium *Bacillus subtilis*. *Arch Biochem Biophys.* 358(2):251-6.

Corrigall AV, Hift RJ, et al(2000) Homozygous variegate porphyria in South Africa: genotypic analysis in two cases. *Mol Genet Metab.* 69:323-30.

Cotter PD, Baumann M, Bishop DF (1992) Enzymatic defect in "X-linked" sideroblastic anaemia: molecular evidence for erythroid δ -aminolevulinate synthase deficiency. *Proc Natl Acad Sci USA* 89: 4028 - 4032

Cox TC et al (1990) Erythroid 5-aminolevulinate synthase is located on the X chromosome. *Am J Hum Genet* 46(1):107-111

Cox TC, Bawden MJ, Martin A, et al (1991) Human erythroid 5-aminolevulinatase synthase: promoter analysis and identification of an iron-responsive element in the mRNA. *EMBO J.* 1991 Jul;10(7):1891-902.

Cox T, Bottomley SS et al (1992) Erythroid 5 Aminolevulinatase synthase deficiency due to a point mutation in a kindred with X-linked sideroblastic anemia. **Blood** 80:341a.

Crespi CL, Penman B et al (1991) A tobacco smoke-derived nitrosamine, 4-(methylnitrosamino)-1-(3-pyridyl)-1-butanone, is activated by multiple human cytochrome P450s including the polymorphic human cytochrome P450D6. *Carcinogenesis* 12 (7) 1197 - 1201

Crespi CL, Langenbach R, Penman B (1993₁) Human cell lines, derived from AHH-1 TK+/- human lymphoblasts, genetically engineered for expression of cytochromes P450.

Crespi CL, Penman B et al (1993₂) Genetic toxicology using human cell lines expressing human P-450. *Biochemical Society Transactions* 21: 1023 -28

Cripps DJ, Peters HA, et al (1984) Porphyria turcica due to hexachlorobenzene – a 20 to 30 year follow-up study on 204 patients. *Brit. J Dermatol.* 111: 413-422

Crouse BR, Sellers VM et al (1995) Site-directed mutagenesis and spectroscopic characterization of human ferrochelatase: identification of residues coordinating the [2Fe-2S] cluster. *Biochemistry.*35(50):16222-9.

Cuevas EC, Bateman AC, et al (1995) Microwave antigen retrieval in immunocytochemistry: a study of 80 antibodies. *Mod Pathol* 8(5):515-20

Dailey HA (1984) Effect of sulfhydryl group modification on the activity of bovine ferrochelatase. *J Biol Chem.* 1984 Mar 10;259(5):2711-5.

Dailey HA, Fleming JE (1986) The role of arginyl residues in porphyrin binding to ferrochelatase. *J Biol Chem.* 261(17):7902-5.

Dailey HA, Karr SM, (1987) Purification and characterization of murine protoporphyrinogen oxidase. *Biochemistry.* 26(10):2697-701.

Dailey HA, Sellers VM, Dailey TA (1994₁) Mammalian ferrochelatase: Expression and characterization of normal and two human protoporphyrin ferrochelatases. *J Biol. Chem.* 269: 390 - 395

Dailey HA, Finnegan MG, Johnson MK (1994₂) Human ferrochelatase is an iron-sulfur protein. *Biochemistry.* 33(2):403-7.

Dailey HA (1994) Expression of a cloned protoporphyrinogen oxidase. *J Biol Chem.* 269(2):813-5.

Dailey TA, Dailey HA (1996₁) Protoporphyrinogen oxidase of *Myxococcus xanthus*. Expression, purification, and characterization of the cloned enzyme. *J Biol Chem.* 271(15):8714-8.

Dailey TA, Dailey HA (1996₂) Human protoporphyrinogen oxidase: expression, purification, and characterization of the cloned enzyme. *Protein Sci.* 5(1):98-105.

Dailey HA, Dailey TA (1997) Characteristics of human protoporphyrinogen oxidase in controls and variegate porphyria. *Cell Mol Biol(Noisy-le-grand)* 43(1): 67 -73

Dandekar T, Stripecke R, Gray NK et al (1991) Identification of a novel iron-responsive element in murine and human erythroid delta-aminolevulinic acid synthase mRNA. *EMBO J.* 10(7): 1903-9.

Dean G, Barnes HD (1958) Porphyria: a South African screening experiment. *Br Med J* 12:298 - 301

Delfau-Larue MH, Martasek P, Grandchamp B (1994) Coproporphyrinogen oxidase: gene organization and description of a mutation leading to exon 6 skipping. *Hum Mol Genet.* (8):1325-30.

Dent AF, Beyersmann D et al (1990) Two different zinc sites in bovine 5-aminolevulinatase distinguished by extended X-ray absorption fine structure. *Biochemistry* 29: 7822 – 7828

Desnick RJ, Glass IA et al (1998) Molecular genetics of congenital erythropoietic porphyria. *Semin Liver Dis.* 18(1):77-84. Review.

De Verneil H, Sassa S, Kappas A (1983) Purification and properties of uroporphorinogen decarboxylase from human erythrocytes. *J Biol. Chem.* 258:2454 - 2460

De Verneuil H, Grandchamp B et al (1984) Assignment of the gene for uroporphyrinogen decarboxylase to human chromosome 1 by somatic cell hybridization and specific enzyme immunoassay. *Hum. Genet.* 66: 202 – 205

DeWitt-Baines, A (1986) Disorders of the Kidney and Urinary Tract. pp 139 – 171 in *Applied Biochemistry of Clinical Disorders*. Ed. A Gornall, JP Lippincott Company, Philadelphia

Deybach, JC; de Verneuil H; Nordmann Y (1981) The inherited enzymatic defect in porphyria varieigata. *Hum Genet* 58: 425 – 428

Deybach JC, daSilva V et al (1984) The mitochondrial location of protoporphyrinogen oxidase. *Eur J Biochem.* 149(2):431-5.

Deybach JC, Puy H (1995) Porphobilinogen deaminase gene structure and molecular defects. *J Bioenerg Biomembr.* 27(2):197-205.

Doss MO, Frank M (1989) Hepatobiliary implications and complications in protoporphyria, a 20-year study. *Clin Biochem* 22(3):223-229

Drew PD, Ades IZ (1986) Regulation of production of embryonic chick liver δ -aminolevulinic synthase: effects of testosterone and of hemin on the mRNA of the enzyme. *Biochem. Biophys. Res. Comm.* 140: 81 – 87

Drew PD, Ades IZ (1989₁) Regulation of the stability of chicken embryo liver δ -aminolevulinic synthase mRNA by hemin. *Biochem. Biophys. Res. Comm.* 182: 102 - 107

Drew PD, Ades IZ (1989₂) Regulation of production of delta-aminolaevulinic synthase in tissues of chick embryos. Effects of porphyrinogenic agents and of haem precursors. *Biochem J* 262(3): 815 -821

Drew PD, Ades IZ (1990) Induction of cytochrome P-450 RNA by porphyrinogenic agents: on the nature of the co-ordinate induction with delta-aminolevulinic synthase in tissues of the chicken embryo. *Int J Biochem* 22(6) : 607 - 610

Dogra SC, Hahn CN, May BK (1993) Superinduction by cycloheximide of cytochrome P450_{2H1} and 5-aminolevulinic synthase gene transcription in chick embryo liver. *Arch. Biochem. Biophys.* 300: 531-534

Dover SB, Graham A et al (1991) Haem arginate plus tin-protoporphyrin for acute hepatic porphyria. *Lancet* 338: 263

Edwards SR, Shanley BC, Reynoldson JA (1984) Neuropharmacology of delta-aminolaevulinic acid—I. Effect of acute administration in rodents. *Neuropharmacology* 23(4): 477-81

Elder GH, Evans JO (1979) Evidence that the coproporphyrinogen oxidase activity of rat liver is situated in the intermembrane space of mitochondria. *Biochem. J* 172: 345-347

Elder GH, Tovey JA, Sheppard DM (1983) Purification of uroporphyrinogen decarboxylase from human erythrocytes. *Biochem. J* (1983) 215: 45 – 55

Elder GH, Roberts AG, de Salamance RE (1989) Genetics and pathogenesis of human uroporphyrinogen decarboxylase defects. *Clin Biochem* 22(3) : 163 - 168

Elder GH, Roberts AG (1995) Uroporphyrinogen decarboxylase. *J Bioenerg Biomembr* 27 (2) : 207 - 214

Elder GH (1998) Porphyria cutanea tarda; *Semin. Liv. Dis.* 18: 67 - 75

Emanuelli T, Pagel FW, et al (2001) 5-Aminolaevulinic acid inhibits [³H]muscimol binding to human and rat brain synaptic membranes. *Neurochem Res* 26: 101-5

Emura I, Sekiya M, Ohnishi Y (1983) Four types of presumptive hemopoietic stem cells in the human fetal liver. *Arch Histol Jpn* 46(5):645-62

Eriksen L, Eriksen N (1997) Urinary excretion of position isomers of penta- and hexa-carboxylated porphyrins belonging to the isomer III series in a case of congenital erythropoietic porphyria. *Scand J Clin Lab Invest* 37:357-61

Erskine PT, Senior N, et al (1997) Crystallization of 5-aminolaevulinic acid dehydratase from *Escherichia coli* and *Saccharomyces cerevisiae* and preliminary X-ray characterization of the crystals *Protein Sci.* 1997 6(8):1774-6.

Erskine PT et al (1999) The Schiff base complex of yeast 5-aminolaevulinic acid dehydratase with laevulinic acid. *Protein Sci.* Jun; 8(6): 1250 -1256.

Erskine PT, Norton E et al (1999) X-ray structure of 5-aminolevulinic acid dehydratase from *Escherichia coli* complexed with the inhibitor levulinic acid at 2.0 Å resolution. *Biochemistry.* 38(14):4266-76.

Falk JE, Dresel EIB, Rimington C (1953). Porphobilinogen as a porphyrin precursor, and interconversion of porphyrins in a tissue system. *Nature* 172: 292.

Felix F, Brouillet N (1990) Purification and properties of uroporphyrinogen decarboxylase from *Saccharomyces cerevisiae*. *Eur. J. Biochem* 188: 393-403

Ferreira GC, Andrew TL et al (1988) Organization of the terminal two enzymes of the heme biosynthetic pathway. Orientation of protoporphyrinogen oxidase and evidence for a membrane complex. *J Biol Chem.* 263(8):3835-9.

Ferreira GC, Pedersen PL (1992) Overexpression of higher eukaryotic membrane proteins in bacteria. Novel insights obtained with the liver mitochondrial proton/phosphate symporter. *J Biol Chem* Mar 15;267(8):5460-6

Ferreira GC, Dailey HA (1993) Expression of mammalian 5-aminolevulinate synthase in *E. Coli*. Overproduction, purification and characterization. *J. Biol. Chem.* 268: 584 – 590

Ferreira GC, Franco R et al (1994) Mammalian ferrochelatase, a new addition to the metalloenzyme family. *J Biol Chem.* 269(10):7062-5.

Ferreira GC (1994) Mammalian ferrochelatase. Overexpression in *Escherichia coli* as a soluble protein, purification and characterization. *J Biol Chem.* 269(6):4396-400.

Ferreira GC (1995) Ferrochelatase binds the iron-responsive element present in the erythroid 5-aminolevulinate synthase mRNA. *Biochem. Biophys. Res. Comm.* 214: 875-878

Ferreira GC (1999) Ferrochelatase. *Int J Biochem Cell Biol* 31(10):995 – 1000

Fischer, H. (1915). Über das Kotporphyrin. II. Mitteilung über das urinporphyrin. *Hoppe-Seyler's Z. Physiol.* 96: 148-182.

Fisher, H. & Orth, H.(1968) In Die Chemie des pyrrols, Johnson Reprint company
New York

Frangioni, JV, Neel, BG (1993) Solubilization and purification of enzymatically active glutathione S-transferase (pGEX) fusion proteins. *Anal Biochem* 210 179 – 187

Frank H, Nelson J et al (1999) Erythropoietic protoporphyria: identification of novel mutations in the ferrochelatase gene and comparison of biochemical markers versus molecular analysis as diagnostic strategies. *J Investig Med* 47(6):278 –284

Frank J, McGrath J, et al (1998) Homozygous variegate porphyria: identification of mutations on both alleles of the protoporphyrinogen oxidase gene in a severely affected proband. *J Invest Dermatol* 110:452-5

Frankenberg N, Erskine PT et al (1999) High resolution crystal structure of a Mg²⁺-dependent porphobilinogen synthase. *J Mol Biol.* 289(3):591-602.

Fruch FW, Zanger UM, Meyer UA (1997) Extent and character of phenobarbital-mediated changes in gene expression in the liver. *Mol Pharmacol* 51(3): 363-9

Fujita H et al (1991) Sequential activation of genes for heme pathway enzymes during erythroid differentiation of mouse Friend virus-transformed erythroleukemia cells. *Biochem Biophys Acta* 1090(3):311-316

Fujita H, Kondo M et al (1994) Characterization and expression of cDNA encoding coproporphyrinogen oxidase from a patient with hereditary coproporphyria. *Hum Mol Genet.* 3(10):1807-10.

Fujita H (1997) Molecular mechanism of heme biosynthesis. *Tohoku J Exp Med* 183 (2) :83-99

Fujiwara, Y., Asogawa, M., and Nakai, K.(1997), Prediction of mitochondrial targeting signals using hidden Markov models, *Genome Informatics Workshop*, 53-60

- Garey JR, Labbe-Bois R et al** (1992) Uroporphyrinogen decarboxylase in *Saccharomyces cerevisiae*. HEM12 gene sequence and evidence for two conserved glycines essential for enzymatic activity. *Eur J Biochem.* 205(3):1011-6.
- Gibbs PNB, Chaudhry A-G, Jordan PM** (1985) Purification and properties of 5-aminolevulinate dehydratase from human erythrocytes. *Biochem. J* 230: 25-34
- Gibbs PNB, Jordan PM** (1986) Identification of lysine at the active site of human 5-aminolevulinate dehydratase, *Biochem. J* 236: 447 – 451
- Gibson KD, Laver WG, Neuberger A** (1958). Initial stages in the biosynthesis of porphyrins. 2. The formation of δ -aminolaevulinic acid from glycine and succinyl coenzyme A by particles from chicken erythrocytes. *Biochem. J.* 70: 71-76.
- Giger U, Meyer UA** (1981) Induction of δ -aminolevulinate synthase and cytochrome P-450 hemoproteins in hepatocyte culture. *J Biol. Chem.* 256: 11182 - 11190
- Gonda DK, Bachmair A, et al** (1989) Universality and structure of the N-end rule. *J Biol Chem* 264 (28):16700-12
- Gonzalez F** (1993) Molecular biology of human xenobiotics-metabolizing cytochromes P450: role of vaccinia virus cDNA expression in evaluating catalytic function. *Toxicology* 82: 77 – 88
- Gopalakrishnan R, Morse MA, et al** (1999) ,Expression of cytochrome P450 2A3 in rat esophagus: relevance to N-nitrosobenzylmethylamine. *Carcinogenesis* 20 (5): 885-91
- Gorchein A, Webber R** (1987) delta-Aminolaevulinic acid in plasma, cerebrospinal fluid, saliva and erythrocytes: studies in normal, uraemic and porphyric subjects. *Clin Sci* 72(1): 103-12

Gornall AG, Luxton AW, Bhavnani BR (1986) Endocrine disorder, pp 285 – 358 in *Applied Biochemistry of Clinical Disorders*, Ed: Gornall AG, JP Lippincott Co. Philadelphia.

Gouya L, Deybach JC et al (1996) Modulation of the phenotype in dominant erythropoietic protoporphyria by a low expression of the normal ferrocheletase allele. *Am J Hum Genet* 58(2):292 - 299

Gouya L, Puy H, et al (1999) Inheritance in erythropoietic protoporphyria: a common wild-type ferrocheletase allelic variant with low expression accounts for clinical manifestation. *Blood* 93(6):2105-2110

Grandchamp B, Phung N, Nordmann Y (1977) Homozygous case of hereditary coproporphyria. *Lancet* ii:1348 – 1349

Grandchamp B, Phung N, Nordmann Y (1978) The mitochondrial localization of coproporphyrinogen oxidase. *Biochem. J* 176: 97 – 102

Grandchamp B, Deybach JC et al (1980) Studies of porphyrin synthesis in fibroblasts of patients with congenital erythropoietic porphyria and one patient with homozygous coproporphyria. *Biochem Biophys Acta* 629: 577-586

Grandchamp B, de Verneuil H, et al (1987) Tissue-specific expression of porphobilinogen deaminase. Two isoenzymes from a single gene. *Eur. J. Biochem.* 162 : 105 – 110

Grandchamp B (1998) Acute intermittent porphyria. *Semin in Liver Dis* 18 (1): 17 - 24

Gray NK, Hentze MW (1994) Iron regulatory protein prevents binding of the 43S translation pre-initiation complex to ferritin and eALAS mRNAs. *EMBO J* 3 (16):3882-91

Guarini L, Piomelli S, Poh-Fitzpatrick MB (1994) Hydroxyurea in congenital erythropoietic porphyria. *N Engl J Med* 330 :1091-2

Guthenberg C, Mannervik B (1979) Purification of glutathione S-transferases from rat lung by affinity chromatography. Evidence for an enzyme form absent in rat liver. *Biochem Biophys Res Commun* 86 :1304-10

Guruprasad K, Reddy BV, Pandit MW (1990) Correlation between stability of a protein and its dipeptide composition: a novel approach for predicting *in vivo* stability of a protein from its primary sequence. *Protein Eng* 4(2):155-61

Hamilton JW, Bement WJ et al (1988) Expression of 5-aminolaevulinate synthase and cytochrome P-450 mRNAs in Chicken embryo hepatocytes *in vivo* and in culture. *Biochem.J* 255: 267 – 275 Erratum in *Biochemical Journal* – 1989 257 (3) 934

Hamilton JW, Bement WJ et al (1992) Inhibition of protein synthesis increases the transcription of the phenobarbital-inducible *CYP2H1* and *CYP2H2* genes in Chick embryo hepatocytes *Arch. Biochem. Biophys.* 298:99-104

Hansson M, Hederstedt L (1994) *Bacillus subtilis* HemY is a peripheral membrane protein essential for protoheme IX synthesis which can oxidize coproporphyrinogen III and protoporphyrinogen IX. *J Bacteriol.* 176(19):5962-70.

Harada FA, Shwayder TA, et al (2001) Treatment of severe congenital erythropoietic porphyria by bone marrow transplantation. *J Am Acad Dermatol* 45:279-8

Harber LC, Bickers DR (1981) in *Photosensitivity diseases: principles of diagnosis and treatment*. Saunders, Philadelphia, 198-223

Harbin BM, Dailey HA (1985) Orientation of ferrochelatase in bovine liver mitochondria. *Biochemistry.* 24(2):366-70.

Hart GJ, Battersby AR (1985) Purification and properties of uroporphyrinogen III synthase (cosynthase) from *Euglena gracilis*. *Biochem. J* 232: 151 - 168

Hart GJ, Miller AD, Battersby AR (1988) Evidence that the pyrromethane cofactor of hydroxymethylbilane synthase (porphobilinogen deaminase) is bound through the sulphur atom of a cysteine residue. *Biochem J* 252: 909 -912

Hasnain SS, Wardell EM et al (1985) Extended-X-ray-absorption-fine-structure investigations of zinc in 5-aminolaevulinate dehydratase. *Biochem J.* 230(3):625-33.

Hasnain SS, Wardell EM et al (1985) Extended-X-ray-absorption-fine-structure investigations of zinc in 5-aminolaevulinate dehydratase. *Biochem J.* 1985 Sep 15;230 (3):625-33.

Hattori N, Fujiwara H et al (2000) Epoxide hydrolase affects estrogen production in the human ovary. *Endocrinology* 141 (9) : 3353 - 65

Hermes-Lima M, Castilho RF, et al (1992) Calcium-dependent mitochondrial oxidative damage promoted by 5-aminolevulinic acid. *BBA* 1180: 201 – 206

Hirling H, Emery-Goodman A, Thompson N et al (1992) Expression of active iron regulatory factor from a full-length human cDNA by in vitro transcription/translation. *Nucleic Acids Res.* 20(1): 33-9.

Hoppe-Seyler, F. (1871). Das Hamatin. *Tubinger Med-Chem. Untersuchungen* 4: 523-533.

Hoppe-Seyler, F. (1879). Über das Chlorophyll der Pflanzen. *Hoppe-Seyler's Z Physiologie Chem.* 4: 193-203.

Horton, P. and Nakai, K (1996) K., A probabilistic classification system for predicting the cellular localization sites of proteins, *Intellig. Syst. Mol. Biol.* 4, 109-115

Horton, P. and Nakai, K.(1997) Better prediction of protein cellular localization sites with the k nearest neighbor classifier, *Intellig. Syst. Mol. Biol.* 5, 147-152

Hentze MW, Caughman SW, Casey JL et al (1988) A model for the structure and functions of iron-responsive elements. *Gene* 1988 Dec 10;72(1-2):201-8

Hunter GA, Ferreira GC (1995) A continuous spectrophotometric assay for 5-aminolevulinate synthase that uses substrate cycling. *Anal. Biochem.* 226: 221 –224

Ish-Horowicz D, Burke JF. (1981)Rapid and efficient cosmid cloning. *Nucleic Acids Res* 9:2989-98
59(1):141-4.

Jacobs JM, Jacobs NJ (1975) Fumarate as alternate electron acceptor for the late steps of anaerobic heme synthesis in *Escherichia coli*. *Biochem Biophys Res Commun.* 65(1):435-41.

Jacobs JM, Jacobs NJ (1976) Nitrate, fumarate, and oxygen as electron acceptors for a late step in microbial heme synthesis. *Biochim Biophys Acta.*449(1):1-9.

Jacobs JM, Jacobs NJ (1977) Evidence for involvement of the electron transport system at a late step of anaerobic microbial heme synthesis. *Biochem Biophys Acta.* 4

Jacobs JM, Jacobs NJ (1984₁) Effect of unsaturated fatty acids on protoporphyrinogen oxidation, a step in heme and chlorophyll synthesis in plant organelles. *Biochem Biophys Res Commun.* 123(3):1157-64.

Jacobs JM, Jacobs NJ (1984₂) Protoporphyrinogen oxidation, an enzymatic step in heme and chlorophyll synthesis: partial characterization of the reaction in plant

organelles and comparison with mammalian and bacterial systems.

Arch Biochem Biophys. 229(1):312-9.

Jacobs JM, Jacobs NJ (1987) Oxidation of protoporphyrinogen to protoporphyrin, a step in chlorophyll and haem biosynthesis. Purification and partial characterization of the enzyme from barley organelles. *Biochem J.* 244(1):219-24.

Jacobs NJ, Borotz SE, Guerinot ML (1971) Protoporphyrinogen oxidation, a step in heme synthesis in soybean root nodules and free-living rhizobia. *J Bacteriol* 171(1):573-6

Jaffe EK, Abrams WR, et al (1992) 5-chlorolevulinate modification of porphobilinogen synthase identifies a potential role for the catalytic zinc. *Biochemistry* 31: 2113 - 2123

Jean G, Lambertenghi G, Tanzi T (1968) Ultrastructural study of the liver in hepatic porphyria. *J Clin. Path* 21: 501-507

Jones MS, Jones OT (1968) Evidence for the location of ferrochelatase on the inner membrane of rat liver mitochondria. *Biochem Biophys Res Commun.* 31(6):977-82

Jones MS, Jones OT (1970) Properties of ferrochelatase in micro-organisms adapting to changes in growth conditions. *Biochem J.* 116(4):19P.

Jones RM, Jordan PM (1993) Purification and properties of the uroporphyrinogen decarboxylase from *Thodobacter sphaeroides*. *Biochem J* 293 (Pt 3) : 703 - 712

Jordan PM & Shemin D (1973) Purification and properties of uroporphyrinogen I synthetase from *Rhodospseudomonas sphaeroides*. *J. Biol. Chem* 248: 1019 - 1024

Jordan PM, Seehra JS (1979) The biosynthesis of uroporphyrinogen III: order of assembly of the four porphobilinogen molecules in the formation of the tetrapyrrole ring. *FEBS Lett.* 104(2):364-6.

Jordan PM , Warren MJ (1987) Evidence for a dipyrromethane cofactor at the catalytic site of *E. Coli* porphobilinogen deaminase. *FEBS Lett.* 225: 87 – 92

Jordan PM, Thomas SD, Warren MJ (1988) Purification, crystallization and properties of porphobilinogendeaminase from a recombinant strain of *Escherichia coli* K12. *Biochem J* 254 (2): 427 - 435

Jordan PM, Mgbeje BI, et al (1988) Nucleotide sequence for the hemD gene of *Escherichia coli* encoding uroporphyrinogen III synthase and initial evidence for a hem operon. *Biochem J* 249 (2): 613 – 616.

Jordan PM, Thomas SD, Warren MJ (1988) Purification, crystallization and properties of porphobilinogen deaminase from a recombinant strain of *Escherichia coli* K12. *Biochem J.*;254(2):427-35.

Jordan PM, Warren MJ, et al (1988) Identification of a cysteine residue as the binding site for the dipyrromethane cofactor at the active site of *Escherichia coli* porphobilinogen deaminase. *FEBS Lett.*;235(1-2):189-93.

Jordan PM, Woodcock SC (1991) Mutagenesis of arginine residues in the catalytic cleft of *E. Coli* porphobilinogen deaminase that affects dipyrromethane cofactor assembly and tetrapyrrole chain initiation and elongation. *Biochem. J* 280: 445 – 449

Jordan PM (1994₁) The biosynthesis of uroporphyrinogen III: mechanism of action of porphobilinogen deaminase. *Ciba Found Symp* 180 : 70 -89

Jordan PM (1994₂) Highlights in haem biosynthesis. *Curr Opin Struct Biol* 4 (6):902-11

Kappas A, Sassa S et al (1995) The porphyrias. In Scriver, CR; Beaudet, A et al (eds.): *Metabolic and molecular basis of inherited disease.* 7th Ed. New York, McGraw-Hill pp 2103-2159

Kaya AH, Plewinska M, Wong DM et al (1994) Human delta-aminolevulinate dehydratase (ALAD) gene: structure and alternative splicing of the erythroid and housekeeping mRNAs. *Genomics*. 19(2):242-8.

Key NS, Rank JM et al (1992) Hemolytic anemia in protoporphyria. Possible precipitating role of liver failure and photic stress. *Am J Hematol* 39: 202 - 207

Khulmann WD, Peschke P (1986) Glucose oxidase as label in histological immunoassays with the enzyme-amplification in a two-step technique: coimmobilized horseradish peroxidase as secondary system enzyme for chromogen oxidation. *Histochemistry* 85: (1):13-17

Kivisto KT, Fritz P et al (1995) Immunohistochemical localization of cytochrome P450 3A in human pulmonary carcinomas and normal bronchial tissue. *Histochem Cell Biol* 103 (1): 25-9

Kirsch RE, Meissner PN, Hift RJ. (1998) Variegate porphyria. *Semin Liver Dis* 18(1): 33-41

Klausner RK, Rouault Ta, Harford JM (1993) Regulating the fate of mRNA: the control of cellular iron metabolism. *Cell* 72(1):19-28.

Ko LJ, Engel JD (1993) DNA-binding specificities of the GATA transcription factor family. *Mol Cell Biol* 13(7):4011-22

Kohno H, Furukawa T, Yoshinaga T, et al (1993) Coproporphyrinogen oxidase. Purification, molecular cloning, and induction of mRNA during erythroid differentiation. *J Biol Chem* 1993 Oct 5;268(28):21359-63

Krantz SB (1991) Erythropoietin. *Blood* 77(3):419-34

Kurashima Y, Hayashi N, Kikuchi G (1970) Mechanism of inhibition by hemin of increase of delta-aminolevulinic acid synthetase in liver mitochondria. *J Biochem (Tokyo)* 67(6) : 863-5

Kuster, W. (1912). Beitrage zur Kenntnis des Bilirubins und Hämins. *Hoppe-Seyler's Z. Physiol. Chem.* 82: 463-483.

Kyte J, Doolittle RF (1982) A simple method for displaying the hydrophobic character of a protein. *J Mol Biol* 157(1):105-32

Laemmli UK (1970) Cleavage of structural proteins during the assembly of the head of the bacteriophage T4. *Nature* 227: 680-685

Laidlaw, P. P. (1904). Some observations on blood pigments. *J. Physiol.* 31: 464-472.

Lander M, Pitt AR et al (1991) Studies on the mechanism of hydroxymethylbilan synthase concerning the role of arginine residues in substrate binding. *Biochem. J* 275: 447-452

Laterriere M, d'Estaintot BL, et al (1998) Expression, purification, crystallization and preliminary X-ray diffraction analysis of human uroporphyrinogen decarboxylase. *Acta Crystallogr D Biol Crystallogr* 54 (Pt 3):476-8.

Laskey JD, Ponka P, Schulman HM (1986) Control of heme synthesis during Friend cell differentiation: role of iron and transferrin. *J Cell Physiol* 120(2): 185 - 192

Lathrop JT, Timko, MP (1993) Regulation by heme of mitochondrial protein transport through a conserved amino acid motif. *Science* 259: 522 - 525

Leeper FJ (1994) The evidence for a spirocyclic intermediate in the formation of uroporphyrinogen III synthase by cosynthase. *Ciba Found. Symp.* 180: 111-123

Leong AS (1993) Microwaves in diagnostic immunohistochemistry. *J Pathol* 171(2):83-98

Lechevrel M, Casson AG (1999) Characterization of cytochrome P450 expression in human oesophageal mucosa. *Carcinogenesis* 20(2):243-8

Lim KC, Ishihara H, Riddle RD et al (1994) Structure and regulation of the chicken erythroid delta-aminolevulinate synthase gene. *Nucleic Acids Res.* 22(7):1226-33.

Lindberg RLP, Porcher C, et al (1996) Porphobilinogen deaminase deficiency in mice causes a neuropathy resembling that of human hepatic porphyria. *Nature Genetics* 12:195 - 199

Lindblad B, Lindstedt S, Steen G (1997) On the enzymic defects in hereditary tyrosinaemia *Proc Natl Acad Sci U S A* 74(10):4641-5

Litman Da, Correia MA (1983) L-tryptophan: a common denominator of biochemical and neurological events of acute hepatic porphyria? *Science* 222(4627): 1031-3

Lok CN, Ponka (2000) Identification of an erythroid active element in the transferrin receptor gene. *J Biol Chem* 275(31): 24185-90

Loots JM, Becker DM, et al (1975) The effect of porphyrin precursors on monosynaptic reflex activity in the isolated hemisectioned frog spinal cord. *J Neural Transm* 36 (1) 71 – 81

Louie GV, Brownlie PD, et al (1992) Structure of porphobilinogen deaminase reveals a flexible multidomain polymerase with a single catalytic site. *Nature* 359: 33 – 39

Louie GV, Brownlie PD, et al (1996) The three-dimensional structure of *Escherichia coli* porphobilinogen deaminase at 1.76-Å resolution. *Protein Sci* 25(1): 48 – 78.

Luo J, Lim CK (1993) Order of uroporphyrinogen III decarboxylation on incubation of porphobilinogen and uroporphyrinogen III with erythrocyte uroporphyrinogen decarboxylase. *Biochem. J.* Jan 15; 289(pt. 2) 529 – 532.

Mancini G, et al (1965) Immunochemical quantitation of antigens by single radial immunodiffusion. *Immunochemistry* 2:235.

Mannervik B, Danielson UH (1988) *CRC Crit. Rev. Biochem.* 23. 283

Martasek P, Kordak V et al (1987) Epidemiology of porphyria cutanea tarda in Czechoslovakia and Mongolia. *Bolletino dell'Instituto Dermatologica S Gallicano* 8: 330-331 – as read in Elders GH (1998) Porphyria Cutanea Tarda (see under Elders)

Martasek P, Camadro JM (1994) Molecular cloning, sequencing, and functional expression of a cDNA encoding human coproporphyrinogen oxidase. *Proc Natl Acad Sci U S A.* 91(8):3024-8.

Martasek P, Miller RT (1999) Assay of isoforms of *Escherichia coli*-expressed nitric oxide synthase. *Methods Enzymol* 301:70-8

May BK, Hansen AJ (1989) Effect of haem on cytochrome P-450 synthesis. *Clin Exp Pharmacol Physiol.* 16(6): 497 – 500.

May BK, Dogra SC et al (1995) Molecular regulation of heme biosynthesis in higher vertebrates. *Progr in Nucl Acid Res* Vol 51 pp1 - 49

McKay R, Druyan R et al (1969) Intramitochondrial localization of delta-aminolaevulate synthetase and ferrochelatase in rat liver. *Biochem J.* 114(3):455-61.

McLellan T, Pryor MA et al (1985) Assignment of uroporphyrinogen decarboxylase to the pter-p21 region of human chromosome 1. *Cytogenet. Cell. Genet.* 39: 224 - 227

McNeill L, Shoolingin-Jordan P (1998) Dipyrrromethane cofactor assembly in porphobilinogen deaminase. *Biochem Soc Trans.*26(3):S286.

Medlock A, Dailey H (1996) Human coproporphyrinogen oxidase is not a metalloprotein. *J Biol Chem.* 271(51):32507-10.

Meissner P, Adams P, Kirsch RE (1993) Allosteric inhibition of human lymphoblast and purified porphobilinogen deaminase by protoporphyrinogen and coproporphyrinogen. *J Clin. Invest.* 91: 1436-1444

Melfors O, Goossen B, Johansson HE, et al (1992) Translational control of 5-aminolevulinate synthase mRNA by iron-responsive elements in erythroid cells. *J Biol Chem.* 268(8):5974-8.

Meyer U, Schuurmans MM, Lindberg RL (1998) Acute porphyrias: pathogenesis of neurological manifestations. *Semin Liver Dis* 18 (1) 43-52

Meyer UA, Hoffmann K (1999) Phenobarbital-mediated changes in gene expression in liver. *Drug Metab Rev.* 31(2) :365 - 373

Mignotte V, Eleouet JF et al (1989) Cis- and trans-acting elements involved in the regulation of the erythroid promoter of the human porphobilinogen deaminase gene. *Proc. Natl. Acad. Sci. USA* 86: 6548 - 6552

Mignotte V, Wall L, et al (1989) Two tissue-specific factors bind the erythroid promoter of the human porphobilinogen deaminase gene. *Nucleic Acids Res.* 17: 37 - 54

Mion FB, Faure JI et al (1992) Liver transplantation for erythropoietic protoporphyria. Report of a new case with subsequent medium-term follow-up. *J Hepatol* 16: 203 -207

Monteiro HP, Abdalla DSP et al (1989) Free radical generation during δ -aminolevulinic acid autoxidation: induction by hemoglobin and connections with porphyriopathies. *Arch. Biochem. Biophys.* 271: 206 – 216

Muir HM, Neuberger A (1950). The biogenesis of porphyrins. 2. The origin of the methyne carbon atoms. *Biochem. J.* 47: 97-104.

Mukerji SK, Pimstone NR (1988) Defective human erythrocyte uroporphyrinogen decarboxylase in familial porphyria cutanea tarda: the metabolic lesion or the result of endogenous porphyrinemia? *Biochem Biophys Res Commun.* 1988 Jul 15;154(1):39-46.

Murakami K, Uchiyama A, et al (2001) Production of biologically active recombinant bovine interferon-gamma by two different baculovirus gene expression systems using insect cells and silkworm larvae. *Cytokine* 13:18-24

Murray GI, Pritchard S et al (1995) Cytochrome P450 CYP3A5 in the human anterior pituitary gland. *FEBS Lett* 364 (1):79-82

Mustajoki P, Tenhunen R et al (1986) Haem arginate in the treatment of acute hepatic porphyrias. *Br Med J Clin Res Ed* 293:538 - 539

Mustajoki P, Kauppinen R et al (1992) Frequency of low erythrocyte porphobilinogen deaminase activity in Finland. *J Intern Med* 231:389 – 395.

Mustajoki P, Mustajoki S, et al (1994) Effects of heme arginate on cytochrome P450-mediated metabolism of drugs in patients with variegate porphyria and in healthy men. *Pharmacokinetics and drug disposition* 56: 9 - 13

Nakahashi Y, Taketani S et al (1990) Molecular cloning and sequence analysis of cDNA encoding human ferrochelatase. *Biochem Biophys Res Commun* 173: 748 - 755

Nakai, K. and Kanehisa, M (1992), A knowledge base for predicting protein localization sites in eukaryotic cells, *Genomics* 14, 897-911

Namba H, Narahara K et al (1991) Assignment of human porphobilinogen deaminase to 11q24.1---q24.2 by in situ hybridization and gene dosage studies. *Cytogenet Cell Genet.* 57(2-3):105-8.

Neal R, Yang P et al (1997) Pro-oxidant effects of delta-aminolevulinic acid (delta-ALA) on Chinese hamster ovary (CHO) cells. *Toxicol Lett* 91 (3) : 169 - 178

Neuberger A, Scott JJ (1953). Aminolaevulinic acid and porphyrin synthesis. *Nature* 172: 1093-1094.

Nishimura K, Tadetani S, Inokuchi H (1995) Cloning of a human cDNA for protoporphyrinogen oxidase by complementation in vivo of a hemG mutant of *Escherichia coli*. *J Biol Chem.* 270(14):8076-80.

Norris PG, Nunn Av et al Genetic heterogeneity in erythropoietic protoporphyria: a study of the enzymatic defect in nine affected families. *J Invest Dermatol* 95: 260-263

Norton E, Sarwar M, Shoolingin-Jordan P (1998) Mechanistic studies on E.coli 5-aminolaevulinic acid dehydratase. *Biochem Soc Trans.* 26(3):S285.

O'Farrell PH (1975) High resolution two-dimensional electrophoresis of proteins. *J Biol Chem* 250:4007-21

Ohashi A, Kikuchi G (1979) Purification and some properties of two forms of 5-aminolevulinic acid synthase. *J.Biol.Chem.* 285: 239 – 247

Onuki J, Medeiros MHG et al (1994) 5-aminolevulinic acid induces single-strand breaks in plasmid pBR322 DNA in the presence of Fe²⁺ ions. *BBA* 1225: 259 – 263

Orkin SH (1992) GATA-binding transcription factors in hematopoietic cells. *Blood* Aug 1;80(3):575-81

Oteiza PI, Kleinman CG et al (1995) 5-aminolevulinic acid induces iron release from ferritin. *Arch. Biochem. Biophys.* 316: 607-611

Ouchterlony O (1949) Antigen-antibody reactions in gels. *Acta Path. Microbiol. Scand.* 26:507.

Pawliuk R, Bachelot T et al (1999) Long-term cure of the photosensitivity of murine erythropoietic protoporphyria by preselective gene therapy. *Nat Med* 5(7):786-773

Percy VA, Shanley BC (1977) Porphyrin precursors in blood, urine and cerebrospinal fluid in acute porphyria. *S Afr Med J* 52 (6) : 219 – 222.

Percy VA, Lamm MC, Taljaard JJ (1981) delta-Aminolaevulinic acid uptake, toxicity, and effect on [14C]-gamma-aminobutyric acid uptake into neurons and glia cells in culture. *J Neurochem* 36 (1):69-76

Phillips J, Whitby F (1997) Characterization and crystallization of human uroporphyrinogen decarboxylase. *Protein Sci.* 6(6):1343-6.

Philpott CC, Haile D, Rouault TA et al (1993) Modification of a free Fe-S cluster cysteine residue in the active iron-responsive element-binding protein prevents RNA binding. *J Biol Chem.* 268(24):17655-8.

Poison RJ, Lim CK et al (1988) The effect of liver transplantation in a 13-year-old boy with erythropoietic protoporphyria. *Transplantation* 46: 386-389

Porcher C, Pitiot G et al (1991) Characterization of hypersensitive sites, protein-binding motifs, and regulatory elements in both promoters of the mouse porphobilinogen deaminase gene. *J Biol. Chem* 266: 10562 - 10569

Potluri VR, Astrin KH, et al (1987) Human δ -aminolevulinic acid dehydratase: chromosomal localization to 9q34 by in situ hybridization. *Hum. Genet.* 76: 236 - 239

Poulson R (1976) The enzymic conversion of protoporphyrinogen IX to protoporphyrin IX in mammalian mitochondria. *J Biol Chem.* 251(12):3730-3.

Poulson R, Polgralse W (1975) The enzymic conversion of protoporphyrinogen IX to protoporphyrin IX. Protoporphyrinogen oxidase activity in mitochondrial extracts of *Saccharomyces cerevisiae*. *J Biol Chem.* 250(4):1269-74.

Price JM, Brown RR, Peters HA (1959) Tryptophan metabolism in porphyria schizophrena and a variety of neurologic and psychiatric diseases. *Neurology* 9: 456-468

Puy H, Robreau AM et al (1996) Protoporphyrinogen oxidase: complete genomic sequence and polymorphisms in the human gene. *Biochem Biophys Res Commun* 226 (1): 226 - 230

Raich N, Romeo PH et al (1986) Molecular cloning and complete primary sequence of human erythrocyte porphobilinogen deaminase. *Nucleic Acids Res.* 14: 5955 – 5968

Raich N, Mignotte V et al (1989) Regulated expression of the overlapping ubiquitous and erythroid transcription units of the human porphobilinogen deaminase gene introduced into non-erythroid and erythroid cells. *J. Biol. Chem* 264: 10186 – 10192

Rank JM, Pascual-Leone A et al (1991) Hematin therapy for the neurologic crises of tyrosinaemia. *J Pediatr* 118: 136 – 139.

Raunio H, Hakkola J et al (1999) Expression of xenobiotics-metabolizing cyp's in human pulmonary tissue. *Exp Toxicol Pathol* 51 (4-5):412-7

Rhode M, Srivastava G et al (1990) Immunocytochemical studies on the localization of 5-aminolevulinate synthase in rat liver. *Arch Biochem Biophys* 280 (2): 331-5

Rimington C (1939). A re-investigation of turacin, the copper porphyrin pigment of certain birds of the *Musophagidae*. *Proc. Roy. Soc. Br.* 127: 106-120.

Roberts AG, Whatley SD et al (1995) Partial characterization and assignment of the gene for protoporphyrinogen oxidase and variegate porphyria to human chromosome 1q23. *Hum. Mol. Genet.* 4(12): 2387 – 2390.

Roberts AG, Elder GH et al (1995) A mutation (G281E) of the human coproporphyrinogen decarboxylase gene causes both hepatocerythropoietic porphyria and over familial porphyria cutanea tarda. *J Invest. Dermatol* 104: 500 – 502

Roberts AG, Puy H et al (1998) Molecular characterization of homozygous variegate porphyria. *Hum Mol Genet* 7:1921-5

Romana M, Dubart A et al (1987) Structure of the gene for human uroporphyrinogen decarboxylase. *Nucleic Acids Res.* 15(18):7343-56.

Romana M, Le Boulch P, Romeo P (1987) Rat uroporphyrinogen decarboxylase cDNA: nucleotide sequence and comparison to human uroporphyrinogen decarboxylase. *Nucleic Acids Res.* 15(17):7211.

Romeo P, Raich N (1986) Molecular cloning and nucleotide sequence of a complete human uroporphyrinogen decarboxylase cDNA. *J Biol Chem.* 261(21):9825-31.

Rouault TA, Tang CK et al (1990) Cloning of the cDNA encoding an RNA regulatory protein – the human iron-responsive element-binding protein. *Proc. Natl. Acad. Sci. USA* 87: 7958-7962

Rufenacht UB, Gouya L et al (1998) Systematic analysis of molecular defects in the ferrocheletase gene from patients with erythropoietic protoporphyria. *Am J Hum Genet* 62(6): 1341-1352

Ryan C, Carter E et al (1993) Isolation and long-term culture of human hepatocytes. *Surgery* 113(1): 48 – 54

Ryan G, Ades IZ (1989) Co-ordinate elevations of liver delta-aminolevulinate synthase and cytochrome P-450 RNA by Phenobarbital in chicken embryos: the effects of heme. *Int J Biochem* 21(9): 1025-1031

Ryan G, Ades IZ (1990) On the mechanism of induction of chick embryo hepatic δ -aminolaevulinate synthase by translational blockers. *Biochem. J.* 274: 619 - 621

Sanger F, Nicklen S, and Coulson AR (1977) DNA sequencing with chain-terminating inhibitors. *Proc. Natl. Acad. Sci. USA* 74: 5463 - 5467

Sano S, Granick S (1961) Mitochondrial coproporphyrinogen oxidase and protoporphyrin formation in beef liver. *J Biol. Chem* 236: 1173 - 1180

Sarkany RPE, Cox TM (1995) Autosomal recessive erythropoietic protoporphyria: a syndrome of photosensitivity and liver failure. *Quart J Med* 88: 541 - 549

Sassa S & Kappas A (1983) Hereditary tyrosinemia and the heme biosynthetic pathway. Profound inhibition of δ -aminolevulinic acid dehydratase activity by succinylacetone. *J. Clin. Invest.* 71: 625 - 634

Scotto AW, Chang L-FL, Beattie DS (1983) The characterization and submitochondrial localization of δ -aminolevulinic acid synthase and an associated amidase in rat liver mitochondria using an improved assay for both enzymes. *J Biol.Chem.* 258: 81-90

Schoenhaut DS, Curtis PJ (1989) Structure of a mouse erythroid 5-aminolevulinate synthase gene and mapping of erythroid-specific DNase I hypersensitive sites. *Nucleic Acids Res* 17(17): 7013-28

Schultz JH (1874): Ein fall von pemphigus leprosus, kompliziert durch lepra visceralis. *Inaugural dissertation, Griefswald.*

Seehra J, Gore M (1981) 5-Aminolevulinic acid dehydratase. The role of sulphhydryl groups in 5-aminolevulinic acid dehydratase from bovine liver.

Eur J Biochem. 114(2): 263-9.

Sellers V, Wang K (1998) Evidence that the fourth ligand to the [2Fe-2S] cluster in animal ferrochelatase is a cysteine. Characterization of the enzyme from *Drosophila melanogaster*. *J Biol Chem.* 273(35): 22311-6.

Senior N, Brocklehurst K, et al (1996) Comparative studies on the 5-aminolaevulinic acid dehydratases from *Pisum sativum*, *Escherichia coli* and *Saccharomyces cerevisiae*. *Biochem J.* 320 (Pt 2): 401-12.

Senior N, Siligardi G (1997) Structural studies on 5-aminolaevulinic acid dehydratase from *Saccharomyces cerevisiae* (yeast). *Biochem Soc Trans.* 25(1):78S

Shanley BC, Neethling AC et al (1975) Neurochemical aspects of porphyria. Studies on the possible neurotoxicity of delta-aminolaevulinic acid. *S Afr Med J* 140: 576 –80

Shaw PH, Mancini AJ, et al (2001) Treatment of congenital erythropoietic porphyria in children by allogeneic stem cell transplantation: a case report and review of the literature. *Bone Marrow Transplant* 27:101-5

Shemin D, Rittenberg D (1945) The utilization of glycine for the synthesis of a porphyrin. *J Biol Chem* 159:567 – 568

Shemin D, Wittenberg D (1946). The biological utilisation of glycine for the synthesis of the protoporphyrin of hemoglobin. *J. Biol, Chem.* 166: 621-625.

Shemin D, Wittenberg J (1951). The mechanism of porphyrin formation - the role of the tricarboxylic acid cycle. *J. Biol. Chem.* 192: 315.

Shemin D, Russell CS (1953). Delta-aminolevulinic acid, its role in the biosynthesis of porphyrins and purines. *J. Amer. Chem. Soc.* 75: 4873-4875.

Shemin D, Russell CS, Abramsky T (1955). The succinate glycine cycle. I. The mechanism of pyrrole synthesis. *J. Biol. Chem.* 215: 613-620.

Shemin D (1976₁) Proceedings: Structure, function and mechanism of delta-aminolevulinic acid dehydratase. *J Biochem (Tokyo)*. 1976 Apr; 79(4):37P-38P.

Shemin D (1976₂) 5-Aminolaevulinic acid dehydratase: structure, function, and mechanism. *Philos Trans R Soc Lond B Biol Sci.* 273(924): 109-15.

Shoolingin-Jordon PM (1995) Porphobilinogen deaminase and uroporphyrinogen III synthase: structure, molecular biology, and mechanism. *J Bioenerg. Biomembr.* Apr; 27(2): 181-195.

Shoolingin-Jordon PM (1998) Structure and mechanism of enzymes involved in the assembly of the tetrapyrrole macrocycle. *Biochem Soc Trans.*26(3):326-36.

Siepkar L, Kramer S (1985) Protoporphyrin accumulation by mitogen stimulated lymphocytes and protoporphyrinogen oxidase activity in patients with porphyria variegata and erythropoietic porphyria: Evidence for a deficiency of protoporphyrinogen oxidase and ferrochelatase in both diseases. *Br J Haematol* 60: 65 - 74

Simons PC, Vander Jagt, DL (1981) Purification of glutathione s-transferases by glutathione-affinity chromatography. *Methods Enzymol.* 77: 236-7

Sinclair PR, Schuetz EG, et al (1990) Role of heme in phenobarbital induction of cytochromes p450 and 5-aminolevulinic acid synthase in cultured rat hepatocytes maintained on an extracellular matrix. *Arch.Biochem. Biophys.* 282: 386 – 392

Smith-Goessling L, Daniels-Mcqueen S et al (1992) Enhanced degradation of the ferritin repressor protein during induction of ferritin messenger RNA translation. *Science* 256: 670 - 673

Smith S (1975) The use of thin layer chromatography in the separation of free porphyrins and porphyrin methyl esters. *Br J Dermatol* 93(3):291-5

Smith S et al (1994) Supplement 28, *Current Protocols in Molecular Biology*. Wiley and Sons, USA

Smythe E, Williams DC (1988) Rat liver uroporphyrinogen III synthase has similar properties to the enzyme from *Euglena gracilis* including the absence of a requirement for a reversibly bound cofactor for activity. *Biochem. J* 253: 275 - 279

Spencer P, Jordan P (1995) Characterization of the two 5-aminolaevulinic acid binding sites, the A- and P-sites, of 5-aminolaevulinic acid dehydratase from *Escherichia coli*. *Biochem J.* 305 (Pt 1):151-8..

Srivastava G, Borthwick IA, et al (1982) Purification of rat liver mitochondrial δ -aminolevulinic acid synthase. *Biochem. Biophys. Res. Comm.* 209: 305 – 312

Srivastava G, Borthwick IA, et al (1983) Hemin inhibits transfer of pre- δ -aminolevulinic acid synthase into chick embryo liver mitochondria. *Biochem. Biophys. Res. Comm.* 117: 344-349

Srivastava G, Bawden MJ et al (1989) Heme may not be a positive regulator of cytochrome-P450 gene expression. *Eur. J. Biochem.* 178:689 – 692

Srivastava G, Hansen, AJ et al (1990) Hemin administration to rats reduces levels of hepatic mRNAs for phenobarbitone-inducible enzymes. *Molecular Pharmacology* 38: 486-493

Srivastava G, Kwong SKY et al (1992) Effect of dexamethasone on mRNA levels for 5-aminolevulinic acid synthase in different tissues. *Eur. J. Biochem.* 203: 59 - 63

Straka JG, Kushner JP (1983) Purification and characterization of bovine hepatic uroporphyrinogen decarboxylase. *Biochemistry* 22: 4664 – 4672

Stamford N, Capretta A, Battersby AR (1995) Expression, purification and characterisation of the product from the *Bacillus subtilis* hemD gene, uroporphyrinogen III synthase. *Eur J Biochem.* 231(1): 236-41.

Stuart KA, Busfield F, et al (1998) The C282Y mutation in the haemochromatosis gene (HFE) and hepatitis C virus infection are independent cofactors for porphyria cutanea tarda in Australian patients. *J Hepatol* 28: 404-9

Taketani S, Inazawa J et al (1992) Structure of the human ferrochelatase gene. Exon/intron gene organization and location of the gene to chromosome 18. *Eur J Biochem.* 1205(1): 17-22

Taketani S, Kohno H et al (1994) Molecular cloning, sequencing and expression of cDNA encoding human coproporphyrinogen oxidase. *Biochim Biophys Acta.* 1183(3): 547-9.

Taketani S, Inazawa J et al (1995) The human protoporphyrinogen oxidase gene (PPOX): organization and location to chromosome 1. *Genomics.* 29(3): 698-703.

Taketani S, Yoshinaga T et al (1995) Induction of terminal enzymes for heme biosynthesis during differentiation of mouse erythroleukemia cells. *Eur J Biochem.* 230(2): 760-5.

Tezcan I, Xu W, et al (1998) Congenital erythropoietic porphyria successfully treated by allogeneic bone marrow transplantation. *Blood* 92(11):4053-8

Thomasc, Ged C, et al (1996) Correction of congenital erythropoietic porphyria by bone marrow transplantation. *J Pediatr* 129: 453-6

Theil EC (1990) Regulation of ferritin and transferrin receptor mRNAs. *J Biol Chem.* 265(9): 4771-4.

Theil EC, McKenzie RA, Sierzputowska-Grasz, H (1994) Structure and function of IRES, the noncoding mRNA sequences regulating synthesis of ferritin, transferrin receptor and (erythroid) δ -aminolevulinic acid synthase. In *Progress in iron research* Ed. C Hershko, Plenum Press, New York

Thunell S, Andersson C et al (1995) Markers for vulnerability in acute porphyria. A hypothesis paper. *Eur J Clin Chem Clin Biochem* 33(4): 179-94

Tobias JW, Shrader TE, et al (1991) The N-end rule in bacteria. *Science* 254 (5036):1374-7

Todd DJ (1998) Molecular genetics of erythropoietic protoporphyria. *Photodermatol Photoimmunol Photomed* 14(2): 70-73

Todd DJ (1994) Erythropoietic protoporphyria. *Br J Dermatol* 131(6): 751-766

Towbin H, Staehelin T, Gordon J (1979) Electrophoretic transfer of proteins from polyacrylamide gels to nitrocellulose sheets: Procedure and some applications. *Proc. Natl. Acad. Sci. USA* 76: 4350-4354

Tsai S-F, Bishop DF, Desnick R (1987) Purification and properties of uroporphyrinogen III synthase from human erythrocytes. *J Biol. Chem.* 262: 1268 - 1273

Tsai S-F, Bishop DF, Desnick RJ (1988) Human Uroporphyrinogen III synthase: molecular cloning, nucleotide sequence, and expression of a full length cDNA. *Proc. Natl. Acad. Sci. USA* 85: 7049 - 7053

Tsukamoto I, Yoshinaga T, Sano S (1980) Zinc and cysteine residues in the active site of bovine liver delta-aminolevulinic acid dehydratase. *Int J Biochem.* 12(5-6): 751-6.

Uvarov VY, Tretiakov VE, Archakov AI (1990) Heme maintains the catalytically active structure of cytochrome P-450. *Febs letters*. 260: 309 - 312

Urban-Grimal D, Volland C, et al (1986) The nucleotide sequence of the HEM1 gene and evidence for a precursor form of the mitochondrial 5-aminolevulinic acid synthase in *Saccharomyces cerevisiae*. *Eur. J Biochem*. 156:511-519

Vince R, Daluge S, Wadd WB (1971) Studies on the inhibition of glyoxalase I by S-substituted glutathiones. *J Med Chem* 14: 402-4

Volland C, Felix, F (1984) Isolation and properties of 5-aminolevulinic acid synthase from yeast *Saccharomyces cerevisiae*. *Eur. J Biochem*. 142: 551 - 557

Waldenstrom, J. (1937). Studien uber porphyrie. *Acta. Med. Scand.* 92 (Suppl.): 1-254

Waldenstrom, J. (1957). The porphyrias as inborn errors of metabolism. *Amer. J. Med.* 22: 758-773.

Wang A-L, Arredondo-Vega FA et al (1981) Regional gene assignment of human porphobilinogen deaminase and esterase A4 to chromosome 11q23-11qter. *Proc. Natl. Acad. Sci. USA* 78: 5734-5748

Warnick GR, Burnham BF (1981) Purification and characterization of 5-aminolevulinic acid synthase. *J.B.C.* 246: 6880 – 6885

Warren MJ & Jordan PM (1988) Investigation into the nature of substrate binding to the dipyrromethane cofactor of *E. Coli* porphobilinogen deaminase. *Biochemistry* 27: 9020 - 9030

Watson CJ, Schwartz S (1941) A simple test for urinary porphobilinogen *Proc. Soc. Exp Biol Med* 47: 393 as described in *Diagnosis of Porphyria Syndromes: A practical*

approach in the era of molecular biology **Bonkovsky HL & Barnard G**, *Seminars in Liver disease*, 1998;18:1 p57 – 65.

Went LN, Klasen EC (1984) Genetic aspects of erythropoietic protoporphyria. *Ann Hum Genet* 48(Pt 2): 105-117

Westall, R. G. (1952). Isolation of porphobilinogen from the urine of a patient with acute porphyria. *Nature* 170: 614.

Wetmur JG, Bishop DF, et al (1986) Human δ -aminolevulinate dehydratase: nucleotide sequence of a full-length cDNA clone. *Proc. Natl. Acad. Sci. USA* 83: 7703 - 7707

Wetmur JG, Kaya AH, et al (1991) Molecular characterization of the human δ -aminolevulinate dehydratase 2 allele: implications for molecular screening of individuals for genetic susceptibility to lead poisoning. *Am. J. Hum. Genet* 49: 757-763

Whitby F, Phillips J (1998) Crystal structure of human uroporphyrinogen decarboxylase. *EMBO J.* 17(9): 2463-71.

Whitcombe D, Carter NP, et al (1991) Assignment of the human ferrochelatase gene (FECH) and a locus for protoporphyria to chromosome 18q22. *Genomics* 11: 1152 - 1154

Whiting MJ, Granick S (1976) δ -aminolevulinic acid synthase from chick embryo liver mitochondria. I Purification and some properties. *J. Biol. Chem.* 251: 1340 – 1346

Williams DC, Morgan GS et al (1981) Purification of porphobilinogen deaminase from *Euglena gracilis* and studies of its kinetics. *Biochem J* 193: 301 - 310

Williams M, Van Der Zee J, Van Stevnick J (1992) Toxic dark effects of protoporphyrin on the cytochrome P-450 system in rat liver microsomes. *Biochem. J* 288: 155-159

Wu WH, Shemin D, et al (1974) The quaternary structure of δ -aminolevulinic acid dehydratase from bovine liver. *Proc. Natl. Acad. Sci. USA* 71: 1767-1770

Wu C, Xu W et al (1996) Mouse uroporphyrinogen decarboxylase: cDNA cloning, expression, and mapping. *Mamm Genome*. 7(5): 349-52.

Wyckoff E, Phillips J, et al (1996) Mutational analysis of human uroporphyrinogen decarboxylase. *Biochim Biophys Acta*. 1298(2): 294-304.

Wyman JF, Gollan JL, et al (1986) Incorporation of haemoglobin haem into the rat hepatic haemoproteins tryptophan pyrrolase and cytochrome P-450. *Biochem. J* 238: 837 - 846

Yamamoto M, Hayashi N, Kikuchi G (1982) Evidence for the transcriptional inhibition by heme of the synthesis of δ -aminolevulinic acid synthase in rat liver. *Biochem. Biophys. Res Comm.* 105: 985 - 990

Yamamoto M, Hayashi N, Kikuchi G (1983) Translational inhibition by heme of the synthesis of hepatic δ -aminolevulinic acid synthase in a cell-free system. *Biochem. Biophys. Res. Comm.* 115: 225 - 231

Yamamoto M, Kure S, et al (1988) Structure, turnover, and heme-mediated suppression of the level of mRNA encoding rat liver δ -aminolevulinic acid synthase. *J Biol. Chem.* 263: 15973 - 15979

Yanase T; Sasano H; et al (1998) Immunohistochemical study of cytochrome b5 in human adrenal gland and in adrenocortical adenomas from patients with Cushing's syndrome. *Endocr J*; 45(1):89-95

Yomogida K, Yamamoto M, et al (1993) Structure and expression of the gene encoding rat nonspecific form δ -aminolevulinate synthase. *J Biochem.* 113: 364 - 371

Yoshinaga T , Sano S (1980) Coproporphyrinogen oxidase I. Purification, properties, and activation by phospholipids. *J Biol. Chem* 255: 4722 – 4726

Yoshinaga T, Sano S (1980) Coproporphyrinogen oxidase II. Reaction mechanism and role of tyrosine residues on the activity. *J. Biol.Chem* 255: 4727 – 4731

Xu K, Elliott T (1993) An oxygen-dependent coproporphyrinogen oxidase encoded by the hemF gene of *Salmonella typhimurium*. *J Bacteriol.* 175(16): 4990-9.

Xu K, Elliott T (1994) Cloning, DNA sequence, and complementation analysis of the *Salmonella typhimurium* hemN gene encoding a putative oxygen-independent coproporphyrinogen III oxidase. *J Bacteriol.* 176(11): 3196-203.

Xu W, Kozak C, Desnick R (1995) Uroporphyrinogen-III synthase: molecular cloning, nucleotide sequence, expression of a mouse full-length cDNA, and its localization on mouse chromosome 7. *Genomics.*26 (3):556-62.

Zon LI, Youssoufian H,et al (1991) Activation of the erythropoietin receptor promoter by transcription factor GATA-1. *Proc Natl Acad Sci U S A* 88(23): 10638-

41

Further conclusions from this study cannot be drawn and further case studies on porphyric subjects unfortunate to die either from acute porphyria or other causes would be helpful.

University of Cape Town